STRUCTURAL EVOLUTION OF THE HIGH HIMALAYA CRYSTALLINE THRUST SHEET IN THE CHUR HALF-KLIPPE, LESSER HIMALAYA, HIMACHAL PRADESH

A THESIS

submitted in fulfilment of the
requirements for the award of the degree
of
DOCTOR OF PHILOSOPHY
in
EARTH SCIENCES

By

BIDYUT KUMAR BHADRA

DEPARTMENT OF EARTH SCIENCES
UNIVERSITY OF ROORKEE
ROORKEE-247 667 (INDIA)

APRIL, 1995

Gratis

CANDIDATE'S DECLARATION

I, hereby, certify that the work which is being presented in this thesis entitled **"STRUCTURAL EVOLUTION OF THE HIGH HIMALAYA CRYSTALLINE THRUST SHEET IN THE CHUR HALF-KLIPPE, LESSER HIMALAYA, HIMACHAL PRADESH"** in fulfilment of the requirement for the award of the Degree of Doctor of Philosophy, submitted in the Department of Earth Sciences of the University, is an authentic record of my own work carried out during a period from April, 1989 to March, 1995 under the supervision of **Dr. D. K. Mukhopadhyay** and **Dr. D. C. Srivastava.**

The matter embodied in this thesis has not been submitted by me for the award of any other Degree.

Bidyut Kr. Bhadra.

BIDYUT KUMAR BHADRA
Candidate's Signature

This is to certify that the above statement, made by the candidate, is correct to the best of our knowledge.

D. C. Srivastava

DR. D. C. SRIVASTAVA
Lecturer
Department of Earth Sciences
University of Roorkee
Roorkee 247667, India

DR. D.K. MUKHOPADHYAY
Lecturer
Department of Earth Sciences
University of Roorkee
Roorkee 247667, India

Signature of Supervisors

The Ph.D. viva-voce examination of Mr. BIDYUT KUMAR BHADRA, Research Scholar was held on 10/01/96

Signature of Supervisors

Signature of External Examiner

ACKNOWLEDGMENTS

I am indebted to the Head of the Department of Earth Sciences, University of Roorkee, Roorkee for providing all the facilities for the work. The work was funded through research grants from the Council of Scientific and Industrial Research, Government of India.

This thesis became a reality due to the constant support and inspiration extended by my parents and Doli, Dilip, Sudipta, Sidhu and Sanjoy. I shall also gratefully and forever remember the moral support and helps extended by Mr. C. B. Majumder during many personal crises.

The entire fieldwork was carried out in association with Tamal Kanti Ghosh, my friend and colleague. Long discussions with him on all aspects of geology both during the fieldwork and in Roorkee had been very informative. Discussions on the Himalayan geology with Prof. A. K. Jain, Dr. R. Manickavasagam, Dr. S. Balakrishnan, Dr. B. K. Chaudhury Dr. N. S. Gururajan and Dr. S. K. Paul were also very useful. Logistic support during the fieldwork was provided by Prof. S. K. Kaushik, Mrs. S. K. Kaushik, Mr. Harichand Sharma and the Public Works and Forest Departments of the Government of Himachal Pradesh. Kali Prasad was the Man-Friday both in the field and in Roorkee. Ram Dal and Amar Singh prepared many of the thin sections. Besides driving the Jeep during the fieldwork, Devender Singh, Bhim singh and Ramesh Chand also helped in many other ways. Puran Sharma printed some of the photographs. Jayaram, Akshaya, Pushpendra, Jai, Manas, Sushil, Vikrant, Swaroop, Ashis, Biju, Rajiv, Dibyajyoti and Sudhir extended invaluable help in putting the thesis together. I am grateful to all of them.

My stay at Rookee was made pleasant through friendship, company and help of Patel, Sandeep, Pankaj, Ramkrishna, Asokan, Hari, Lalan, Anurag, Manoj, Veneet, Thomas, Ajay, Sundaram, Binayak, Karki, and the families of A. Deb, A. C. Das, A. Roy, A. L. Guha, S. Deb, J. Das, S. Sarkar, and S. Chakraborty.

The work was carried out under the supervision of Dr. D. K. Mukhopadhyay and Dr. D. C. Srivastava. Their suggestions, advice and criticism in all stages, from suggesting the problem through field and laboratory works to the completion of the final draft, are gratefully acknowledged.

Bidyut Kr. Bhadra.

(Bidyut Kumar Bhadra)

CONTENTS

LIST OF FIGURES
(Figures are given at the end of the corresponding chapter)

LIST OF TABLES

(Tables are given at the end of the corresponding chapter)

ABSTRACT

The High Himalaya Crystalline Zone (HHCZ) representing a 25-30 km thick thrust sheet rides over the rocks of the Lesser Himalaya Zone (LHZ) along the Main Central Thrust (MCT), the most important intracontinental thrust in the Himalaya. The rocks of the HHCZ are the most highly deformed and metamorphosed rocks in the Himalaya. Around the Chur peak in the Lower Himachal Himalaya the frontal part of the HHCZ thrust sheet, locally called the Jutogh Group, is exposed in a half-klippe. Large-scale map pattern together with detailed analyses of structures from thin section to outcrop scales have been used to elucidate the deformational history of these rocks.

The frontal part of the HHCZ thrust sheet in this area can be considered to be a 5-6 km thick ductile shear zone in which ductile shearing is most intense in three restricted horizons. In this zone, however, two generations of pre-shearing folds (F_1 and F_2) which are tight to isoclinal and recumbent to gently-plunging reclined/inclined with E or W axial trend can be recognized. A penetrative cleavage (S_1) parallel to the axial planes of F_1 folds is the dominant planar structure and a crenulation cleavage (S_2) parallel to the F_2 axial planes is sporadically developed. The F_1 and the F_2 folds are coaxial resulting in type-3 interference patterns. In the ductile shear zones the structures of the early (i.e. F_1-F_2) generations have been extensively modified. Structures developed during progressive ductile shearing include: (1) mylonites, mylonitic foliations and S-C composite planar fabrics, (2) folds on layering and crenulations on pre-existing cleavage surfaces, (3) interference structures such as sheath folds, type 2 and type 3 patterns, (4) several generations of crenulation cleavage, (5) extensional structures, such as extension crenulation cleavage, foliation boudinage, rotated boudinage and pinch-and-swell structures. Small-scale thrusts giving imbricate or schuppen structures are also common in the shear zones. A set of very open and upright folds (F_3) have affected all these structures. The last deformation episode is represented by a set of subvertical fractures some of which are faults with a normal sense of displacement. Four large-scale thrusts can be recognized, viz., the Chail thrust, the Jutogh thrust, the Rajgarh thrust and the Chur thrust, the last two are reported for the first time. These four thrusts cut up the crystalline rocks of the area into four thin thrust slices giving rise to imbricate structure in large scale. A granite body (the Chur granite) occurs in this area at the highest topographic and structural levels and belongs to the Lesser Himalaya granite belt. It has been shown that the Chur granite is a thrust slice which suggests that there is another, probably basement-involved, thrust in the HHCZ sitting at a higher structural level than the MCT.

The main phase of regional progressive metamorphism is completely pretectonic with respect to the ductile shearing. It is argued that the inversion of metamorphic zones in this area is due to imbrication of thrust slices derived from a terrain with normal Barrovian metamorphic zones.

CHAPTER - 1
INTRODUCTION

1.1 PREAMBLE

The arcuate Himalayan mountain belt (about 3000 km long and 200 to 300 km wide, Fig. 1.1) marks the most recent and type example of continent-continent collision between the northward moving Indian plate and the northern Eurasian plate (e.g. Dewey & Bird 1970; Powell & Conaghan 1973; Le Fort 1975; Molnar & Tapponnier 1975, 1978; Bird 1978). The Indus-Tsangpo Suture Zone (ITSZ) marks the site of the collision (Figs. 1.1, 1.2). The northern margin of the Indian continental crust, that was caught up in the post-collision deformation, has been doubled up to about 70-80 km under Tibet due to overthrusting along a gently dipping detachment thrust (Fig. 1.2). Within the Himalaya orogenic segment, i.e. south of the ITSZ, a number of thrust planes characteristically slice up the rock sequences to form a crustal stacking wedge (Mattauer 1986).

The initial contact between the two continents took place in the Kohistan-Ladakh area in the northwestern Himalaya. Subsequently, the Indian plate rotated counterclockwise and the suturing process between the Greater India and Asia propagated eastward (Powell & Conaghan 1973; Powell 1979; Klootwijk 1984; Klootwijk *et al.* 1985). Klootwijk *et al.* (1992) suggested that the initial contact was already established by Cretaceous-Tertiary time (ca. 65 Ma) and the terminal collision occurred at about 55 Ma when the India's northward movement slowed down from 18-19.5 cm/year to 4.5 cm/year (see also Powell & Conaghan 1973; Molnar & Tapponnier 1975; Powell 1979; Besse *et al.* 1984; Patriarch & Achache 1984; Besse & Courtillot 1988). Therefore, a reasonable estimate of the total amount of post-collision continental crustal shortening between the stable part of the Eurasian plate and India is of the order of about 3000 km (Besse & Courtillot 1988). It has been suggested that about 2000 km of the total shortening was partitioned within the Tibetan block north of the ITSZ (Achache *et al.* 1984; Besse & Courtillot 1988) and was absorbed by overthrusting

along the detachment as well as through block rotation and sideways extrusion along large-scale strike-slip faults (Tapponnier *et al.* 1982). The estimate of the crustal shortening within the Indian indenter (i.e. south of the ITSZ) varies widely from about 1000 km (Besse *et al.* 1984) to about 200-300 km (Schelling & Arita 1991; Schelling 1992). A significant part of this shortening has been taken up by displacement along several thrust planes, such as the Main Central Thrust, the Main Boundary Thrust, the Main Frontal Thrust (see Figs. 1.1, 1.2) and others.

Thrusting is one of the major manifestations of collision tectonics in the Himalaya along which large-scale crustal shortening has occurred. Therefore, it is important to understand the structural details of these thrust planes. In this thesis a detailed structural analyses of a segment of the Main Central Thrust, supposedly the most important intracontinental thrust in the Himalaya, is presented.

1.2 TECTONIC DIVISIONS OF THE HIMALAYA

Physiographically the Himalaya orogenic belt is separated from the northern Tibetan Plateau by a rather depressed topography of the Indus-Tsangpo valleys. The very low and flat topography of the Indo-Gangetic alluvial plain marks the southern limit of the mountain belt. Himalaya is often loosely divided into three longitudinal topographic zones - the Higher Himalaya, the Lower Himalaya and the Sub-Himalaya (Fig. 1.2).

Geologically, the Indus-Tsangpo Suture Zone (ITSZ) separates the Himalayan belt from the northern Trans-Himalaya zone which is an integral part of the Eurasian plate. South of the ITSZ four longitudinally continuous lithotectonic zones, have traditionally been recognized. These are, from north to south, the High Himalaya Sedimentary Zone (HHSZ), the High Himalaya Crystalline Zone (HHCZ), the Lesser Himalaya Zone (LHZ) and the Sub-Himalaya Zone (SHZ). Each of these zones is bounded by major tectonic planes or zones (Figs. 1.1, 1.2). Detailed geological descriptions of these zones have been given, among others, by Gansser (1964, 1974),

Fuchs (1975, 1981), Le Fort (1975, 1989), Stocklin (1980), Valdiya (1980b), Sinha (1981), Searle *et al.* (1987), and Windley (1988). Brief accounts of each of these zones are given below.

1.2.1 The High Himalaya Sedimentary Zone (HHSZ)

This zone is made up of 11-14 km thick essentially conformable sequence of Cambro-Ordovician to the lower Cretaceous sedimentary rocks. Structurally it is a very complex zone with south-vergent recumbent folds and thrusts, north-vergent back-folds and back-thrusts and extensional structures (Searle 1983; Burg & Chen 1984; Herren 1987; Patel *et al.* 1993). At places the lower part of the HHSZ are metamorphosed (e.g. Schneider & Masch 1993; Kakkar 1988; Gururajan 1994). The contact of the HHSZ with the underlying HHCZ (Fig. 1.1) is a low angle north-dipping normal fault, regionally called the South Tibetan Detachment System (STDS, Burchfiel *et al.* 1992). The Trans-Himadri Thrust in Kumaun (Valdiya 1988), Annapurna Detachment Fault in central Nepal (Brown & Nazarchuk 1993) and Zanskar Shear Zone in the northwestern Himalaya (Searle 1983; Burg & Chen 1984; Herren 1987) correspond to the same fault system. Originally the STDS was probably a thrust but reactivated as a normal fault during the late Tertiary extension (Burg *et al.* 1984; Burchfiel & Royden 1985; Burchfiel *et al.* 1992).

1.2.2 The High Himalaya Crystalline Zone (HHCZ)

The HHCZ forms the basement to the HHSZ and represents the leading edge of the Precambrian Indian crust, reactivated and remobilized during the Tertiary Himalayan orogeny. It is also known as the Central Crystallines/Himadri in the Kumaun Himalaya, the Jutogh/Vaikrita Group in the Himachal Himalaya, the Tibetan Slab in the Nepal Himalaya, the Darjeeling Gneiss in the Sikkim Himalaya and others (Pilgrim & West 1928; Heim & Gansser 1939, Gansser 1964; Le Fort 1975; Valdiya 1980a,b, 1988; Stocklin 1980). The rocks of the HHCZ are the most highly metamorphosed and deformed rocks in the Himalaya. One of the most important

features of the HHCZ is that the metamorphic isograds are inverted, i.e., the higher grade rocks occur at successively higher topographic levels. This inverted metamorphism has been reported from the entire orogen (e.g. Pilgrim & West 1928; Ray 1947; Bhattacharyya & Das 1982; Arita 1983; see also reviews by Le Fort 1975; Sinha-Roy 1982; Windley 1983; Barnicoat & Treloar 1989). Two-mica anatectic S-type leucogranites of Tertiary age formed due to partial melting of the HHCZ have intruded the upper part of crystalline complex as well as the overlying HHSZ (e.g. Le Fort 1981; Dietrich & Gansser 1981; Deniel *et al.* 1987; Le Fort *et al.* 1987; Gururajan & Islam 1991; Harris *et al.* 1993; Searle *et al.* 1993). The Main Central Thrust (MCT) separates the HHCZ from the underlying Lesser Himalaya zone.

1.2.3 The Lesser Himalaya Zone (LHZ)

This zone is characterized by a sequence of sedimentary rocks and low-grade metamorphic rocks of upper Proterozoic to lower Palaeozoic age. Amphibolite facies metamorphic assemblages have been described from the structurally highest portions in some of the areas, such as Midland Formations in Nepal which also shows inverted metamorphism (Arita 1983; Pecher 1989). Determinations of definitive age relations and lateral correlations are difficult and uncertain owing to lack of fossils, paucity of exposures in many areas and later structural complications. The boundary of the LHZ and the Sub-Himalaya Zone to the south is known as the Main Boundary Thrust (MBT) which is probably still tectonically active (Valdiya *et al.* 1992).

1.2.4 The Sub-Himalaya Zone (SHZ)

It is made up of early Tertiary shallow marine Subathu and Dagshai-Kashauli Formations and molassic sediments of the Siwalik Group. This zone is now actively overriding the Indo-Gangetic alluvial plain along the Main Frontal Thrust (MFT) (Nakata *et al.* 1990; Yeats & Lillie 1991; Gahlaut & Chander 1992).

1.3 THE MAIN CENTRAL THRUST (MCT)

1.3.1 The importance of the MCT

As mentioned in section 1.2 there are four major tectonic boundaries which can be traced along the entire length of the Himalaya (Fig. 1.1). Of these, the MCT has a critical significance in the overall geodynamic evolution of the Himalayan orogenic belt for several reasons. (1) The MCT is considered to be a major intracontinental thrust which has accommodated significant amount of crustal shortening within the Indian indenter. (2) The metamorphic grades are inverted in the vicinity of the MCT giving rise to now-famous inverted metamorphism. The metamorphism including the inverted metamorphism has been related to the movement along the MCT. (3) The thrusting along the MCT is believed to be responsible for the generation and emplacement of leucogranite bodies. (4) At least a part of the present-day high topography has been caused by the MCT. (5) The thermal structure in the crust under the Himalaya must have been significantly perturbed during the development of the MCT.

However, the identification and location of the MCT in different sectors are far from certain (Le Fort 1975; Stocklin 1980; Valdiya 1980a).

1.3.2 The tectonic position of the MCT

The MCT was originally defined by Heim & Gansser (1939) in the eastern Kumaun between Pinder and Kali rivers (Fig. 1.3). In this area the MCT separates the medium-grade metamorphic rocks belonging to the Central Crystalline Zone (mica schists and orthogneisses) from the underlying Lesser Himalaya sedimentary rocks (Berinag quartzite and calcareous zone of Tejam composed of partly-argillaceous limestones, siliceous dolomites and interbanded slates). Towards south Heim & Gansser (1939) also recognized another crystalline sequence, "The Crystalline Almora Zone", a klippe of the Central Crystalline Zone. Gansser (1964) extended this definition to the whole of the Himalaya and marked the MCT at the contact between the HHCZ and the LHZ (Fig. 1.1).

Valdiya (1980a) recognized another thrust, the Vaikrita thrust, higher up in the section that separates the underlying medium-grade Munsiari Formation (sericite-chlorite-biotite schists, amphibolites, marble with granites and augen gneisses) from the high-grade metamorphic rocks of the Vaikrita Group (kyanite-sillimanite-garnet psammatic gneiss, granulites and migmatites). The Vaikrita thrust has been identified on the exclusive basis of an abrupt and dramatic change in the grade of metamorphism though no structural discordance exists (Valdiya 1980a, p. 107). Valdiya (1980a,b) redesignated the Vaikrita thrust as the MCT and redefined the original MCT of Heim & Gansser (1939) as the Munsiari thrust (Fig. 1.3). The redefined MCT (i.e. Vaikrita thrust) has been extended by Valdiya (1980b) to whole of the Himalaya (Fig.1.3).

In central Nepal the MCT has been marked at the top of the Midland Formation (Pecher 1977). In contrast to the original definition of the MCT, the rocks of the Midland Formation are metamorphosed upto garnet-grade and has been correlated with the Munsiari Formation by Valdiya (1980b).

Many workers now consider that the MCT is not a plane but a several kilometer thick ductile shear zone introducing the notion of 'Main Central Thrust Zone'(see Le Fort 1989). For example, Pecher (1977) suggests that the global deformation around the MCT is absorbed by sliding on many parallel planes and thus the MCT is a large and complex crustal-scale shear zone. Arita (1983) proposed a 'Main Central Thrust Zone' bounded by two thrust planes - a basal and southern MCT-I and MCT-II bounding the upper and northern limit. Metcalfe (1993) and Searle *et al.* (1993) consider the whole of Munsiari Formation as a 12-km wide north dipping ductile shear zone (Fig. 1.3).

1.3.3 The MCT and the Inverted Metamorphic Zones

Central to the problem of identification and location of the MCT is its relation with inverted metamorphic zones (cf. Ray 1947; Bhattacharyya & Das 1982). For example, Sinha-Roy (1982) defines the MCT to occur at the base of the inverted

metamorphic sequence whereas Lal *et al.* (1981) put the inverted metamorphism below the MCT. Others put the MCT within the inverted metamorphic pile, usually to coincide with the kyanite isograd (e.g. Pecher 1975; Stocklin 1980; Bouchez & Pecher 1981). Finally, MCT is taken to be a several kilometers thick ductile shear zone within which inverted metamorphism occurs (e.g. Mohan *et al.* 1989). Thus all the possible relations between the MCT and inverted metamorphic zones have been suggested by different authors working in different parts of the Himalaya.

1.4 THE SCOPE OF THE PRESENT INVESTIGATION

From the foregoing discussion it is apparent that the identification and location of the MCT and its relation with the inverted metamorphic zones are still enigmatic problems. This is a manifestation of the fact that in a terrain with post-thrusting metamorphism with or without deformation, a thrust plane or zone can be obliterated with near-complete thoroughness (Knopf 1935; Naha & Ray 1971). Thermal modelling shows that in overthrust terrains post-thrusting heating can be significant given appropriate physical and thermal parameters (e.g. Oxburgh & Turcotte 1974; England & Thompson 1984). Depth to thrust plane is one of the more important parameters that control the amount of heating and consequent increase in temperature. On a dipping thrust plane, such as the MCT, syn- to post-thrusting temperature rise should be much less in the frontal part as compared to the root zone (Shi & Wang 1987; Molnar & England 1990). It is, therefore, expected that in the root zone in the Higher Himalaya the MCT may have been obliterated to varying extent through syn- to post-thrusting metamorphism. In the frontal part of the MCT metamorphism may have been much less intense and in such areas both pre-thrusting and thrust related structures and fabrics can be studied in detail. A number of klippe and half-klippe representing the frontal part of the HHCZ thrust sheet are well exposed in the physiographic Lower Himalaya (Fig. 1.3). However, barring a few notable contributions (e.g. Naha & Ray 1971 & 1972) detailed structural work in these klippe has not yet been attempted.

In the eastern Himachal Pradesh the rocks of the HHCZ occur as a klippe around Simla town and as a half-klippe around the Chur peak (3647 m; ca. 40 km SE of Simla). The half-klippe of the HHCZ around the Chur peak has been chosen for detailed structural study for several reasons. (1) From this area Pilgrim & West (1928) documented for the first time a large-scale thrust, the Jutogh thrust, which Gansser (1964) considered to be a continuation of the MCT described in the Kumaun Himalaya by Heim & Gansser (1939). (2) Also from this area Pilgrim & West (1928) documented an inverted metamorphic zonation which has drawn attention of a large number of later workers from North America, Europe, Japan and India. (3) A granite body, the Chur granite, occurs at the Highest topographic levels and belongs to the 'Lesser Himalaya Granite Belt' of Le Fort (1988). The structural setting of the granite bodies of this belt in general and the Chur granite in particular is yet to be completely understood. (4) The area surrounding the Chur peak attains an elevation in excess of 3000 m and from this area topography slopes away in all direction. This domal topography together with gentle dips of rock formations makes this area ideal for studying a significant section of the HHCZ within a relatively small area. (5) In 1928 Pilgrim & West published for this area a very detailed geological map which must stand as one of the best from anywhere in the world. The availability of an excellent geological base map saved a lot of time as geological mapping is a very time consuming exercise. (6) The area is easily accessible by road via Solon and Nahan. Further, there are a number of roads and Guest Houses in this area constructed by the Himachal Pradesh Public Works and the Forest Departments. These are important because accessibility and logistic support are the major problems that one faces while working in the Himalaya.

An area of about 850 km^2 between 77°15'N-77°35'N and 30°43'E-31°E around the Chur peak in the Simla and Sirmour districts of Himachal Pradesh was chosen for a detailed study to elucidate the structural history of a frontal part of the HHCZ thrust sheet. The area falls under the Survey of India Toposheet Nos. 53F/5, 53F/6, 53F/9,

53F/10. Structural mapping was carried out at 1:50000 scale with maps in larger scale in certain key areas. More than 5000 compass readings of planar and linear structures were collected and analyzed using equal-area lower hemisphere stereographic projection technique. Map patterns together with analyses of small-scale structural elements, such as folds, foliations and lineations, and microstructural studies have helped in deciphering the geometry, sequence and mechanics of development of structures in different scales. Microstructural studies have helped in elucidating the time relation between the growth of metamorphic minerals and the deformational episodes. A detailed study of metamorphism is, however, totally beyond the scope of the present work.

FIGURES

CHAPTER - 1

FIGURE 1.1 Geological sketch map of the Himalaya showing major lithotectonic zones (after Gansser 1974). THZ: Trans Himalaya Zone; HHSZ: High Himalaya Sedimentary Zone; HHCZ: High Himalaya Crystalline Zone; LHZ: Lesser Himalaya Zone; SHZ: Sub Himalaya Zone; ITSZ: Indus-Tsangpo Suture Zone; STDS: South Tibetan Detachment System; MCT: Main Central Thrust; MBT: Main Boundary Thrust; MFT: Main Frontal Thrust.

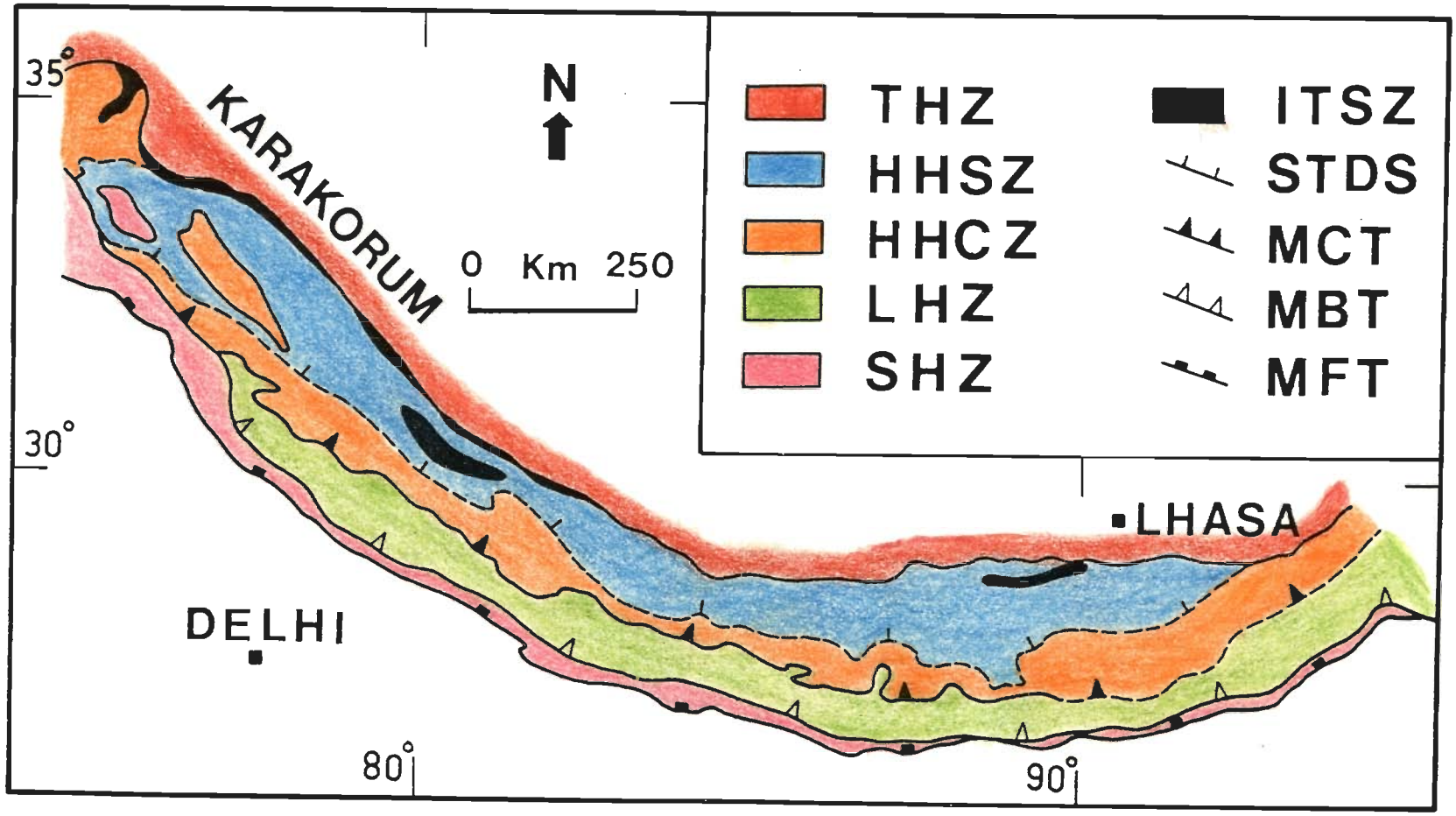
35°
KARAKORUM
N
0 Km 250
THZ
HHSZ
HHCZ
LHZ
SHZ
ITSZ
STDS
MCT
MBT
MFT
30°
LHASA
DELHI
80°
90°

Fig. 1.1

FIGURE 1.2 Schematic N-S cross section of the Himalaya based primarily on geophysical data (after Seeber *et al.* 1981; Hirn *et al.* 1984; Ni & Barazangi 1984) showing that the MFT, the MBT and the MCT are splay faults from a gently dipping detachment thrust. Note that the movement along the MCT has left the HHCZ as klippe on the LHZ in the Lower Himalaya. SHZ: Sub-Himalaya zone, LHZ: Lesser Himalaya Zone, HHCZ: High Himalaya Crystalline Zone, HHSZ: High Himalaya Sedimentary Zone, ITSZ: Indus-Tsangpo Suture Zone, MFT: Main Frontal Thrust, MBT: Main Boundary Thrust, MCT: Main Central Thrust.

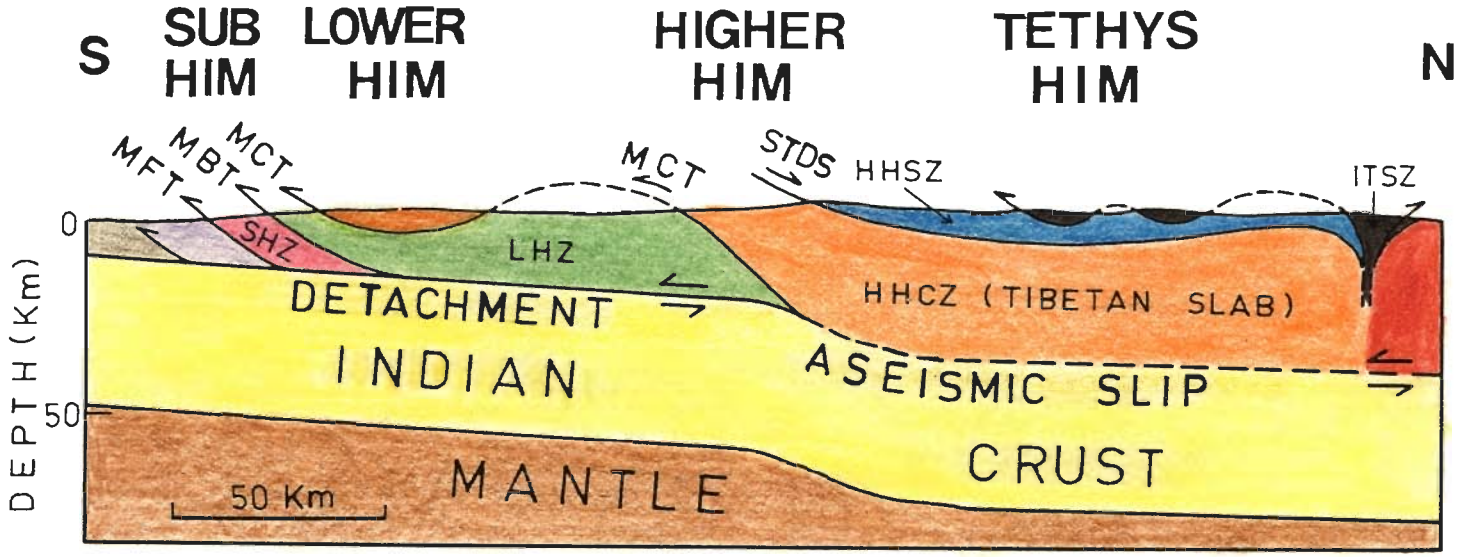
S
SUB HIM
LOWER HIM
HIGHER HIM
TETHYS HIM
N
MFT
MBT
MCT
MCT
STDS
HHSZ
ITSZ
SHZ
LHZ
DETACHMENT
INDIAN
HHCZ (TIBETAN SLAB)
ASEISMIC SLIP
CRUST
MANTLE
50 Km
DEPTH (Km)
0
50

Fig. 1.2

FIGURE 1.3 Geological map of the northwestern Himalaya showing the area of study in relation to the regional geology (adapted from the compilation by Paul & Roy 1991 after Gansser 1964; Virdi 1979; Valdiya 1980b).

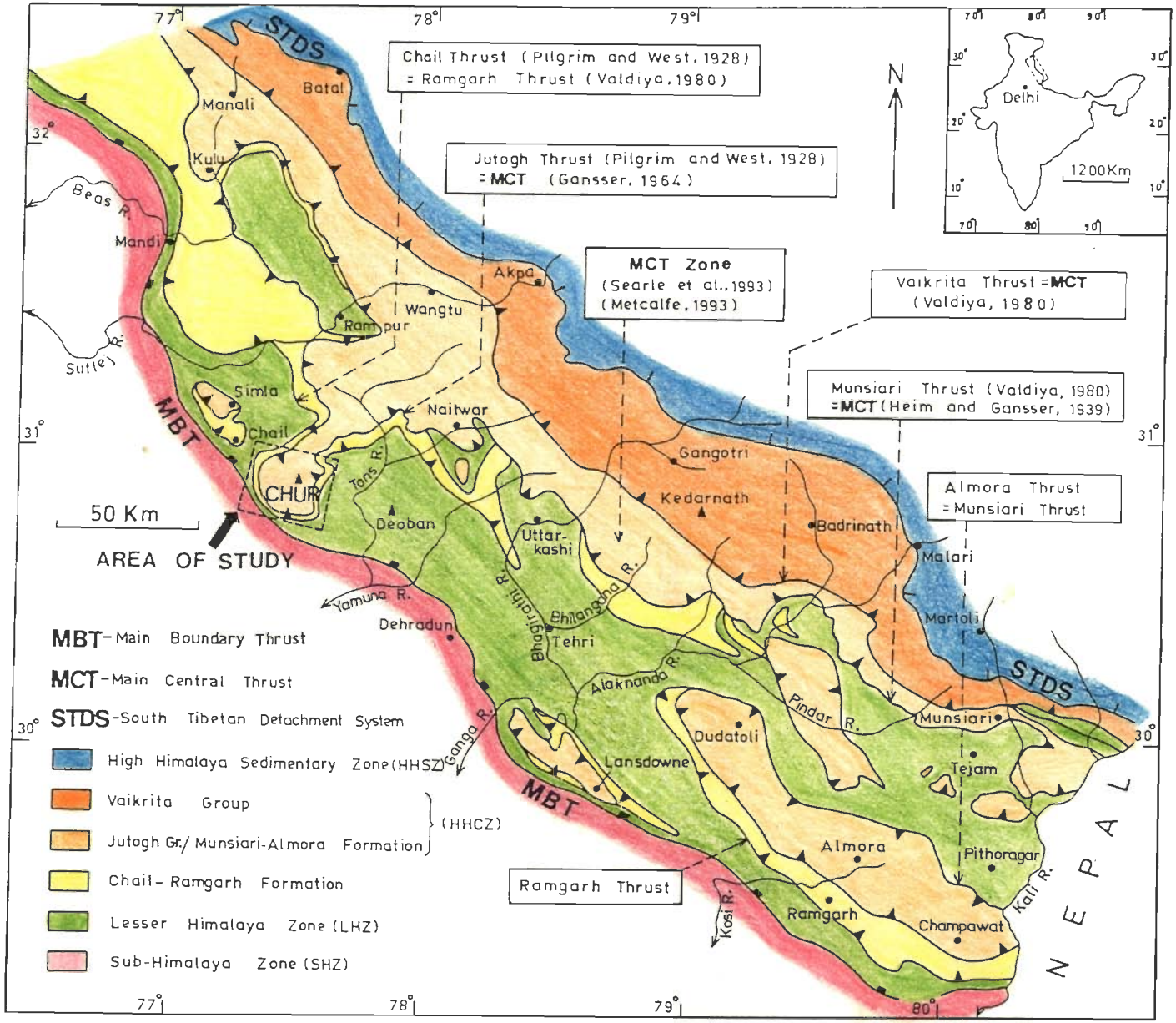
77°
78°
79°
80°
32°
31°
30°
STDS
Chail Thrust (Pilgrim and West, 1928)
= Ramgarh Thrust (Valdiya, 1980)
Jutogh Thrust (Pilgrim and West, 1928)
= MCT (Gansser, 1964)
MCT Zone
(Searle et al., 1993)
(Metcalfe, 1993)
Vaikrita Thrust = MCT
(Valdiya, 1980)
Munsiari Thrust (Valdiya, 1980)
= MCT (Heim and Gansser, 1939)
Almora Thrust
= Munsiari Thrust
Ramgarh Thrust
MBT
MBT
N
Delhi
1200Km
Batal
Manali
Kulu
Beas R.
Mandi
Sutlej R.
Akpa
Wangtu
Rampur
Simla
Chail
Naitwar
CHUR
Tons R.
Deoban
Uttar-
kashi
Gangotri
Kedarnath
Badrinath
Malari
Martoli
Munsiari
Tejam
Pithoragar
Almora
Ramgarh
Champawat
Kali R.
Kosi R.
Lansdowne
Dudatoli
Pindar R.
Alaknanda R.
Bhagirathi R.
Bhilangana R.
Tehri
Dehradun
Yamuna R.
Ganga R.
50 Km
AREA OF STUDY
NEPAL
MBT- Main Boundary Thrust
MCT- Main Central Thrust
STDS- South Tibetan Detachment System
High Himalaya Sedimentary Zone (HHSZ)
Vaikrita Group
Jutogh Gr./ Munsiari-Almora Formation
(HHCZ)
Chail- Ramgarh Formation
Lesser Himalaya Zone (LHZ)
Sub-Himalaya Zone (SHZ)

Fig. 1.3

CHAPTER - 2
GEOLOGY OF THE AREA

2.1 REGIONAL SETTING

As mentioned in chapter-1, the High Himalaya Crystalline Zone (HHCZ) forms a huge thrust sheet that can be traced all along the Himalayan orogenic belt. The HHCZ has been thrust over the Lesser Himalaya Zone (LHZ) along the Main Central Thrust (MCT). The crystalline rocks of the HHCZ are divided into an inner crystalline belt representing the root zone of the HHCZ thrust sheet and an outer crystalline belt in the frontal part of the HHCZ thrust sheet (Thakur 1981). The later occurs as a series of klippe and half-klippe in the LHZ of the Lower Himalaya (Fig. 1.3).

In the northwestern Himalaya two distinct crystalline thrust sheets, viz., the Jutogh Thrust Sheet and the Chail Thrust Sheet have been recognized (Pilgrim & West 1928; Virdi 1979, 1981; Srikantia & Bhargava 1974,1985; Valdiya 1980a; Thakur 1981). The medium grade metamorphic rocks of the Jutogh thrust sheet constitute the frontal part of the HHCZ thrust sheet. The status of the low grade metamorphic rocks of the Chail Thrust Sheet is uncertain but Fuchs (1981) consider them to be part of the LHZ. The base of the Jutogh Thrust Sheet is marked by the Jutogh thrust which is considered to be a continuation of the MCT (Heim & Gansser 1939; Gansser 1964).

Valdiya (1980b) divided the HHCZ into the Munsiari Formation and the Vaikrita Group occurring at lower and higher tectonic levels respectively. The contact between them has been taken to be Vaikrita thrust which lies at a higher structural level than the MCT as originally defined by Heim & Gansser (1939). The Jutogh Group in the Himachal Himalaya has been correlated with the Munsiari Formation by Valdiya (1980a). However, the Vaikrita thrust has never been established on the structural arguments in any area.

In the higher reaches of Himachal Himalaya the root zone of the HHCZ is very well exposed between the Satluj and Beas rivers. The frontal part of the HHCZ is well preserved as a pear-shaped klippe around Simla town and as a half-klippe around the

Chur peak in the Lower Himachal Himalaya (Fig. 1.3). In the Chur area a much thicker section, as compared to the Simla area, is preserved. Further, from the Chur area the HHCZ can be traced northward into the Higher Himalaya (Fig. 1.3).

2.2 PREVIOUS WORK

Pilgrim & West (1928) mapped the area around the Chur peak, including the area around the Simla town to the NW, and described the geology in detail (Fig. 2.1). Their classification of the rocks of the Simla-Chur peak area is given in Table 2.1.

The Jutogh Series and the Chail Series have been redesignated as the Jutogh Group and the Chail Formation respectively in order to conform to the recent stratigraphic codes (Srikantia & Bhargava 1988). The Chur granite occurs at the highest topographic and tectonic levels. The rocks of the Jutogh Group, the Chail Formation and the Lesser Himalaya Zone occur at successively lower topographic levels. Pilgrim & West (1928) assumed that the medium-grade metamorphic rocks of the Jutogh Group, the low-grade rocks of the Chail Formation and the Blaini boulder beds are of early Precambrian (Archean), late Precambrian (Proterozoic) and Upper Carboniferous (Lower Gond wana) age respectively. Based on this assumed stratigraphy in this area of unfossiliferous rocks, Pilgrim & West (1928) proposed two important overthrusts from this area: the Jutogh thrust marking the contact between the Jutogh Group and the Chail Formation and the Chail thrust at the base of the Chail Formation. Further, the occurrence of gently dipping carbonaceous schist at more than one topographic levels in this area was explained by large-scale recumbent folding. However, it is to be noted that neither the large-scale overthrusting nor the recumbent folding was demonstrated from any structural criteria.

The Chur granite which is completely surrounded by the rocks of the Jutogh Group was thought to be a laccolithic intrusion by Pilgrim & West (1928). They also showed that the grade of metamorphism in the Jutogh rocks increases towards the higher topographic levels as well as near the Chur granite. This now-famous inverted

metamorphism has subsequently been described from almost the entire orogenic belt. Pilgrim & West (1928) postulated that the superposition of contact metamorphism due to the intrusion of the Chur granite on already regionally metamorphosed Jutogh rocks caused this apparent inversion of metamorphic zones.

In the Simla klippe, Naha & Ray (1971) presented several lines of evidence to prove the occurrence of the Jutogh thrust at the base of the Jutogh Group. Naha & Ray (1972) showed that the Jutogh Group has been involved in folding of three generations and metamorphism in two phases. The earliest structures, present in outcrop to map scales, are isoclinal, recumbent/reclined folds with a shallow plunge toward east or west. The axial surfaces of these folds have been folded coaxially into open, upright antiforms and synforms which become tight to isoclinal at places causing local involution. These two generations of folds have been affected locally by a third set of conjugate and chevron folds on N-S striking axial surfaces. The overthrusting is broadly contemporaneous with the development of second generation of folding. Naha & Ray (1970) also showed that the main metamorphism in these rocks is post-F_1 recumbent folding. Kanwar & Singh (1979) have remapped the rocks of Jutogh Group and part of the granite body in the southwest of Chur area and upholds the interpretation of Naha & Ray (1971, 1972). However, the structural interpretation of Naha & Ray (1970, 1971, 1972) has been disputed by Dubey & Bhatt (1991) who suggest that there is no large-scale recumbent folding in the Simla area and that the initiation of fold and thrust movements were simultaneous.

Kishore & Kanwar (1984a,b) concluded that the Chur granite is not a single homogeneous body but it consists of two components: foliated granite along the margin and non-foliated granite in the central part, the non-foliated component intruding the foliated component. They further suggest that the contact of the foliated granite and the metasediments is discordant to the bedding plane in the metasediments and the regional foliation (axial planar to first set of folds in the country rocks) is parallel to the

foliated granite. Das (1991) concluded that the Chur granite is typical S-type granite derived by partial melting of the crustal sedimentary rock under syn-collision regime.

Das & Rastogi (1988) studied the petrology of the Jutogh metasediments in the north of Chur peak and deciphered three deformation episodes (D1, D2, D3) associated with the two metamorphic episodes (M1 and M2) in these rocks. The peak metamorphic condition during the M1 phase is syn- to post-kinematic to D1 deformation but pre-kinematic to D2 deformation. The second metamorphism (M2) which is of retrogressive nature superposed M1 during D2 deformation. Roy & Mukherjee (1976) have studied the relation between the growth of metamorphic minerals and deformation episodes in the Jutogh metasediments in the western part of the Chur peak. They suggest two prograde metamorphic episodes (M1 and M2) followed by a retrograde metamorphism. They contend that the M1 phase is syn- to post with respect to the first deformation episode and the M2 phase completely post-dates the second deformation.

2.3 THE GEOLOGICAL MAP

A thorough field check shows that the geological map (Fig. 2.1) prepared by Pilgrim & West (1928) is very precise. However, the following main departures are observed during the course of mapping on 1:25000 scale in some critical areas.

(1) Remapping around Rajgarh shows that in this area the map pattern is slightly different and the faults (displacing the carbonaceous schist bands) marked by Pilgrim & West are not present (Fig. 2.1).

(2) According to Pilgrim and West (1928) the upper carbonaceous schist band does not continue beyond Bagi in the southeastern part and near Thandidhar in the northwestern part (see Fig. 2.1). Remapping shows that this band continues northward as very thin and discontinuous lenticular bodies.

(3) In the Jutogh Group Pilgrim & West (1928) recognized two major rock types, viz., carbonaceous schists and quartzite (Boileaugunge quartzite). Detailed

mapping around Rajgarh show that the two carbonaceous schist bands have separate identities although they are petrographically very similar. The rocks between the two carbonaceous bands are dominantly fine-grained quartzite with a few thin intercalations of pelites. Above the upper carbonaceous band and upto the granite, the rocks are essentially coarse-grained mica schist with thin intercalations of quartzite and marble.

All these modifications have been incorporated in Fig. 2.2. Brief descriptions of the different rock units are given below.

2.4 ROCK TYPES

2.4.1 Jutogh mica schist

The Jutogh mica schist is a medium- to coarse-grained schistose rock with a wide variation in colour and composition. The rocks rich in quartz and muscovite are dull grey whereas biotite-rich rocks are dark grey in colour. On weathered surfaces mica schists appear brownish grey due to iron staining. The fine-grained varieties are phyllite and the coarse grained varieties are typically schist. The schistosity is defined by parallel alignment quartz and phyllosilicates (muscovite, biotite and chlorite). The grain size of the constituent minerals increases towards the granite body. With increasing proportion of quartz the pure mica schist grades into quartz-mica schist. In the south (between Churwadhar and Haripurdhar) the rock is more micaceous as compared to the rocks in the north (between Painkufar and Sarahan). Mica schist layers are often traversed by quartz veins running either parallel to the foliation or across the foliation.

In a major part, mica schist is essentially composed of quartz, muscovite, biotite and garnet with minor proportions of plagioclase, chlorite, tourmaline, epidote, apatite, sphene, zircon and ilmenite. Muscovite and biotite occur in varying proportion, although biotite is more dominant. Large staurolite porphyroblasts (upto 2-3 cm) are common in the western part but occur sporadically in the rest of the area. Kyanite and fibrolitic sillimanite, recognized only in thin sections, are confined to the mica schists

near the granite contact. Large porphyroblasts of garnet (diameter exceeding 1 cm at some places) are present in almost every outcrop. Chlorite mainly occurs as retrograde product of garnet and biotite.

Within the mica schist a thin, conformable but discontinuous band of marble occurs between Chogtali and Haripurdhar. There is no trace of marble in mica schist in the rest of the area. The impure marble is milky-white to greyish-white, medium- to coarse-grained, schistose rock essentially composed of calcite with varying proportions of quartz, talc, plagioclase, tremolite, epidote, sphene and opaque minerals. Purer varieties of marble show granoblastic texture with equant, polygonal grains of calcite. The dimensional preferred orientation of the inequant calcite grains and prismatic talc and tremolite crystals mark the cleavage planes in impure marble.

Amphibolites are quite common in mica schist. They occur as small lenticular bodies which are conformable to the local cleavage surfaces. Amphibolites are greenish black, medium- to coarse-grained and are well foliated. They are essentially made up of actinolitic-hornblende with minor amounts of quartz, plagioclase, epidote, garnet, biotite, apatite, sphene and opaque minerals.

Dolerite dykes, cross cutting the local foliation planes are present at places in mica schists. They are composed of plagioclase, pyroxene, epidote and opaque minerals and exhibit ophitic texture in thin sections.

2.4.2 Jutogh quartzite

Quartzites are medium to fine grained, grey to yellowish white, and very well-foliated rock. The fine grained quartzites are phyllitic in nature and grade into schistose varieties with increasing grain size. At places quartzites are massive. Quartz is the most dominant mineral which may constitute more than 90% of the rock. Muscovite, biotite, garnet and chlorite are the other important minerals present. Plagioclase, tourmaline, epidote, apatite, sphene and ilmenite occur in minor amounts. Thin mica schist bands commonly occur within quartzite throughout the area.

2.4.3 Jutogh carbonaceous schist

The two carbonaceous schist bands in the Jutogh Group have the same appearance in the megascopic and microscopic scales. The carbonaceous schist is essentially composed of quartz, muscovite, biotite and varying proportion of carbon content. Plagioclase, chlorite, garnet, tourmaline, epidote, calcite and pyrite are the other constituents. Muscovite dominates over the biotite and is often impregnated with carbonaceous particles. The carbon content varies from place to place and at places the rock resembles coal due to very high carbon content.

Irregular patches of calc-silicate rocks and impure marble are intimately associated with carbonaceous schists. These are dark grey to pale brown, medium- to coarse-grained and well-foliated rocks. They are mainly composed of calcite and quartz with varying proportions of talc, tremolite, zoisite, grossular garnet, diopside, apatite, sphene and opaque minerals.

2.4.4 Chail phyllite and quartzite

Phyllite and quartzite belonging to the Chail Formation underlie the Jutogh Group. These phyllite and quartzite are so closely interlayered that they cannot be separately mapped. The thickness of the quartzite layers vary from few cm to a few tens of meters.

The phyllite is a medium to fine-grained, grey to buff coloured rock with well developed phyllitic structure. In outcrops these rocks easily break into tabular blocks along the closely spaced cleavage surfaces. The quartzites are dull grey, fine-grained and are weakly foliated. Alternate quartzite and phyllitic layers mark the bedding plane in Chail Formation. Phyllites are essentially composed of quartz, muscovite and chlorite with minor proportions of feldspars (albite-oligoclase), epidote, tourmaline and opaque minerals. Preferred orientation of the muscovite and chlorite flakes and inequant quartz grains mark the cleavage planes in Chail phyllite. Only in one restricted locality (near Haripurdhar) biotite has been observed.

2.4.5 Chur Granite

The granite occurring at the central part of the area occupies the highest topographic levels around the Chur peak. It is surrounded on all sides by the Jutogh mica schists. The upper contact of the granite is not exposed within this area.

The Chur granite is a coarse grained, pinkish white to dark grey, massive to foliated igneous rock. It shows porphyritic texture in which very large K-feldspar megacrysts occur in a coarse-grained groundmass. The massive or non-foliated granite is exposed in the central part and gradually becomes foliated variety nearer to the contact with the mica schist. The K-feldspar megacrysts vary in size (few mm to more 15 cm long) and shape (rectangular, square, rhombus and irregular). The well-foliated varieties have the appearance of augen gneiss where the foliation swerves around the megacrysts. Tourmaline-bearing pegmatite veins are commonly emplaced into the granite either parallel to the foliation or across the foliation. Small (few cm^2) xenoliths of pelitic rocks have occasionally been observed in the granite.

The granite is essentially composed of K-feldspar, quartz, biotite and muscovite. Epidote, sphene, tourmaline, apatite, zircon and opaque minerals occur in minor proportions. Garnet, kyanite and sillimanite are present at some of the localities. A detailed description of the Chur granite has been given in the chapter-5.

FIGURES AND TABLES

CHAPTER - 2

FIGURE 2.1 Geological map of the Simla-Chur peak area (after Pilgrim & West 1928).

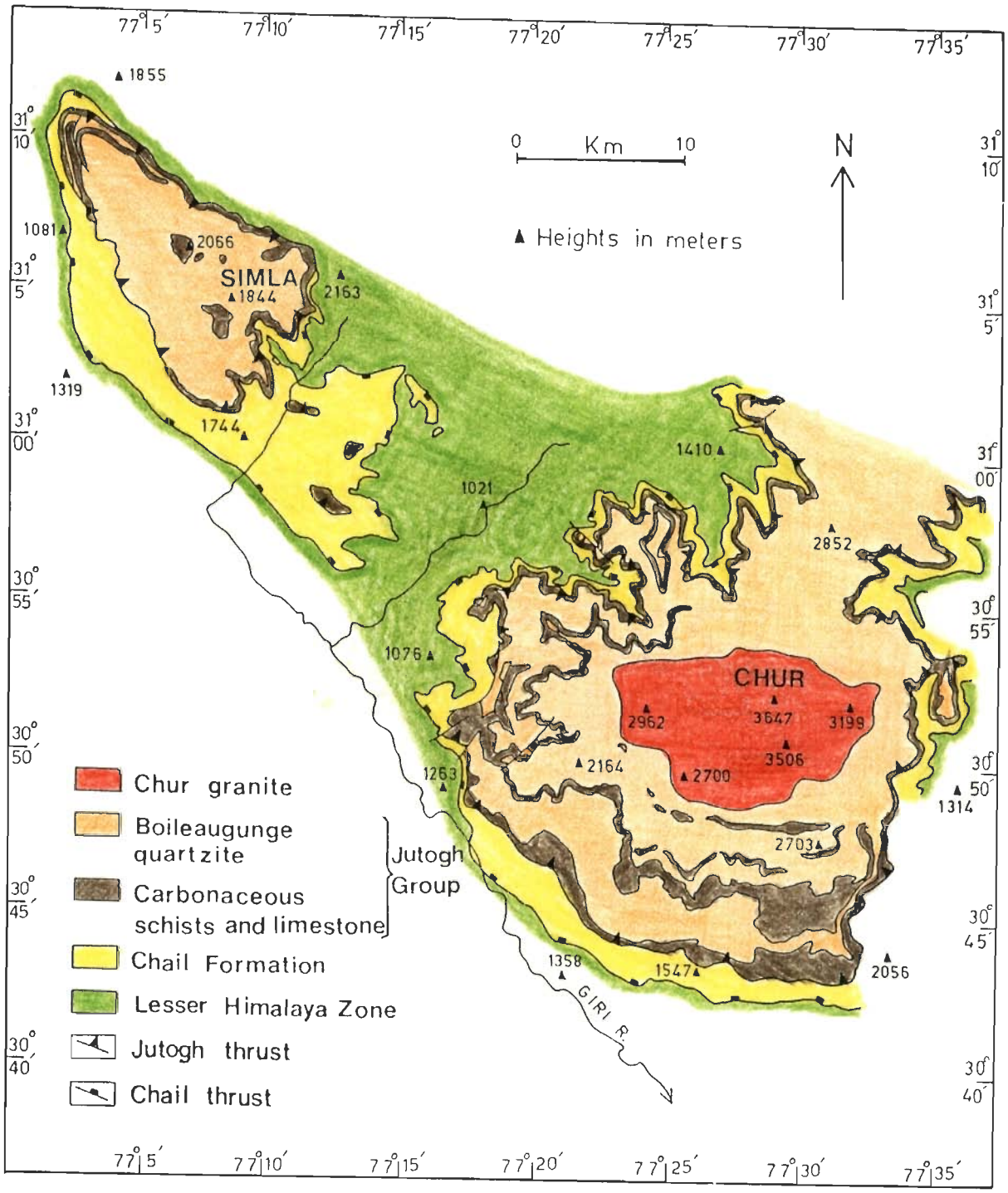
77°5′
77°10′
77°15′
77°20′
77°25′
77°30′
77°35′
31° 10′
31° 5′
31° 00′
30° 55′
30° 50′
30° 45′
30° 40′
0 Km 10
N
▲ Heights in meters
▲1855
1081▲
2066
SIMLA
▲1844
2163
1319
1744▲
1410▲
1021
2852
1076▲
CHUR
2962
3647
3198
3506
2700
▲2164
1263
2703▲
1314
1358
1547▲
2056
GIRI R.
Chur granite
Boileaugunge quartzite
Carbonaceous schists and limestone
Jutogh Group
Chail Formation
Lesser Himalaya Zone
Jutogh thrust
Chail thrust

Fig. 2.1

FIGURE 2.2 Geological map of the area around the Chur peak (modified after Pilgrim & West 1928). 1: Chur granite; 2: Mica schist; 3: Marble; 4: Upper carbonaceous schist; 5: Quartzite; 6: Lower carbonaceous schist; 7: Chail Formation; 8: Lesser Himalaya Zone (LHZ). 2-6 belong to Jutogh Group.

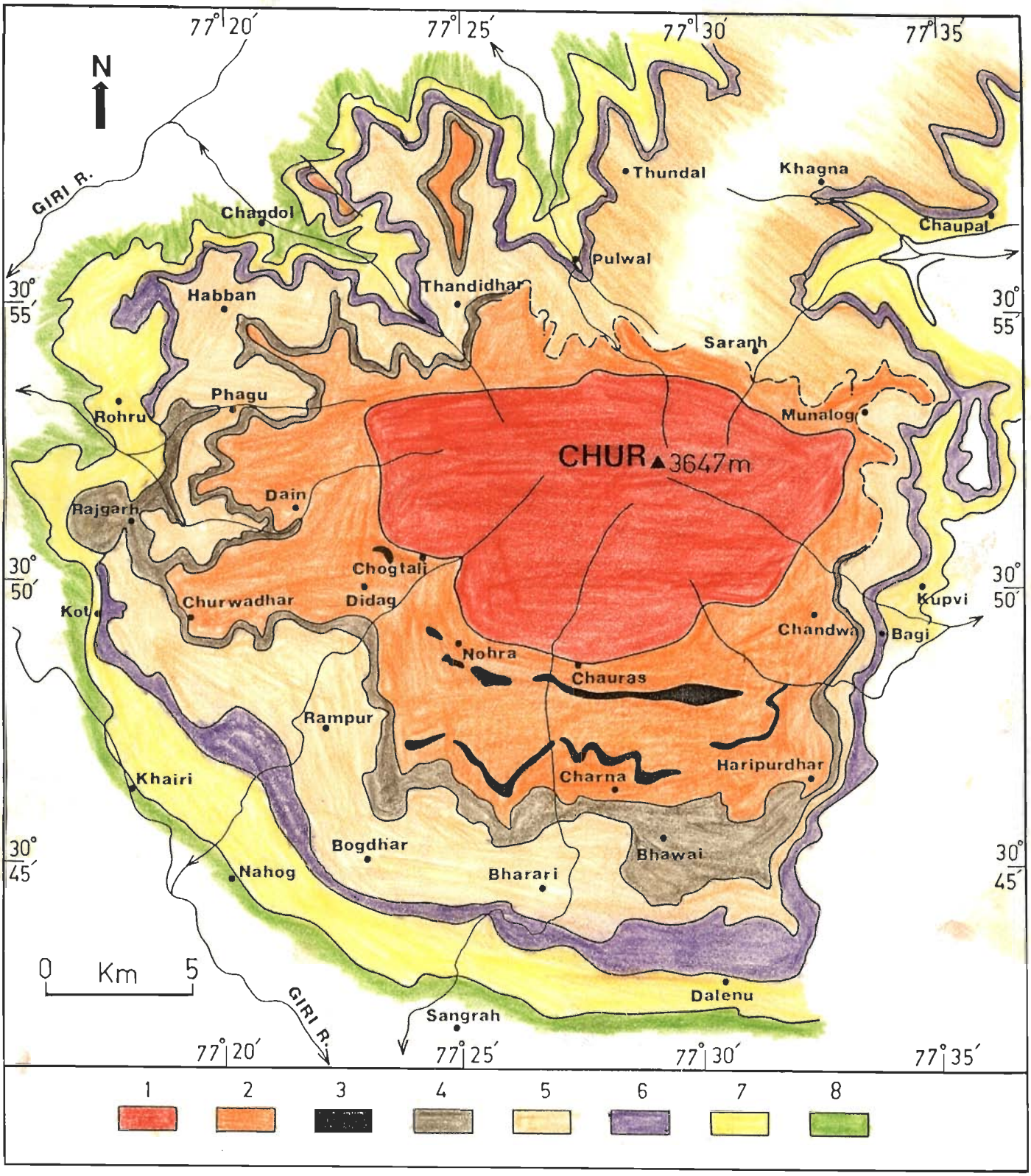
77°20′
77°25′
77°30′
77°35′
N
GIRI R.
Chandol
Thundal
Khagna
Chaupal
Pulwal
Habban
Thandidhar
30°55′
Saranh
Phagu
Rohru
Munalog
CHUR ▲3647m
Dain
Rajgarh
30°50′
Chogtali
Churwadhar
Didag
Kot
Kupvi
Chandwa
Bagi
Nohra
Chauras
Rampur
Haripurdhar
Khairi
Charna
30°45′
Bogdhar
Bhawai
Nahog
Bharari
0 Km 5
Dalenu
Sangrah
GIRI R.
1
2
3
4
5
6
7
8

Fig. 2.2

Table 2.1

CLASSIFICATION OF THE ROCKS OF THE SIMLA-CHUR PEAK AREA (AFTER PILGRIM & WEST 1928)

BLAINI BOULDER BED - Slates with pebbles — **Up. Palaeozoic**

..... Unconformity .....

SIMLA SERIES — **Lr. Palaeozoic**

Slates and micaceous sandstones
Limestone

..... Unconformity .....

JAUNSAR SERIES — **Late Precambrian**

Sub-schistose slates
Micaceous slates and phyllites
Phyllites and Conglomerate
Quartzites
Slates with vein quartz

..... Unconformity .....

CHAIL SERIES — **Late Precambrian**

Schistose slates and quartz-schist
Talcose flaggy quartzites and quartz-schist
Talc-schist
Grey slates with interbedded lime-stones

..... Unconformity .....

Intrusion of Chor granite into the Jutogh Series
Intrusion of olivin dolerites into the granite and the Jutogh series.

JUTOGH SERIES — **Early Precambrian**

Quartzite and Schists
Carboneceous dolomitic limestones
Carboneceous slates and phyllites
Quartzites and mica-schists (Boileagunge beds)

CHAPTER - 3
SMALL-SCALE STRUCTURES

The geometry and orientation of different structural elements show wide variations due to multiple deformations in this area. In order to reconstruct the sequence of deformation episodes it is necessary to document structural elements of different generations systematically. The spatial variation in the orientations of these small-scale structures then can be used to interpret the large-scale structural geometry of the area.

Structures directly observable in the scale of thin section, hand specimen and outcrop and their interrelations are discussed in this chapter.

3.1 STRATIFICATION

The earliest planar structure recognizable in the metasedimentary rocks is stratification (S_0) which is defined by colour and compositional bands, ranging in thickness from mm, as seen under microscope, to tens of meters in outcrop (Figs. 3.1a-b). In quartzite thin pelitic layers and in mica schists thin quartzite layers mark the stratification surfaces. Stratification is especially difficult to decipher in zones of thick units of schistose rocks. Even where thin quartzose layers occur parallel to the dominant cleavage in the mica schist, it is difficult to decide whether they are of depositional significance or not. However, where these layers are oblique to the cleavage in these rocks, their depositional origin is unequivocal. In impure marble, thin carbonaceous-rich layers (Fig. 3.1a) and calc-silicate (tremolite-actinolite) layers define stratification. In the Chail Formation alternate pelitic and psammatic layers define stratification (Fig. 3.1b). Sedimentary structures, such as crossbedding, are rare and have been observed in quartzites.

In major part of the area stratification is subhorizontal to gently dipping and parallels the local cleavage surfaces.

3.2 EARLY STRUCTURES

3.2.1 Folds of the first generation (F_1) and related structures

The earliest folds, observed in all the metasedimentary rocks of the area, are a set of very tight to isoclinal folds (F_1) traced by S_0 surfaces and the earliest recognizable cleavage (S_1) is axial planar to these folds (Figs. 3.1c,d, 3.2, 3.3). These folds are defined by quartzite, micaceous quartzite and impure marble layers in mica schist and carbonaceous schist. They are also defined by quartz (Figs. 3.2a,c) and calcite veins in mica schist and calc-silicate rocks respectively.

Most of the F_1 folds have class-1C geometry (Ramsay 1967) but there is a wide variation in shape depending on the viscosity contrast between the folded layers and the matrix. Where the viscosity contrast is high, such as quartz vein in mica schist, the folds are typically ptygmatic with class-1B geometry in the vicinity of the hinges (Fig. 3.2d). As the viscosity contrast decreases the shape of the folds become class-1C, eventually becoming approximately similar (i.e. class-1C tending towards class-2). In a multilayered sequence the competent and the incompetent layers show Class-1C and Class-3 geometry (Fig. 3.3a) respectively. A majority of the F_1 folds have thickened hinges and thinned limbs (Figs. 3.1c, 3.2b). The shapes of the hinges vary widely ranging from very sharp to concentric (Figs. 3.2c,d). Disharmony due to sharp variation in shapes of hinges involving multilayered rocks in a single fold profile (Figs. 3.2b, 3.3a), as well as multiple and box-shaped and parasitic folds with reversal of curvature at the hinges of folds of larger order are very common. Radial tension joints (Fig. 3.3a) at the outer arcs of folds and prominent joint surfaces perpendicular to fold hinges have been noted. The folds on thicker bands have larger wavelengths. All these characteristics suggest that the F_1 folds have developed by buckling (Ramsay 1967; Hudleston 1986; Ramsay & Huber 1987; Ghosh 1993). Most of the F_1 folds show extremely high amplitude/wavelength ratio (Figs. 3.1c, 3.2c, 3.3b). Pinch-and-swell structures, boudinage and rootless floating hinges (Fig. 3.3d) are common. These

features indicate considerable amount of post-buckle shortening perpendicular to the axial planes of the folds.

The axial planes of the majority of the F_1 folds have very gentle dips. These folds are recumbent to gently plunging reclined/inclined in geometry. However, due to later folding the axial planes show variation in dip such that they become upright at places.

A cleavage (S_1) which is axial planar to the F_1 is very well developed in all the rock types of the Jutogh Group and the Chail Formation (Figs. 3.2d, 3.3b,c, 3.4, 3.5a,b). Owing to the fact that most of the F_1 folds are very tight to isoclinal, the S_0, S_1, and the F_1 axial planes are all effectively parallel to each other except at the hinges where S_0 and S_1 are at high angles.

The S_1 is a continuous cleavage and the fabric varies from slaty cleavage through phyllitic structure to schistosity (cf. Dennis 1972; Hobbs *et al.* 1976; Powell 1979; Davis 1984). In the Chail phyllite and carbonaceous schist the S_1 is a slaty cleavage. The S_1 is typically a schistosity in coarser varieties of mica schist and amphibolite. In purer varieties of marble S_1 is usually not seen in hand specimen but the impure varieties show well developed schistosity. Under the microscope the schistosity in marble is defined by strong preferred orientation of elongated calcite grains, tremolite prisms and mica flakes.

Under the microscope, S_1 shows all variations from domainal cleavage (Figs. 3.4d, 3.5b) to a cleavage defined by evenly dispersed mica flakes and inequant quartz grains with preferred orientation (Figs. 3.4a,c). In the domainal structure clusters of lenticular quartz and feldspar grains (QF-domains) are anastomosed by M-domains (mica domain or cleavage domain) where phyllosilicates show very strong preferred orientation. In amphibolite and calc-silicate rocks amphibole prisms (Fig. 3.5a) and elongated calcite grains (Fig. 3.4b) define S_1 cleavage.

The intersection of S_0 and S_1 surfaces is the most common linear structure of the first generation. This lineation is always parallel to the local fold axis. On the cleavage surfaces (S_1) this lineation occurs as colour stripes which is called striping lineation (Fig. 3.5c). On the bedding planes (S_0) this lineation occurs as grooves and ridges. A mineral lineation defined by the preferred orientation of streaks of muscovite or biotite in mica schist and inequant quartz grains in quartzite has also developed. In amphibolite the mineral lineation is marked by hornblende prisms. Fold mullions have been observed at the interface of pelitic and psammatic layers in both Jutogh and Chail rocks (Fig. 3.5d).

3.2.2 Folds of the second generation (F_2) and related structures

The folds of the second generation (F_2) have affected the F_1 axial planes and cleavage (S_1) as well as S_0 surfaces (Figs. 3.6a-d, 3.7a,b, 3.8b). The F_2 folds vary from open to isoclinal but the interlimb angles in most of the cases vary between 20° to 50°. The shapes of the F_2 folds vary widely from nearly chevron to concentric style, sometimes along a single fold profile (Fig. 3.7a). In mica schist the F_2 folds are often crenulation microfolds (Fig. 3.8b). At the hinge zones of F_2 folds of larger order the crenulations are symmetric but at the limbs they are markedly asymmetric.

The F_2 folds follow competency rule with more competent layers showing folds with class-1B geometry in the vicinity of the hinges. The more incompetent layers show thickening of the hinges and thinned limbs resulting in class-1C geometry. The wavelength of the F_2 folds depends on the thickness of the layers involved in folding -- thicker layers showing folds with larger wavelength. Parasitic folds and disharmony with the reversal of curvature at the fold hinges are common (Fig. 3.6b). Radial tension joints parallel to the F_2 fold axis (Fig. 3.6d) and extension joints perpendicular to the F_2 fold axis (Fig. 3.6c) are usually present. All these features indicate that the F_2 folds were also developed by buckling.

The F_2 fold hinges are subhorizontal or plunge at low angles towards E to ESE directions. In most of the cases the axial planes of the F_2 folds have subhorizontal to gentle dips resulting in recumbent/reclined geometry. In rare cases the F_2 folds are subhorizontal-upright. The F_2 folds are common in the rocks of the Jutogh Group but they are absent in the Chail Formation.

A discontinuous cleavage (S_2; cf. Davis 1984) which is of the nature of crenulation cleavage (cf. Rickard 1961; Gray 1977a,b; 1979; Gray & Durney 1979) approximately parallel to the axial planes of the F_2 crenulation folds has developed at some places in mica schist. In quartzite and marble the S_2 occurs as spaced cleavage (Davis 1984). Various stages of development of S_2 crenulation cleavage (Bell & Rubenach 1983) are traceable under the microscope. In this area the development of S_2 crenulation cleavage has rarely reached the stage 5 and has never reached the stage 6 of Bell & Rubenach (1983). That is, the S_1 cleavage has nowhere been completely obliterated by the development of S_2. A few grains of micas with (001) traces subparallel to the axial planes define a crude cleavage where F_2 crenulations are gentle or open (Fig. 3.7c). With increasing tightness the cleavage traces of phyllosilicates become approximately parallel to the axial planes of F_2 microfolds and define a well developed crenulation cleavage (Fig. 3.7d; Hobbs et al. 1976; Gray 1977a,b). Both `zonal' and `discrete' crenulation cleavages (Gray 1977a) are present (Fig. 3.7d). The two types of crenulation cleavages often grade into each other.

Pucker lineation defined by the hinges of the F_2 crenulations on S_1 surfaces is the most common linear structure of the second generation in the mica schist (Fig 3.8a,b). The puckers vary in shape from round- to sharp-hinged and often die out, bifurcate or converge. Intersection of crenulation cleavage (S_2) and the folded S_1 cleavage sometimes define an intersection lineation of second generation (Fig. 3.8b).

3.2.3 Interrelation of structures of first and second generations

As discussed in the previous sections, folds of different styles and/or orientations have developed in the area. However, folds of similar style and/or orientation need not have developed during the same deformation episode (see Williams 1970). The tight to isoclinal F_1 folds are characterized by the facts that they have developed only on the stratification (So) and the earliest recognizable cleavage (S_1) cuts across the hinges at high angles. Therefore, these folds are the earliest diastrophic structures developed in this area. The lineation due to intersection of S_0 and S_1 cleavage and the mineral lineations parallel to this lineation must also be contemporaneous. The F_2 folds, varying from close to tight, affect S_0 as well as S_1 cleavage surfaces and therefore must be later in age. The S_2 crenulation cleavage parallel to the F_2 axial planes and the pucker lineation parallel to the axes of F_2 folds must also be of the same generation.

The coaxial superposition of F_2 folds on F_1 folds result in type-3 interference pattern (Figs. 3.8c,d; Ramsay 1967). As the F_1-F_2 linear structures mostly have subhorizontal to gentle plunge this interference is usually seen on subvertical faces of the outcrops. As a result of this interference, the F_1 folds are nonplane cylindrical but the F_2 folds are plane cylindrical. When F_2 folds are isoclinal the axial planes of F_1-F_2 folds are co-planar except at the hinges of F_2 folds (Fig. 3.8d). Though the F_1-F_2 folds are nearly coaxial, the angle between the two axes can be as high as 40°-50° in some domains. The F_1 linear structures curve around the F_2 fold hinges in such cases and the F_1 folds become non-plane as well as non-cylindrical.

In many exposures neither the S_1 cleavage (and the F_1 linear structures) nor any overprinting relationship is present. In such cases it is virtually impossible to group a particular fold into either F_1 or F_2 generation. Since these folds are nearly coaxial in most cases, they are grouped together as ``early folds'' predating the development of the shear zones described in the next section.

3.3 STRUCTURES IN THE SHEAR ZONES

3.3.1 Mylonite and Mylonitic foliation (S_m)

Mylonite and mylonitic foliations (S_m) are the characteristic features of many fine-grained rocks in ductile shear zones. The term mylonite was originally coined by Lapworth (1885) who considered the mylonites to be the products of intense brittle deformation. In a classic paper, Bell & Etheridge (1973) have shown that the mylonite results primarily via ductile flow and crystal-plastic grain-size reduction (dynamic recrystallization and neomineralization) though brittle deformation in some minerals, such as feldspar, may occur (see also Hobbs *et al.* 1976; Sibson 1977; White *et al.* 1980; Wise *et al.* 1984). The definition of mylonite and terminologies associated with the rocks in mylonite zones as given by different workers are confusing and too complicated at times (e.g. Zeck 1974; Tullis *et al.* 1982). In the following description the terminologies of Bell & Etheridge (1973), Hobbs *et al.* (1976), White *et al.* (1980) and, in particular, Wise *et al.* (1984) are followed. Mylonites are classified into protomylonite, orthomylonite and ultramylonite in which surviving porphyroclasts constitute more than 50%, between 50 to 10% and less than 10% of the rock respectively. With the increase in the rate of strain mylonites grade into cataclasite, a characteristic product of brittle faults. Where rate of recovery dominates over rate of strain, porphyroblastic gneiss or augen gneiss forms (Wise *et al.* 1984).

In the present area all the rock types of both the Chail Formation and the Jutogh Group as well as the Chur granite (see chapter 5) have been mylonitized to varying extent (Figs. 3.9-3.12). All gradation from protomylonite through orthomylonite to ultramylonite have been observed. At the initial stage of the mylonitization quartz grains show strong undulose extinction. Recrystallization nearer to the grain boundaries of these deformed grains leads to the formation of core-and-mantle texture (Fig. 3.9a; cf. White 1976). With increase in recrystallization (Fig. 3.9c) the rocks acquire a 'pseudoporphyritic' texture with surviving deformed porphyroclasts in a fine-grained

matrix (Figs. 3.9b,d). Where the grains are favourably oriented quartz-ribbon mylonite has developed (Figs. 3.10b,c). Porphyroclasts may (Fig. 3.10a) or may not (Fig. 3.10b) survive in a quartz-ribbon mylonite. The quartz grains in the ribbons are invariably recrystallized and show well formed subgrains (Fig. 3.10c). Finally, complete recrystallization obliterates the original fabric and the rock is composed of small polygonal relatively strain-free grains (Fig. 3.11a). The quartz-rich rocks, in such cases, become blastomylonite (Fig. 3.11a). The mica (muscovite and biotite) grains also undergo similar sequence of deformation. The fine recrystallized micas are often smeared along mylonite foliaiton (Fig. 3.10d).

In the ortho- and ultramylonites a mylonitic foliation (S_m) is usually very well developed (Figs. 3.9c, 3.10, 3.11a-c) and obliterates the early cleavages to varying extent. In hand specimen and outcrops the S_m in ultramylonites is often the penetrative cleavage and has the appearance of slaty cleavage especially in quartzite (see Fig. 3.15d). Even where the S_m is the only discernible cleavage, the S_1 cleavage may be preserved in relict porphyroclasts (Fig. 3.11d). The S_m is easily recognized in thin sections but in many outcrops and hand specimens it is virtually impossible to distinguish it from the S_1 cleavage. The degree of mylonitization varies from the scale of thin section (Fig. 3.11b,c) to the scale of the map.

In the Jutogh Group the two carbonaceous bands are most intensely mylonitized. The Chail phyllite at the contact with the lower carbonaceous band and the Jutogh mica schist at the contact with both the upper carbonaceous band and the Chur granite are also highly mylonitized. The mylonitisation in the Chur granite is restricted to the margin i.e. near the contact with the surrounding mica schist. The central part of the granite is relatively undeformed. A detailed description of granite mylonites has been given in chapter-6.

The S-C composite planar fabric (Berthe *et al.* 1979; Lister & Snoke 1984) has developed in all the rock types but most extensively in the carbonaceous schists (Fig. 3.12). The S-surfaces are defined by any penetrative cleavage which is the result of the accumulation of finite strain and are approximately parallel to the X-Y plane of the finite strain ellipsoid. The C-surfaces are defined as the loci of zones of intense shear strain (Lister & Snoke 1984). The S-surfaces in this area can be either mylonitic foliation (S_m) (Figs. 3.12a-c, 3.24c) or S_1 cleavage surface. In the original description by Berthe *et al.* (1979) both the S- and C-surfaces develop simultaneously. Where the S_1 cleavage is the S-surface this is clearly not correct (cf. Platt & Visser 1980; Platt 1984). Both type-I and type-II S-C mylonites (Lister & Snoke 1984) have developed in the shear zones. Type-II S-C mylonite, defined by mica fish (Fig. 3.12d), is common in quartzite and granite mylonites whereas in the metasedimentary rocks type-I S-C mylonite is more frequently observed (Figs. 3.12a-c).

3.3.2 Folds in the shear zones (F_{SZ})

In ductile shear zones layers having competency contrast with the matrix may undergo folding if the initial angle (α, measured counterclockwise, Fig. 3.13a) between the layer and the shear direction is high (Ramsay & Allison 1979; Ramsay 1980; Mukhopadhyay 1989). In such cases the layers lie in the zone of contraction of the finite strain ellipsoid. In anisotropic rocks, pre-existing cleavage surfaces (e.g. S_1) with similar orientation will be crenulated due to interplanar slip (Fig. 3.14a; e.g. Dennis & Secor 1987,1990). In a progressive shear the mylonitic foliation (S_m) developed during the same shearing movement may also be crenulated (e.g. Platt 1983). The early formed folds in the shear zones as well as the pre-existing folds caught up in the shear zones may be modified during the continued shearing movement (Figs. 3.13b-d). The modifications may lead to the formation of type-1 (sheath folds, Carreras *et al.* 1977; Bell 1978; Quinquis *et al.* 1978; Cobbold & Quinquis 1980; Ramsay 1980), type-2 or type-3 superposed fold geometries of Ramsay (1967). The interference fold geometries

may be traced by a layer (e.g. S_0 or quartz vein), a pre-existing cleavage surface (e.g. S_1) or even a cleavage formed during the early stage of the same shearing movement (e.g. a crenulation cleavage or a mylonitic foliation) .

In the present area folds of varying attitude and style have been observed in the shear zones (Figs. 3.15-3.19). Quartz veins and lithological layerings in carbonaceous bands, calc-silicate rocks and quartzite trace folds in the shear zones. These folds are tight to isoclinal with thickened hinges and thinned limbs. The folds follow competency rule and thicker bands show folds of larger wavelength. Disharmony at the fold hinges are also common. In general these folds show all the evidence of buckling (cf. Ramsay 1967; Hudleston 1986; Ramsay & Huber 1987; Ghosh 1993). Most of the folds in the shear zones are, however, traced by cleavage planes (Figs. 3.15d, 3.16) and they are of the nature of kinks (Figs. 3.16a,b) or crenulation folds (Figs. 3.16c,d) and are usually asymmetric.

Besides folds that have developed during shearing movement, the folds of the early generations (i.e. F_1-F_2) are also caught up and preserved in the shear zones. In many handspecimen- and outcrop-scale folds the 'generation' of a particular fold can not be decided. Only in thin sections this relationship becomes clear. In many folds a cleavage parallel to the axial planes can be very well seen (Figs. 3.15a,b). In thin sections it has been seen that this axial plane cleavage can be an S_1 cleavage, a crenulation cleavage or a mylonitic foliation. For example, the fold shown in Fig. 3.15a which has been collected from a shear zone appears to be an F_1 fold on S_0 with a very good axial plane cleavage. But the thin sections cut perpendicular and parallel to the hinge line show that the folding is on S_1 slaty cleavage which has been crenulated. The axial plane cleavage seen in hand specimen is actually a discrete crenulation cleavage. Since mylonite fabric and texture are absent this fold appears to be of F_2 generation. However, owing to the fact that crenulation and crenulation cleavage on S_1 surfaces have also developed during shearing movement (see below), it is not possible

to exclude this possibility either. In thin section of the fold in Fig. 3.15b crenulations and axial planar crenulation cleavage similar to the fold in Fig. 3.15a are observed. However, in this case the folding is on a mylonitic foliation and the stretching lineation parallel to the hinge line is defined by quartz ribbons. Therefore, this fold is not of an early generation (F_1 or F_2) but has developed during shearing movement. Only in very rare instances in an outcrop it may be concluded that a particular fold has developed during the shearing movement (Fig. 3.15d).

In shear zones some of the crenulations with well developed crenulation cleavage are on S_1 surfaces (Fig. 3.16d). However, a majority of the kinks and crenulations are on mylonitic foliation (Figs. 3.16b,c). The quartz-ribbons in mylonites are often folded (Figs. 3.17a,b). These folds are usually very tight to isoclinal with thickened hinges and thinned limbs (Fig. 3.17b). Both symmetric and asymmetric (Fig. 3.17a) folds have been observed. Folded quartz ribbons also show all the evidence of buckling. Mylonitic foliations are not only crenulated but an accompanying crenulation cleavage is also very commonly observed (Fig. 3.17c).

Sheath folds (Figs. 3.17d, 3.18a) with plane non-cylindrical geometry (akin to type-1 interference geometry of Ramsay 1967) is a common feature in many shear zones. In this area hinge-line folds are very acute and as a consequence, only the tips of the "sheaths" with elliptical outcrop pattern are normally seen (Fig. 3.18a). Type-3 interference pattern is also very common (Figs. 3.18b, 3.19a,b). In an illustrative outcrop the type-3 pattern (Fig. 3.18b) has the appearance of F_1-F_2 interference. But in thin section it is seen that the "early hinge" of this interference structure is traced by a mylonitic foliation (Fig. 3.18c). Therefore, the "early hinge" is not of F_1 generation but corresponds to a fold developed early in the shear zone. Quartz ribbons in mylonites (Fig. 3.19b) as well as crenulations (Fig. 3.19a) also show type-3 interference patterns. Type-2 interference patterns where the "early" axial planes as well the hinge lines are curved have also been observed (Figs. 3.19c,d).

Therefore successive generations of folds have developed in the shear zones. In addition folds of early generations (F_1-F_2) are also caught up in the shear zones. In the field often it is impossible to decide to which generation a particular fold belongs (see section 3.3.3 below). For this reason, all the folds in the shear zones have been grouped together (F_{SZ}).

3.3.3 Repeated crenulations and crenulation cleavage development

Bell & Rubenach (1983) have shown that a cleavage can be progressively destroyed to completion through the development of a crenulation cleavage and a new cleavage can form. Six stages through which a pre-existing cleavage can be obliterated were recognized (Fig. 4, Bell & Rubenach 1983). In an area with one dominant cleavage, the evidence for the existence of earlier cleavages come from the inclusion trails that define internal fabric (S_i) in porphyroblasts (e.g. Zwart 1962; Spry 1969; Vernon 1978, 1989; Bell & Rubenach 1983; Bell & Johnson 1989). In this area stages 1 through 6 of Bell & Rubenach (1983) have been repeated several, but unknown, times. Various stages of different generations of cleavage formations can be documented (Figs. 3.16, 3.17a-c, 3.19a,b, 3.20, 3.21, 3.22). Further, these structures are remarkably well preserved in the most intensely sheared rocks such as the two carbonaceous schist bands and the Chail phyllites near the contact with the lower carbanaceous band. The following stages of repeated crenulation cleavage development have been recognized:

(1) The earliest stage is a crenulation on S_1 cleavage without any development of a new fabric (Fig. 3.20a) provided that the S_1 was lying in the zone of contraction (see Fig. 3.14a).

(2) Development of crenulation cleavage along the axial planes of the crenulation folds (Figs. 3.20b). The crenulation cleavage may be `discrete' (Figs. 3.16d, 3.21a) or `zonal'.

(3) Dissolution and transfer of quartz grains may lead to the formation of

differentiated crenulation cleavage. The quartz grains, if favourably oriented, may form ribbons (Figs. 3.20c, 3.22b). A mylonitic foliation parallels the differentiated layering (Fig. 3.22b). The differentiated crenulation cleavage may completely be homogenized and the S_1 may be totally obliterated (stage 6 of Bell & Rubenach 1983).

(4) If the S_1 was in the zone of extension (see Fig. 3.14b) then instead of crenulation a mylonitic foliation (S_m) may be superimposed on S_1. In this case S_m would be a continuous cleavage (Fig. 3.10d). However, if S_1 is completely obliterated then this stage cannot be distinguished from homogenized differentiated cleavage formed in stage (3) described above.

(5) The differentiated mylonitic crenulation cleavage (Fig. 3.16c, 3.22a,c) or the continuous mylonitic cleavage (Fig. 3.21b) may again be crenulated (Fig. 3.20d). This is most spectacularly shown by kinked (Fig. 3.16b) and folded quartz ribbons (Figs. 3.17a,b). A new crenulation cleavage may develop along the axial planes of these folds (Figs. 3.20e, 3.21c,d, 3.22a,c).

(6) The stage (5) above may be followed by the development of a new differentiated crenulation cleavage (Fig. 3.20f) which may obliterate the earlier mylonitic crenulation cleavage to varying extent. Unless the earlier differentiated cleavage is preserved (Fig. 3.17a), this complex story may be lost.

(7) The refolded isoclinal folds traced by quartz ribbons (Fig. 3.19b) or crenulations (Fig. 3.19a) suggest that this process may have repeated several but unknown number of times. The mica-rich differentiated layers are often disrupted (possibly due to shearing at low angle to the layering), form mica 'fish' (Fig. 3.22d) and give the rocks a spotted appearance in handspecimen.

The development of repeated crenulation cleavage (often differentiated and mylonitized) leads to a serious problem. In a majority of instances in shear zones it is not possible to pigeonhole a particular cleavage to a definite generation. For example, the two stages of differentiated and mylonitized crenulation cleavage surfaces shown in

Figs. 3.20c and 3.20f cannot be distinguished unless the former is preserved in the latter as seen in Fig. 3.17c. Moreover, there is no way to prove that the earlier cleavage in Fig. 3.17c is also the earliest cleavage. Even where differentiated layering is not present (Fig. 3.21b), it can always be argued that this mylonitic foliation represents a homogenized earlier differentiated crenulation cleavage (stage 6 of Bell & Rubenach 1983). Finally, in many cases where in hand specimen only one set of cleavage is discernible, a complex history of cleavage formation is revealed in thin sections. Fig. 3.17c clearly shows atleast two generations of differentiated and mylonitized crenulation cleavage. But the outcrop from where the sample was collected shows only one set of cleavage (parallel to the later cleavage) which resembles the S_1 slaty cleavage to naked eye.

3.3.4 Problem of refolding and repeated crenulation cleavage development in shear zones

The development of buckle folds or crenulation folds in a simple shear model (Ramsay & Graham 1970; see also Ramsay & Huber 1983) are possible if layers with viscosity contrasts or a cleavage surface lie in the zone of contraction of the instantaneous flow field (Fig. 3.13a). However, it is not immediately clear how superposed fold geometry (Ramsay 1967) or refolding of mylonite cleavage (Platt 1983) in shear zone can form. In the 'ideal' shear zone model of Ramsay & Graham (1970), the plane of shear is a plane of no finite and instantaneous elongation. With progressively increasing shear strain the X-Y principal plane of the finite strain ellipsoid rotates towards the plane of shear but can never reach it and consequently cannot pass through it. Therefore, once a material line gets into the zone of extension (Fig. 3.13a) it cannot get back into the zone of instantaneous contraction in a progressive simple shear.

In this area superposed fold interference patterns as well as refolded mylonitic cleavage are very common in shear zones. They have developed via several me· chanisms as discussed below.

(1) Some of the refolded folds in the shear zones (particularly type-3 patterns) are obviously pre-shearing F_1-F_2 interference (section 3.2.7) now preserved in the relatively less deformed parts of the shear zones.

(2) The early folds (F_1 or F_2) caught up in the shear zones may get refolded (cf. Mukhopadhyay 1989). There are three possibilties (cf. Ramsay 1967): (a) The early axial plane is parallel or at low angle ($\alpha << 45°$) to the plane of shear but the hinge line is at high angle to the shear direction and has undulations. In such a case the axial plane will remain planar but the hinge line will be folded leading to the formation of sheath folds resembling type-1 interference pattern (Fig. 3.13b). (b) The early axial plane is at high angle to the plane of shear ($\alpha \approx 135°$) and the hinge line is at low angle to the shear direction but at high angle to the plane of shear. Both the early axial plane and the hinge line will get folded giving rise to boomerang or mushroom (type-2) interference pattern (Fig. 3.13b). (c) The early axial plane is at high angle to the plane of shear ($\alpha \approx 135°$) and the hinge line is at high angle to the shear direction but lying on the plane of shear. The early axial plane will get folded but both the early and later folds will be cylindrical. The resulting interference pattern will be hook-shaped (type-3, Fig. 3.13c). It is possible that the later folds in type-2 and type-3 superposed patterns may be modified into sheath folds during progressive shearing if undulations develop on the hinge lines.

(3) The quartz ribbons and the mylonitic foliations are often folded, as has been observed in thin sections (e.g. Figs. 3.16c, 3.17a,b). These folds have developed by buckling (or flexural slip). Since mylonitic foliation supposedly traces the X-Y plane of the finite strain ellipsoid it should not enter the zone of contraction and consequently

cannot be folded. Therefore, the main problem of folding and refolding of mylonitic foliation is the initiation of folds in shear zone (Platt 1983) because once nucleated a fold can amplify during progressive deformation. Several mechanisms have been proposed: (i) The flow fields in a deforming matrix can be perturbed around rigid inclusions (e.g. Ghosh & Ramberg 1976; Ghosh 1977; Ildefonse & Mancktelow 1993), such as porphyroblasts, boudins, rootless hinges or pebbles. This perturbation can bring the mylonitic foliation, momentarily atleast, in the zone of contraction. A fold can be initiated and subsequently amplified (Bell 1978; Cobbold & Quinquis 1980). Folds on mylonite foliation have been observed to occur around garnet porphyrobalsts (see Fig. 6.) in support of this hypothesis. However, such folds also occur where no such rigid inclusion is present (Fig. 3.17a). (ii) Platt (1983) showed that the foliation formed in a ductile shear zone can be folded by continuing shear without the foliation having to enter the contraction sector of the flow field. Small decreases in the rate of shear strain cause forward rotation of the foliation that may amplify into folds. (iii) Successive development of folds in progressive deformation has been explained by inhomogeneity of the rocks and heterogeneous character of strain by Ghosh & Sengupta (1984). (iv) Ghosh & Sengupta (1987) argued that in a major ductile shear zone the total shear displacement is accomplished by separate displacements along numerous small anastomosing shear zones which give lens-shaped pods. In a newly formed shear lens, superimposed on already sheared rocks, the pre-existing shear foliation will make acute angle with the lens wall. When this acute angle is counter to the sense of shear, the pre-existing foliaiton will lie in the instantaneous shortening field and become deformed into a set of asymmetric folds. It is not easy to discriminate between the above mentioned possible mechanisms; all of them were probably responsible for folding mylonitic foliation in different sectors.

(4) The three types of interference patterns (Figs. 3.13b,c,d) have also been observed on mylonitic foliation (e.g. Figs. 3.18a,b, 3.19c). Of course if folds on

mylonitic foliation can be initiated and amplified via any of the mechanisms described above, then refolding of a folded quartz ribbon or mylonitic foliation is not a serious problem. It is generally assumed that hinge lines of folds developed in a simple shear are approximately parallel to Y-axis of the finite strain ellipsoid and perpendicular to the shear direction. In such a situation refolding can produce type-1 or type-3 interference patterns (Figs. 3.13b,d). Dennis & Secor (1987, 1990) showed that the hinge lines of crenulation folds in shear zones can be perpendicular, subparallel or at an oblique angle. Therefore, type-2 interference pattern where crenulation axes need to be at low angle to the shear direction (Fig. 3.13c) can form.

3.3.5 Extensional structures

Extensional structures are quite widespread in the ductile shear zones in this area (Figs. 3.23, 3.24). These structures develop when a planar fabric (layering, Fig. 3.13a or cleavage, Fig. 3.14b) is in the zone of extension of the finite strain ellipsoid. An extension crenulation cleavage (ecc) is the most common extensional structure in this area (Fig. 3.23; cf. Platt 1979; Platt & Visser 1980; White *et al.* 1980; William & Price 1990). The *ecc* is microstructurally and genetically distinct from other types of crenulation cleavage in the sense that it develops along the limbs of very open crenulations (Fig. 3.23c) and does not occur as an axial planar structure. In this area the *ecc* has been observed in the scale varying from outcrop to thin section (Fig. 3.23). The *ecc* has developed on S_1 (Fig. 3.23b) as well as on mylonite foliation (Fig. 3.23c). It occurs both as conjugate sets (Fig. 3.23b) and as a set of approximately parallel planes (Fig. 3.23a,c). Where the *ecc* has developed on quartz-ribbon mylonites, the ribbons asymptotically curve into the *ecc* (Fig. 3.23d). In some instances neomineralization, preferentially along the *ecc*, has been observed.

If layers get caught up in the extension field they develop boudinage (Fig. 3.24b) or pinch-and-swell structures depending on the viscosity contrast with the matrix. Boudinage structures are invariably rotated (Ramsay 1967). Cleavage planes in similar

situations develop quartz-filled foliation boudinage (Fig. 3.24a). Relatively rigid minerals such as garnet, staurolite or clinozoisite are fractured, boudinaged, torned asunder and sometimes strewn along the mylonitic foliation (Fig. 3.24c,d).

Extensional structures/tectonics at the northern margin of the HHCZ have been described by many workers and have been related to the late N-S orogenic crustal extension in the overall compressional tectonics in the Himalaya (e.g. Burg *et al.* 1984; Burchfiel & Royden 1985; Searle 1986; Herren 1987; Royden & Burchfiel 1987; Patel *et al.* 1983). In this area extensional structures do not suggest any large-scale crustal extension. They have merely formed where pre-existing cleavage surfaces lie in the extension field of the strain ellipsoid.

3.3.6 Linear structures

Shear zone rocks are often very strongly lineated with the lineation lying on the mylonitic foliation. The most common linear structure is a stretching lineation (Fig. 3.15b, 3.25a,b) which is usually defined by quartz- or mica-ribbons. Sometimes elongated mica clots are parallel to this lineation (Fig. 3.25a). Lineation due to intersection of mylonitic foliation and the folded s-surfaces and crenulation lineation are also present.

The lineations in shear zones are usually very straight in outcrop scale but sometimes curved along with (Fig. 3.25c) and around fold hinges (Fig. 3.25d). The linear structures of F_1 generation are usually approximately parallel to the mylonitic lineations but they are at acute angles in some of the exposures. On planar S_1 cleavage surface folded striping (i.e. S_1 intersection lineation) lineations with a mylonitic lineation approximately bisecting the fold traced by the striping lineation have been seen. This particular feature forms in the vicinity of F_1 fold hinges if the S_1 axial planar cleavage is parallel to the plane of shear (Ramsay 1967, p. 473).

3.3.7 Small-scale thrusts

Gently-dipping small-scale thrusts are very common in the carbonaceous schist bands and adjacent rocks (Figs. 3.26). In the hanging wall block the mylonitic foliaiton is usually subparallel to the thrust plane. But in the foot wall block the thrust planes often cut across the mylonitic foliation (Figs. 3.26a,b). Dragging effect in the foot wall block has been noted (Fig. 3.26b). A number of thin thrust sheets, each measuring less than a metre thick, ride over each other giving rise to imbricate or schuppen structures (Fig. 3.26c). At places in carbonaceous schists duplex structures have developed. In some cases the roof and floor thrusts merge to give lensoid duplex structure. Splays from a floor thrust have also been observed. The Jutogh quartzite, which underlies the upper carbonaceous band everywhere, sometimes occur above the upper carbonaceous band due to small-scale thrusting. In most of the cases the thrust planes dip at low angle (20°-30°) with sense of movement towards west or southwest.

3.4 LATE STRUCTURES

3.4.1 Folds of the third generation (F_3)

A set of very broad-hinged upright warps (F_3, Fig. 3.27a) have affected all the structures of both the F_1-F_2 generations and in the shear zones. The effect of these structures is seen in broad undulations of the cleavage surfaces in outcrop to intermediate scales.

3.4.2 Late fractures

A set of subvertical to steeply dipping fractures cut across all the planar fabric of the rock types (Figs. 3.27b-c). These fractures are the latest structures in this area. They occur either as one set of subvertical fractures (Fig. 3.27b) or as steeply dipping conjugate sets (Fig. 3.27c). At some places they show normal sense of displacement (Fig. 3.27d).

FIGURES

CHAPTER - 3

FIGURE 3.1 STRATIFICATION (S_0) AND F_1 FOLDS

(a) Bedding planes (S_0) marked by colour banding in impure marble. The dark bands are rich in carbonaceous matter. Looking N325°. Location: 1 km S of Nohra.

(b) Bedding planes (paralleled by S_1 cleavage) traced by alternate pelitic and psammatic layers in Chail phyllite. Note the psammatic layer in the lower part of the photograph shows boudinage and pinch-and-swell structure. Looking N350°. Location: 4 km W of Rajgarh.

(c) Profile section of an isoclinal F_1 fold defined by quartzite layers in mica schist. Note thickened hinges and thinned limbs and very high amplitude/wavelength ratio. Looking N290°. Location: 2 km E of Charna.

(d) Isoclinal, gently-plunging F_1 fold traced by marble layers in mica schist. Looking N135°, oblique to the hinge line. Location: 1.5 km N of Charna.

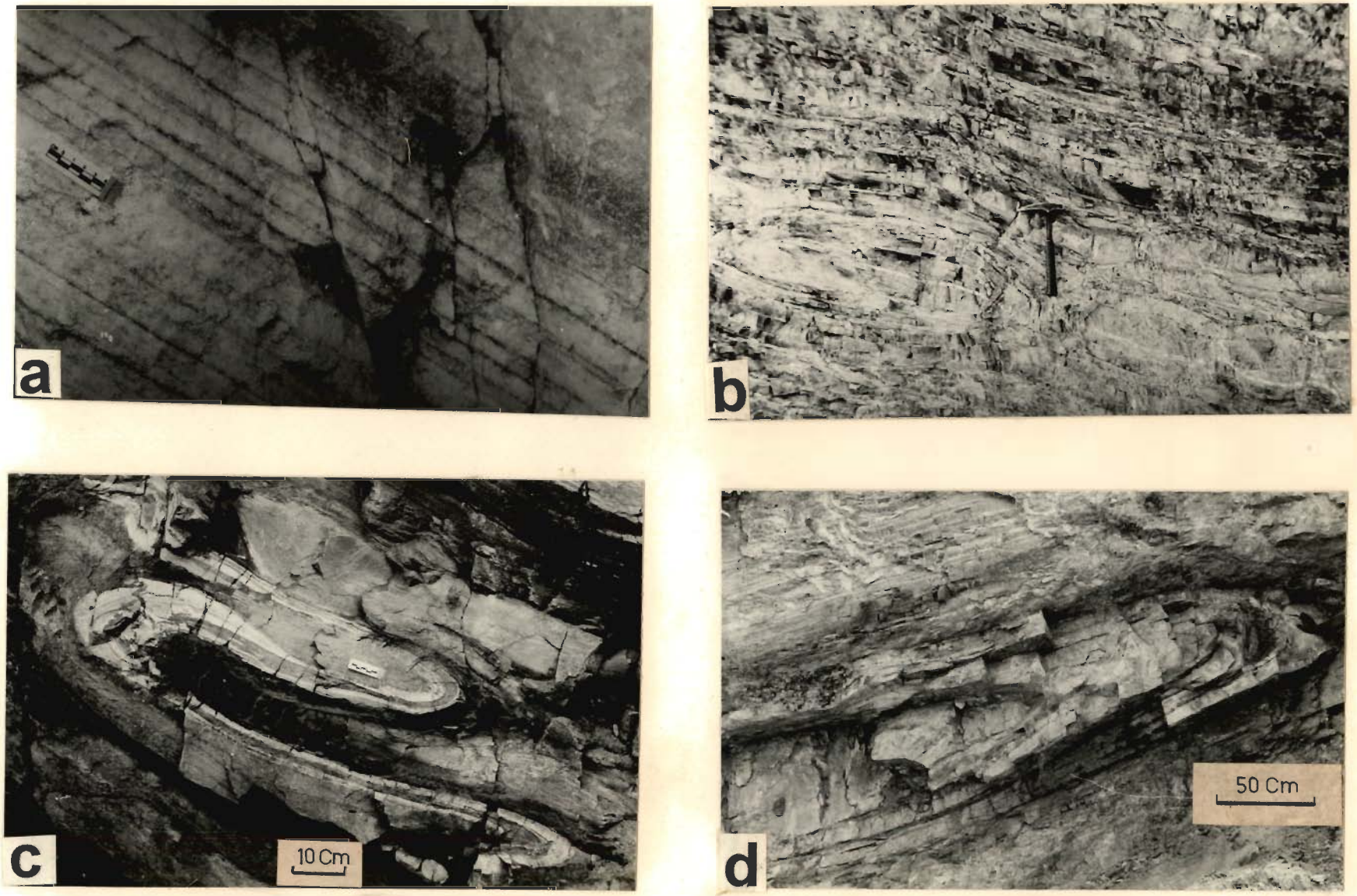

Fig. 3.1

FIGURE 3.2 F_1 FOLDS

(a) Rootless isoclinal F_1 fold traced by quartz vein in mica schist showing straight hinge line. Looking N. Location: 2 km W of Didag.

(b) Very tight to isoclinal F_1 folds defined by colour banding in impure marble. Disharmony at the fold hinges due to reversal of curvature noticeable. Looking N110°. Location: 2.5 km NW of Nohra.

(c) Sharp-hinged, recumbent and isoclinal F_1 fold traced by quartz vein in micaceous quartzite. Location: 5 km SW of Phagu.

(d) Quartz vein in mica schist involved in ptygmatic F_1 folding. Note that some of the folds have clear 1B geometry in the vicinity of the hinge zones. Axial plane cleavage (S_1) is noticeable. Location: 3 km NW of Charna.

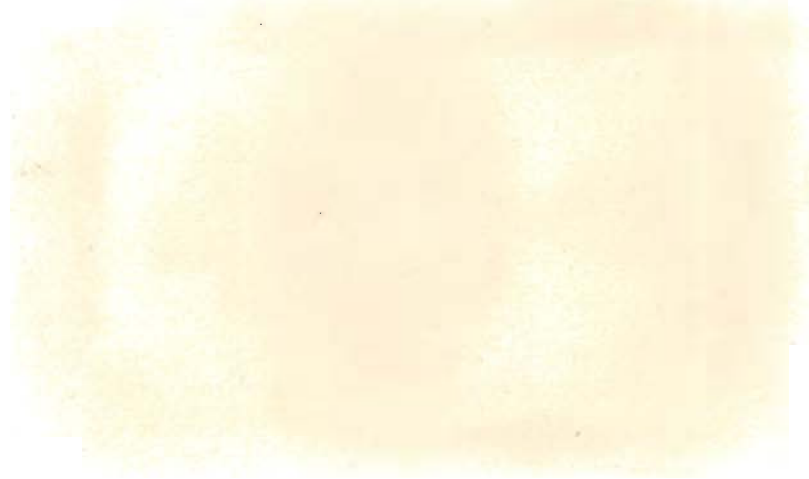

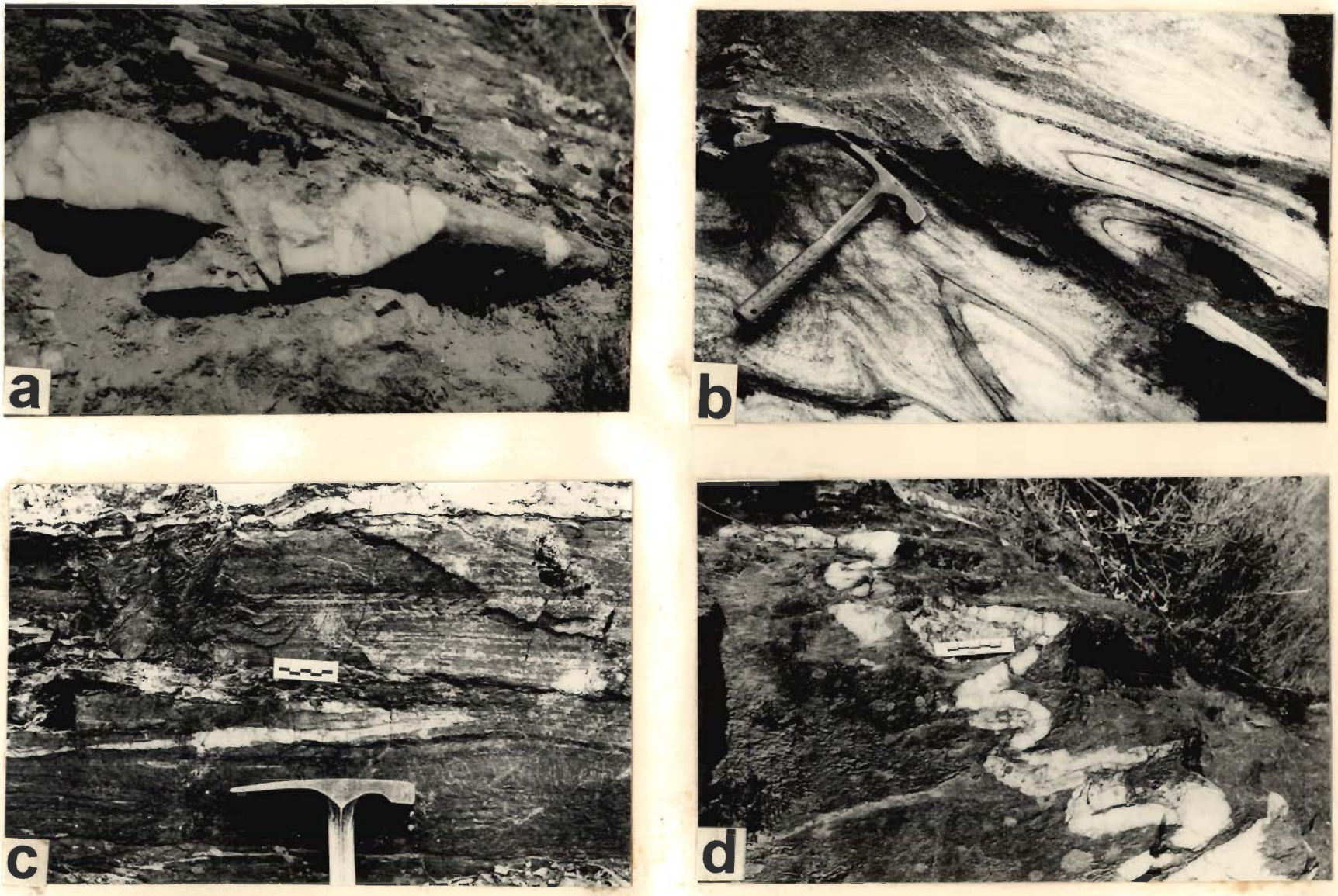

Fig. 3.2

FIGURE 3.3 F_1 FOLDS

(a) Hinge zone of a tight F_1 fold affecting multilayered sequence in the quartz-mica schist. Thickening at the hinges, disharmony and radial tension cracks are noticeable. Location: 3 km W of Haripurdhar.

(b) F_1 isoclinal recumbent fold defined by quartzo-feldspathic vein in quartz-biotite gneiss. Axial planar cleavage (S_1) cuts across the hinge. The fold show very high amplitude/wavelength ratio. Looking N25°. Location: Didag.

(c) Quartzite layer in mica schist showing round hinged, tight, gently plunging inclined F_1 folds. Axial planar cleavage cut across the hinge. Looking N40°. Location: 3 km E of Churwadhar.

(d) Rootless fold hinges (F_1) and boudinage structures traced by quartzose layer in mica schist. Looking: N345°. Location: 2 km W of Didag.

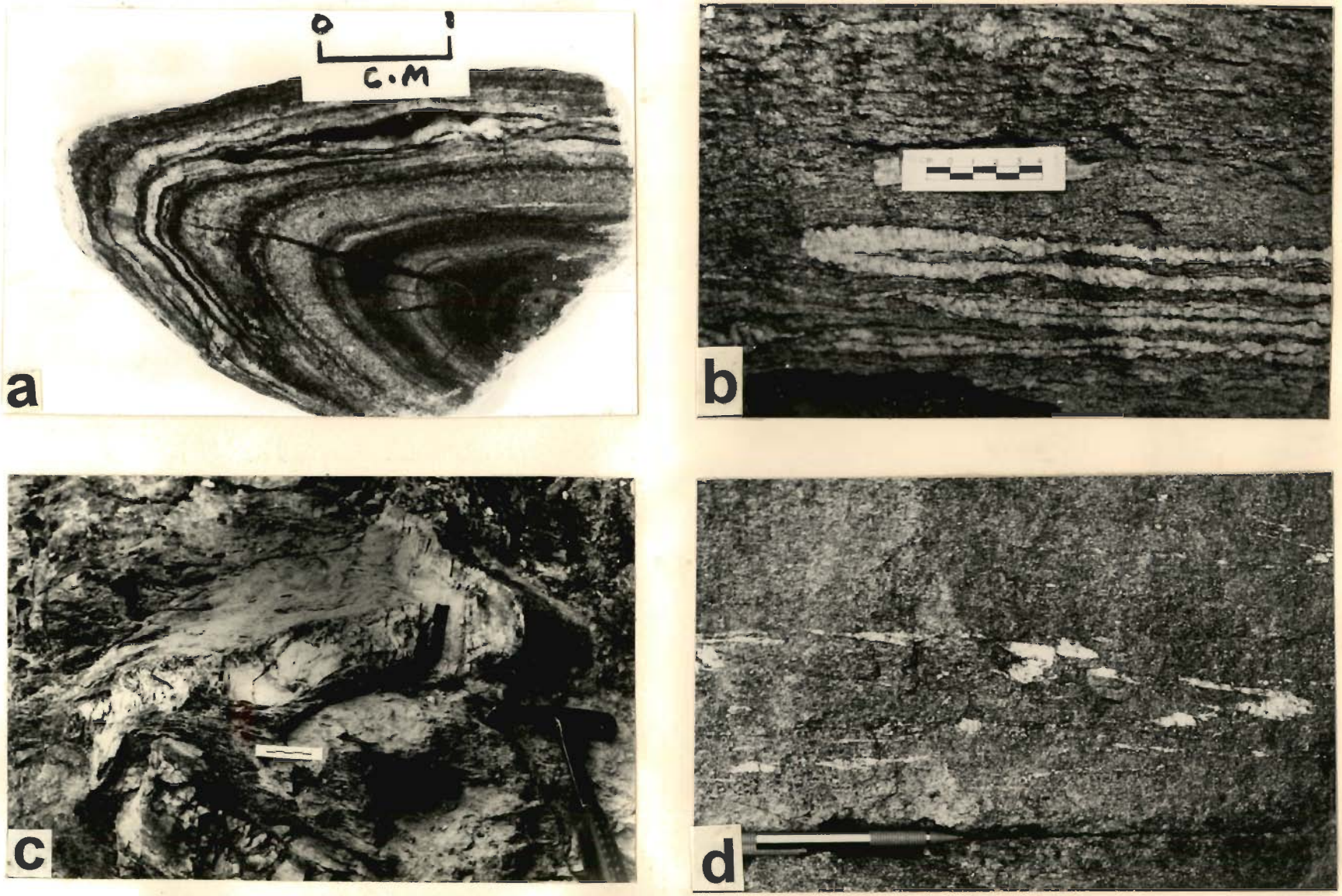

Fig. 3.3

FIGURE 3.4 CLEAVAGE OF THE FIRST GENERATION (S_1)

(a) Slaty cleavage (S_1) defined by preferred orientation of inequant quartz grains and uniformly distributed mica flakes in quartzite. Base: 1.3 mm. Oblique nicols. Location: Near Saranh.

(b) S_1 schistosity in calc-silicate rock defined by preferred orientation of inequant quartz and calcite grains. Base: 1.3 mm. Oblique nicols. Location: Saranh.

(c) S_1 cleavage in mica schist showing uniformly distributed mica flakes. Base: 2 mm. Plane-polarized light. Location: 4 Km E of Pulwal.

(d) S_1 domainal cleavage defined by lenticular quartz domains and anastomosing mica domains in quartz-mica schist. Base: 1.3 mm. Oblique nicols. Location: 4 Km E of Pulwal.

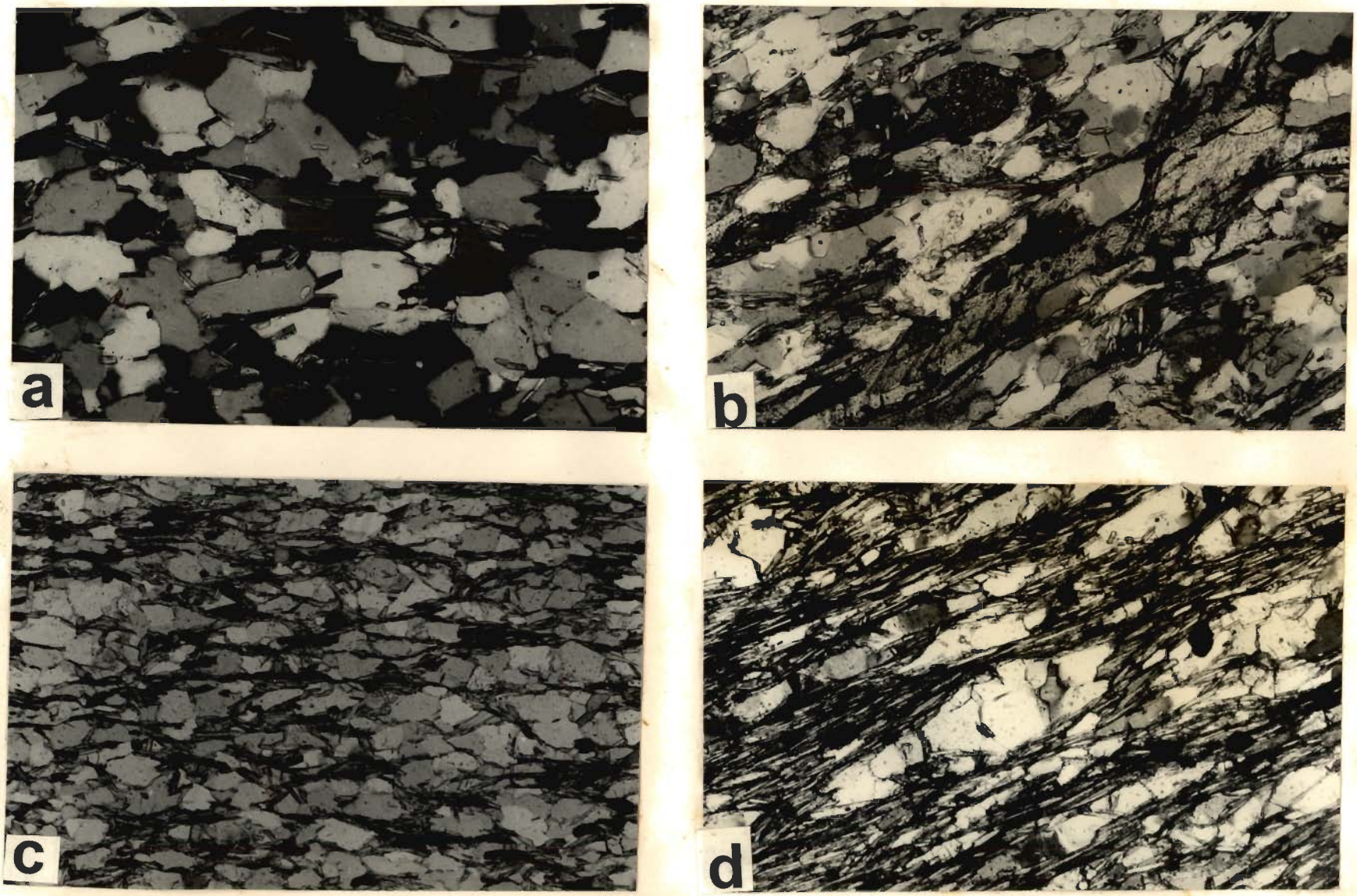

Fig. 3.4

FIGURE 3.5 S_1 CLEAVAGE AND LINEATION OF THE FIRST GENERATION

(a) Amphibolite showing S_1 cleavage traced by preferred orientation of hornblende and elongated quartz grains. Base: 2 mm. Oblique nicols. Location: Churwadhar.

(b) Domainal S_1 slaty cleavage in Chail phyllite defined by lenticular Q-domains with dimensional preferred orientation and M-domains rich in fine grained micas. A few opaque minerals are randomly distributed in the rock. Opaques oriented oblique to the foliation show pressure shadow zones. Base: 5.2 mm. Plane-polarized light. Location: Dalenu.

(c) Traces of bedding plane on S_1 schistosity defines stripping lineation (parallel to the scale). A stretching lineation at an angle to striping lineation is noticeable. Looking N315°. Location: 7 km south of Nohra.

(d) Fold mullion in Chail phyllite. Location: 3 km N of Rajgarh.

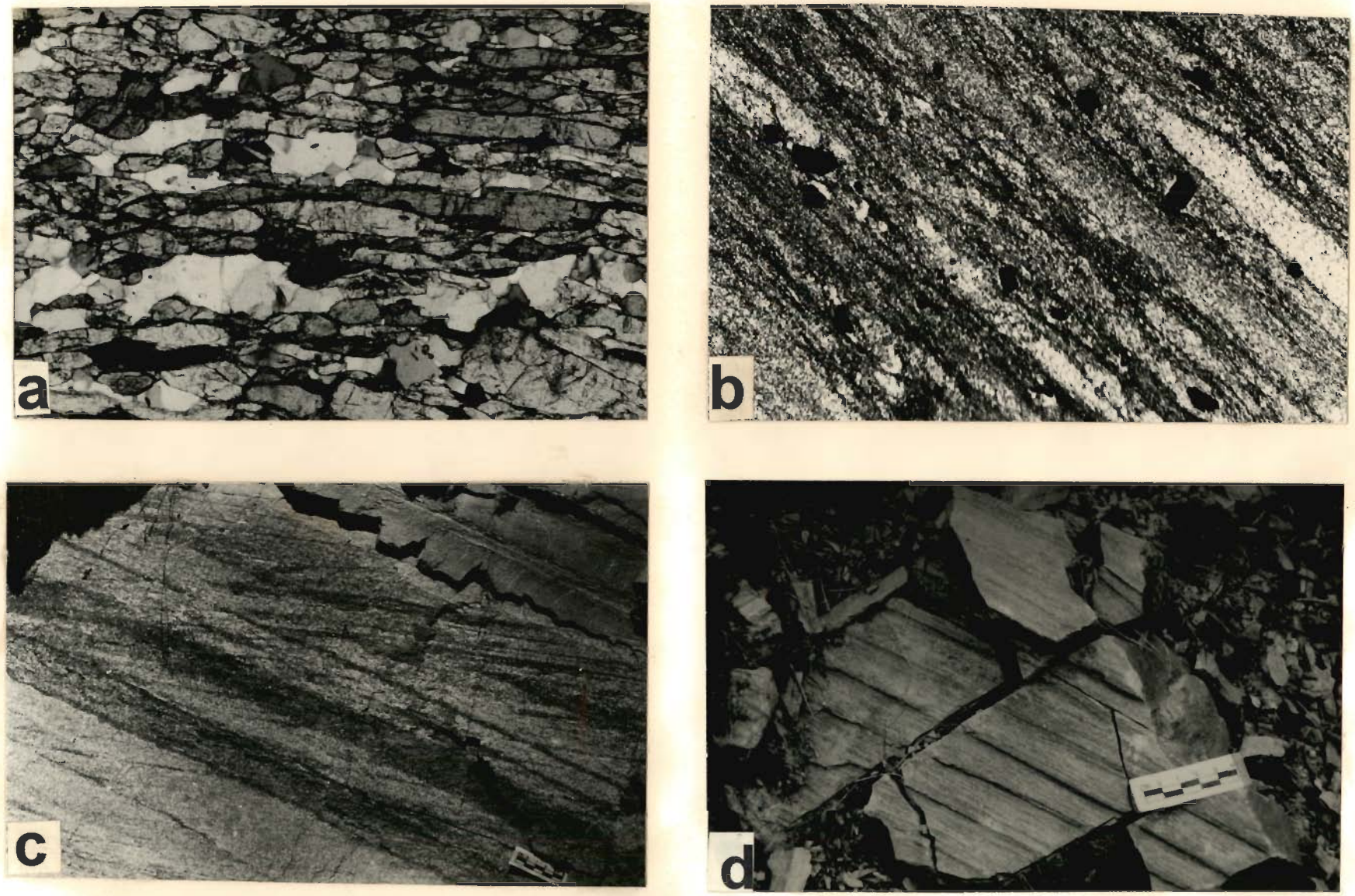

Fig. 3.5

FIGURE 3.6 F_2 FOLDS

(a) An asymmetric, gently-plunging, isoclinal reclined fold (F_2) defined by S_1 schistosity in mica schist. Looking N130°. Location: Nohra.

(b) Gently-plunging, inclined F_2 fold traced by S_0 and S_1 surfaces in quartz-mica schist. Note that the hinges in the upper right hand side of the photograph are nearly chevron type. The hinges on the left hand side is rather broad and show disharmony due to reversal of curvature. Looking N340°. Location: 2 km south of Nohra.

(c) Broad, round-hinged, gently-plunging inclined fold (F_2) defined by S_1 schistosity in mica schist. Fracture perpendicular to the hinge line is present. Looking N65°. Location: 2 km S of Chauras.

(d) Round-hinged, gently plunging inclined fold (F_2) defined by S_1 schistosity in quartz-mica schist. Note radial tension fractures. Looking N310°. Location: 2 km W of Haripurdhar.

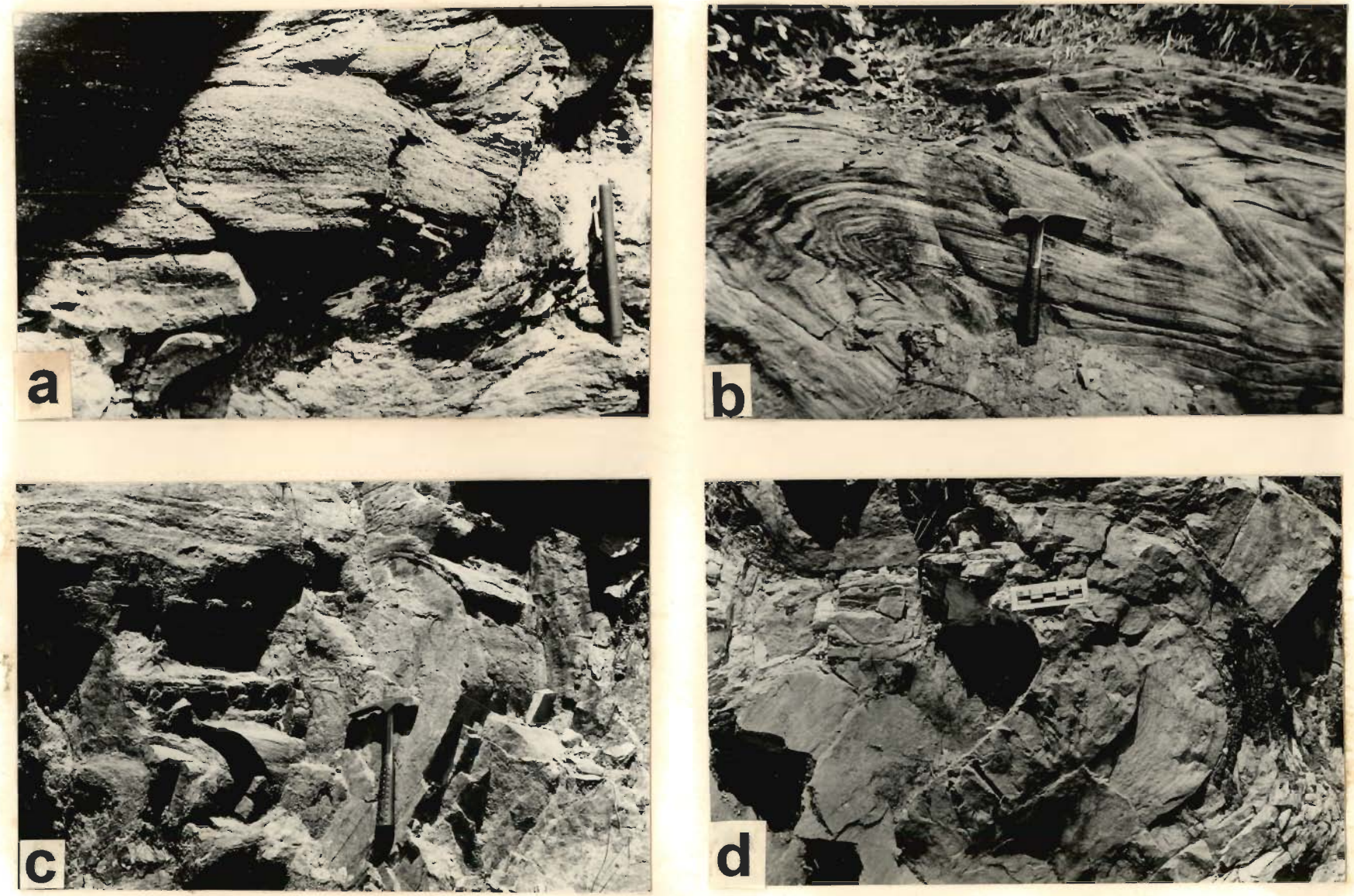

Fig. 3.6

FIGURE 3.7 F_2 FOLDS AND S_2 CRENULATION CLEAVAGE

(a) Tight F_2 fold traced by quartzose layers (S_0) and S_1. The fold varies from round-hinged to nearly chevron type along the axial surface. Looking: N145°. Location: Nohra.

(b) Horizontal-inclined F_2 fold traced by both S_0 and S_1 in mica schist. Looking N135°. Location: 2 km south of Chauras.

(c) Incipient crenulation cleavage marked by newly developed muscovite flakes along the axial surface of the crenulation. Base: 2 mm. Crossed nicols. Location: Chauras.

(d) Discrete and zonal crenulation cleavage (S_2) axial planar to the F_2 crenulations, in mica schist. Base: 8 mm. Plane-polarised light. Location: 4 km NW of Kupvi.

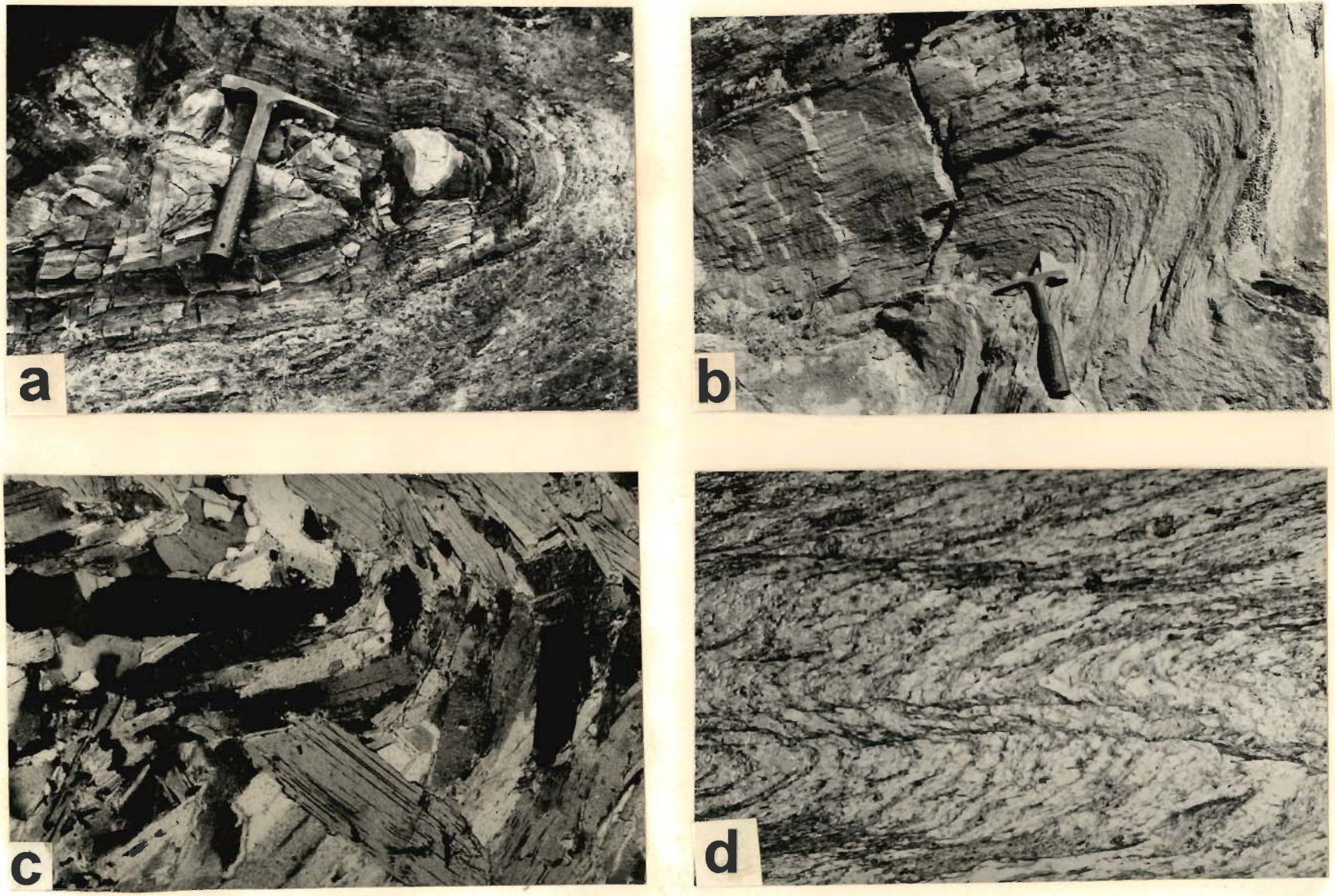

Fig. 3.7

FIGURE 3.8 F_2 LINEATIONS AND F_1-F_2 INTERFERENCE PATTERNS

(a) F_2 pucker lineation in mica schist, oriented at an oblique angle to the fold mullions of F_1 generation (left to right). Looking: N. Location: 2 km south of Chauras.

(b) F_2 lineation due to intersection between S_2 crenulation cleavage and folded S_1 schistosity surface in mica schist. Note pucker lineations form grooves and ridges on the folded surface and parallel the intersection lineation. Location: 1 km S of Habban.

(c) F_1 fold with boudinaged limbs traced by quartz vein in mica schist is coaxially refolded by open, round-hinged F_2 fold resulting in hook-shaped (type-3) interference pattern. Location: Charna.

(d) Type-3 interference pattern due to coaxial superposition of F_2 folding on F_1 fold in impure marble. The F_1 fold is isoclinal whereas the F_2 fold is very tight. Looking: N16°. Location: 6 km SW of Nohra.

Fig. 3.8

FIGURE 3.9 MYLONITES

(a) Protomylonite in quartzite showing original quartz grains with serrated grain boundaries and strong undulose extinction. Recrystallization and subgrain developement along the grain boundaries give core-and-mantle (e.g. mortar) texture. The rock is devoid of any cleavage surface. Base: 1.3 mm. Crossed nicols. Location: Bogdhar.

(b) Protomylonite in mica schist with surviving quartz porphyroclasts in a very fine-grained recrystallized matrix. Base: 6.5 mm. Crossed nicols. Location: 4 km W of Didag.

(c) Quartzite protomylonite with surviving quartz porphyroclasts embedded in a matrix composed of small recrystallized quartz grains. Note that recrystallization is more extensive than in **(a)** above. Base: 2 mm. Crossed nicols. Location: Bogdhar.

(d) Quartz porphyroclasts in a very fine-grained matrix composed of quartz and sericite in Chail phyllonite. Overall the rock is orthomylonite. Base: 1.8 mm. Crossed nicols. Location: Kot.

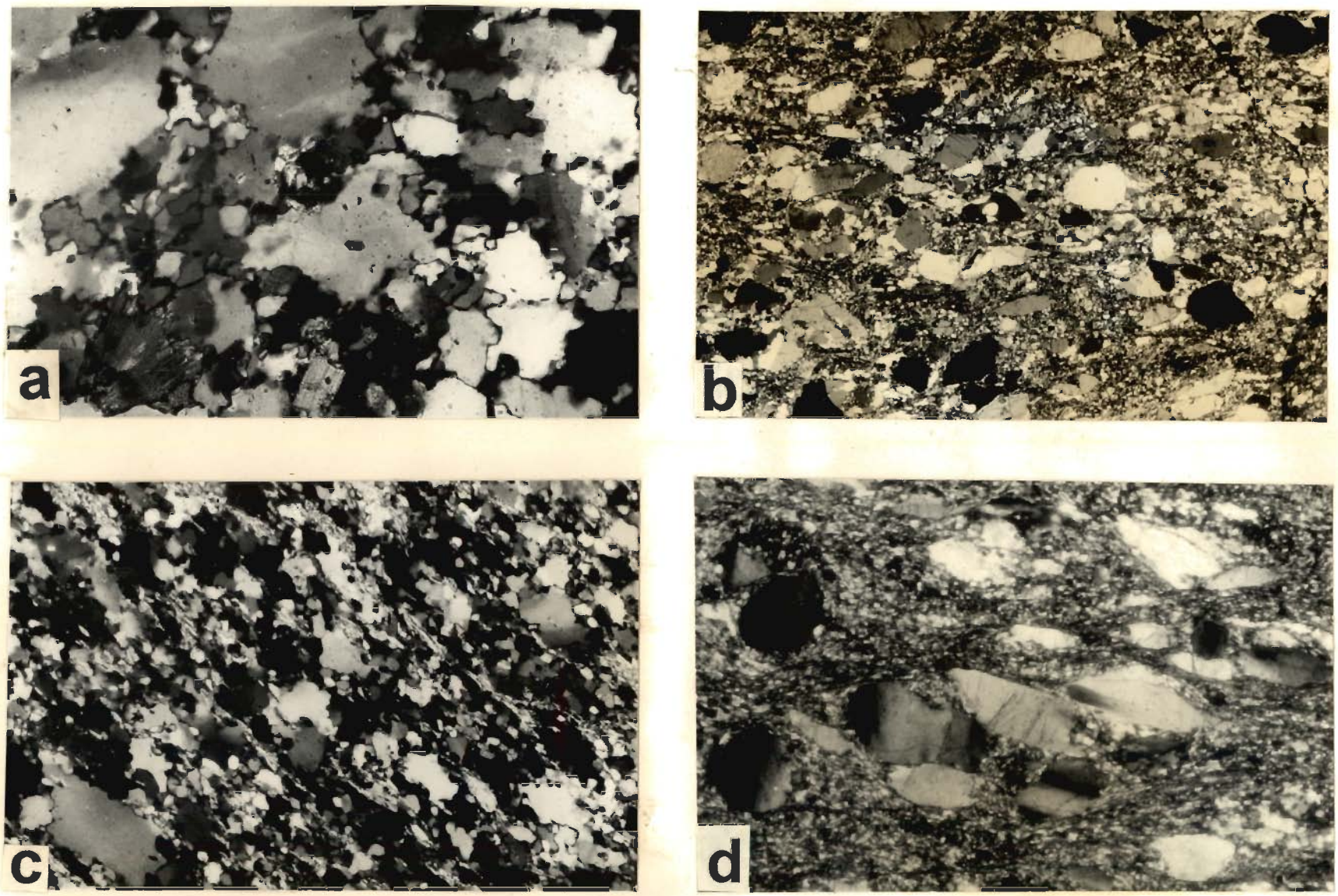

Fig. 3.9

FIGURE 3.10 MYLONITES

(a) Mica schist orthomylonite showing development of mylonitic foliation traced by quartz ribbons with few surviving quartz porphyroclasts. Base: 2 mm. Oblique nicols. Location: Thandidhar.

(b) Quartz-ribbon mylonite with very well developed mylonitic foliation in mica schist ultramylonite. Base: 8 mm. Plane-polarized light. Location: 4 km W of Didag.

(c) Details of (b) above showing recrystallized quartz ribbons in mica schist. Preferred orientation of recrystallized micas and quartz ribbons define a mylonitic foliation. Base: 2 mm. Crossed nicols.

(d) Well developed mylonitic foliation defined by elongated strain-free quartz grains and mica ribbons in micaceous quartzite ultramylonite. Note that in hand specimen the foliation has the appearance of slaty cleavage. Base: 2 mm. Crossed nicols. Location: 4 km south of Habban.

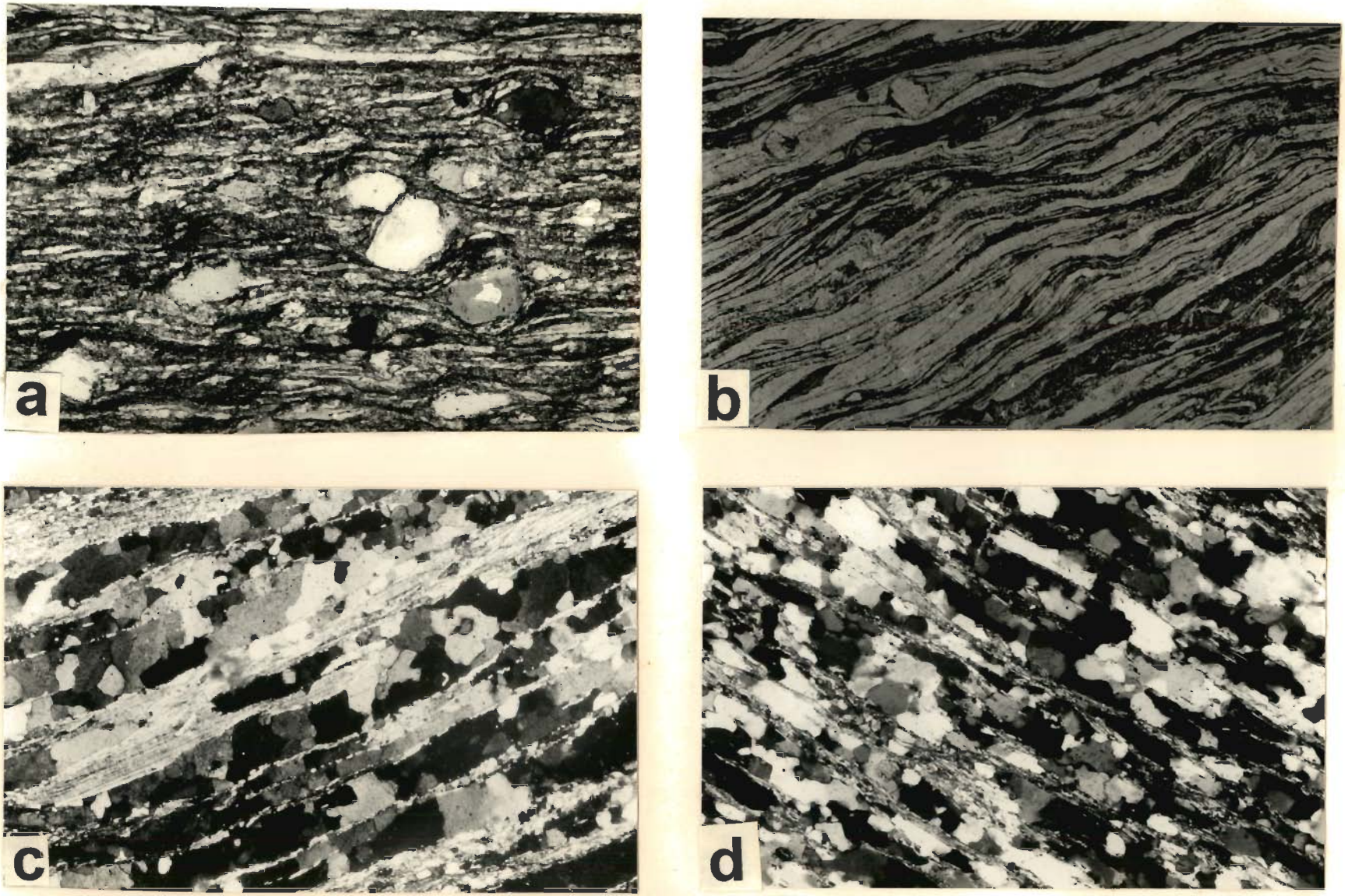

Fig. 3.10

FIGURE 3.11 MYLONITES

(a) Completely recrystallized quartzite ultramylonite. Note that the quartz grains are almost strain-free, polygonal and show triple-points. Base: 1.8 mm. Crossed nicols. Location: 2 km W of Phagu.

(b) Carbonaceous schist ultramylonite with well developed mylonitic foliation. Base: 5.2 mm. Crossed nicols. Location: 4 km south of Habban.

(c) Variation in the intensity of mylonitization in thin section scale as shown by variation in grain-size reduction and recrystallization. Base: 5.2 mm. Crossed nicols. Location: 3 Km NE of Phagu.

(d) S_1 cleavage traced by straight inclusion trails (carbonaceous matter) in relict feldspar porphyroclast in quartzite ultramylonite. The S_i (= S_1) is perpendicular to the S_e (=mylonitic foliation). Base: 0.45 mm. Crossed nicols. Location: 2 km W of Phagu.

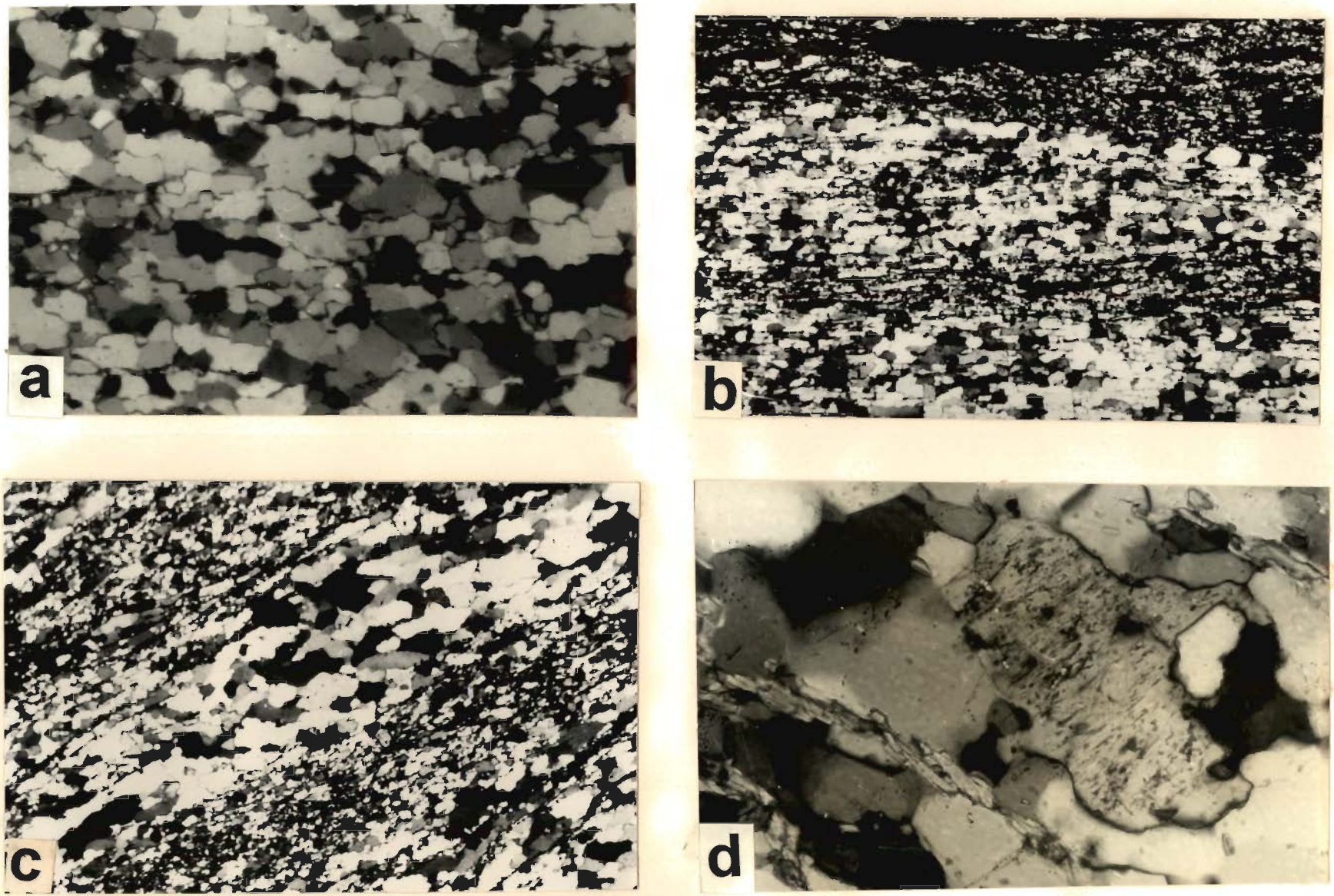

Fig. 3.11

FIGURE 3.12 S-C MYLONITE

(a) S-C structure in lower carbonaceous band. Looking N190°. Location: 2 km E of Kot.

(b) S-C structure in lower carbonaceous band in thin section scale. Note that the S-surfaces are defined by a mylonitic foliation which sigmoidally curve into C-surfaces along which no new fabric has developed. Base: 8 mm. Oblique nicols. Location: 1 km SE of Habban.

(c) S-C structure in quartz-mica schist. The S-surfaces, defined by a mylonitic foliation, asymptotically meet the C-surfaces which is marked by intense grain-size reduction. Base: 5.2 mm. Plane-polarized light. Location: 1 Km S of Bogdhar.

(d) Muscovite "fish" in granite define type-II S-C mylonite. The muscovite grain show strong undulose extinction whereas the quartz grains are recrystallized and relatively strain free. Base: 1 mm. Oblique nicols. Location: 3 Km E of Bagi.

Fig. 3.12

FIGURE 3.13 DEFORMATION OF LAYERS IN DUCTILE SHEAR ZONES

Schematic diagrams showing characteristic geometric features that can develop when layers with competency contrast are involved in ductile shearing. All the diagrams are for dextral shear zones. In sinistral shear zones the geometries will be mirror-image of the sketches shown.

(a) A section perpendicular to shear-zone wall and parallel to shear direction (adapted from Mukhopadhyay 1989, Fig. 4). α is the initial angle, measured counterclockwise, between the layer and the shear direction. If the α is high the layer (layer 3) will be in the zone of contraction and z-shaped (s-shaped in dextral shear zone) folds will develop. Pre-shear folds (layer 4) will get refolded. If the α is low the layers will lie in the zone of extension. The layers and early axial planes (layer 1) will get sigmoidally curved. Boudinage or pinch-and-swell structure will be given by layers with high competency contrast (layer 2). If α is zero (not shown) the layer will neither be elongated nor shortened.

(b) Development of sheath fold (adapted from Ramsay 1980; Ghosh 1986). Note that the α is low (i.e. the axial plane and the limbs are subparallel to the shear zone wall) and the hinge line with initial undulations is at high angle to the shear direction.

(c) Development of type-2 interference pattern (adapted from Ramsay 1967). Note that the α is high and the early hinge line is at low angle to the shear direction.

(d) Development of type-3 interference pattern (adapted from Ramsay 1967). Note that the α is high and the early hinge line is also at high angle to the shear direction.

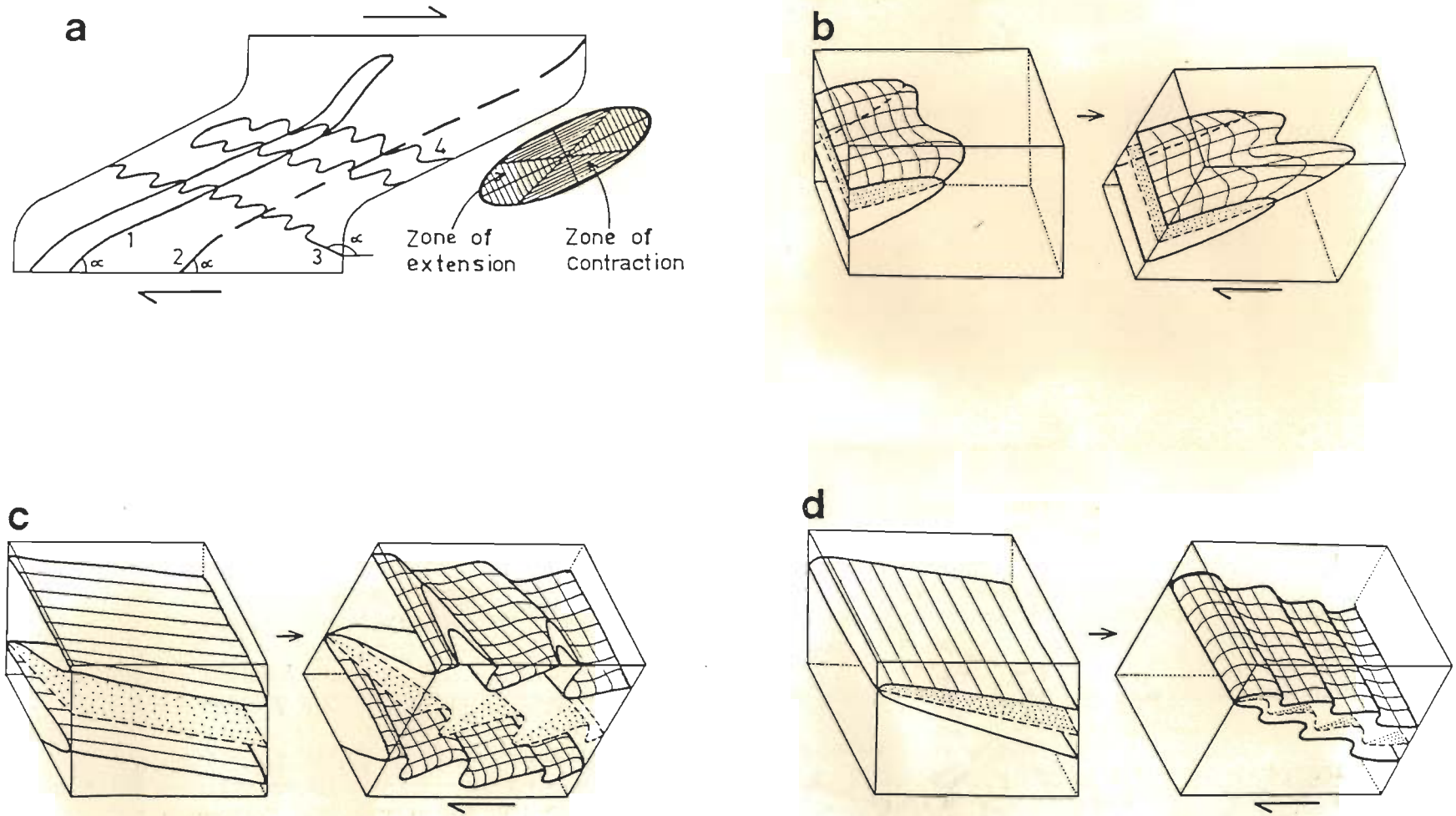

Fig. 3.13

FIGURE 3.14 SCHEMATIC MODELS FOR DEFORMATION OF CLEAVAGE SURFACES IN DUCTILE SHEAR ZONES (adapted from Dennis and Secor 1987, 1990)

(a) Cleavage surfaces with high α (Fig. 3.13a) are in the zone of contraction. Crenulation and crenulation cleavage may form.

(b) Cleavage surfaces with loω α (Fig. 3.13a) are in the zone of contraction. Extension crenulation or foliation boudinage may form.

(c) Cleavage surfaces subparallel to the shear zone wall (α approximately zero) are not deformed.

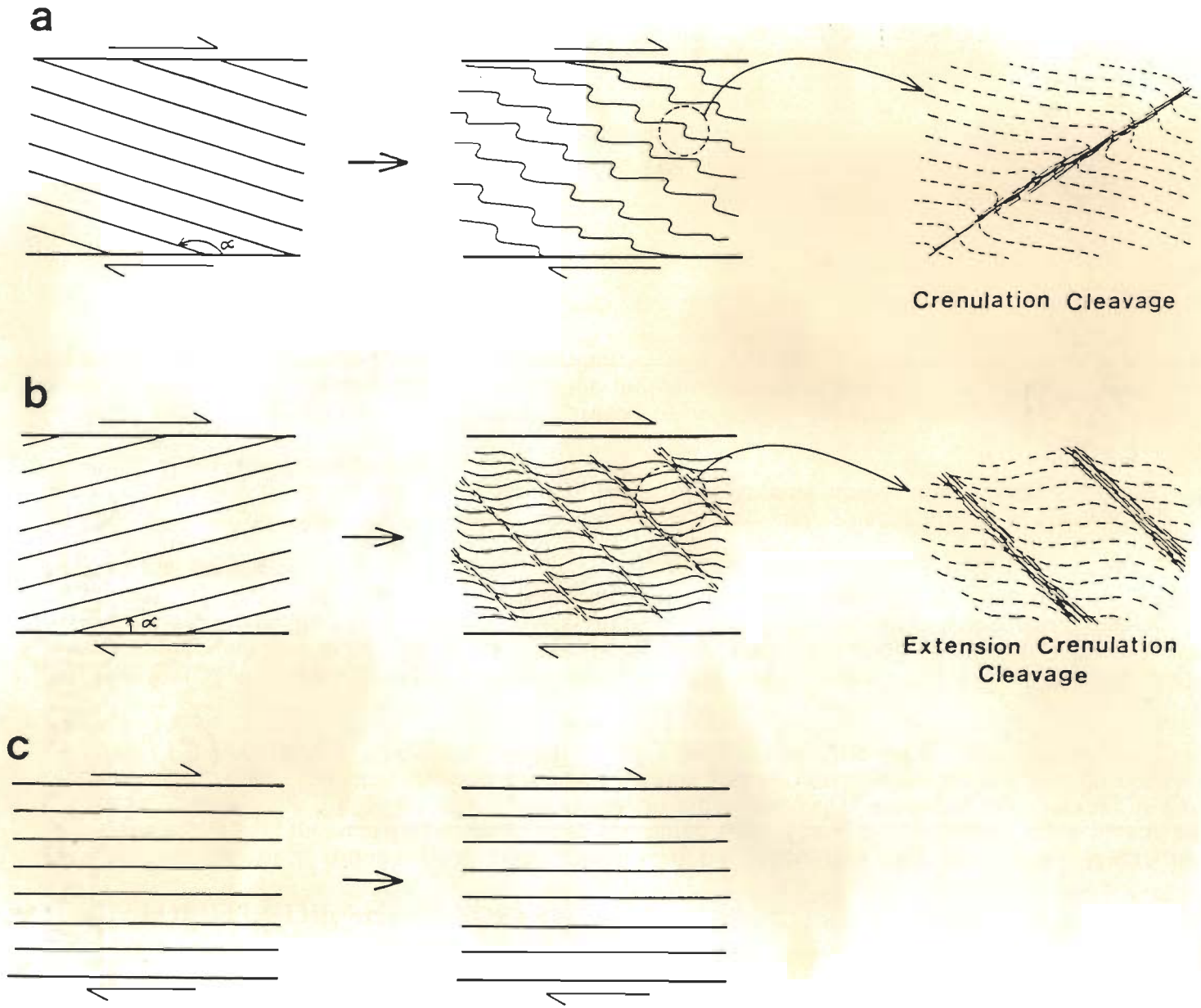
a
α
Crenulation Cleavage
b
α
Extension Crenulation
Cleavage
c

Fig. 3.14

FIGURE 3.15 FOLDS IN THE SHEAR ZONES

(a) Polished slab of a round-hinged tight fold traced by quartz-rich and carbon-rich layers in upper carbonaceous schist. the slab is cut oblique to the hinge line. The well-developed axial planar cleavage apparently suggests the fold to be of F_1 generation. In thin section it is seen that this cleavage is a discrete crenulation cleavage. Two thin sections prepared parallel and perpendicular to hinge line do not show any evidence of mylonitization. Therefore, this fold is F_2 caught up in the shear zone. Location: 2 km N of Rajgarh.

(b) The fold seen in this figure is exactly similar to the fold shown in (a) except that the rock is an ultramylonite with the axial planar cleavage being a mylonite foliation. Stretching lineation oriented parallel to the hinge line is given by quartz ribbons. Therefore, this fold has formed during shearing movement. An F_1 striping lineation perpendicular to the stretching lineation is noticeable. Location: 5 km NNE of Haripurdhar.

(c) Calcite veins showing isoclinal folds, boudinage structure and isolated hinges in calc-silicate rock in upper carbonaceous schist. Axial planar mylonitic foliation cuts across the hinges. Looking: N305°. Location: 1 km N of Haripurdhar.

(d) Very tight, gently-plunging inclined fold traced by mylonitic foliation in quartzite. The shape of the hinge varies along the axial plane. Note that the mylonitic foliation has the appearance of slaty cleavage. Looking: N36°. Location: 6 km N of Haripurdhar.

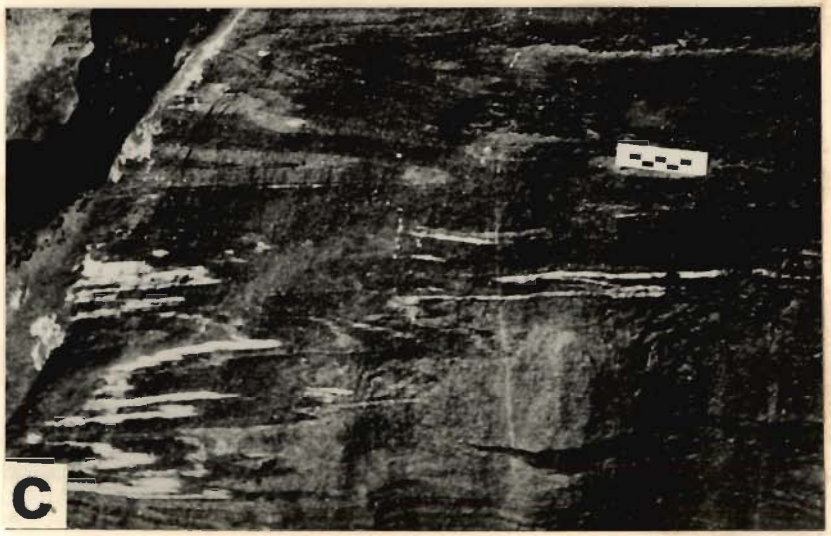

Fig. 3.15

FIGURE 3.16 CRENULATION AND CRENULATION CLEAVAGE IN SHEAR ZONES

(a) Asymmetric kinks on mylonitic foliation in mica schist at the contact with granite. Looking N60°. Location: 1.5 km E of Chogtali.

(b) Kink bands on mylonitic foliation in upper carbonaceous schist. Note kinked quartz ribbons at upper right and lower left. Base: 2 mm. Plain-polarized light. Location: 1.5 km NNW of Bharari.

(c) Round-hinged crenulation fold in upper carbonaceous schist. The alternate quartz-rich and mica-rich domains are differentiated layers developed during an earlier but unknown event of crenulation foliation formation. The differentiated layering *now* defines a mylonitic foliation. At the core of the fold a crenulated quartz ribbon is noticeable. Base: 5.2 mm. Plane-polarized light. Location: Haripurdhar.

(d) Discrete crenulation cleavage developed during shearing affecting S_1 cleavage in carbonaceous schist. In hand specimen the penetrative cleavage is parallel to the crenulation cleavage. Base: 1.8 mm. Plane-polarized light. Location: Kot.

Fig. 3.16

FIGURE 3.17 CRENULATION, CRENULATION CLEAVAGE AND FOLD INTERFERENCE IN SHEAR ZONES

(a) Mylonitic foliation in mica schist traced by quartz ribbons is asymmetrically crenulated. Base: 2 mm. Oblique nicols. Location: 4 km W of Didag.

(b) Very tight fold in mica schist traced by recrystallized quartz ribbons. Note that the hinge is thickened and limbs are thinned. Base: 5.2 mm. Oblique nicols. Location: Phagu.

(c) Discrete crenulation cleavage (left to right) with a relict earlier crenulation cleavage preserved within the Q-domain (microlithon) in mylonitized upper carbonaceous schist. Both the cleavages show differentiated layering. Note that in hand specimen and outcrop, only one cleavage surface, parallel to the crenulation cleavage oriented left-to-right could be recognized. Base: 2 mm. Plane-polarized light. Location: 5 km S of Phagu.

(d) Two isoclinal folds on mylonitic foliation having planar and similarly oriented (subvertical) axial planes show hinge-lines (parallel to pen and the black line) plunging in opposite directions suggesting sheath-fold geometry in carbonaceous schist. Location: Rajgarh.

Fig. 3.17

FIGURE 3.18 FOLD INTERFERENCE IN SHEAR ZONES

(a) Cross-sectional view of the tip of a sheath fold in upper carbonaceous schist. Looking N80°. Location: 2 km W of Dain.

(b) Hook-shaped (type-3) interference pattern in upper carbonaceous schist. The 'early' (not F_1) hinge is noticeable at right-central part of the photograph. As both the folds are isoclinal the two axial planes are parallel to each other except at the later hinge seen to the left-central part. Thin section of the early hinge show that the entire interference pattern is on a mylonitic foliation. Looking N75°. Location: 2 km NE of Haripurdhar.

(c) Photomicrograph of the hinge-zone of the early isoclinal fold in **(b)** above showing that the fold is traced by mylonitic foliation. Base: 5.2 mm. Slightly oblique nicols.

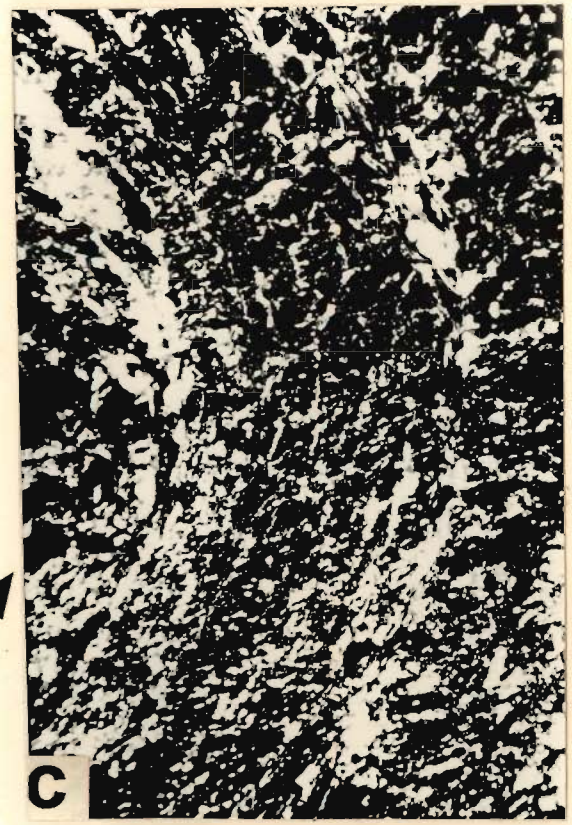

Fig. 3.18

FIGURE 3.19 FOLD INTERFERENCE IN SHEAR ZONES

(a) Refolded crenulations in mica schist giving type-3 interference pattern. The "early" (not F_1) hinge is noticeable at lower right. Bold and dashed lines are drawn along early and later axial planes respectively. Base: 8 mm. Plane-polarized light. Location: Chogtali.

(b) Isoclinally folded quartz ribbon in mica schist refolded into open folds giving type-3 interference pattern. Note crenulations in mica-rich portions with axial planes parallel to both the early (bold line) and later (dashed line) axial planes. Base: 5.2 mm. Crossed nicols. Location: Chogtali.

(c) Isoclinal fold traced by mylonitic foliation in carbonaceous schist with curved hinge line and folded axial plane across an open fold (with axial plane oriented from upper right to lower left) giving type-2 interference pattern. Sketches from colour transperancy. Location: Rajgarh.

(d) Early hinge-line folded around an open later fold in Lower carbonaceous schist. Sketches from colour transperancy. Location: 2 km NE of Kot.

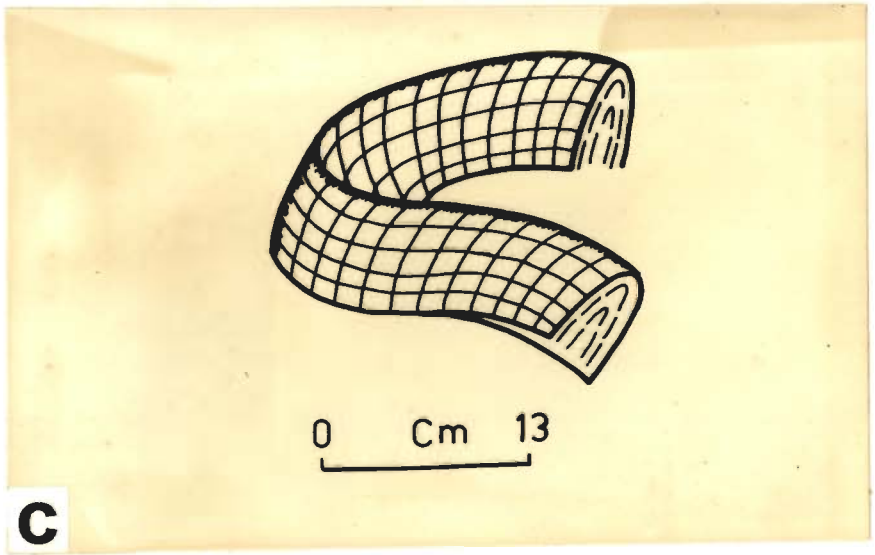

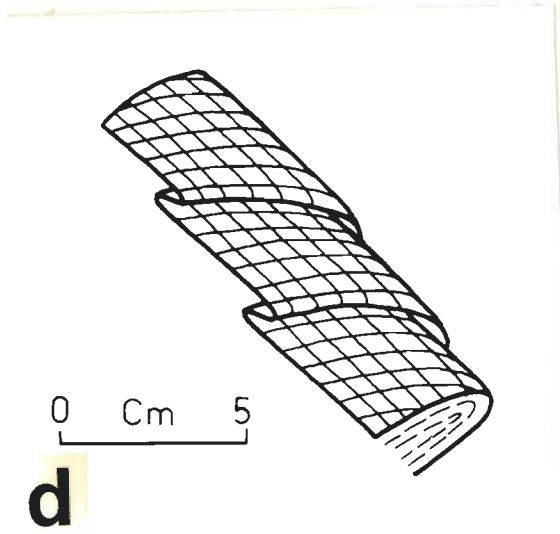

Fig. 3.19

FIGURE 3.20 SCHEMATIC DIAGRAMS SHOWING REPEATED CRENULATION CLEAVAGE FORMATION IN SHEAR ZONES

During progressive shear a pre-existing cleavage (i.e. S_1, S_2 or even a mylonitic foliation) is crenulated (**a**) and a zonal crenulation cleavage develops (**b**) leading to the formation of differentiated layering (**c**). The grain-size reduction via recrystallization and neomineralization leads to the formation of mylonite and mylonitic foliation. The quartz grains in the Q-domains may form ribbons (**c**), if favourably oriented. The differentiated crenulation cleavage (c), which is also a mylonitic foliation, is again crenulated (**d**) followed by formation of crenulation cleavage (**e**) and differentiated crenulation cleavage (**f**). In detail there could be many variations from these schematic diagrams. For example, quartz ribbons (**c,f**) may not form, the pre-existing cleavage may or may not be preserved within the differentiated layers in (**c**) and (**f**) or instead of forming discontinuous cleavage the fabric may be homogenized and a continuous cleavage may develop. Note that if earlier foliation is not preserved then stages (**c**) and (**f**) cannot be distinguished. Further, stages (**c**) to (**f**) may be repeated unknown number of times.

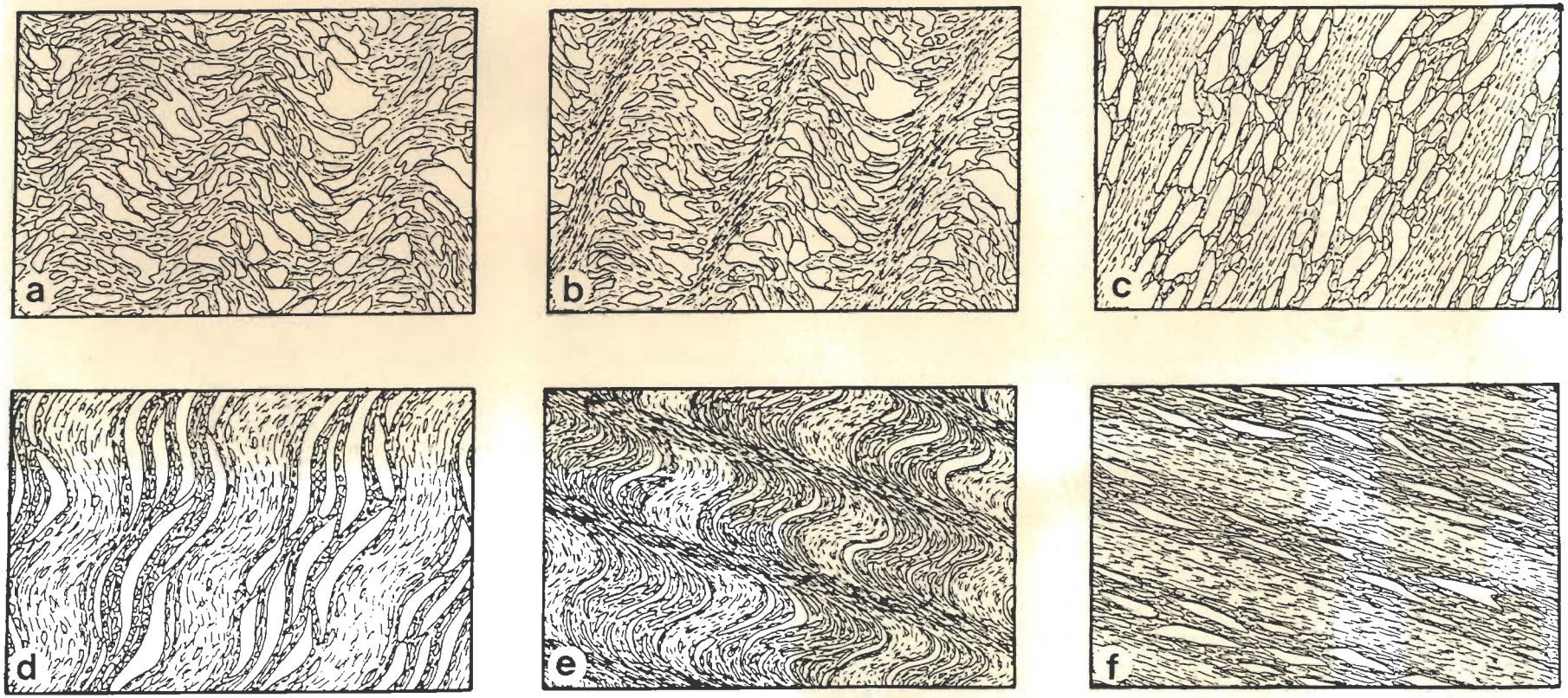

Fig. 3.20

FIGURE 3.21 FOLIATIONS IN SHEAR ZONES

(a) S_1 slaty cleavage in Chail phyllite involved in symmetric crenulations and formation of discrete crenulation cleavage. Unornamented grains are quartz. The crenulation cleavage is the penetrative cleavage in hand specimen. Base: 1.3 mm. Plane-polarized light. Location: Dalenu.

(b) Open to gentle crenulations affecting mylonitic foliation in upper carbonaceous schist. Base: 2 mm. Plane-polarized light. Location: Bharari.

(c) Mylonitic foliation in carbonaceous schist involved in isoclinal crenulations. An incipient crenulation cleavage parallel to the axial plane is noticeable. Base: 1.8 mm. Crossed nicols. Location: 3.5 km NNE of Boghdhar.

(d) Crenulation cleavage affecting a mylonitic foliation in a recrystallized ultramylonite in upper carbonaceous schist. Mylonitic foliation continues through both the cleavage domains and microlithon domains. This is an initial stage of formation of differentiated layering in a mylonite. Base: 2 mm. Oblique nicols. Location: 1 km S of Dain.

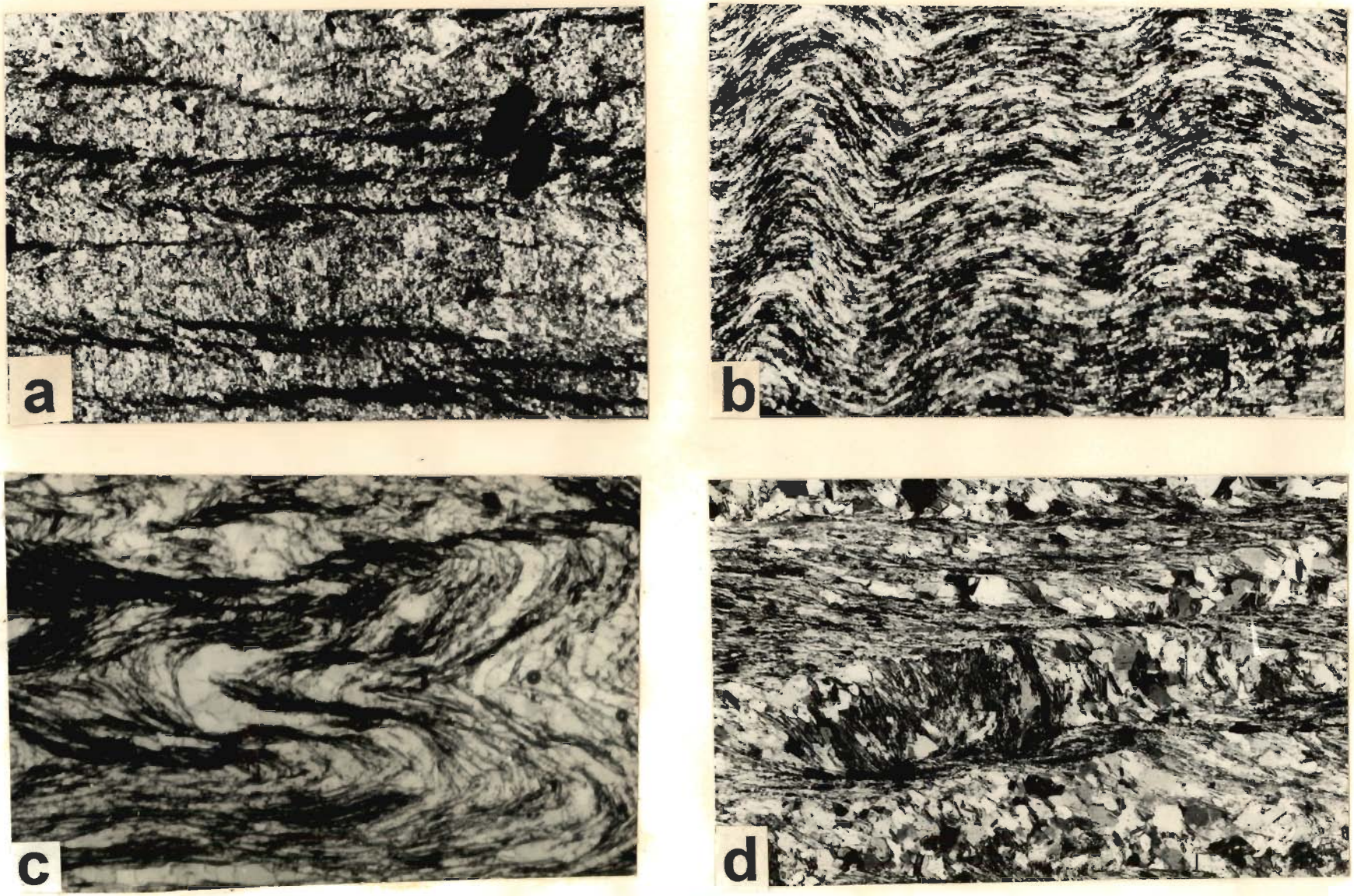

Fig. 3.21

FIGURE 3.22 FOLIATION IN SHEAR ZONES

(a) An early stage of development of differentiated crenulation cleavage in mylonitized lower carbonaceous schist. The crenulation cleavage is zonal with mylonitic foliation continuous through both Q- and M-domains. Base: 0.65 mm. Plane-polarized light. Location: Chandol.

(b) Alternate quartz-rich and sericite-rich layers giving differentiated cleavage in Chail phyllite. Note mylonitic foliation parallel to the layering. Base: 2 mm. Oblique nicols. Location: Bogdhar.

(c) Folds traced by differentiated crenulation cleavage which represents a mylonitic foliation. Crenulations and crenulation cleavage noticeable at the core of the fold. Base: 8 mm. Crossed nicols. Location: 4 km ENE of Habban.

(d) Carbon impregnated differentiated mica-rich layer sheared and disrupted giving mica "fish" structure in carbonaceous schist. Base: 1.8 mm. Crossed nicols. Location: 3.5 km NNE of Boghdhar.

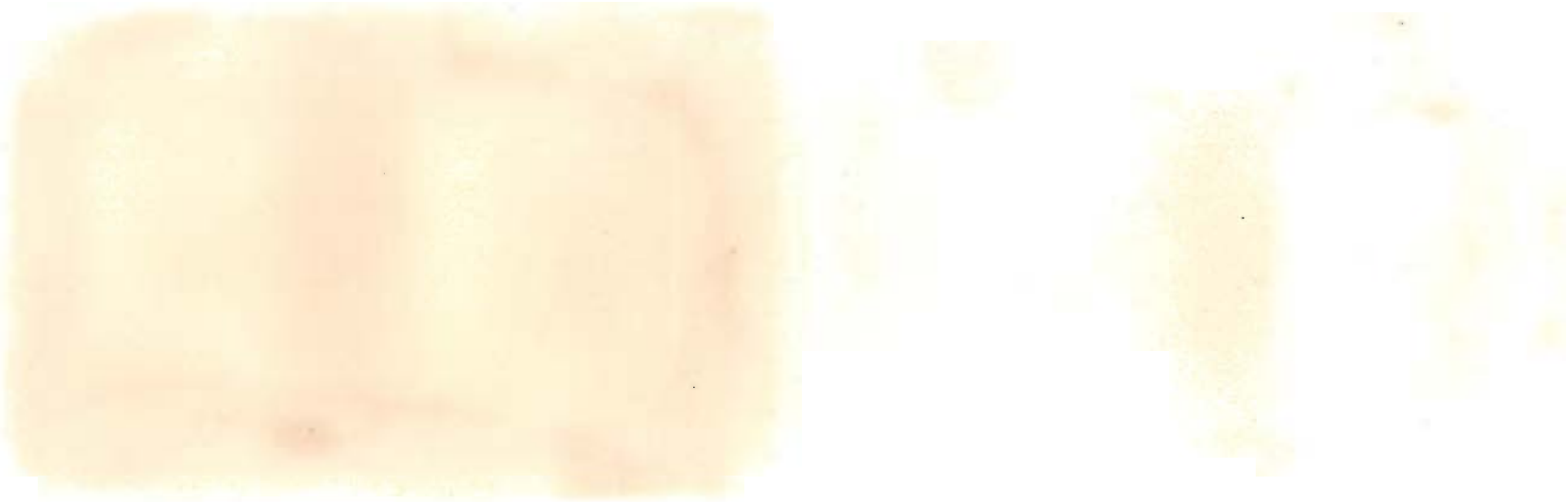

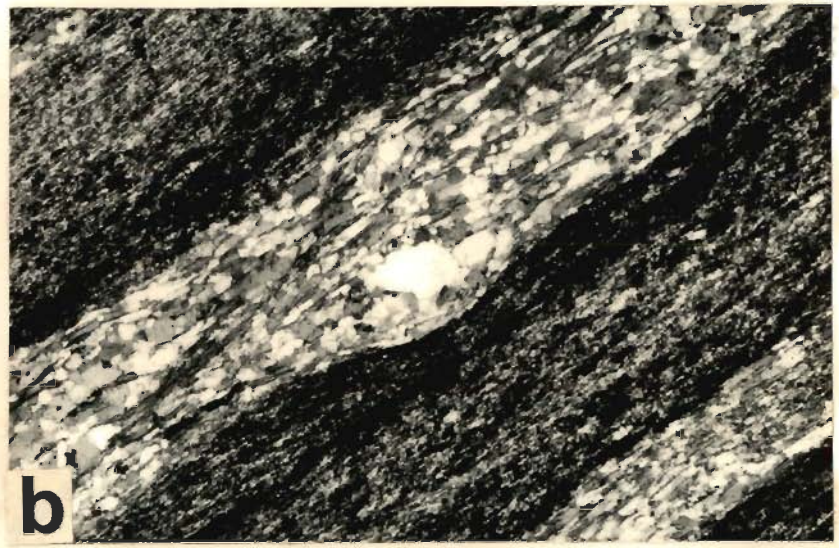

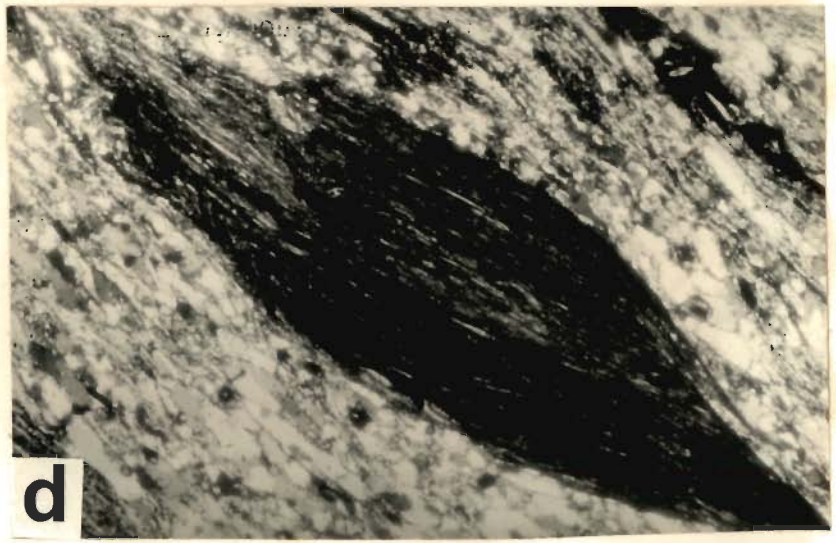

Fig. 3.22

FIGURE 3.23 EXTENSIONAL STRUCTURES IN SHEAR ZONES

(a) Extension crenulation cleavage (ecc) developed at high angle to the main foliation (dipping gently to the right) in Chail phyllite. The foliation along with boudinaged quartz veins are sigmoidally curved between two ecc surfaces. Looking N289°. Location: 3 km W of Kupvi.

(b) Conjugate extension crenulation cleavage affecting S_1 schistosity in amphibolite. Base: 8 mm. Oblique nicols. Location: 4 km W of Didag.

(c) A set of subparallel extension crenulation cleavage surfaces superposed on quartz-ribbon mylonite in upper carbonaceous schist. Base: 5.2 mm. Oblique nicols. Location: 2 km SW of Haripurdhar.

(d) Details of (c) above showing sigmoidally curved quartz ribbons within two subparallel extension crenulation cleavage surfaces. Oblique nicols. Base: 2 mm. Location: 2 km SW of Haripurdhar.

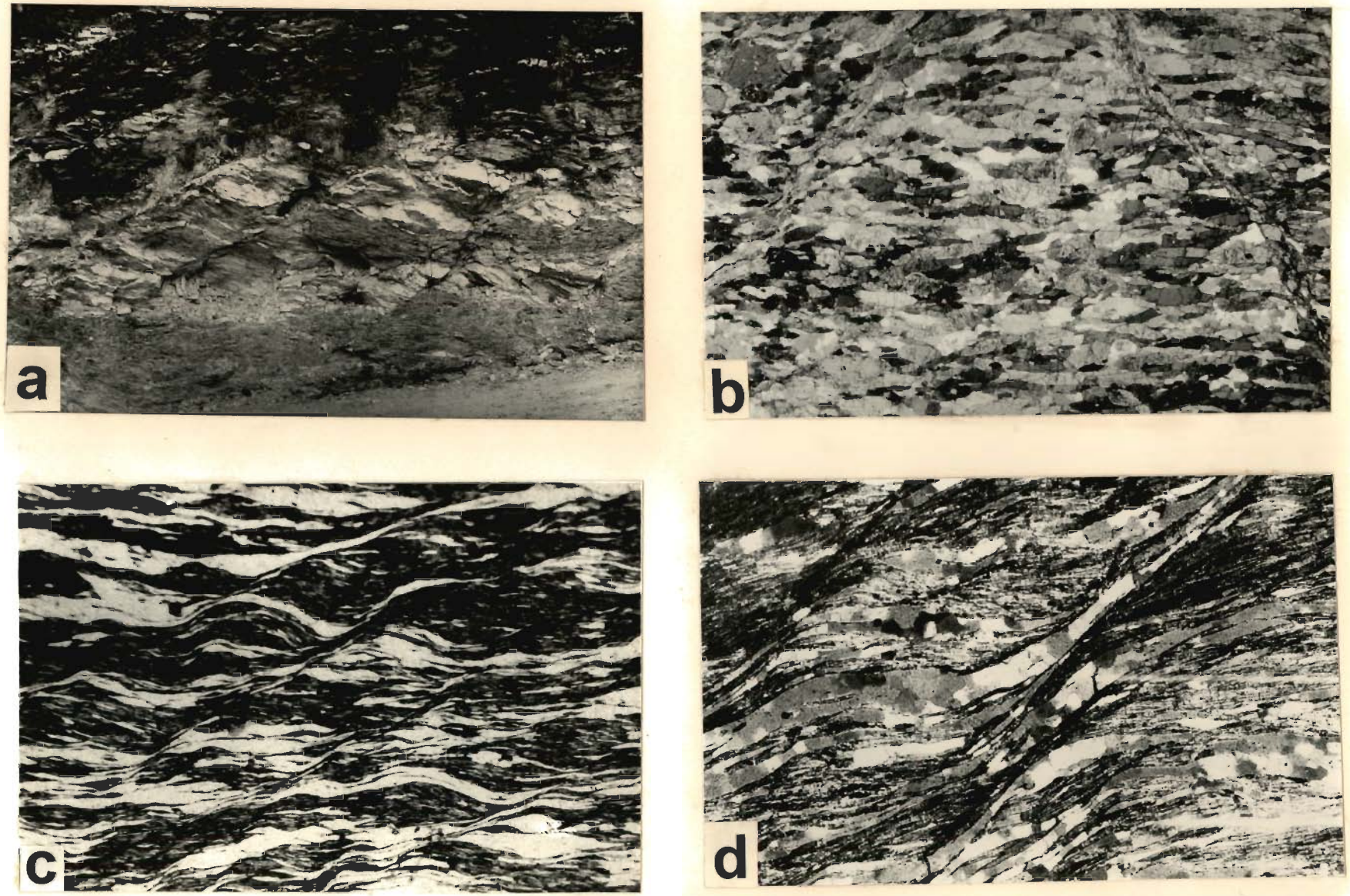

Fig. 3.23

FIGURE 3.24 EXTENSIONAL STRUCTURES IN SHEAR ZONES

(a) Symmetric foliation boudinage in quartz-mica schist. Foliation planes are symmetrically bent at the quartz filled fracture zone. Looking: N336°: Location: 0.5 km N of Phagu.

(b) Rotated boudins traced by quartz vein in the upper carbonaceous band. A shear foliation continues through the necking point. Location: 6 km NE of Rajgarh.

(c) Boudinaged garnet crystals aligned along the mylonitic foliation in mica schist. Note S- and C-surfaces. Base: 1.6 mm. Plane-polarized light. Location: 5 km ESE of Rajgarh.

(d) Extension fractures in clinozoisite(?) in carbonaceous schist. Base: 2 mm. Crossed nicols. Location: Bogdhar.

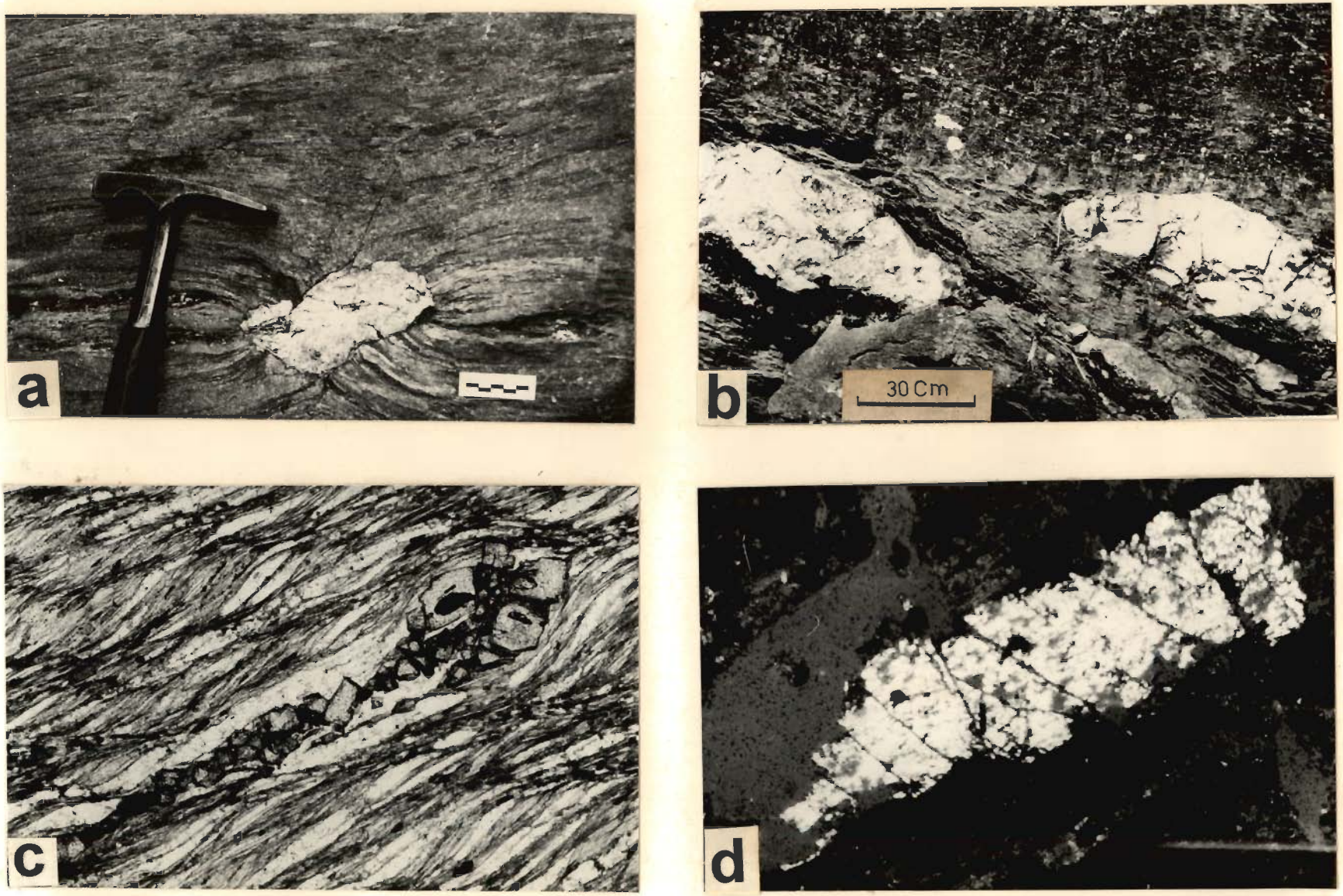

Fig. 3.24

FIGURE 3.25 LINEAR STRUCTURES IN SHEAR ZONES

(a) Stretching lineation on mylonitic foliation in quartzite. Note elliptical mica clots aligned parallel to lineation. Subhorizontal surface. Location: 3 km E of Rajgarh.

(b) Stretching lineation on mylonitic foliation defined by mica grains. Subhorizontal surface. Location: 5 Km SSW of Bagi.

(c) Hinge line of a recumbent fold on mylonitic foliation in Upper carbonaceous schist curved along with a stretching lineation. Note that the fold is plane-noncylindrical. Looking: N330°. Location: 3 km NW of Bagi.

(d) Strongly curved stretching lineation around the hinge of an open fold traced by mylonitic foliation in upper carbonaceous schist. Location: Rajgarh.

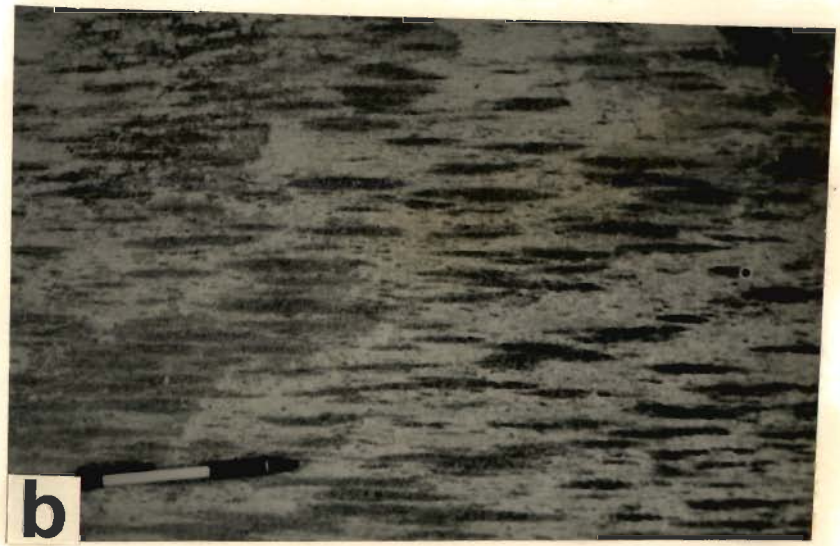

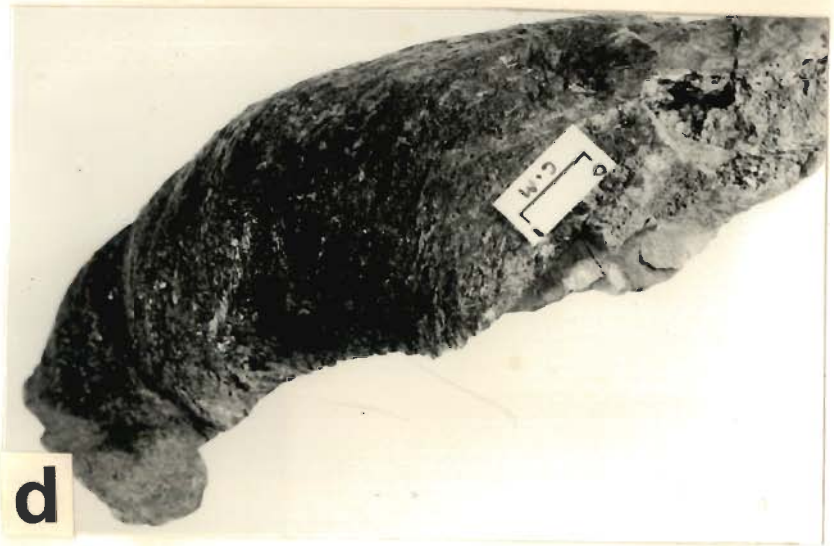

Fig. 3.25

FIGURE 3.26 SMALL-SCALE THRUSTS

(a) Small-scale thrust in quartzite underlying the upper carbonaceous band. In the hanging wall block mylonitic foliation is parallel to the thrust plane. The foliation in the foot wall block is steeply dipping to the left and is truncated by the thrust plane. Looking N60°. Location: 3 km S of Bhawai.

(b) Drag fold in the foot wall block of a small-scale thrust in quartzite. The gently dipping (to the left) foliation in the hanging wall block is parallel to the thrust plane. Note that the quartzite above the thrust is more massive. The exposure is at the lower contact of the upper carbonaceous band. Looking: N32°. Location: 4 km S of Rajgarh.

(c) Thrust imbrication in outcrop scale in quartzite at the contact with upper carbonaceous schist The more prominent thrust planes have been emphasized. Looking N38° Location: Churwadhar

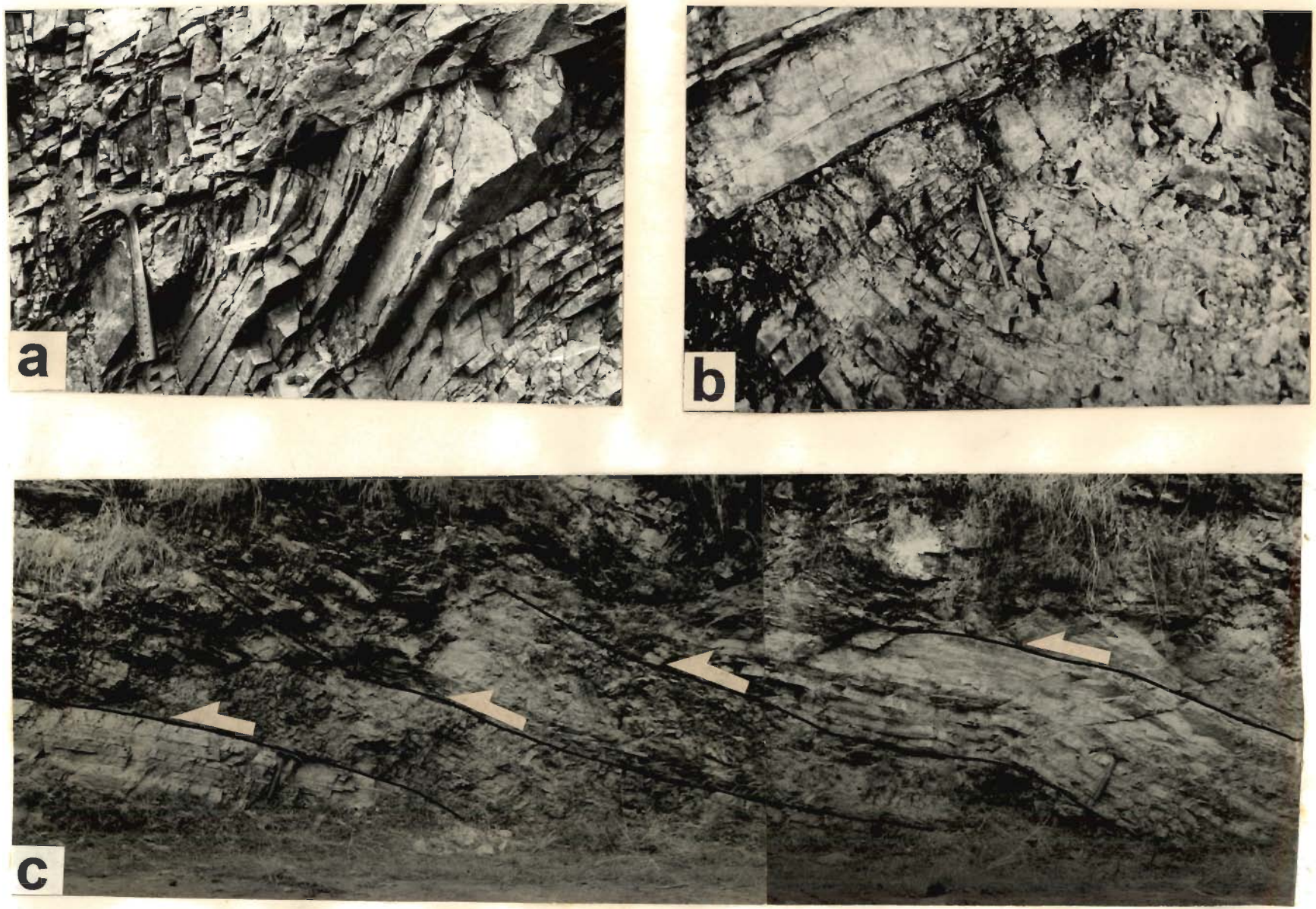

Fig. 3.26

FIGURE 3.27 LATE STRUCTURES

(a) F_3 warp traced by quartzite layer in mica schist. Looking: N36°. Location: 3 km NE of Churwadhar.

(b) Closely spaced subvertical fractures cutting across gently-dipping mylonitic foliation and small-scale thrust in quartzite. Looking: N95°. Location: 4 Km ESE of Nohra.

(c) Conjugate late fractures in upper carbonaceous schist. The fracture dipping to the right has a small amount of normal displacement. Looking: N28°. Location: 5 km SSW of Haripurdhar.

(d) Normal sense of displacement along steeply dipping fault planes in amphibolite occurring within mica schist. Looking: N290°. Location: 2 km W of Didag.

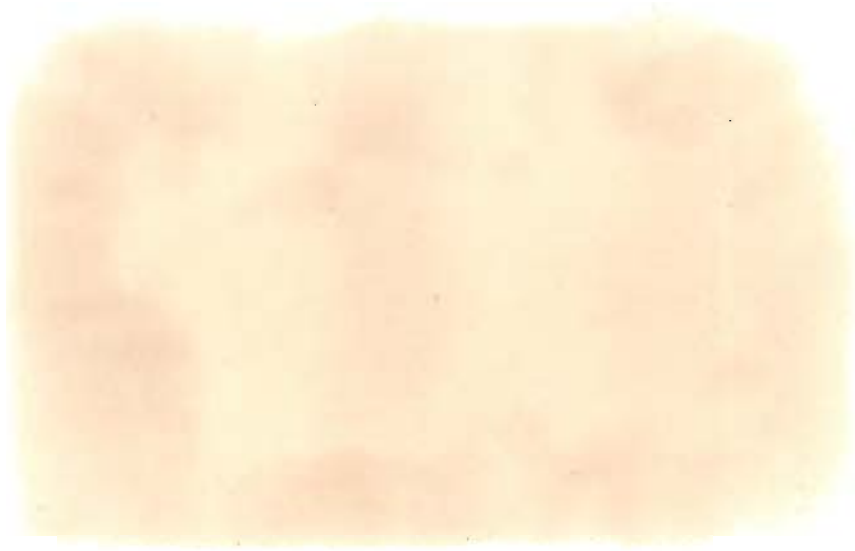

Fig. 3.27

CHAPTER - 4
LARGE-SCALE STRUCTURES

4.1 A LIMITATION

The standard methods of structural analyses in an area with polyphase folding are very well known (Turner & Weiss 1963) and have been applied successfully in many deformed terrains from all the world over (see Hobbs *et al.* 1976, p.407-432). These methods essentially involve stereographic analyses of structural elements, such as axial planes of folds, foliation surfaces, fold axes and other linear structures of different generations. The spatial variation in orientation of small-scale structures together with map pattern is often used to decipher the geometry of large-scale structures.

The traditional methods of structural analyses are, however, difficult to apply in the present area. In chapter-3 it has been shown that two generations of early folding (F_1-F_2) and related structures have been overprinted by the structures developed during a progressive ductile shearing. A late stage folding (F_3) has affected all the structures developed earlier. The most serious difficulty found during the fieldwork is that the cleavage surfaces of different generations are indistinguishable from each other in a large number of outcrops. For example, in many cases S_1 slaty cleavage and mylonitic foliation have the same appearance in outcrops. This caused a serious limitation because if the cleavage surfaces of different generations cannot be discriminated in an outcrop then the folds of different generations cannot be distinguished from each other. This problem is most severe particularly in the intensely sheared rocks. Thus only in thin sections distinctions among structures of different generations are possible. But obviously it was not possible to collect samples (and make thin sections) from thousands of outcrops where orientation data were taken.

In spite of these limitations, however, in some of the outcrops small-scale early folds could unambiguously classified into different generations (F_1-F_2) based on overprinting relations.

4.2 THE MAP PATTERN

The map pattern of an area becomes meaningful only when the variation of the lithological contacts is considered together with the variation in the topography. The highest elevations in this area is around the Chur peak from where the topographic surface slopes away in all directions giving an inverted bowl type of topography. This is clearly shown by the drainage pattern and the topographic contours in Fig. 4.1. Except in the northeastern part of the area, the map patterns of all the lithological units are approximately semicircular about the Chur peak. Each rock type is also more or less restricted to a particular altitude. In detail there are many 'V's pointing upslopes and downslopes along valleys and spurs respectively. In the northcentral part there is a closed outcrop of upper carbonaceous band around a ridge and detached from the main exposure at the present topographic level. From the area around the Chur peak a ridge extends in the northeasterly direction and the Jutogh/Chail rocks open out instead of closing giving rise to the half-klippe type of outcrop pattern (see Fig. 5.2). A cursory examination of the map pattern apparently suggests flat-lying or gently dipping and homoclinal rock sequence with a normal startigraphy in this area (Srikantia & Bhargava 1988). This suggestion is further strengthened by the subhorizontal or gentle dips of *s*-surfaces in a majority of the exposures.

A closer scrutiny, however, reveals that the subhorizontal *s*-surfaces are invariably penetrative cleavage surfaces of deformational origin. They are also axial planar to isoclinal folds with long drawn-out and extremely attenuated limbs. Further, several generations of small-scale folds with varying style, geometry and orientations are very common. The superposed fold geometries can be demonstrated from thin section to outcrop scales. Finally successive generations of structures developed during

ductile shearing can be easily documented. Since the small-scale structures mimic the large-scale structures the simple outcrop pattern and the sub-horizontal to gently dipping rock sequences conceal a very complex large-scale structural geometry in this area.

4.3 REGIONAL VARIATION IN THE ORIENTATION OF *S* PLANES

The most dominant *s*-surface in the area are the axial planar cleavage of the first generation (S_1) along with the crenulation cleavage/mylonitic foliations (S_m) developed repeatedly during a progressive ductile shearing. A crenulation cleavage of the second generation (S_2) is sporadically developed. In many outcrops it is impossible to decide whether the penetrative cleavage is S_1- or S_m-surface. Also it may not be possible to disinguish between a crenulation cleavage of the second generation and a crenulation cleavage developed during shearing. For this reason all the penetrative *s*-surfaces have been grouped together as "foliations" and plotted with the same symbol on the structural map (Fig. 4.2). The term "foliation" has been used as a non-genetic term that include any penetrative s-surface of any generation in a particular outcrop. Similarly all the linear structures have also been grouped together and plotted with the same symbol in Fig. 4.2.

Fig. 4.2 shows that the dip amounts of the dominant foliations are gentle to moderate. The synoptic stereogram of all the foliation planes gives a well defined point maximum (Fig. 4.3a). The modal foliation plane has a dip of 10°/N59°. The synoptic stereogram of all the linear structures also show a point maximum corresponding to a plunge of 10°/N57° (Fig. 4.3b). This stereogram suggests that in large scale there is a recumbent or low-plunging reclined fold with NE-SW axial trend of axes. The spread in the orientations of the foliations and lineations (Fig. 4.3) could be an effect of F_3 folding.

A closer scrutiny of Fig. 4.2 shows that the foliations in the eastern part dip gently to the west whereas the foliations in the western part dip gently to the east.

Similarly in the southern part the foliations dip towards north and the foliations in the northern part dip towards south. Only in the area between Nohra and Chauras (south of the Chur peak) there are some steeply dipping foliation planes. Therefore, the area was subdivided into five subareas on the basis of homogeneity with respect to the orientations of the foliations. Stereographic plots of the foliations and the lineations for all five subareas are given in Fig. 4.4.

The foliations and lineations in subareas 1,2,4 and 5 show point maxima (Fig. 4.4). The modal foliation planes in these subareas have gentle dips (11° to 21°). But the dip directions vary from N93° in subarea 1, through N314° and N14° in subarea 2 and 4 respectively, to N80° in subarea 5. The lineations also show point maxima and they have gentle northeasterly or southwesterly plunge. Moreover, the modal foliation planes always pass through the point maximum of the lineations. Therefore the foliation and lineation data suggest recumbent or gently plunging reclined/inclined folds in the scale of individual subarea. Further, the variation in the orientation of the modal foliation planes in subareas 1, 2, 4 and 5 suggests an overall basin type of structure.

Only in the subarea 3 the foliations are distributed along a well-defined girdle around a ß axis plunging 16°/N105° (Fig. 4.4c). The lineations plunge gently to the east (20°/N93°). This suggest an open folding of the foliation planes. However, the maximum on the girdle corresponding to a gently dipping (16°/N90°) modal foliation suggests that the axial plane of the open fold is subhorizontal or gently dipping. This is further corroborated by the fact that in this subarea a number of open folds on subhorizontal axial planes have been observed. These folds with wavelengths several tens of meters have been observed on steep hill slopes where measurements on axial planes and axes could not be taken. These folds are not F_3 which are mostly upright. As will be shown in chapter 5, the contact between the Chur granite and the Jutogh metasedimentary rocks is a thrust. These open folds are probably related to thrusting.

4.4 REGIONAL VARIATION IN THE ORIENTATION OF AXES AND AXIAL PLANES OF FOLDS

The orientations of axial planes and axes of mesoscopic folds are show in Fig. 4.5. In some of the exposures where early folds are traced by S_0 surfaces, neither any axial plane cleavage nor any overprinting relationship was observed. At such places whether an early fold belongs to F_1 or F_2 generation could not be unambiguously determined. Further, as discussed in section 3.3.2, in shear zones and specially in the carbonaceous bands it is virtually impossible in many instances to distinguish between early folds (F_1-F_2) and the successive generations of folds developed during progressive shearing. Owing to this serious limitation, the axial planes and axes of all the folds of the area have been plotted with the same symbols in Fig. 4.5. The axial planes and axes of folds in general have similar orientations as that of the foliations and lineations (compare Fig. 4.2 with Fig. 4.5). This is to be expected since most of the cleavage surfaces in the area are axial planar in nature.

4.4.1 Early folds

The F_1 and F_2 folds are coaxial in most of the instances and, therefore, the axes of early folds have been grouped together. The axes of most of the early folds have gentle easterly plunge (Fig. 4.6a). There is, however, a significant amount of spread from the maximum orientation. This is due to two reasons: (i) the F_1 and F_2 folds are not strictly coaxial everywhere resulting in some spread in the orientation of the F_1 fold axes and (ii) this primary spread has been accentuated by superposition of later folds. However, on some outcrops the F_1 and F_2 folds can be distinguished on the basis of overprinting relationships. The orientations of F_1 and F_2 axial planes from such outcrops are depicted in Fig. 4.6b-d. The poles to the axial planes of F_1 folds define a partial girdle around a ß axis plunging 14°/N85° (Fig. 4.6b). Since the ß axis coincides with the maximum of the early axes (Fig. 4.6a) the partial girdle is due to F_2 folding. A well-defined point maximum (dip 13°/N70°) within the partial girdle (Fig. 4.6b) indicates that the axial planes of large-scale F_1 as well as F_2 folds are gently dipping

and that both these folds are very tight to isoclinal. This is further corroborated by a point maximum of the F_2 axial planes (Fig. 4.6c) which corresponds to a modal F_2 axial planes having 21° dip towards N54°. Since the axial planes of both the early folds have similar orientations (Fig. 4.6b,c) they have also been plotted together in the stereogram (Fig. 4.6d). The combined stereogram also defines a point maximum that gives a gently dipping (20°/N59°) modal early axial plane.

From the foregoing discussion we can conclude that the early folds in large scale vary from tight to isoclinal, recumbent to gently plunging reclined/inclined with gentle plunge towards west. Based exclusively on the argument of repetition of beds Pilgrim and West (1928) suggested that the two carbonaceous schist bands represent two limbs of a huge recumbent fold, a postulate upheld by later workers (e.g. Kanwar & Singh 1979). As will be shown later (section 4.5) this interpretation is not correct. A discontinuous marble band occurs at two different topographic levels within the Jutogh mica schist between Nohra and Haripurdhar (see Fig. 2.2). This marble probably traces a large-scale isoclinal recumbent fold with the hinge exposed in between Ruinsdhar and Haripurdhar. In this sector the foliation (Fig. 4.2) as well as axial planes of folds (Fig. 4.5) turn around along with the marble band suggesting that this fold is of later (i.e. F_2) generation. Owing to extremely rugged topography detailed mapping could not be carried out. Except for this probable F_2 fold no other large-scale early fold could be demonstrated.

4.4.2 Folds in shear zones

As mentioned earlier the two carbonaceous schist bands are the most intensely sheared rocks of the area. The axial planes of the folds in these rocks mostly have gentle dips but there is a wide scatter (Fig. 4.7a). The hinge lines of these folds in general have gentle plunge but the variation in trend is extreme (Fig. 4.7a). In a ductile shear zone, with increasing shear strain the axial planes of folds should become subparallel to the plane of shear and the hinge lines should rotate towards the shear

direction (Ramsay & Graham 1970; Ramsay 1980; Ramsay & Huber 1983). The variation in the orientation of axial planes and hinge lines of folds as seen in Fig. 4.7b is therefore rather baffling.

In order to check if these bewildering variation is spatial three small sectors were chosen viz., the lower carbonaceous band near Kot, the upper carbonaceous band north of Bogdhar and both the bands near Haripurdhar (Fig. 4.7, inset) and the data on axial planes and hinge lines were plotted in separate stereograms (Figs. 4.7b-d). In all the three sectors the axial planes have dominantly gentle dips but the poorly defined modal axial planes have different dip directions. The trends of the gently-plunging fold axes show large variations (upto about 180°). Most interestingly the hinge lines are distributed about the modal axial planes in the three sectors suggesting approximately planar axial planes with variably oriented hinge lines. This is a typical geometry of a sheath fold where hinge line curves on a planar axial plane. This is further corroborated by the presence of sheath folds in small scales. The "limbs" of "hinge-line folds" tend to become parallel and consequently scatter in the hinge line should decrease with increase in shear strain. The amount of scatter in the orientations of fold axes apparently suggests low shear strain during ductile shearing.

In a simple shear the pre-existing cleavage surfaces lying in the zone of contractions are crenulated. Dennis & Secor (1987, 1990) have shown that the hinge lines of the crenulations may be perpendicular, parallel or oblique to the shear direction. Once formed the hinge lines should rotate towards the shear direction. Further, during progressive shear successive generations of folds have developed (section 3.3.3). Consequently the early formed folds in the shear zones must have rotated more than the later formed folds. Finally, folds of the early (F_1 and F_2) generations with variable orientation of hinge lines (Fig. 4.6a) have also been caught up and modified in the shear zones. The extreme scatter in the orientations of hinge lines, as seen in Fig. 4.7a is a combined manifestation of these factors.

4.5 THE RAJGARH AREA

The map pattern of the area as a whole is rather simple with outcrops of different rock types more or less restricted to specific topographic levels. In particular the two carbonaceous bands occurring at two topographic levels maintain their separate and flat-lying identities throughout the area. However, in the western part around Rajgarh the two carbonaceous bands come very close to each other and the map pattern is very complex. Detailed mapping in this area (Figs. 4.8, 4.9) brings out the following facts:

(1) The topography in the southern part of Fig. 4.8 is such that the upper carbonaceous band should have turned around north of Jon. The upper contact of the upper carbonaceous band (i.e. with the mica schist) precisely does the same. The lower contact (i.e. with the quartzite), on the other hand, suddenly opens out towards north and after following a tortuous course around Rajgarh returns near Jon and then follows eastward. In this sector the upper carbonaceous band is both underlain and overlain by the quartzite. Also only in this area the upper carbonaceous band comes directly in contact with Chail Formation.

(2) The lower and the upper carbonaceous bands are not physically connected as can be clearly seen in the southwestern part near Dharoti and in the northern part near Thaina. In these two areas the lower carbonaceous band terminates against quartzite and Chail phyllites and the three different rock types occur together.

(3) In the rest of the area the upper carbonaceous band is overlain and underlain by the mica schist and quartzite of the Jutogh Group respectively. But around Rajgarh the same band is overlain by the Jutogh quartzite and underlain by the Chail phyllites.

(4) As is clearly indicated by the drainage pattern in the central part of Fig. 4.8 the upper carbonaceous band is repeated along the same topographic slope. The lower carbonaceous band, on the other hand, maintains its simple map pattern.

(5) Around Rajgarh the cleavage surfaces at most of the outcrops have gentle dips (Fig. 4.8). The stereographic plot shows that the cleavage surfaces are distributed along a partial girdle around a β axis plunging 6°/N22° (Fig. 4.10a). The lineations plunge at low angle to NE or SW. The lineation maximum (10°/N52°) is oblique (about 30°) to the β axis. The modal cleavage surface, dipping 16°/N86° contains both the β axis and the lineation maximum (Fig. 4.10a).

(6) The axial planes of small-scale folds have gentle dips in variable directions (Fig. 4.9). Stereographic plot (Fig. 4.10b) show a point maximum with gentle easterly dipping modal axial plane although a crude partial girdle around a gentle easterly plunging β axis may be considered. The gently plunging hinge lines of small-scale folds, however, show extreme variation in trend.

The above observations show that the Rajgarh area cannot locate the hinge zone of a large isoclinal recumbent fold whose two limbs are supposedly represented by the two carbonaceous bands (Pilgrim & West 1928; Kanwar & Singh 1979). In fact the two carbonaceous bands are not physically connected and therefore have separate identities. Further, the lower carbonaceous band maintains its flat lying attitude without any exception. Whereas the upper carbonaceous band around Rajgarh has a very tortuous map pattern suggesting a complex structural geometry. Consequently, there must be a structural discordance between the two carbonaceous bands at least in the Rajgarh area.

The repetition of the gently dipping upper carbonaceous band along the same hill slope (as shown by the drainage pattern east of Thaina, Fig. 4.8) suggests folding in the scale of the map involving this band only. Since most of the cleavage surfaces and axial planes of folds are subhorizontal (Figs. 4.8, 4.9, 4.10) the large-scale folds must be isoclinal and recumbent or gently-plunging inclined/reclined. The extreme variation in trend of the gently-plunging axes of small-scale folds (Fig. 4.10b) prove that the fold are non-cylindrical from small to large scales. It can, therefore, be concluded that large-scale folds are plane but non-cylindrical suggesting sheath fold geometry. The β

axis in Fig. 4.10a probably corresponds to F_3 warps in map scale.

Interestingly, most of the cleavage surfaces in this sector are on mylonitic foliation, as seen in a large number of thin sections. The large-scale folds, then, are on mylonitic foliation and the folding must be related to the ductile shearing. Two points need to be emphasized here: (1) the large-scale folding in the Rajgarh area affect the upper carbonaceous band but the lower carbonaceous band maintains its flat lying attitude, (2) This folding is not related to early, i.e. F_1 or F_2, deformation episodes but developed during later ductile shearing.

In order to depict large-scale structures, cross sections perpendicular and parallel to the fold axis are usually drawn. Since the folds in the Rajgarh area are non-cylindrical, a series of sections in different orientations were drawn. Two of them, approximately perpendicular to each other are shown in Fig. 4.11. The approximately E-W cross section (Fig. 4.11a) show that the upper carbonaceous band along with the quartzite are involved in refolded isoclinal recumbent folding. The abnormally huge thickness of the carbonaceous band near Rajgarh is due to fold involution in large-scale. The structural discordance between the two carbonaceous bands is also very clearly seen in this section. The NNE-SSW cross section (Fig. 4.11b) show an isolated band of the upper carbonaceous band which represents the lower limb of the isoclinal recumbent fold. But interestingly the two terminations of this isolated carbonaceous band are hinges which are at high angle to the cross section. This large scale folding does not affect the lower carbonaceous band.

From a series of cross sections in different directions a schematic three-dimensional diagram depicting the large-scale structure has been constructed (Fig. 4.12). Fig. 4.12 shows non-cylindrical refolded fold with sheath like geometry affecting the upper carbonaceous band and the quartzite unit. This explains the small closed outcrop of the quartzite within upper carbonaceous band west of Rajgarh (Fig. 4.8). An appropriate cross sections perpendicular to the front face of Fig. 4.12 an

isolated layer of the upper carbonaceous band may appear as in Fig. 4.11b.

Interestingly, in the Simla klippe Naha and Ray (1971b) have shown that the lower carbonaceous band and the quartzite are involved in large-scale refolded isoclinal fold. However, they consider these structures are to be of earliest generation. In the Simla area the Jutogh Group is represented by the lower carbonaceous band and the quartzite. The rest of the rocks have been removed by erosion. It is possible that the large-scale fold traced by Naha and Ray (1971b) is on mylonitic foliation and is akin to the large-scale fold affecting the upper carbonaceous band around Rajgarh.

Finally, the other possibility may be considered that the two carbonaceous bands indeed represent two limbs of a huge F_1 recumbent fold with the lower limb torned asunder during ductile shearing and the thrusting may be considered. Although this possibility cannot be ruled out, it is unlikely for two reasons: (1) In this event mica schist should appear below the lower carbonaceous band (i.e. the lower limb) at least at some places. But in Simla-Chur peak area the lower carbonaceous band is underlain by the rocks of the Chail Formations without any exceptions. (2) At the hinge of an F_1 recumbent fold the S_0 surfaces should be vertical with sub-horizontal axial planar cleavage. However, no such unambiguous relationship has been observed.

4.6 LARGE-SCALE THRUSTING

In the Simla-Chur peak area Pilgrim and West (1928) recognized two thrusts, viz., the Chail thrust and the Jutogh thrust (see Fig. 2.1) on the basis of an assumed stratigraphic sequence. The Chail thrust separates the low-grade metamorphic rocks of the Chail Formation from the underlying sedimentary rocks of the LHZ. The Chail Formation in turn is separated from the overlying medium grade rocks of the Jutogh Group by the Jutogh thrust. These two thrust sheets, viz., the Jutogh thrust sheet and the Chail thrust sheet, have subsequently been recognized and mapped in much of the western Himalaya. A plethora of local names have been given to these two thrust sheets by different workers working in different sectors of the western Himalaya. The Jutogh

thrust was considered by Gansser (1964) to be a continuation of the MCT as defined by Heim & Gansser (1939) in the Kumaun Himalaya.

The extension of the Chail thrust sheet northward from the Simla-Chur peak area has been shown by Virdi (1979, 1981). The Chail thrust is not studied in detail here but a critical cross checking of the evidence given by the previous workers supports the presence of the Chail thrust.

In addition to the Jutogh thrust, well-established elsewhere, two new thrusts, viz., the Rajgarh thrust and the Chur thrust, have been recognized in the Jutogh Group (Fig. 4.13). The Jutogh thrust is marked by the lower carbonaceous schists band as was originally suggested by Pilgrim & West (1928). The upper carbonaceous schist band marks the Rajgarh thrust and the contact between the Chur granite and the Jutogh mica schists marks the Chur thrust. Of these the Chur thrust has a much greater regional significance and therefore has been described in detail separately in the next chapter (chapter 5). The evidences for the Jutogh and Rajgarh thrusts follow.

As will be shown in chapter 6, the contact between the phyllites of the Chail Formation and the lower carbonaceous band of the Jutogh Group mark a significant break in the metamorphic grade. Every outcrop of the Jutogh Group of rocks including the lower carbonaceous band contains biotite and large porphyroblasts of garnet. Garnet is totally absent in the rocks of the Chail Formation. Except in a small area southeast of Haripurdhar biotite is also absent in the Chail phyllites. Chlorite and sericite are the most common minerals in these rocks. Northward of the present area the Chail rocks pass from low-grade phyllites through biotite schists to garnet-mica schists (Virdi 1981). Sporadic occurrence of garnet and chloritoid pophyroblasts have been reported from the Chail thrust sheet exposed in the Satluj valley (Gururajan 1994). The biotite zone of the Barrovian sequence is therefore, missing, or truncated at the Jutogh-Chail contact.

Staurolite is present in the mica schists occurring above the upper carbonaceous schist. This mineral has never been observed in the pelitic layers occurring within the Jutogh quartzite. The upper carbonaceous band, therefore, marks a transition from the garnet zone to the staurolite. Further, staurolite is very profusely developed in the mica schist in the western part but is rarely seen in the mica schists in the eastern part. This tentatively suggest that garnet-staurolite isograd is truncated by the upper carbonaceous band. However, since formation of staurolite requires a restricted bulk chemistry no attempt has been made to draw this isograd.

In this area ductile shearing is most intense in the two carbonaceous bands. In this rock type the penetrative cleavage in a majority of the instances is a mylonitic foliation. Repeated crenulation cleavage development on mylonitic foliation is very common. Folds of different generations were produced on the mylonitic foliation during the course of a progressive ductile shearing. The rocks adjacent to the carbonaceous bands are also mylonitized but intensity of mylonitization, in general, decreases away from both the carbonaceous bands.

Small-scale thrusts are very common in the carbonaceous bands and quartzite unit. They are rare away from the carbonaceous bands. These thrusts some times reverse the order of occurrence of the rocks.

Although the contact of the carbonaceous bands with the adjacent rocks are parallel to the foliations, at some of the exposures the *s*-surfaces are truncated by the contact.

The F_1 folds are common in both the Chail and the Jutogh rocks. But the folds of the second generation (F_2) are absent in the Chail Formation. This suggests a structural discordance between the two rock groups. Further, this structural discordance also suggests that the pre-ductile shearing (i.e. early) deformations in these two rock groups are possibly unrelated.

The detailed microstructural studies indicate that the fabric develop ment during ductile shearing is much more evident in Jutogh quartzite than in the Jutogh mica schists. The Jutogh quartzite as a whole may be considered as blastomylonite. The early fabrics are more commonly preserved in the Jutogh mica schists.

The different rock types are restricted to specific topographic levels and nowhere repetition of rock types, suggesting large-scale early folding, have been observed. This is surprising because in small scale early folds are common.

The most dramatic example of structural discontinuity is seen in the Rajgarh area, as discussed in the previous section. In this area the upper carbonaceous band and quartzite have involved in noncylindrical, refolded isoclinal folds traced by mylonitic foliation in the scale of the map but the lower carbonaceous band remains unaffected. The cleavage surfaces in the Chail Formation show only gentle undulations, an effect of F_3 folding. Further, the Jutogh-Chail contact is truncated by the upper carbonaceous band (Figs. 4.11, 4.12).

All these features suggest that the two carbonaceous bands in this area represent two separate thrusts. Since the Jutogh thrust is truncated by the Rajgarh thrust, the former is older than the Rajgarh thrust.

Around the Chur peak four thrusts can be recognized. These are: the Chur thrust (see chapter 6), the Rajgarh thrust, the Jutogh thrust and the Chail thrust (Fig. 4.13). A general ENE-WSW cross-sections (Fig. 4.14) through Chur peak show that this area can be considered to consist of four thin imbricated thrust sheets. The shearing movement responsible for this was initially ductile as indicated by abundant meso-structures typically found in ductile shear zones. The rocks deformed by early ductile shearing were later sliced up through brittle thrusts. In the carbonaceous schists which are the most intensely sheared rocks, stretching lineations along with sense of shear direction from S-C fabric were measured (Fig. 4.15). The stretching lineations plunge gently towards NE or SW but the sense of shear is consistently towards SW. Only two

data show sense of displacement towards NE whose significance is not clear. Note that the stretching lineations in Figs. 4.15 and 4.3b are similar.

From this area alone it is not possible to postulate which of these four thrusts is equivalent to the MCT. According to Gansser (1964) the Jutogh thrust is a continuation of the MCT. If one is to accept the suggestion of Valdiya (1980b) then the Chur thrust should be equivalent of MCT. Sinha-Roy (1982) suggests that the MCT in this area is represented by the Chail thrust. In a later publication Sinha-Roy (1988) redefined the Chail and Jutogh thrusts as MCT-I and MCT-II (cf. Arita 1983). It is probably not a worthwhile exercise to reconcile between these conflicting views. The significant point is that the MCT in this area represents a `zone' within which ductile shearing and imbrication of thin thrust slices can be recognised. Further, within this `zone' presence of pre-ductile shearing structures and a regional metamorphism can be demonstrated.

FIGURES

CHAPTER - 4

FIGURE 4.1 Map patterns of different lithological units in terms of topography (geology after Pilgrim & West 1928). Dashed lines are topographic contour lines. Note that the highest elevations are around the Chur peak (3647 m) and the topography slopes away in all directions which is most dramatically shown by the radial drainage pattern (thin lines). In the NE a ridge extends in the norteasterly direction and marked by the 2600 m contour. Contour interval 400 m. 1: Chur granite, 2: Mica schist, 3: Upper carbonaceous schist, 4: Quartzite, 5: Lower carbonaceous schist, 6: Chail Formation, 7: Lesser Himalaya Zone (LHZ). 2-5 belong to the Jutogh Group.

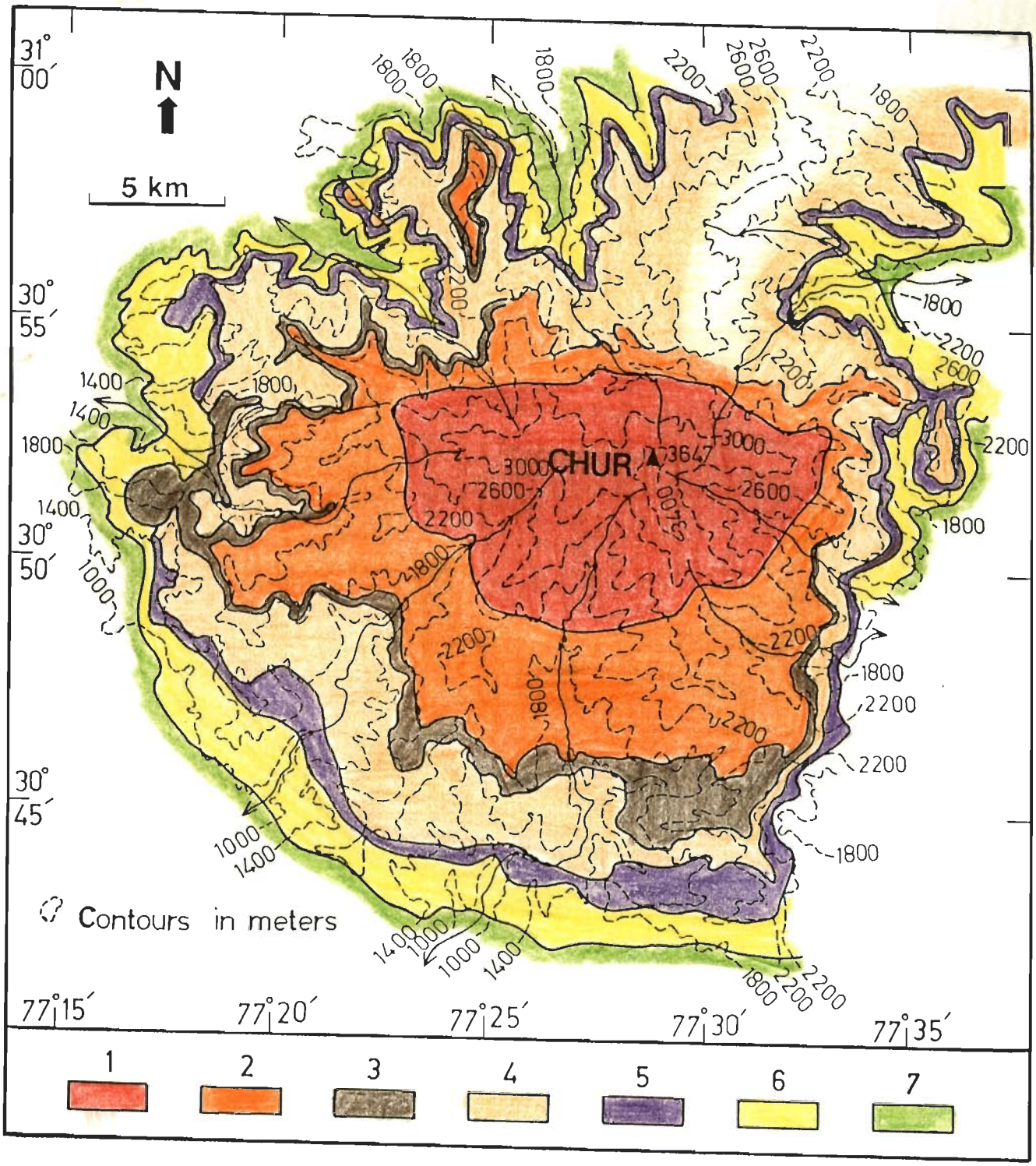
N
5 km
31° 00′
30° 55′
30° 50′
30° 45′
77° 15′
77° 20′
77° 25′
77° 30′
77° 35′
CHUR
3647
Contours in meters
1
2
3
4
5
6
7

Fig. 4.1

FIGURE 4.2 Structural map of the area showing orientaions of the foliations and lineations.

FIGURE 4.3 Synoptic stereograms of foliations (a) and lineations (b). Continuous contours: 2086 poles to foliations, contours: 0.5-1-3-5-7% per 1% area. Dashed contours: 677 lineations, contours: 1-3-5-10-13% per 1% area.

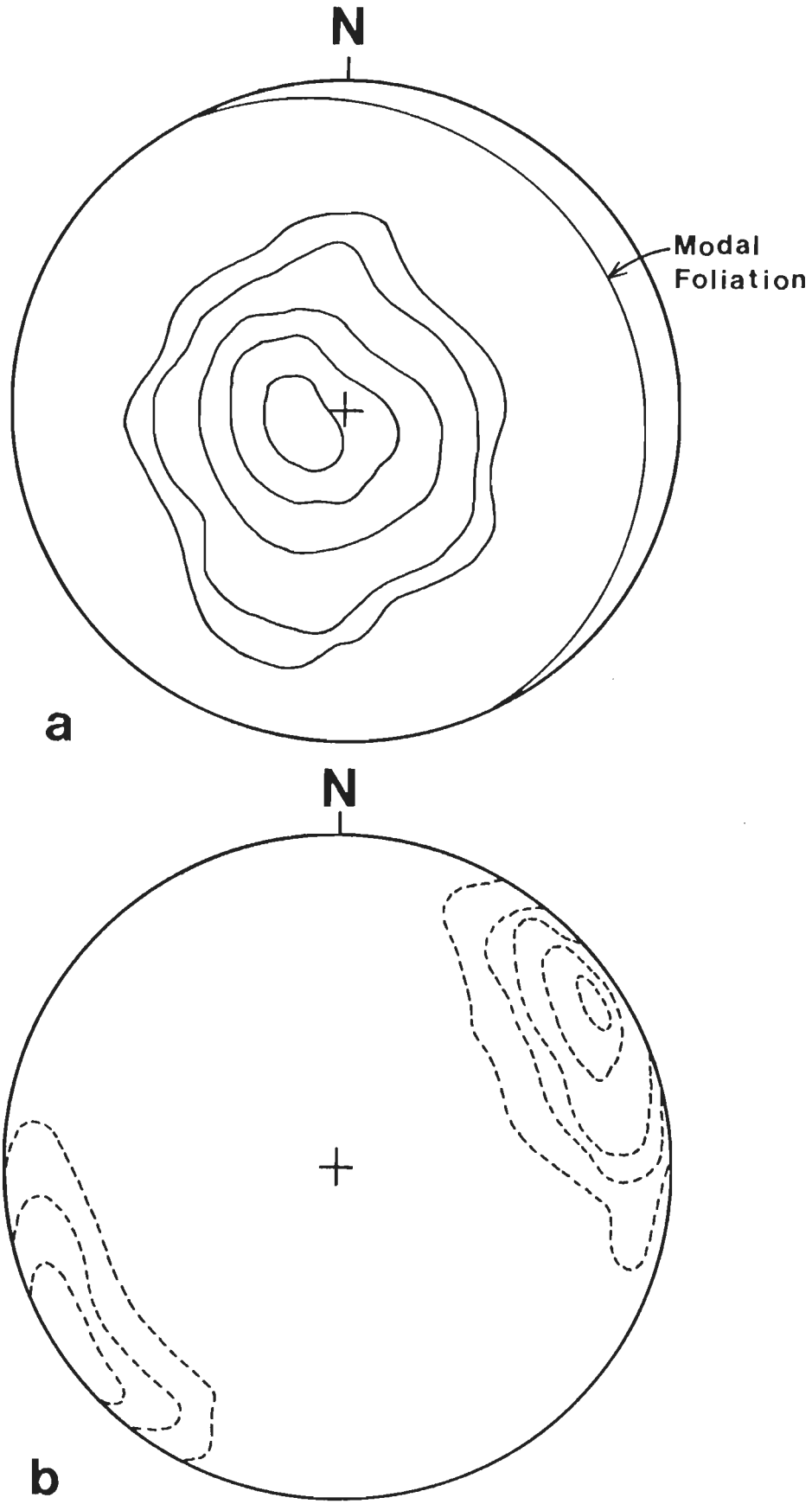

Fig. 4.3

FIGURE **4.4** Orientations of foliations and lineations in the five (1-5) different tectonic subareas. Inset shows the location of the subareas. Md: modal foliation; continuous contours: poles to foliations; dashed contours: lineations.

(a) Subarea 1; 493 poles, contours: 0.3-2-5-10-15% per 1% area; 230 lineations, contours: 0.5-2-5-10-12.5% per 1% area.

(b) Subarea 2; 333 poles, contours: 0.4-2-5-10-15% per 1% area; 116 lineations, contours: 1-3-5-10-16% per 1% area.

(c) Subarea 3; 307 poles, contours: 1-3-5-6% per 1% area; 29 lineatioins, contours: 4-9-15-25% per 1% area.

(d) Subarea 4; 223 poles, contours: 0.5-2-5-10-18% per 1% area; 50 lineations, contours: 2.5-10-20-32% per 1% area.

(e) Subarea 5; 730 poles, contours: 0.5-2-5-10% per 1% area; 252 lineations, contours: 0.5-2-5-10-15% per 1% area.

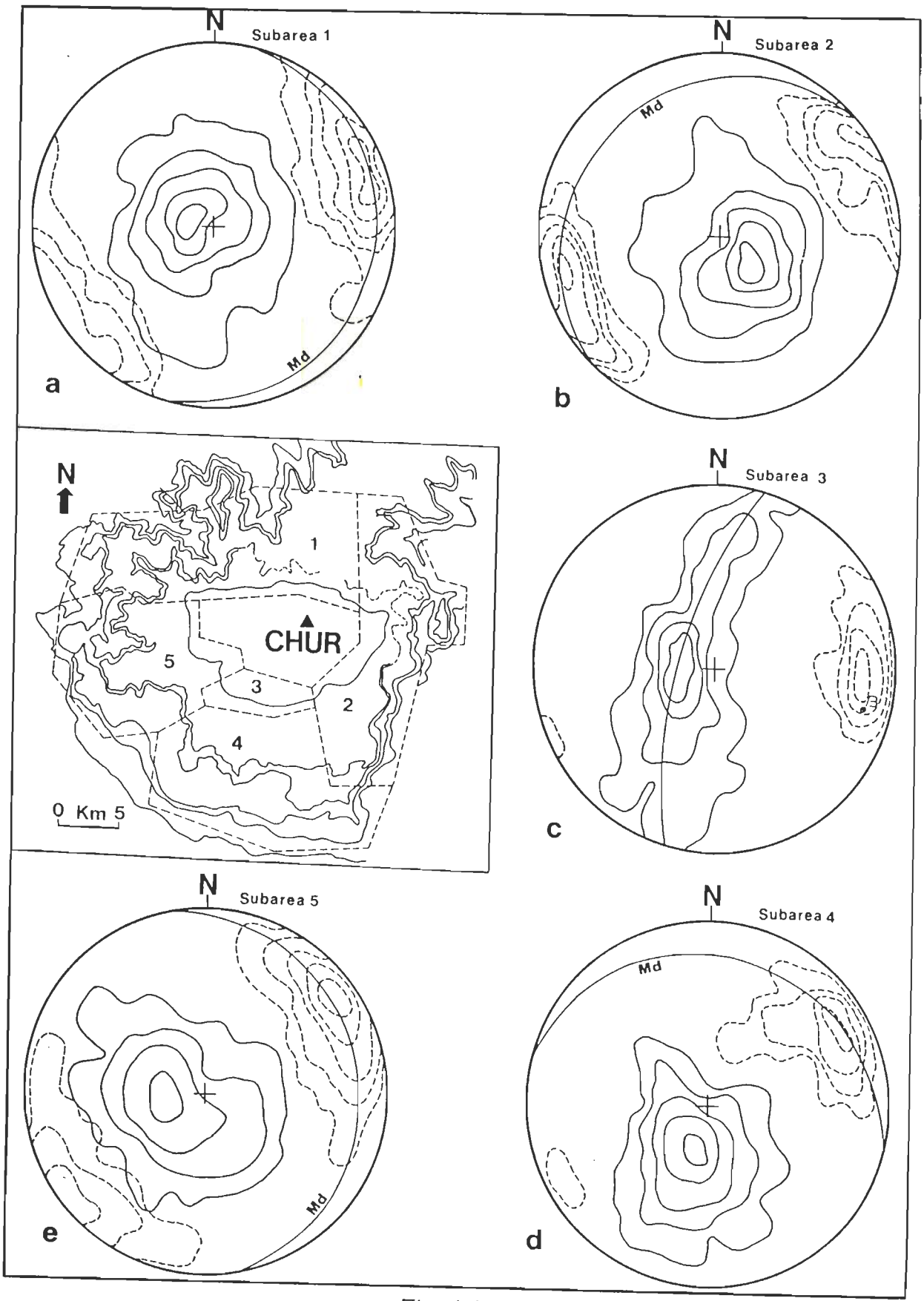
N
Subarea 1
Md
a
N
Subarea 2
Md
b
N
CHUR
1
2
3
4
5
0 Km 5
N
Subarea 3
c
N
Subarea 5
Md
e
N
Subarea 4
Md
d

Fig. 4.4

FIGURE 4.5 Structural map of the area showing orientaions of axial planes and axes of small-scale folds.

FIGURE 4.6 Orientations of small-scale early folds (F_1-F_2).

(a) 185 early (F_1-F_2) fold axes, contours: 0.6-3-6-9% per 1% area.

(b) 67 poles to F_1 axial planes, contours: 1.4-3-5-8-11% per 1% area.

(c) 72 poles to F_2 axial planes, contours: 2-4-6-8-10% per 1% area.

(d) 139 poles to early(F_1-F_2) axial planes,contours: 1-3-5-8-11% per 1% area.

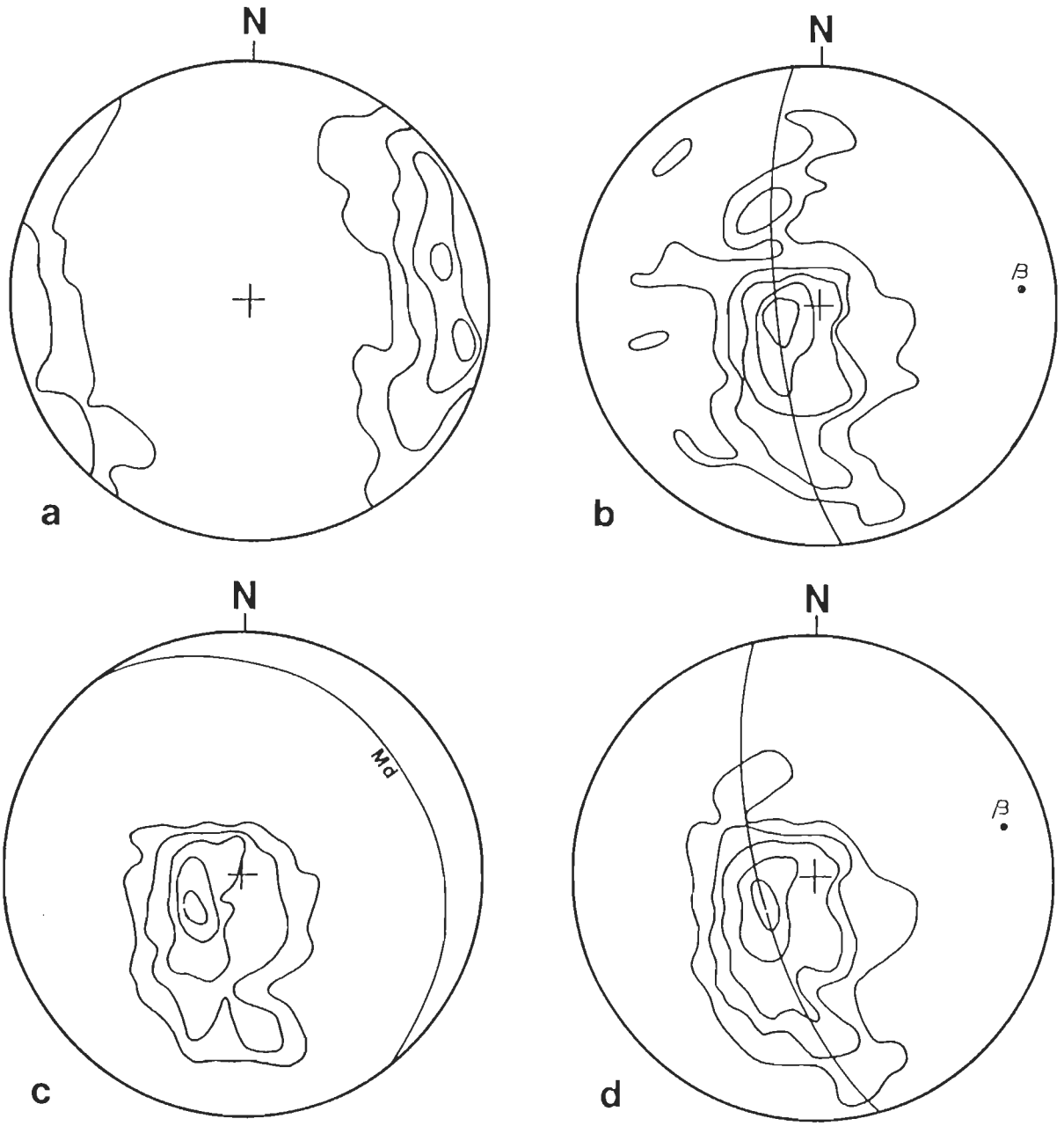

Fig. 4.6

FIGURE 4.7 Orientations of axial planes and axes of small-scale folds in the two carbonaceous bands. Contour in **(a)** and dots in **(b-d)**: poles of axial planes; open circles: fold axes; Md: modal axial planes (approximate). Inset shows location of three areas near Kot, Bogdhar and Haripurdhar from where data have been separately analyzed in **(b)** to **(d)**.

(a) Synoptic stereogram for the whole area. 217 poles, contours: 0.5-2-3-5-6% per 1% area.

(b) Data from Kot area.

(c) Data from Bogdhar area.

(d) Data from Haripurdhar area.

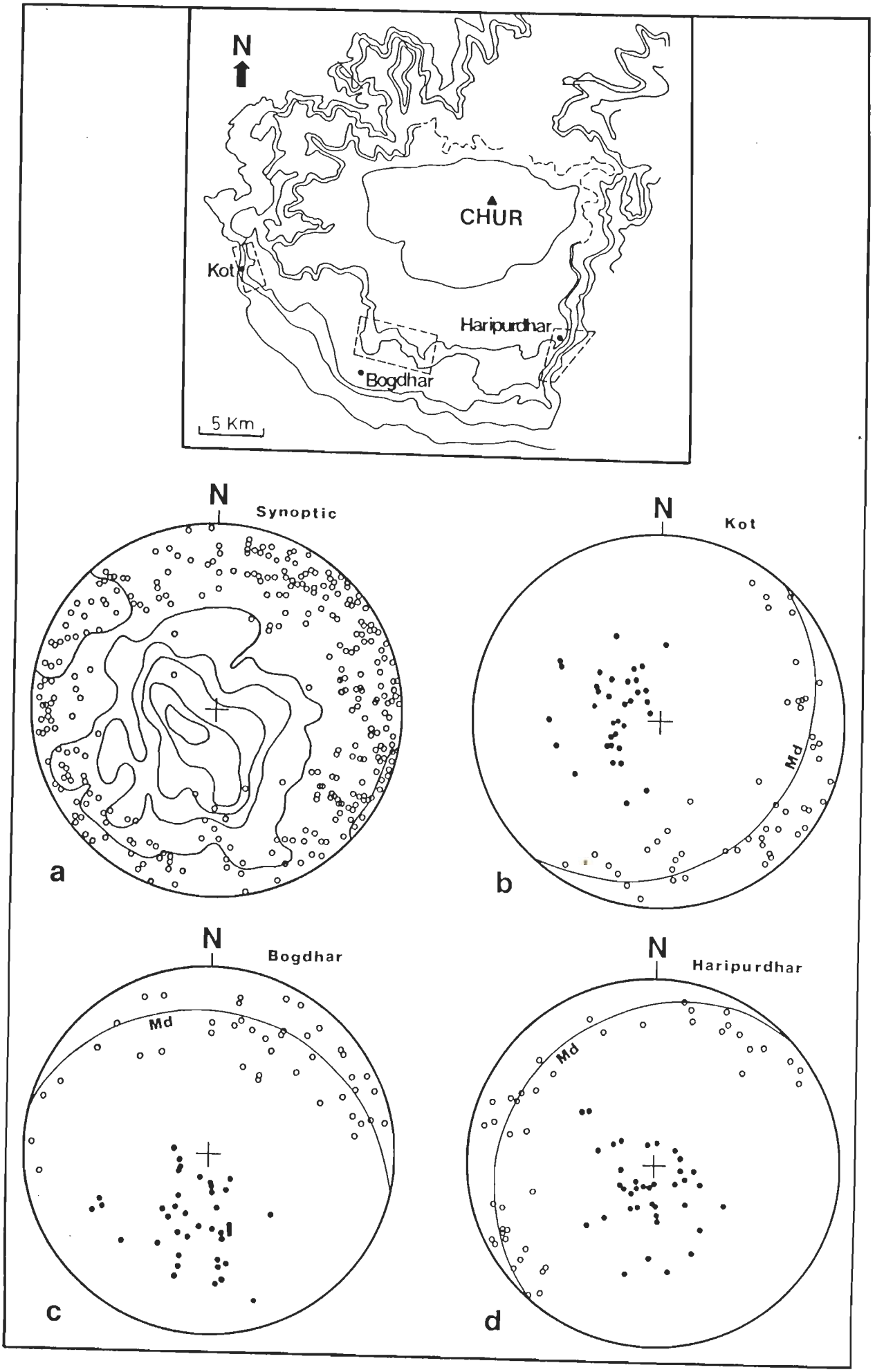
N
CHUR
Kot
Haripurdhar
Bogdhar
5 Km
N
Synoptic
a
N
Kot
Md
b
N
Bogdhar
Md
c
N
Haripurdhar
Md
d

Fig. 4.7

FIGURE 4.8 Structural map of the area around Rajgarh showing the orientations of the foliations and lineations.

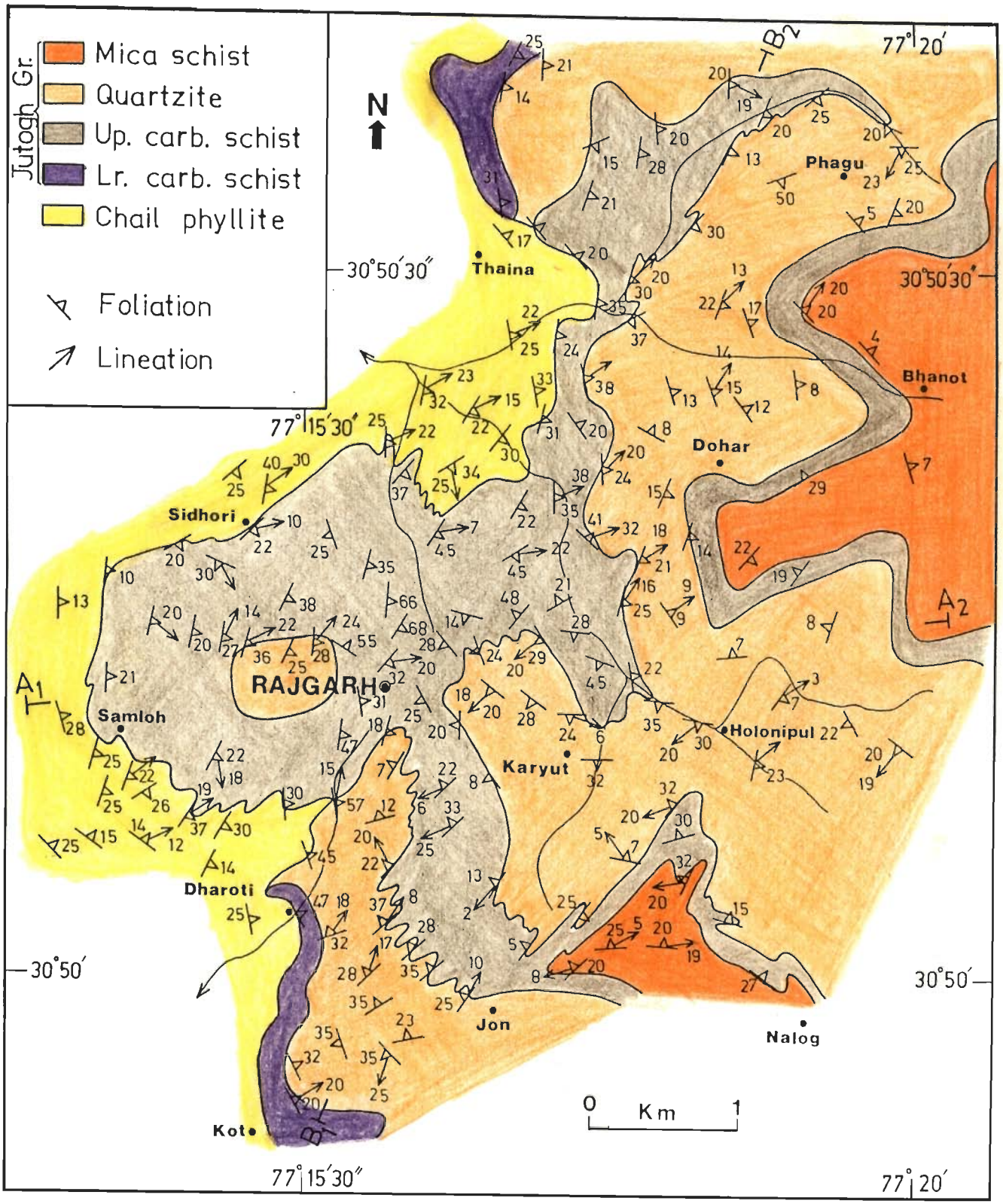
Jutogh Gr.
Mica schist
Quartzite
Up. carb. schist
Lr. carb. schist
Chail phyllite
Foliation
Lineation
N
77°20′
77°15′30″
30°50′30″
30°50′
Thaina
Phagu
Bhanot
Dohar
Sidhori
RAJGARH
Samloh
Karyut
Holonipul
Dharoti
Jon
Nalog
Kot
TB2
A1
A2
B
0 Km 1

Fig. 4.8

FIGURE 4.9 Structural map of the area around Rajgarh showing the orientations of the axial planes and axes of small-scale folds in the carbonaceous bands.

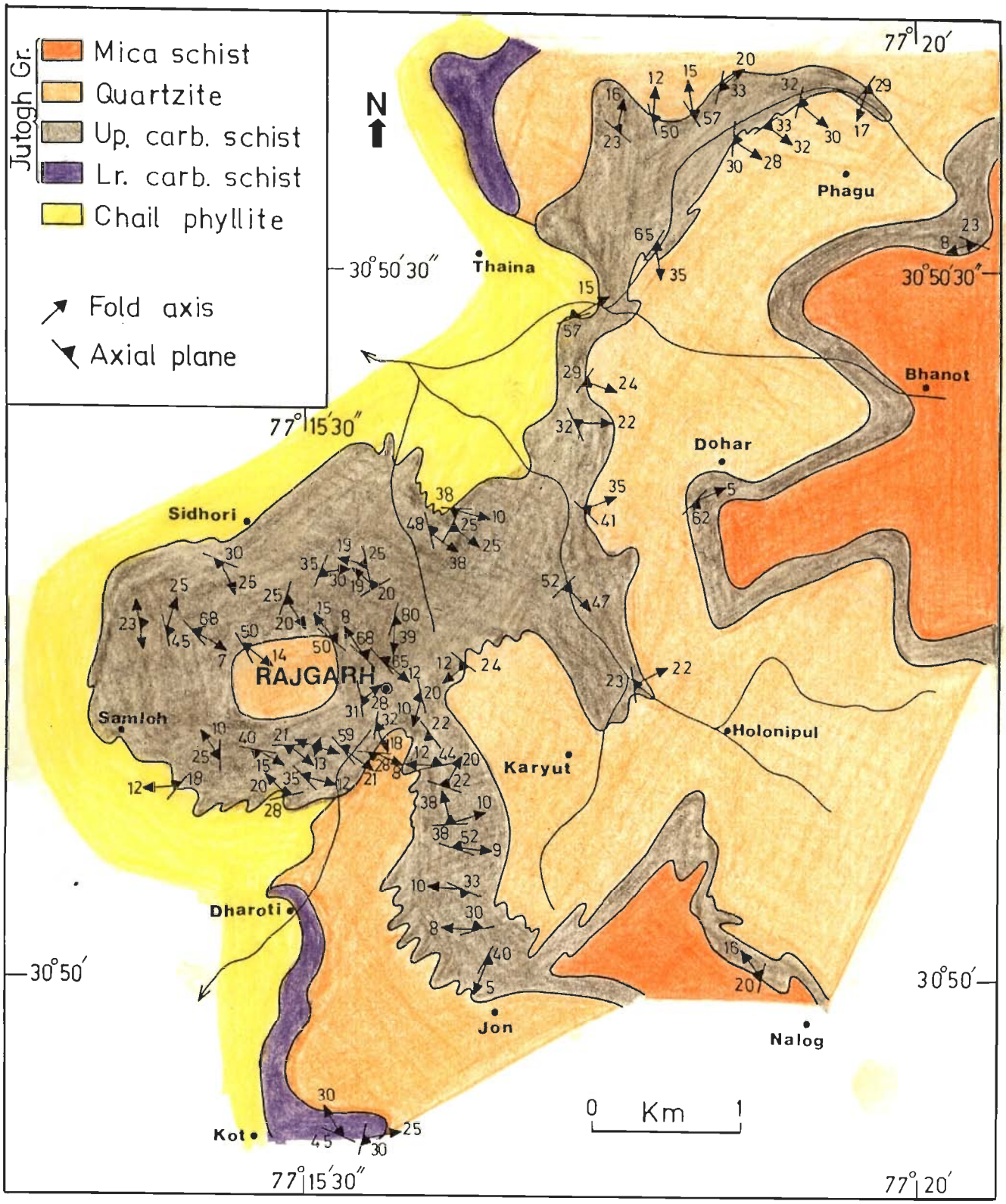
Jutogh Gr.
Mica schist
Quartzite
Up. carb. schist
Lr. carb. schist
Chail phyllite
Fold axis
Axial plane
N
77°20′
30°50′30″
77°15′30″
30°50′
Thaina
Phagu
Bhanot
Dohar
Sidhori
RAJGARH
Samloh
Karyut
Holonipul
Dharoti
Jon
Nalog
Kot
0 Km 1

Fig. 4.9

FIGURE **4.10** Stereograms for the planar and linear structures around Rajgarh (Fig. 4.8 and 4.9).

(a) Foliations and lineations. Continuous contours, 383 poles to foliations, contours: 1-2-5-10-12% per 1% area; dashed contours, 151 lineations, contours: 1-3-5-10-15% per 1% area. Md: modal foliation.

(b) Axial planes and axes of small-scale folds. Dots: poles to axial planes; open circles: fold axes.

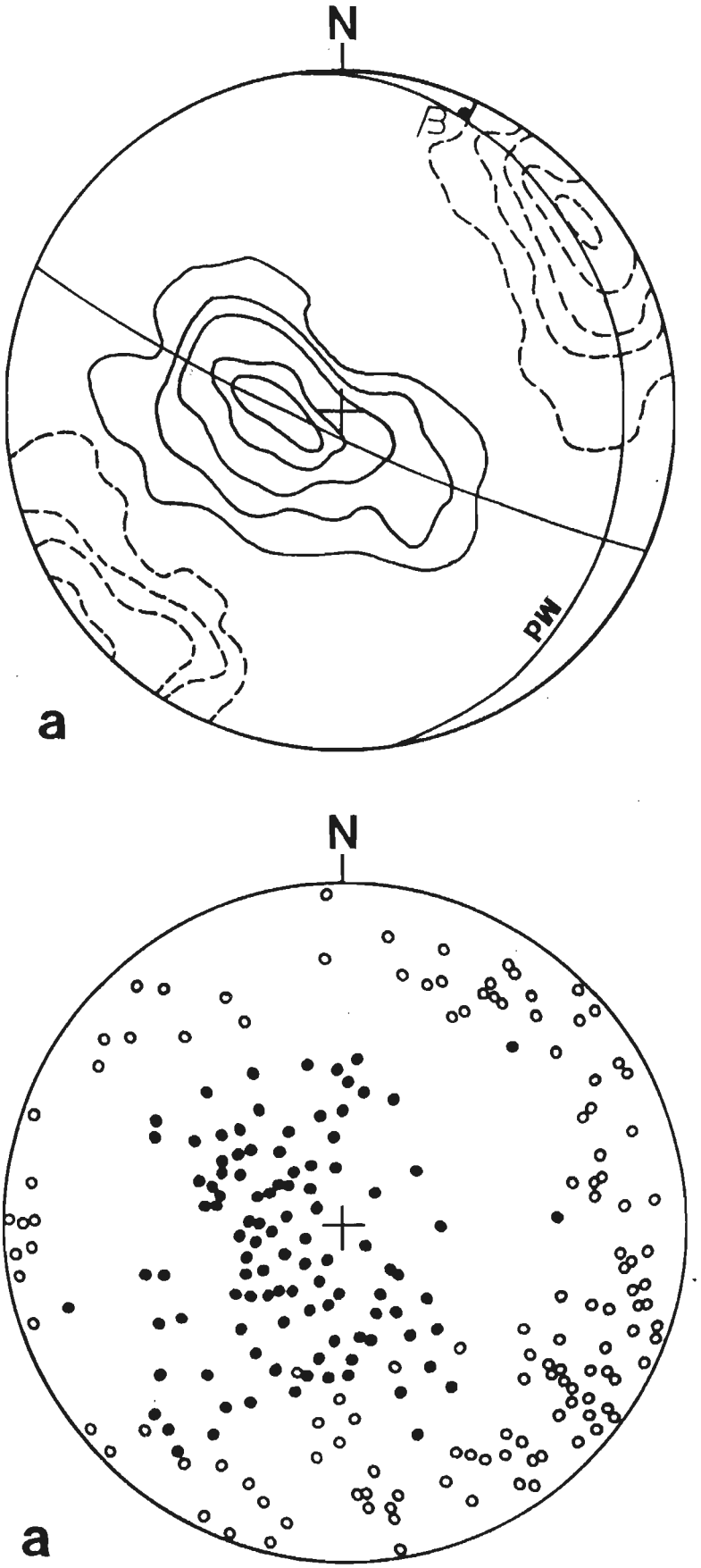

Fig 4.10

FIGURE 4.11 Geological cross sections in Rajgarh area. Section lines are shown in Fig. 4.8. **(a)** Along A_1-A_2. **(b)** Along B_1-B_2. See text for details. MS: mica schist; UCS: Upper carbonaceous schist; Q: Quartzite; LCS: Lower carbonaceous schist; CP: Chail phyllite; JT: Jutogh thrust; RT: Rajgarh thrust.

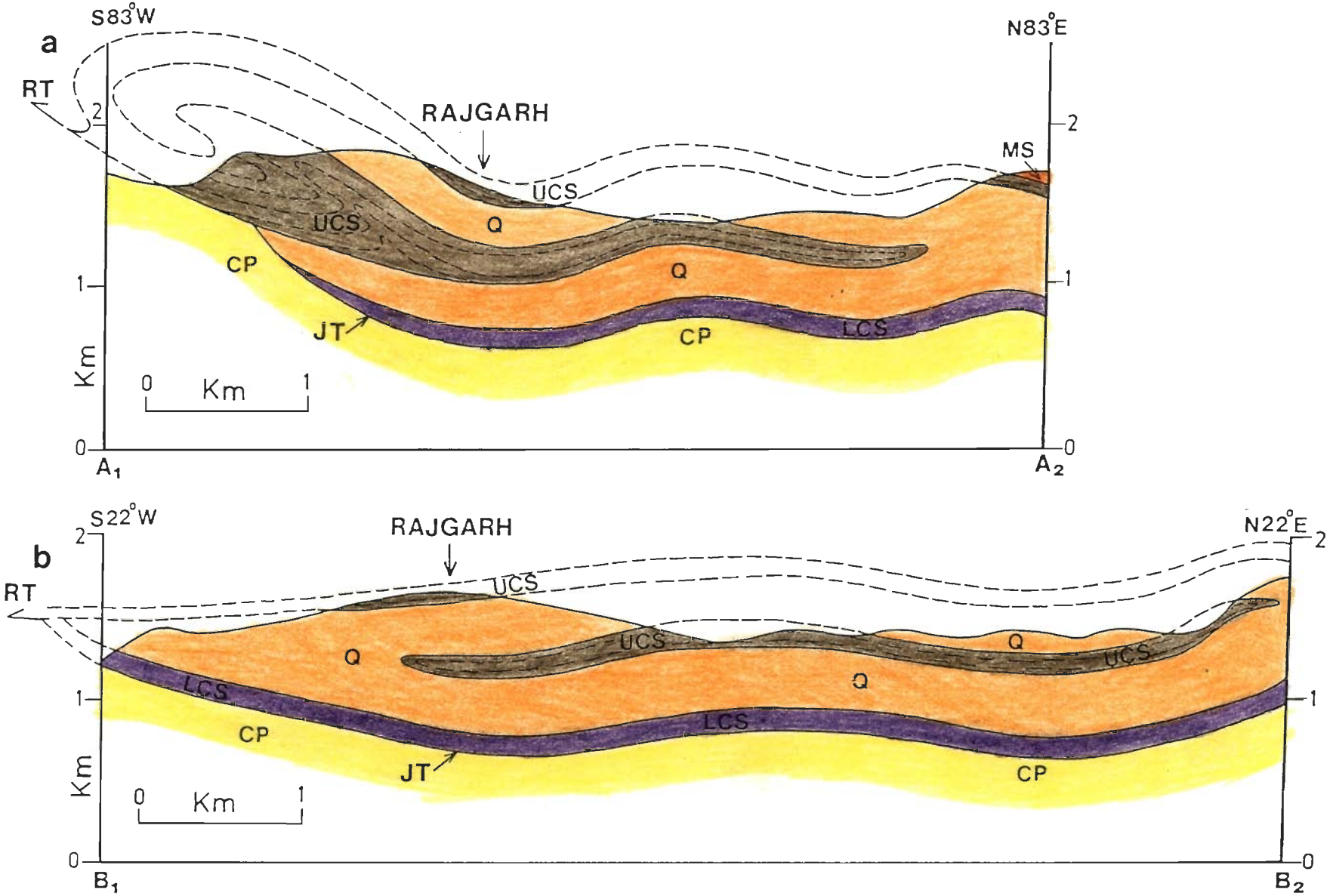
a
S83°W
N83°E
RT
RAJGARH
MS
UCS
UCS
Q
Q
CP
JT
CP
LCS
Km
0 Km 1
2
1
0
A1
A2
b
S22°W
N22°E
RT
RAJGARH
UCS
UCS
UCS
Q
Q
Q
LCS
LCS
CP
CP
JT
Km
0 Km 1
2
1
0
B1
B2

Fig. 4.11

FIGURE 4.12 Schematic three-dimensional diagram showing the large scale refolding, traced by upper carbonaceous band, around Rajgarh. Note strong non-cylindricity of the large-scale folds resulting in sheath fold type of geometry.

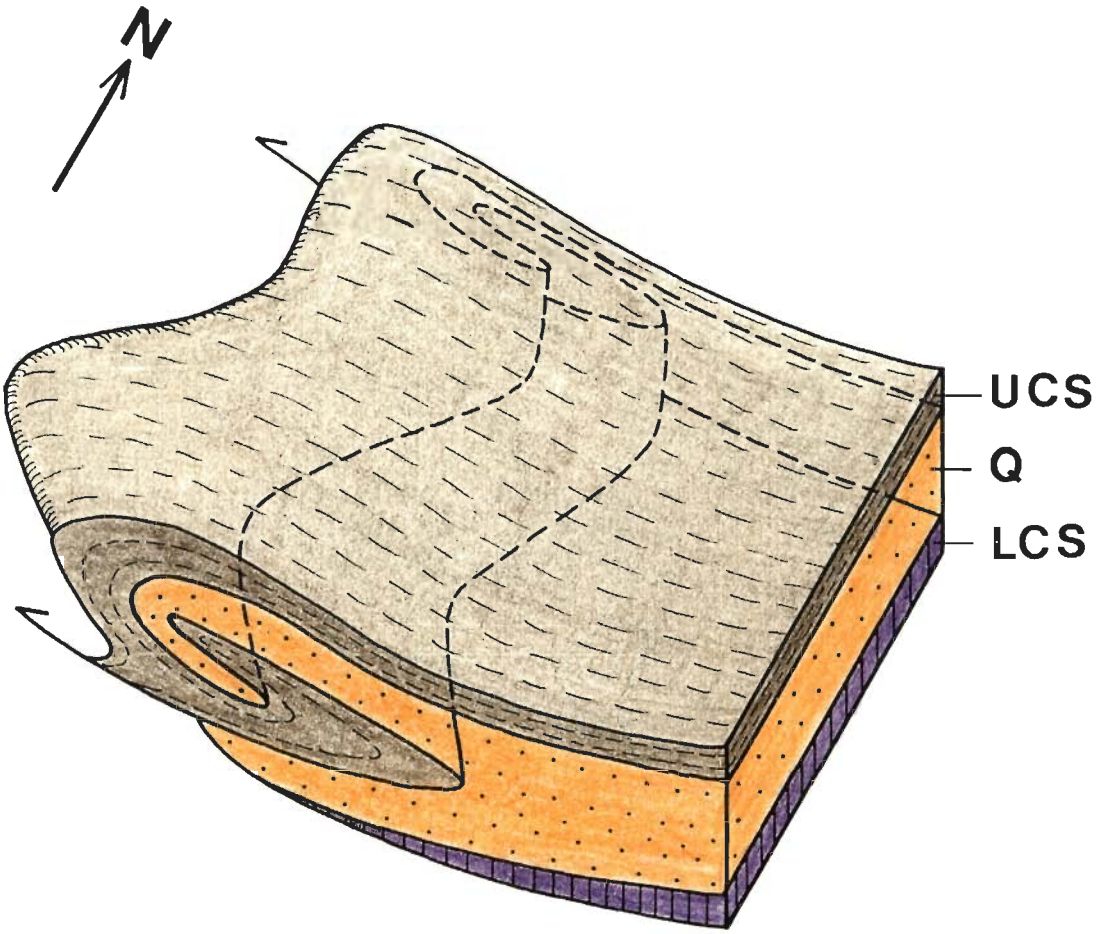

UCS-Up. Carb. Schist

Q -Quartzite

LCS-Lr. Carb. Schist

Fig. 4.12

FIGURE 4.13 Geological map around the Chur peak showing the locations of four thrust planes. 1: Chur granite; 2: Mica schist; 3: Upper carbonaceous schist; 4: Quartzite; 5: Lower carbonaceous schist; 6: Chail Formation; 7: Lesser Himalaya Zone (LHZ); 8: Thrusts. 2-5 belong to Jutogh Group.

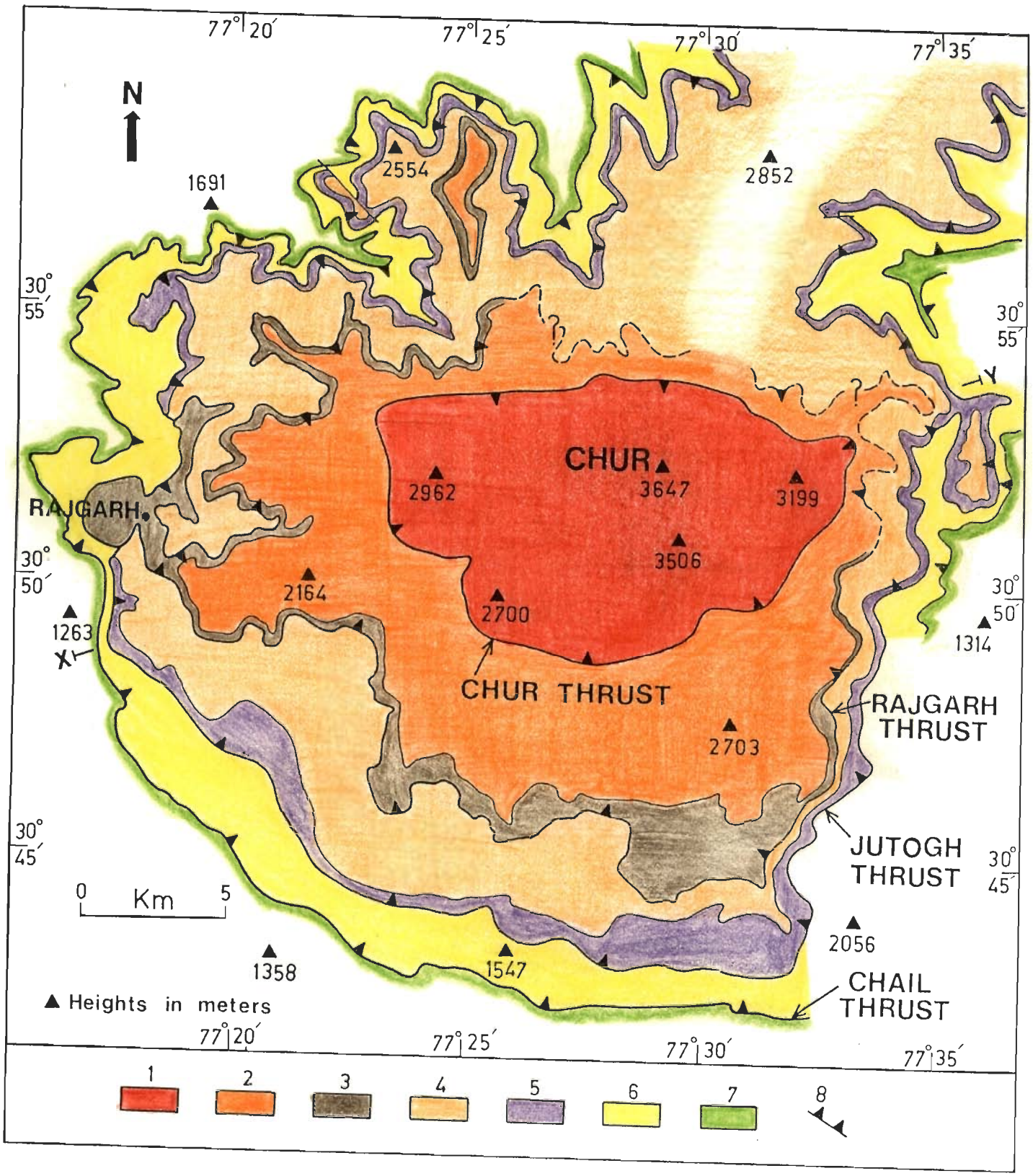
77°20′
77°25′
77°30′
77°35′
N
2554
2852
1691
30°55′
CHUR
2962
3647
3199
3506
RAJGARH
30°50′
2164
2700
1263
X
Y
1314
CHUR THRUST
RAJGARH THRUST
2703
30°45′
JUTOGH THRUST
0 Km 5
2056
1358
1547
CHAIL THRUST
▲ Heights in meters
1
2
3
4
5
6
7
8

Fig. 4.13

FIGURE 4.14 Generalised cross section along X-Y (Fig. 4.13) through the Chur peak showing imbrication of four thin thrust sheets. G: Chur granite; MS: Mica schist; Q: Quartzite; CP: Chail phyllite; LH: Lesser Himalaya Zone (LHZ).

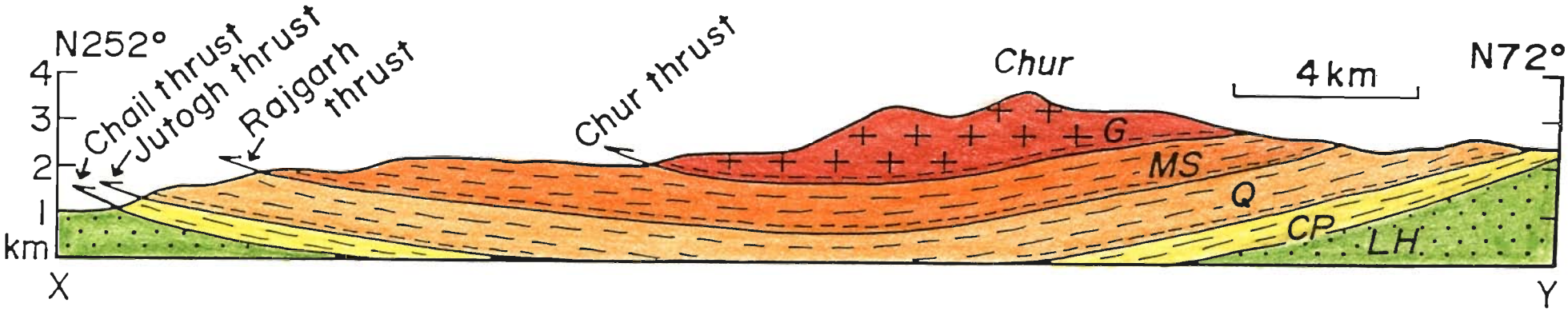
N252°
Chail thrust
Jutogh thrust
Rajgarh thrust
Chur thrust
Chur
4 km
N72°
4
3
2
1
km
G
MS
Q
CP
LH
X
Y

Fig. 4.14

FIGURE 4.15 Orientations of shear lineations (dots) measured where sense of shear directions (arrows) could be determined from the S-C fabric and the asymmetric crenulations. Note that the sense of shear is approximately from NE to SW.

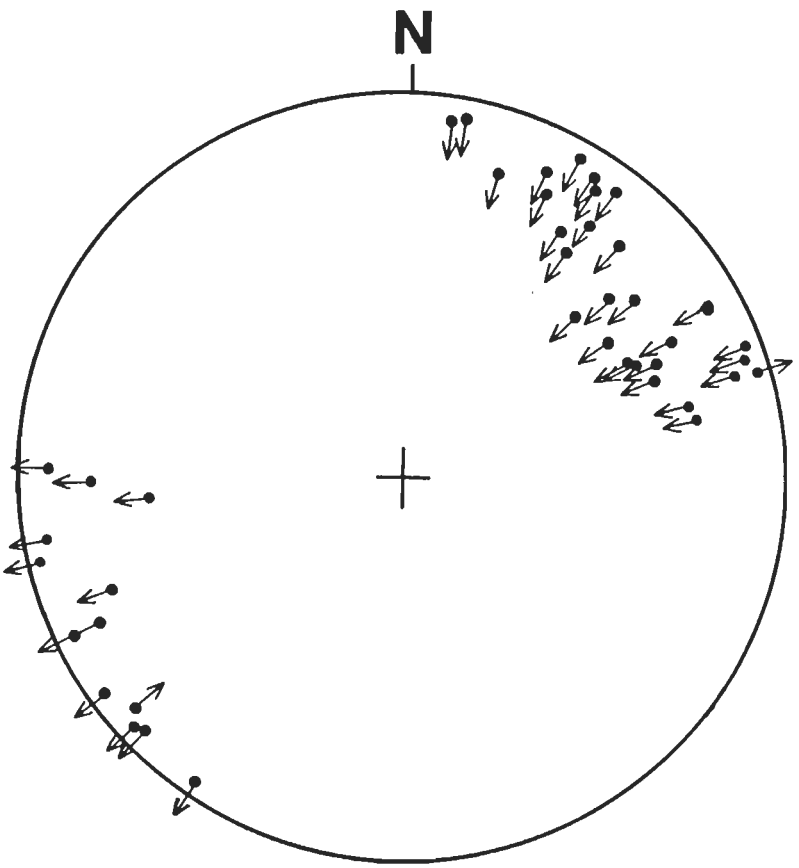

Fig. 4.15

CHAPTER-5

THE CHUR GRANITE

5.1 THE LESSER HIMALAYA GRANITE BELT

Within the Himalayan orogenic segment (i.e. south of ITSZ) numerous granitic bodies occur in all the lithotectonic zones, except the SHZ. Le Fort (1988) grouped these granitic bodies into three belts each running parallel to the orogen. These are, from north to south: (1) the North Himalaya Belt, (2) the High Himalaya Belt, and (3) the Lesser Himalaya Belt. The first two belts are related to the India-Eurasia collision and subsequent evolution of the Himalayan crust (Le Fort 1988 and references therein). In particular it has been shown that the leucogranites of the High Himalaya Belt have formed by partial melting of the Himalayan crust during thrusting along the MCT (e.g. Deitrich & Gansser 1981; Le Fort 1981; Le Fort et al. 1987; Vidal *et al.* 1982; Deniel *et al.* 1987).

The southernmost Lesser Himalaya granite belt, consisting of a series of porphyritic peraluminous quartz-rich granite bodies, is particularly well marked in the physiographic Lower Himalaya of Himachal, Garhwal and Kumaun (Fig. 5.1; Thakur 1983). Most of these granites are only few km^2 to a few tens of km^2 in areal extent and are hosted by the HHCZ and LHF nappe sequences within short distances from the MCT. In addition, there are also a large number of "augen gneisses" of granitic composition in this belt (e.g. Pecher & Le Fort 1977; Valdiya 1980b; Gururajan 1990). The isotopic ages of these granites vary from Proterozoic to early Paleozoic (e.g. Le Fort *et al.* 1980; Scharer & Allegre 1983; Trivedi *et al.* 1984) and therefore the formation and emplacement of the granitic rocks of this belt are unrelated to the Himalayan orogeny which is essentially Tertiary in age.

The structural settings of these granites and the augen gneisses are surprisingly still ambiguous. They are commonly mapped as rootless plutons that intruded the metamorphic country rocks exposed in the erosional outliers of the HHCZ (hanging wall of the MCT) (Valdiya 1980b; Chatterjee & SwamiNath 1977; Thakur 1983).

This is important, because if these granites intruded the country rocks during the Proterozoic-early Paleozoic time then they have merely been transported to the present locations along with the nappe sequences and may not have much tectonic significance to the Tertiary Himalayan orogeny. Some workers (e.g. Sinha-Roy & Sengupta 1986), on the other hand, consider that all the deformed granites in the LHZ are thrust wedges. If this postulation is correct then the Lesser Himalaya granites may have important bearing on the overall geodynamic evolution of the Himalayan orogen. Unfortunately, the contact relations of these granitic bodies with the surrounding country rocks have never been conclusively demonstrated.

The Lesser Himalaya granite occurring around the Chur peak in the Himachal Himalaya is one of the most famous of these bodies (the Chur granite, Figs. 5.1, 5.2). Pilgrim & West (1928) suggested that the Chur granite is a laccolithic intrusion from the north into the surrounding metamorphic rocks. This view has been upheld by most of the later workers (e.g. Kanwar & Singh 1979; Kishore & Kanwar 1984a,b). In this chapter the status of the Chur granite vis-a-vis the Jutogh Group of rocks is discussed.

5.2 THE CHUR GRANITE

5.2.1 The geology

The isolated Chur granite occurs where altitude exceeds about 3000 m around the Chur peak (Figs. 5.1, 5.2). It also occurs at the highest structural levels in the sense that it overlies the topmost Rajgarh thrust sheet (Fig. 4.14). The granite body has an approximately oval or circular shape and is surrounded by the Jutogh mica schist. Except near the margin, the granite is coarse grained, massive and porphyritic with very large (occasionally exceeding 15 cm in length) K-feldspar megacrysts. The megacrysts constitute as much as 20-30% of the volume and occur as randomly oriented nearly perfect rectangular crystals (Fig. 5.5a).

About 25 km NE of the Chur peak several similar, but much smaller granite bodies are also exposed around the Kainchwa peak (3462 m, Fig. 5.2; Srikantia &

Bhargava 1988) where altitudes exceed above 3000 m. It is interesting to note that the exposures of granite occur only when the elevation exceeds about 3000 meters. Around Simla town (about 40 km NW of the Chur peak) where the same Jutogh rocks are exposed in a pear-shaped klippe there is no exposure of granitic rocks. In this area the maximum elevation is about 2000 m (Fig. 5.2). This observation suggests that the granitic rocks occurring around the Chur and Kainchwa peaks are the erosional remnants of one larger subhorizontal sheet-like granite body.

5.2.2 The contact relation

The contact between the granite and the surrounding Jutogh mica schist is razor-sharp wherever exposed (Fig. 5.6b) and can be very precisely located in the field. The contact and the foliation in both the granite and the adjacent mica schist are all strictly parallel (Figs. 5.3, 5.6b). Elsewhere, thin slices of granite in mica schist and thin mica schist slices in granite have been observed. These slices with thickness never more than a few tens of cm are restricted near the contact and are strictly parallel to the adjacent cleavage planes. In order to check the contact relation, about twelve km of the granite contact was mapped in detail between Chogtali and Chauras southwest of the Chur peak (Fig. 5.4). This area was chosen particularly because the dip of the contact varies from gentle near Chogtali to rather steep near Chauras. Nowhere any cross-cutting relationship or apophyses has ever been observed from outcrop to map scale. Irrespective of the amount of dip the contact is always conformable with the local foliation planes. Stereographic plot of foliation planes measured near the contact, however, show folding on a gentle easterly plunging open fold (Fig. 5.4) which explains the variation in the amount of dips. The stretching lineations in this area have gentle plunge towards NE. Close to the contact in both the rocks a large number of pegmatitic and quartz veins are usually present but they disappear within a short distance from the contact. Some of the pegmatitic veins contain xenoliths of granite. These veins often cross cut the foliation surfaces. Where veins are profusely developed

it may erroneously be interpreted that the granite has an intrusive relation with the mica schist. These veins are syn- to late-kinematic with respect to the Tertiary thrusting movements, derived from the surrounding rocks possibly due to shear heating and fluid interaction.

5.2.3 The outcrop pattern

The southern contact dips towards the granite whereas the northern contact locally dip away from the contact. This led Pilgrim & West (1928) to conclude that the mica schist overlies the granite in the north since in the direction of the dip the overlying rocks should be exposed. The occurrence of garnet near the Chur peak was taken to indicate as the presence of mica schist outcrops. Therefore, Pilgrim & West (1928) suggested that the granite is a laccolithic intrusion into the Jutogh mica schist. Kanwar & Singh (1979) further suggested that this laccolithic intrusion took place along the core of a huge isoclinal fold with gentle dip of axial plane. In a rugged terrain such as this where the slope is steeper than the dip of the contact, underlying rocks should be exposed in the direction of the dip of the contact. Further, the garnet bearing rocks near the Chur peak are granites and not mica schist. Finally, if the contact is isoclinally folded with gently dipping axial planes (Kanwar & Singh 1979) then the contact and the S-surfaces should have rotated through vertical at some places which is not the case here. Therefore, the postulates of Pilgrim & West (1928) and Kanwar & Singh (1979) are clearly not tenable.

The closed outcrop pattern indicates that it is the same contact everywhere. In a major part the contact as well as the concordant cleavage planes in both the granite and mica schist dip gently towards the granite (Fig. 5.3). Therefore, the contact has an overall shallow basin type of configuration. This, together with the topography which slopes away in all directions rather steeply from the area around the Chur peak, readily explains the closed outcrop pattern of the granite. Locally, dip of the contact becomes steeper (Fig. 5.4) and at some places in the northeastern part the dip direction is away

from the granite body. This is due to the late stage gently plunging upright folding (F_3) as well as due to thrust related folding (section 4.3). The upper contact of the granite is not exposed in this area.

5.2.4 Mylonitization of the Chur granite

As has been mentioned earlier, the granite body is massive in most part but is strongly foliated near the margin. In the massive granite very large randomly oriented rectangular K-feldspar megacrysts impart the rocks a typical porphyritic texture in outcrop (Fig. 5.5a). Nearer to the contact with the Jutogh metasediments a foliation gradually becomes very prominent. Concomitant with the development of the foliation the K-feldspar megacrysts are broken into smaller fragments, become elliptical or lensoid-shaped (or "augen"-like) and they are aligned parallel to the foliation. This sequence has been shown in Figs. 5.5a to 5.6a. In Fig. 5.8 histograms of the angles between the long dimensions of the megacrysts and a reference line are shown. The reference line is either the trace of the foliation plane or arbitrary where foliation is not seen. It is clearly seen that as the foliation becomes more and more prominent the long dimensions of the megacrysts come to lie (sub)parallel to the foliation planes.

In the very well foliated granite, megacrysts are some times difficult to recognize and at times become indistinguishable from the mylonitized mica schists. The gradation from massive to foliated granite is perfectly gradual. The thickness of the foliated zone near the margin varies from a few meters to more than a hundred meters. Consequently, the outcrop width of the foliated granite also varies widely. The massive granites in the central part has also been foliated in discrete zones of limited width and length. However, these zones are insignificant in areal extent.

Towards the centre where the granite is massive or weakly foliated, anomalous extinction, kinked and bent cleavage traces in micas and twin lamellae in feldspars and development of small recrystallized grains at the boundaries of larger grains (mortar texture) are the characteristic features in thin sections (Figs. 5.6c,d). This grades into

rocks where highly strained surviving megacrysts occur in a matrix consisting of fine grained recrystallized, polygonal and strain-free grains (Fig. 5.7a). This in turn grades into rocks where surviving megacrysts are very few in number and a very well-developed foliation is traced by very long and recrystallized quartz ribbons (Fig. 5.7b-d). The mica grains are broken into smaller grains and are smeared along the foliation planes. They also form ribbons and are recrystallized at places. The K-feldspar megacrysts invariably show core-and-mantle texture (Fig. 5.7c). As discussed in section 3.3.1, all these lines of evidence prove beyond doubt that the foliated granite at the margin is nothing but a mylonitised granite. The mylonitization varies from protomylonite through mylonite to ultramylonite sometimes even in a single thin section. In outcrops and in thin sections it is clear that the foliation is undoubtedly mylonitic and not flow banding (Pilgrim & West 1928) or gneissosity (Kanwar & Singh 1979). In highly deformed rocks mylonitic foliation traced by quartz ribbons and aligned micas often wrap around relict lensoid K-feldspar megacrysts (Fig 5.7b). The deformed, lensoid-shaped K-feldspar megacrysts are confined to the mylonitized zone near the contact with the surrounding mica schist and together with the mylonitic foliation the rock has an appearance of a typical "augen gneiss". In thin sections and in outcrops S-C fabric is quite common (see Fig. 3.12d). However, one may erroneously interpret the anastomosing mylonite foliation around K-Feldspar megacrysts as S-C fabric (Fig. 5.5b). Since the variation in the intensity of development of the mylonitic foliation and also the variation in mylonite microstructures are gradual in space, it can be concluded that the foliated granite near the margin is the deformed and mylonitized part of the granite seen towards the center. The postulation of Kishore & Kanwar (1984) that the foliated and unfoliated granites are the two different intrusive phases is clearly not correct.

The ultramylonites without any surviving K-Feldspar megacrysts near the contact are sometimes indistinguishable from the underlying mica schist and the contact may be

incorrectly interpreted to be gradational (Fig. 5.6b). It is interesting to note that gradational contacts have been suggested for some of the Lesser Himalayan granites.

5.2.5 Metamorphism

As will be shown in the next chapter, there is no contact metamorphic effect on the country rocks. The mica schist adjacent to the granite contains staurolite, kyanite and sillimanite. Neither hornfelsic texture nor andalusite or cordierite has ever been found. This area shows the classic inverted metamorphic zonation with the grade of metamorphism increasing towards higher topographic/structural levels and towards the granite. Detailed petrographic and microstructural studies in the metasedimentary rocks of the Jutogh Group have shown that the main metamorphic minerals are completely pre-tectonic with respect to the development of the mylonitic foliations. Finally, geothermobarometric studies (T.K. Ghosh and D.K. Mukhopadhyay, pers. comm.) show that there is no systematic increase in temperature of metamorphism in the metamsediments from Jutogh thrust to the granite contact. It is interesting to note that inverted metamorphic zones are also present adjacent to some other Lesser Himalaya granites where the granites occur above the highest grade rocks (e.g. Le Fort *et al.* 1980).

5.3 STATUS OF THE CHUR GRANITE

The characteristic features of the Chur granite can be summarized as follows: (1) It is an erosional remnant of a large subhorizontal sheet-like body. (2) It occurs at the highest topographic levels as well as at the highest tectonic levels and is underlain by several thin subhorizontal thrust sheets composed of metasedimentary rocks. (3) The central portion of the granite body is massive, porphyritic with large K-feldspar megacrysts and is largely undeformed. (4) Near the contact with the surrounding mica schist the granite shows all the features of a typical mylonite with a well developed mylonitic foliation. (5) The variation from undeformed granite in the central part to granite mylonite near the margin is gradual. (6) The deformed and lensoid-shaped K-

feldspar megacrysts along with well developed mylonitic foliation imparts the granite an appearance of a typical "augen-gneiss". (7) The contact of the granite is everywhere concordant with the gently dipping mylonitic foliation present in both the granite and the underlying mica schist. (8) Neither any cross-cutting relationship nor any effect of contact metamorphism has been observed.

All these lines of evidence taken together prove beyond doubt that the Chur granite is a thrust sheet and not an intrusion into the surrounding HHCZ either in its present position or at its pre-thrusting original location. This thrust sheet was of much larger areal extent but now occurs as small and isolated bodies around the Chur peak owing to deep erosion. We have named the thrust at the base of the Chur granite as Chur thrust (Bhadra *et al.* 1993; Mukhopadhyay *et al.* 1994).

5.4 REGIONAL EXTENSION OF THE CHUR THRUST

The granite bodies around the Kainchwa peak have the same geologic and tectonic settings as the Chur granite. We may, therefore, extend the Chur thrust upto this area. Further extension of the Chur thrust northward into the Higher Himalaya can only be *speculative* at present. A granite body (locally called the Wangtu Gneissic Complex, WGC) has been reported from the Satluj valley around Wangtu (see Fig. 1.3 for location), about 80 km NNE of the Chur peak (Sharma 1976; Kakkar 1988). Although the exposures of the WGC are extensive in the Satluj valley, it's extension towards NW or SE are not well known because of rugged terrain and poor accessibility. Reconnaissance survey in the Satluj valley shows that the WGC is similar in many respect to the Chur granite. The porphyritic granite of the WGC contains deformed K-feldspar megacrysts which together with well developed mylonitic foliation gives the rocks a gneissic appearance. However, compared to the Chur granite the WGC is deformed throughout and the mylonitization is much more extensive. Whereas the contact of the Chur granite and the foliations are subhorizontal, the contact of the WGC and the concordant foliations dip 40-50° to NE. The WGC is both underlain and

overlain by metasedimentary rocks of the HHCZ with razor-sharp contacts. The upper contact of the WGC is called Karcham thrust (Kakkar 1988) and coincides with the Vaikrita thrust of Valdiya (1980a; see Sharma 1976). The lower contact may possibly be equivalent to the Chur thrust. It is tentatively suggested that the root zone of the Chur thrust sheet is represented by the WGC which is sandwiched by the lower (Jutogh Group, Pilgrim & West 1928) and upper (Vaikrita Group, Valdiya 1980b) parts of the HHCZ.

A granite body (the Lansdowne granite) of small areal extent (ca. 10 km^2) occurs in the Klippe of the HHCZ around Lansdowne town (see Fig. 5.1 for location), about 150 km SE of the Chur area (Auden 1937; Shanker & Ganessan 1973). The thrust at the base of the HHCZ metamorphic rocks is locally called the Amri thrust and is possibly equivalent of the Jutogh thrust of the Chur area. This granite is remarkably similar to the Chur granite in it's tectonic setting and physical appearance. The Lansdowne granite, originally thought to be an intrusion into the surrounded metamorphic rocks (Auden 1937), has been suggested to have a thrust contact (the Lansdowne thrust, Gupta 1973). It is possible that the Chur thrust and the Lansdowne thrust are equivalent.

5.5 TECTONIC IMPLICATIONS

Many of the granites and the augen-gneisses in the Lesser Himalaya belt are similar to the Chur granite in their structural setting, petrography and field relations (for reviews see Valdiya 1980b; Thakur 1983). Most of them are porphyritic in the central part but become (augen) gneissic near the margin and occur as gently-dipping concordant sheet-like bodies. In general they have been interpreted to be loccolithic/sheet intrusions in the metasedimentary country rocks. A granitic magma rich in large megacrysts would be very viscous and should be expected to be diapiric rather than laccolithic intrusion. Further, if the mylonitized contact is due to the forceful intrusion then the mylonite fabric should be early Paleozoic or older in age

which is the age of most of these granites. However, the age of mylonitisation is invariably Tertiary (e.g. Hubbard & Harrison 1989). A careful survey of the published descriptions of many of the so-called augen gneisses suggest that they are granite mylonite. For example, an 800 m thick concordant "augen gneiss", supposedly an intrusion into the metamorphic country rocks, has been shown to be a granite mylonite (Gururajan 1990). Therefore, it seems likely that some or even majority of these granites and augen gneisses occurring in the Lesser Himalaya belt are thrust slices. It is necessary to map these granites and re-examine their tectonic settings because most of them have not been studied in detail. The root zone of these possible thrust sheets are also not known. If the (unexposed) basement to the metasedimentary rocks of the HHCZ is granitic then some of the granites and augen gneisses belonging to the Lesser Himalaya belt may represent basement thrust slices.

The conclusion that the Chur granite corresponds to a thrust sheet and suggestion that many of the Lesser Himalayan granites may have the same contact relations potentially have regional implications. The implication is that there is another, probably basement involved thrust sheet sitting at a higher structural level than the MCT. If this is true it would require us to rethink about the amount of shortening that was partitioned into the Himalaya per se rather than distributed over Tibet and SE Asia in Miocene time which is the probable age of this thrust. However, the estimation of the shortening during the Himalayan orogeny is beyond the scope of the present investigation.

FIGURES

CHAPTER - 5

FIGURE 5.1 Geological map of the Himachal-Garhwal-Kumaun Himalaya showing the locations of the Chur and some of the other granite bodies of the "Lesser Himalaya" belt of Le Fort (1988). The geological map is after Paul & Roy (1991) and the locations of the granite bodies are from Thakur (1980, 1981).

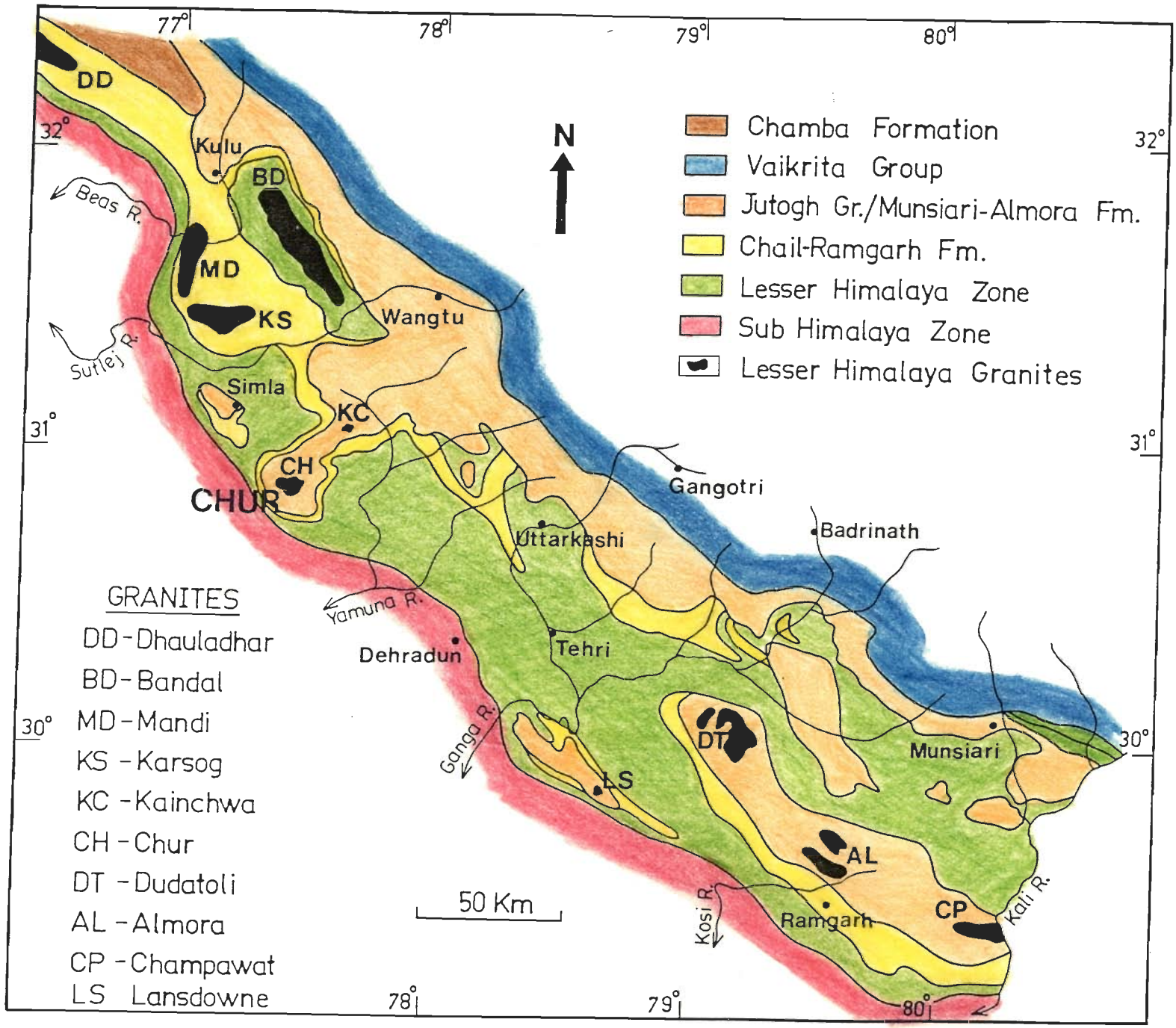
77°
78°
79°
80°
32°
31°
30°
N
Chamba Formation
Vaikrita Group
Jutogh Gr./Munsiari-Almora Fm.
Chail-Ramgarh Fm.
Lesser Himalaya Zone
Sub Himalaya Zone
Lesser Himalaya Granites
DD
Kulu
BD
Beas R.
MD
KS
Wangtu
Sutlej R.
Simla
KC
CH
CHUR
Gangotri
Badrinath
Uttarkashi
Yamuna R.
Dehradun
Tehri
Ganga R.
DT
Munsiari
LS
AL
Kosi R.
Ramgarh
CP
Kali R.
50 Km
GRANITES
DD - Dhauladhar
BD - Bandal
MD - Mandi
KS - Karsog
KC - Kainchwa
CH - Chur
DT - Dudatoli
AL - Almora
CP - Champawat
LS Lansdowne

Fig. 5.1

FIGURE 5.2 The klippe and half-klippe of the HHCZ thrust sheet (locally called the Jutogh thrust sheet) in the Simla-Chur peak area (simplified after Pilgrim & West 1928; Srikantia *et al.* 1978; Bhargava 1980; Srikantia & Bhargava 1988) showing that the exposures of granite are preserved only when the elevation exceeds above 3000m. For example, in the Simla klippe where the maximum elevation is about 2000m, there is no exposure of granite.

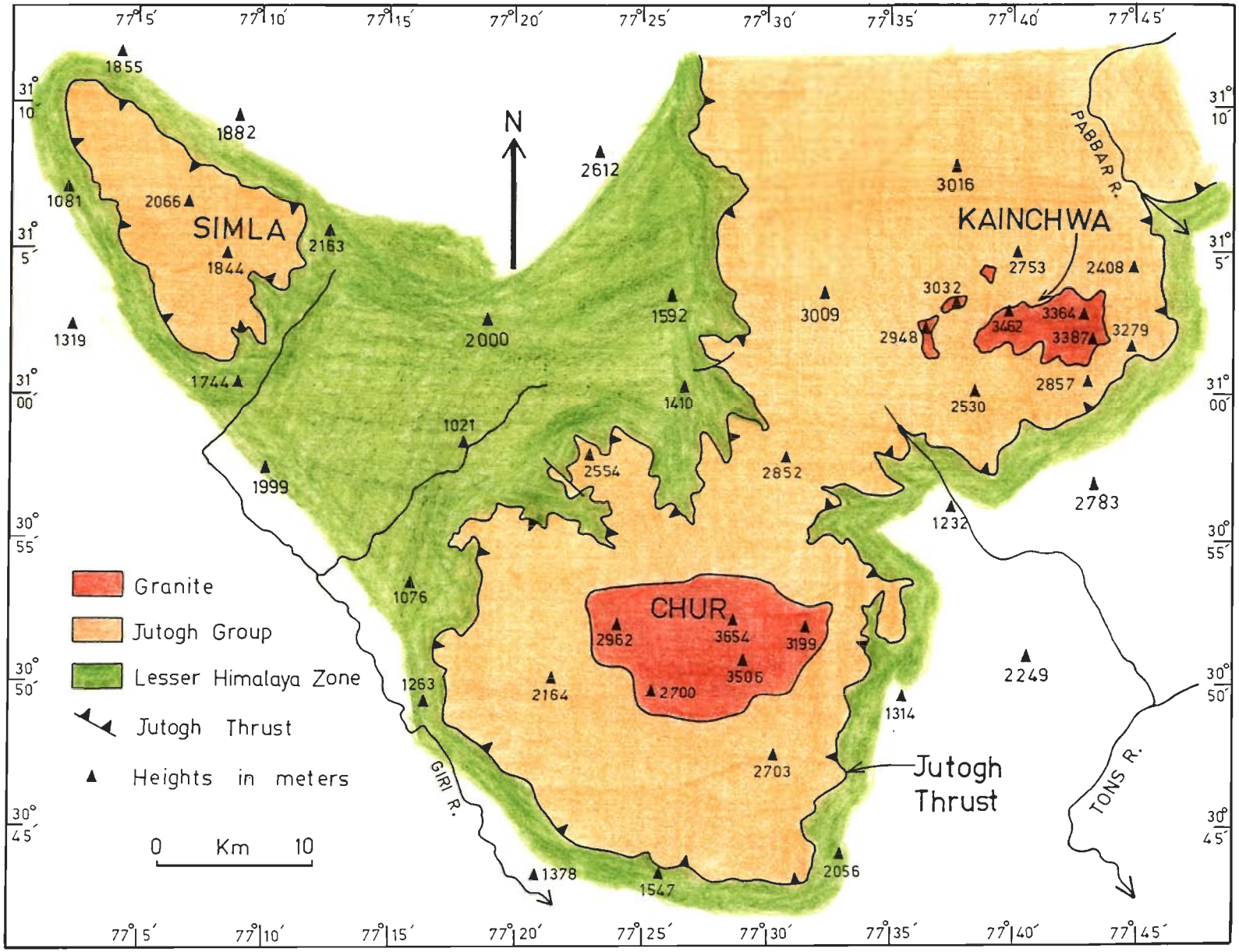
77°5′
77°10′
77°15′
77°20′
77°25′
77°30′
77°35′
77°40′
77°45′
31° 10′
31° 5′
31° 00′
30° 55′
30° 50′
30° 45′
N
SIMLA
KAINCHWA
CHUR
PABBAR R.
GIRI R.
TONS R.
Jutogh Thrust
Granite
Jutogh Group
Lesser Himalaya Zone
Jutogh Thrust
Heights in meters
0 Km 10
1855
1882
1081
2066
2163
1844
1319
1744
2000
2612
1592
1410
1021
1999
2554
2852
3009
3016
2753
2408
3032
3364
3462
3387
3279
2948
2857
2530
2783
1232
1076
2962
3654
3199
3506
2700
2164
1263
2249
1314
2703
1378
1547
2056

Fig. 5.2

FIGURE 5.3 Structural map of the Chur granite. The contact of the granite is slightly modified after Pilgrim & West (1928).

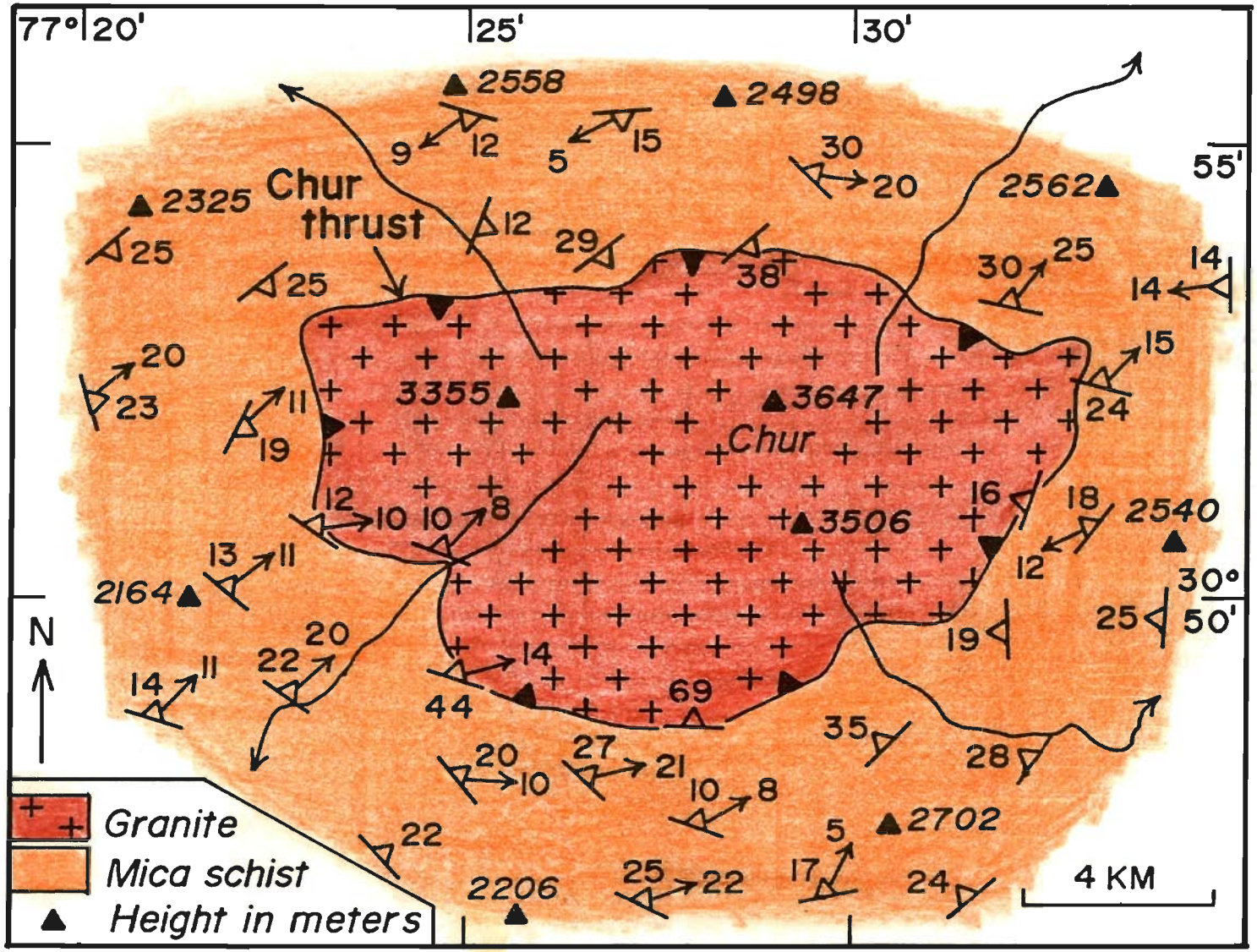
77°
20'
25'
30'
55'
30°
50'
2558
2498
2562
2325
Chur thrust
2164
3355
3647
Chur
3506
2540
2702
2206
N
Granite
Mica schist
Height in meters
4 KM

Fig. 5.3

FIGURE 5.4 Structural map of the granite contact in the SW of the Chur peak showing that the contact is concordant with the foliation planes in both the granite and surrounding mica schist. Inset shows stereographic plots of poles to foliation planes (contoured) and stretching lineations (dots) measured from near the contact. The β-axis corresponds to the folds developed during thrusting.

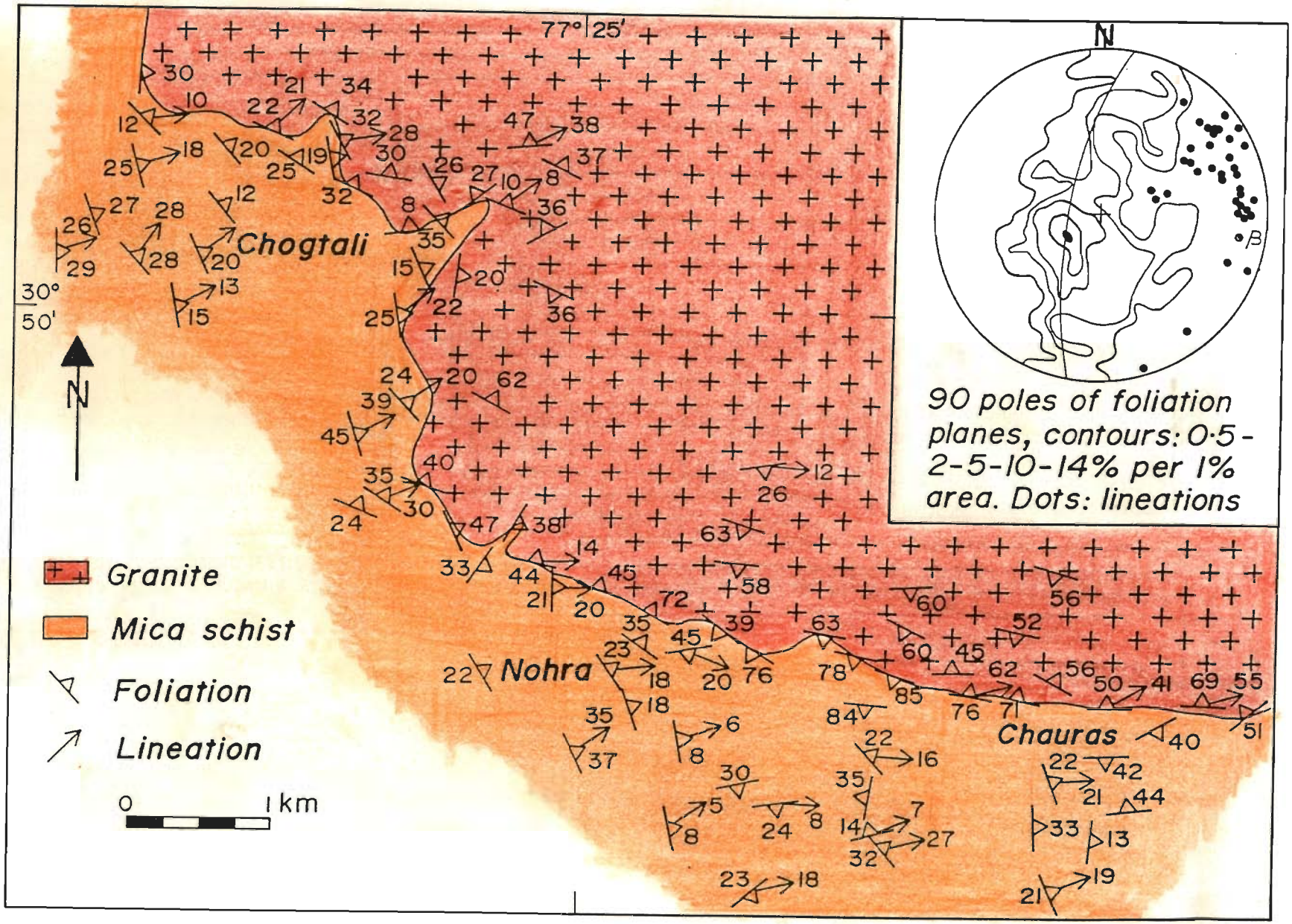
77° 25'
30° 50'
Chogtali
Nohra
Chauras
N
β
90 poles of foliation planes, contours: 0·5 - 2-5-10-14% per 1% area. Dots: lineations
Granite
Mica schist
Foliation
Lineation
0
1 km

Fig. 5.4

FIGURE 5.5 GRANITES IN OUTCROP AND HAND SPECIMEN

(a) Undeformed granite with large randomly oriented K-feldspar megacrysts in a coarse grained matrix defining porphyritic texture. Location: Chur peak.

(b) Polished slab of a deformed granite with mylonitic foliation anastomosing around large K-feldspar megacrysts. Location: 1 Km SW of Munalog.

(c) Deformed granite with preferred dimensional orietation of elliptical K-feldspar megacrysts parallel to the mylonitic foliation. Some of the megacrysts have been broken into much smaller peices. Note very long quartz ribbons wrap around megacrysts. Location: Chauras.

(d) Polished slab of a deformed granite showing only a few megacrysts in strongly foliated matrix. Location: NE of Chogtali.

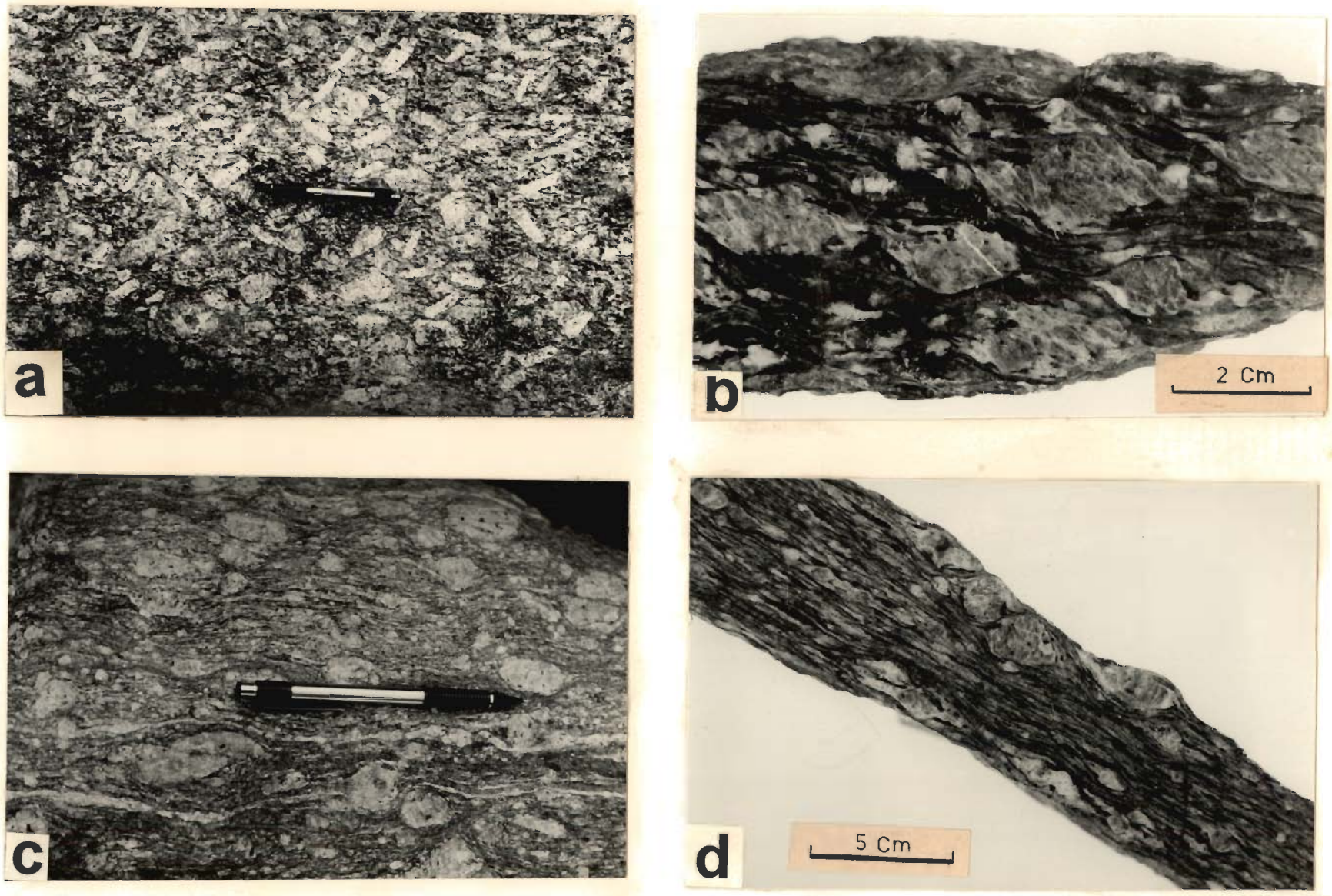

Fig. 5.5

FIGURE 5.6 GRANITES IN OUTCROP AND THIN SECTION

(a) Highly deformed granite near the contact with mica schist (not seen in the photograph) showing lenticular megacrysts in a well foliated matrix. The rock has the appearance of augen gneiss. Location: 4 Km E of Nohra.

(b) Gently-dipping razor-sharp contact (parallel to pen) between the granite ultramylonite (upper part) and the Jutogh quartzose mica schist. The granite is devoid of any megacryst. A few meters above the contact as well as along the strike (outside the field of view) megacrysts are present and help in recognizing the ultramylonite to be granite. A thin concordant quartzose mica schist (arrow) can be seen within the granite. Location: 1 Km NW of Chogtali.

(c) Photomicrograph of an undeformed (as seen in hand specimen) granite. Base: 1.6 mm. Crossed nicols. Location: 1.5 Km NE of Chogtali.

(d) Weakly deformed granite showing undulose extinction and fine recrystallized grains at the grain boundaries giving core-and-mantle texture. Base: 2 mm. Crossed nicols. Location: 4 Km E of Phagu.

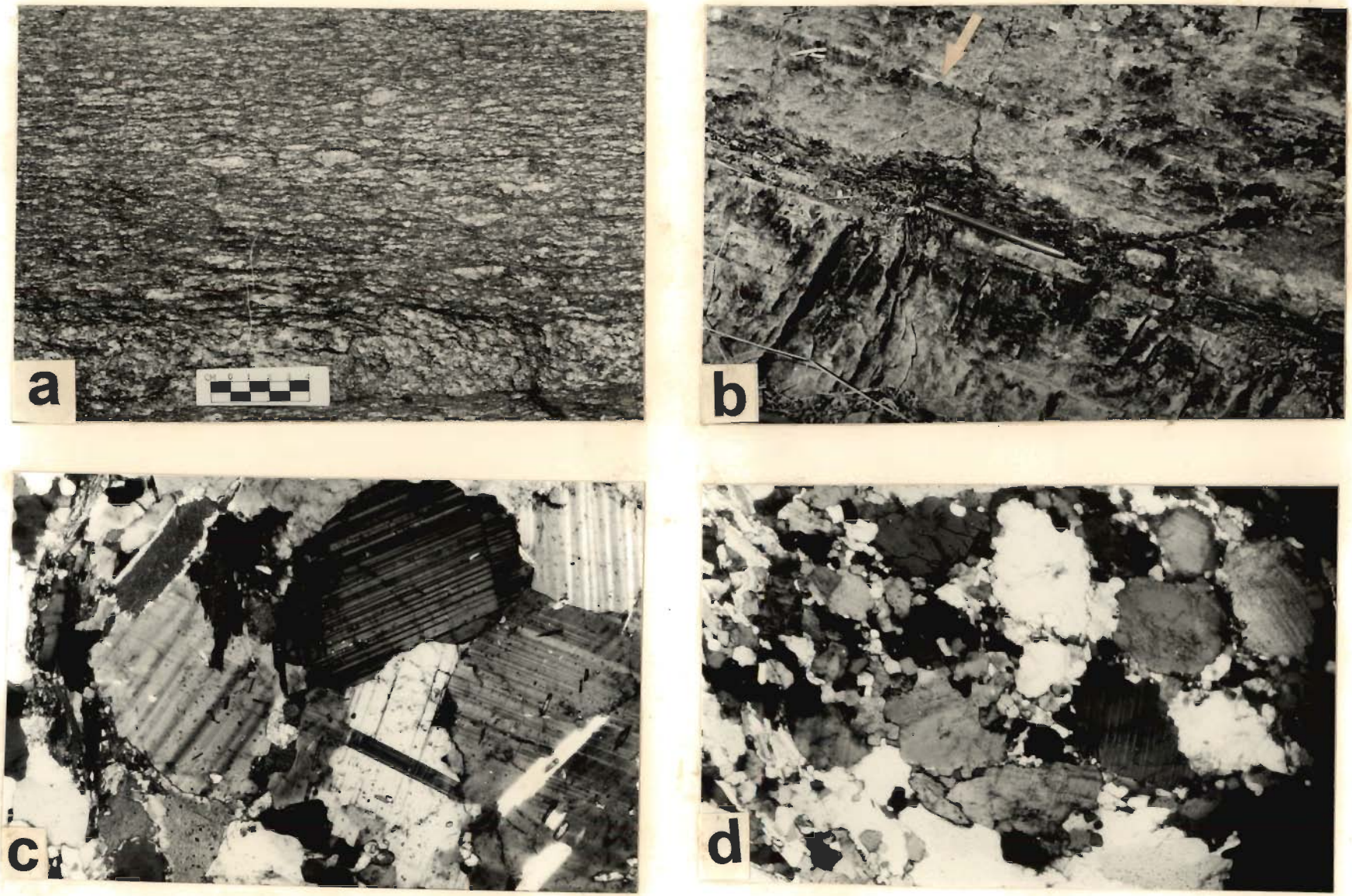

Fig. 5.6

FIGURE 5.7 PHOTOMICROGRAPHS OF GRANITE MYLONITE

(a) Protomylonite showing strained porphyroclasts of quartz and feldspars in fine grained recrystallized matrix. Note a weakly developed mylonitic foliation. Base: 5.2 mm. Crossed nicols. Location: 2.5 Km SW of Sarahan.

(b) Negative print of an orthomylonite showing mylonitic foliation wrapping around highly strained elliptical K-feldspar megacrysts. Base: 3.9 Cm. Crossed nicols. Location: NE of Chogtali.

(c) Boudinaged K-feldspar megacryst (Kf) with strain-free subgrains near the margin. Note mylonitic foliation in the lower part. Crossed nicols. Base: 8 mm. Location: 4 Km east of Phagu.

(d) Mylonitic foliation defined by recrystallized quartz and mica (dark) ribbons. Base: 5.2 mm. Crossed nicols. Location: NE of Chogtali.

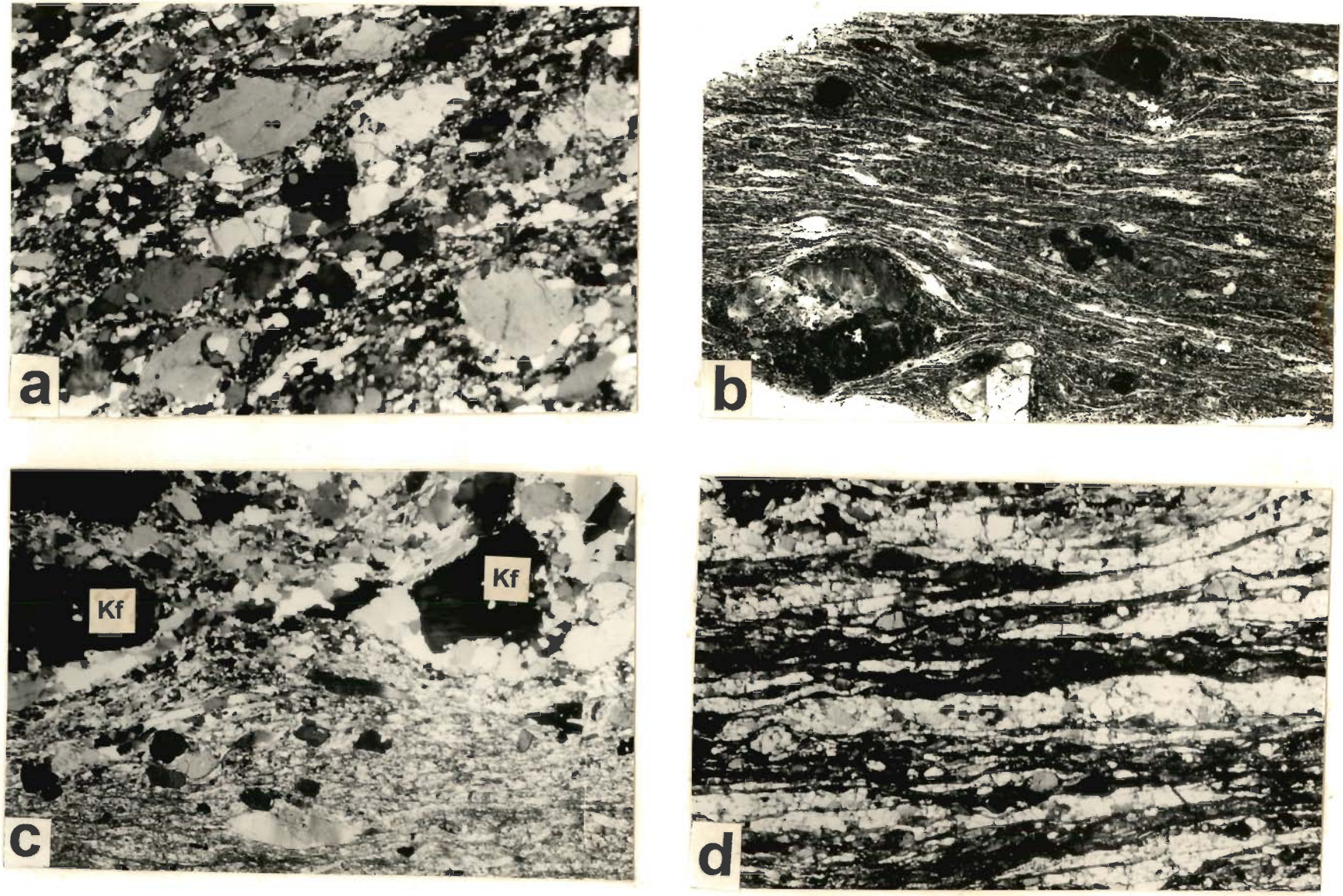

Fig. 5.7

FIGURE 5.8 Histograms of the angles (ø, clockwise positive, between the long axis of the K-feldspar megacrysts and the reference line) and the % frequency of the number of grains. Reference lines are traces of mylonitic foliation in (d) to (i) and arbitrary in (a) to (c). a-c: unfoliated/very weakly foliated granites, d-f: moderately foliated granites, and g-i: strongly foliated granites. Note that with the increase in the degree of development of the (mylonitic) foliation the long axes of the megacrysts acquire a preferential orientation (sub)parallel to the trace of the foliation. All measurements were made on field photographs. N: number of data.

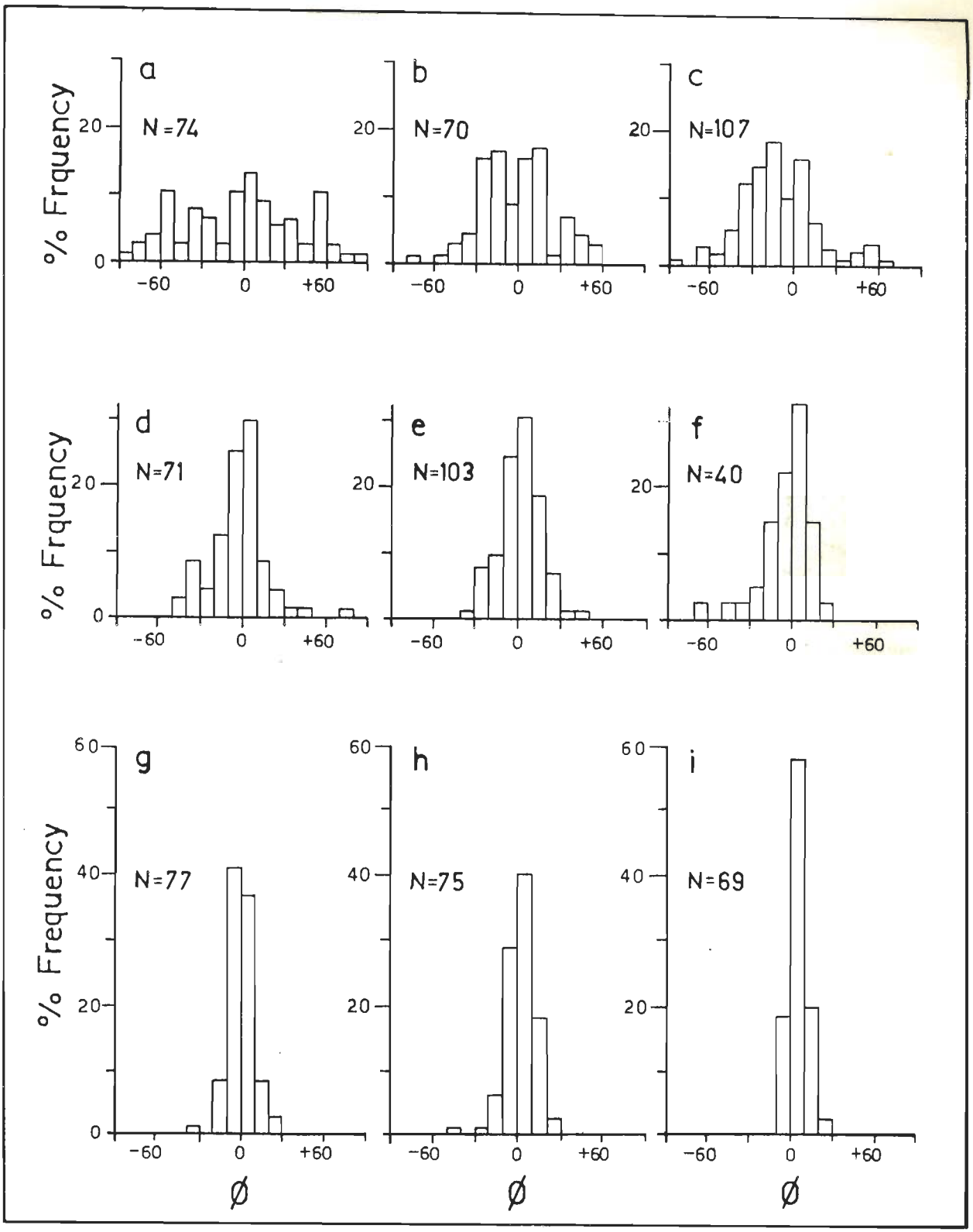
a
N=74
b
N=70
c
N=107
d
N=71
e
N=103
f
N=40
g
N=77
h
N=75
i
N=69
% Frquency
% Frequency
20
40
60
0
-60
0
+60
ø

Fig. 5.8

CHAPTER - 6
MICROSTRUCTURES AND METAMORPHISM

6.1 PORPHYROBLAST-MATRIX RELATIONSHIPS

The microstructural relationships between porphyroblasts and matrix foliations (Zwart 1962; Spry 1969) have been used by many workers to elucidate relative timing between the episodes of metamorphism and deformation. Lucid reviews on this topic have been given by Vernon (1978, 1989).

Following general practice the cleavage in the matrix will be designated as S_e (e for "external") and the cleavage inside the porphyroblast traced by inclusion trails will be referred to as S_i (i for "internal"). The microstructural criteria that are often used are sometimes ambiguous, leading to equivocal tectono-thermal interpretations (e.g. Vernon 1978; Bell 1985; Bell &Johnson 1989, Bell *et al.* 1992; Johnson 1993). As emphasized by Vernon (1978), it is insufficient to describe a porphyroblast as "pretectonic", "syntectonic" or "post-tectonic" without detailed characterization of the s-surfaces (S_e) or the fold sets in the matrix. It has been shown in chapter-3 that there are three types of cleavage surfaces (i.e. S_e), viz., S_1, S_2 and S_m related to F_1 folding, F_2 folding and ductile shearing respectively in this area. Further, S_m include several (but unknown number of) generations of mylonitic foliations developed during the progressive ductile shearing. It is also probably necessary to clearly state the criteria that have been used in a particular study to elucidate relative time relations between the crystallization of metamorphic minerals and the deformation episodes. some of the more important criteria used in this study have been summarised in Fig. 6.1.

Owing to its critical significance in the present area the microstructural relation where S_e or axial planes of folds are deflected (i.e. swerves) around porphyroblasts (Figs. 6.1a,b,e,i) needs a detailed discussion. The relative chronology between porphyroblast and the matrix foliation in this type of microstructural relation has been much debated. Some workers (e.g. Misch 1971, 1972) suggest that the matrix cleavage is deflected by the growing crystals which implies that such porphyroblasts are

postkinematic with respect to the matrix cleavage. Others suggest that the growth of the porphyroblasts is prior to the deformation that produced the cleavage in the matrix i.e., the S_e (Zwart 1962). The second view is favoured here for several reasons: (1) The maximum compressive stress is in general inferred to be perpendicular to a cleavage surface. Therefore, intuitively it seems unlikely that a syntectonic porphyroblast would grow and deflect cleavage surfaces against maximum compressive normal stress (Vernon 1978). (2) Very common occurrence of S_i (sometimes of several generations, e.g. Bell & Johnson 1989) prove that in a very well foliated rock a growing porphyroblast usually incorporates matrix cleavage traces as S_i. If a growing porphyroblast deflects S_e then S_i should indeed be rare. (3) Numerical experiments by Ghosh (1977; see also Ghosh 1975; Ghosh & Ramberg 1976) show that the drag patterns in the deforming matrix swerve around a pre-existing rigid inclusion. (4) A very convincing evidence comes from the Chur granite of this area. It has been shown (chapter-5) that in the undeformed portions of the granite randomly oriented rectangular K-feldspar megacrysts occur in an unfoliated matrix. This granite is strongly mylonitized near the Chur thrust where augen-shaped K-feldspar megacrysts occur in a matrix that shows very well developed mylonitic foliation. The mylonitic foliations in the granite mylonite are always strongly deflected around the megacrysts (Fig. 6.1i). Of course there is no doubt that the megacrysts are prekinematic with respect to the formation of the mylonitic foliation. Therefore, porphyroblast showing similar textural relationship should be treated as pre-kinematic with respect to the development of S_e.

6.2 MINERAL FORMATION IN RELATION TO DEFORMATION EPISODES

6.2.1 Chlorite

Chlorite shows wide variation in microstructural relations. Some of the chlorite grains occur as flakes. They are evenly dispersed and are aligned parallel to the S_1 cleavage suggesting that they are synkinematic with F_1. These chlorite grains have formed during the progressive metamorphism and not during retrogression. Sometimes

chlorite porphyroblasts overgrow and incorporate S_1 cleavage where S_i and S_e are continuous (Fig. 6.2a,b) indicating that these chlorites are post-F_1. Where S_1 is involved in F_2 crenulations the S_i ($=S_1$) is either straight (Fig. 6.2a) or crenulated (Fig. 6.2b). In the later case the crenulations in the matrix are tighter than the crenulation defined by S_i. Strong undulose extinction and kinked cleavage traces in these chlorite porphyroblasts suggest that they have been deformed by the F_2 folding. In summary, the chlorites started forming synkinematically with respect to F_1 and continued to crystallize during the F_2 deformation. However, the crystallization of chlorite does not outlast the second deformation. In the Chail phyllites the syn-F_1 chlorites are common but post-F_1 porphyroblast absent. In the rocks of the Jutogh Group both syn- and post-F_1 chlorites are very common near the base but become progressively scarce upwards and finally disappear at the middle levels of the mica schist unit. In the Jutogh rocks post-F_1 chlorite porphyroblasts are retrograded from garnet and biotite. In some examples garnets form armoured relicts around which chlorite porphyroblasts grow (Fig. 6.2c). At other places garnets are completely destroyed and pseudomorphed by a "pool" of fibrous chlorite grains. S_1 cleavage traces sometimes form S_i trails in such chlorite porphyroblasts suggesting chloritization to be post-F_1.

Chlorite grains have crystallized very extensively during ductile shearing. Relatively inclusion-free chlorite flakes are sometimes oriented parallel to the mylonitic foliation (S_m) suggesting that they are synkinematic with respect to the S_m (Fig. 6.2d). Some of these grains, however, show evidence of extensive post-crystalline deformation and could also be relict syn-F_1 chlorite grains. In ductile shear zones and specifically in the two carbonaceous bands chlorite porphyroblasts usually contain S_i which is continuous with S_e ($= S_m$) (Fig. 6.3a). When these porphyroblasts are favourably oriented they show typical "mica fish" structure (Fig. 6.3b, cf. Lister & Snoke 1984). In some porphyroblasts the straight S_i are at high angle to and abut

against the S_e (Figs. 6.3c,d) indicating that they are prekinematic with the matrix foliation. But most interestingly both the S_i and S_e are mylonitic foliations. The S_i represents an early mylonitic foliation which has been completely obliterated by the later mylonitic foliation represented by the S_e (stage 6 of Bell & Rubenach 1983). In the pressure shadows of these chlorite as well as garnet porphyroblasts fine needles of chlorite are oriented parallel to the S_e (= S_m) (Fig. 6.3d). These are synkinematic with the mylonitic foliation in the matrix. All these features show that crystallization of chlorite grains was very extensive during the progressive ductile shearing.

6.2.2 Biotite

Biotite is absent in the Chail Formation except at a small locality near Haripurdhar. It makes its first appearance at the Jutogh thrust and is present in all the rock types of the Jutogh Group and the Chur granite.

Biotites with strong preferred dimensional orientations defining the S_1 cleavage are syntectonic with respect to the F_1 deformation. At some places prismatic biotite porphyroblasts with cleavage traces at high angle to the S_1 are present. Straight inclusion trails in some of these porphyroblasts are continuous with S_e (= S_1). These are late- to post-tectonic with reference to F_1. At the hinge zones of F_2 crenulations the biotites show kinking, bending and undulose extinction and are prekinematic with reference to F_2. However, at some of the hinges of F_2 crenulation folds biotites are sharply recrystallized. Where S_2 crenulation cleavage is very well developed the same is sometimes defined by the recrystallized biotite grains. Therefore, the crystallization of biotite started syntectonically with F_1 but outlasted the F_2 deformation.

The biotite in the ductile shear zones shows strong post-crystalline deformation. Often biotite porphyroblasts are broken into small pieces, recrystallized and smeared along the mylonitic foliation. These recrystallized biotite are synkinematic with ductile shearing. Rarely, prismatic biotite porphyroblasts occur randomly oriented in a mylonitized matrix. Some of these biotites are deformed indicating that they formed at

an early stage of ductile shearing. However, some of these biotite porphyroblasts are relatively strain-free suggesting that they grew at the later stage of the ductile shearing. Therefore, rather recrystallization of biotite has taken place syntectonically with the progressive ductile shearing. But the recrystallisation of biotite is less extensive during ductile shearing than the recrystallisation of chlorite.

6.2.3 Garnet

The garnet porphyroblasts (Figs. 6.4, 6.5) make their first appearance in the lower carbonaceous band (i.e. above the Jutogh thrust). They are present in all the rock types of the Jutogh Group but are completely absent in the rocks of the Chail Formation in this area. There is a bimodal distribution of the size. The bigger grains are subrounded to irregular in shape (Figs. 6.4a,c,d, 6.5a,c) and are usually inclusion rich (Figs. 6.4a, 6.5a,c). The smaller grains, on the other hand are polygonal and they are either inclusion free or contain a few unoriented inclusions (Figs. 6.4b, 6.5b).

Some of the garnet porphyroblasts have small (as compared to the grains in the matrix) unoriented inclusions and occur in a matrix with well developed S_1 cleavage. These are possibly pre- or early-tectonic with respect to the formation of S_1 cleavage. Others have inclusion-trails defining S_i that are either spiral-shaped (Fig. 6.4a) or straight which are continuous with the S_1 cleavage ($=S_e$). These porphyroblasts are syn- to post-kinematic with reference to F_1. In some of the larger porphyroblasts unoriented inclusions are present throughout the porphyroblasts giving a skeletal appearance. The included quartz grains are usually equant and relatively coarse. These porphyroblasts are elongate along S_1 and are sometimes fractured and boudinaged suggesting syntectonic growth during F_1. More often the garnets have inclusion-rich cores and inclusion-free rims (Fig. 6.5c). The inclusions in the core are either unoriented (Fig. 6.5c) or they form straight or spiral-shaped S_i. Less common are those large porphyroblasts which are virtually inclusion free. This type of microstructure suggest two stage growth. The inclusion-rich cores are early- to late-tectonic with

respect to F_1 but the inclusion-free rims possibly overgrew in a static phase post-dating F_1 deformation. The inclusion-free porphyroblasts and small polygonal grains are contemporaneous with this phase. The axial planes of F_2 microfolds (Fig. 6.4c) and S_2 crenulation cleavage swerves around the garnet porphyroblast suggesting pre-kinematic crystallisation with reference to F_2.

The garnet porphyroblasts in the ductile shear zones (Figs. 6.4d, 6.5a-d) show some interesting microstructural relations. The mylonitic foliation invariably swerves around the garnet porphyroblasts (Figs. (6.5a,c). Nowhere, the S_i in garnet is continuous with the mylonitic foliation in the matrix ($S_m = S_e$). The axial planes of isoclinal folds traced by quartz ribbons in ultramylonites also swerves around the garnet porphyroblasts (Fig. 6.5c). Microfolds on mylonitic foliations abut sharply against garnets. The tightness of these microfolds decreases away from the garnet porphyroblasts (Fig. 6.5b). Strain-shadow zones (Figs. 6.3d, 6.4d) are usually present in which often there is a mylonitic foliation. The mylonitic foliation in the strain shadows often asymptotically meets the mylonitic foliation in the matrix (Fig.6.4d). Broken pieces of garnet are often strewn along the mylonitic foliations (Fig. 6.5d). The garnet porphyroblasts are, therefore, completely pretectonic with respect to the ductile shear deformation.

6.2.4 Staurolite

The staurolite porphyroblasts are present only in the mica schist between the upper carbonaceous band and the Chur granite. They are absent in all other rock types. They are very common in the western part but occur sporadically in the rest of the mica schist unit.

The staurolite porphyroblasts have the similar microstructural relations as that of garnet. Spiral-shaped or straight S_i are continuous with the S_e (= S_1) suggesting syn- to post-tectonic growth with respect to F_1. The axial planes of F_2 microfolds and S_2 crenulation cleavage are usually deflected around the staurolite porphyroblasts

indicating prekinematic growth with respect to the second deformation (F_2). Within staurolite porphyroblasts garnets are sometimes present pointing to garnet to staurolite transformation during progressive metamorphism. In the ductile shear zones the mylonitic foliations are invariably deflected around the staurolite porphyroblasts (Fig. 6.6a). They usually show strong undulose extinction indicating post-crystalline deformation. They are often boudinaged (Fig. 6.6b), broken into small pieces and are strewn along the mylonitic foliation (Fig. 6.6a). Strain-shadow zones are commonly present. All these lines of evidence suggest that the staurolite porphyroblasts are completely prekinematic with reference to the ductile shearing. In the shear zones staurolites retrograde to biotite and rarely to chlorite. These retrograded biotite and chlorite laths usually occur in the strain shadow zones and in the necking zones between the boudinaged staurolites (Fig. 6.6b).

6.2.5 Kyanite and sillimanite

Kyanite and sillimanite have been observed only in a few thin sections. They occur in mica schist near the Chur thrust and in the Chur granite at a few places. Owing to their restricted occurrence and small grain sizes microstructural relations of these two minerals are relatively less certain. Bladed crystals of kyanite and fibrolitic sillimanite, however, invariably show evidence of strong post-crystalline deformation. Only in one thin section, kyanite blades are sufficiently large to show that mylonitic foliation swerves around the porphyroblast (Fig.6.6c), similar to garnet and staurolite porphyroblasts. Kyanites sometimes show straight S_i (= S_1) traced by fine biotite flakes and elongated quartz grains. The S_i is usually oblique to and abut against S_e (= S_m). These features, together with strong post-crystalline deformation indicate that kyanite and sillimanite are prekinematic with respect to the ductile shearing.

6.2.6 Amphiboles

Tremolite-actinolite in calc-silicate rocks and hornblende in amphibolites usually define S_1 cleavage and are therefore syntectonic with F_1. Where S_1 is involved in F2

crenulations, amphibole prisms are bent, broken and show undulose extinction suggesting deformation during F_2. A few amphibole grains have grown across S_2 crenulation cleavage suggesting that crystallization of amphiboles outlasted F_2 deformation. Hornblende in amphibolite caught up in ductile shearing usually shows evidence of post-crystalline deformation. However, at places where shearing is very intense grain-size reduction via recrystallization and neomineralization have been observed in amphibole. The recrystallized grains are extremely fine-grained in such cases. No prismatic crystal syn- to post-kinematic with ductile shearing has ever been observed.

6.2.7 Other minerals

Quartz, muscovite and calcite grains have (re)crystallized over a wide range of time. Crystallization of these minerals started at an early stage of the F_1 deformation and outlasted the ductile shearing episode. Tourmaline and epidote group of minerals are fairly common in the rocks of the Jutogh Group. When porphyroblastic these minerals are invariably syn-tectonic with early deformations (i.e. F_1-F_2) but prekinematic with reference to the ductile shearing (Fig. 6.6d). Small equant grains of tourmaline and epidote have however, crystallized syntectonically in shear zones. Plagioclase mostly crystallised during F1 and F2 deformations but syntectonic recrystallisation with respect to ductile shearing is also common.

6.3 COMMENTARY ON METAMORPHISM

The rocks of the Chail Formation in this area contain only chlorite among the metamorphic index minerals of the Barrovian sequence. Garnet is totally absent and biotite is present only in a small area near Haripurdhar. Both biotite and garnet mark their first appearance in the lower carbonaceous band i.e. at the Jutogh-Chail contact indicating a break in metamorphic grade at the Jutogh thrust where the biotite zone of the Barrovian sequence is absent. In all the rock types of the Jutogh Group both biotite and garnet are present. Staurolite is unevenly distributed in the mica schist occurring

above the upper carbonaceous band. Therefore, the mica schist unit is in the staurolite grade while the quartzite unit is in the garnet grade. Since staurolite forms in rocks with restricted bulk composition (Mueller &Saxena 1977 p.192, Yardley 1989 p.67-68) no attempt has been made to draw the garnet-staurolite isograd. Kyanite and sillimanite are present in both the Chur granite and the mica schist in the vicinity of the Chur thrust. In this area the sedimentary rocks of the LHZ are overlain by progressively higher grade metamorphic rocks which occur at successively higher topographic levels as was originally shown by Pilgrim & West (1928). This so-called inverted metamorphism has subsequently been described in other parts of the Himalaya by many workers (see section 1.3.3).

The microstructural relations show that the garnet, staurolite and possibly kyanite/sillimanite are pretectonic with respect to the ductile shearing. They are mostly syn- to post-F_1 deformation but pretectonic with respect to the F_2 deformation. Chlorite has crystallized very extensively during both F_1 and F_2 folding and ductile shearing. Biotite has the same relation as chlorite but (re)crystallization during the ductile shearing is much less extensive as compared to chlorite. We can, therefore, conclude that the main phase of progressive metamorphism is broadly synchronous with the early deformation episodes or, in other words, completely predates the ductile shearing. During ductile shearing a retrograde metamorphism commonly producing chlorite and less extensively biotite can only be recognized. The relationship between the crystallisation of the main metamorphic minerals in relation to the deformation events has been shown in Table 6.1.

In this area it is certain that the progressive metamorphism is earlier than the ductile shearing and is broadly synchronous with early (i.e. F_1-F_2) deformation episodes. The ductile shearing and thrusting in this area can be confidently related to deformations during Himalayan orogeny. Radiometric age determination on ductile shear zones in the Himalaya normally yield Tertiary ages (e.g. Hubbard & Harrison

1989). The leucogranites of the Higher Himalaya that have been derived by partial melting of the Himalayan crust (e.g. Le Fort 1981, Deitrich & Gansser 1981) also give Tertiary ages (e.g. Deniel *et al.* 1987, Copeland *et al.* 1991). The age of pre-shearing early deformation and metamorphism seen in this area is not available. Elsewhere in the Himalaya polyphase metamorphism has been documented (e.g. Pecher 1989; Pognate & Lombardo 1989; Staubli 1889). Some of these studies postulate that the earliest metamorphism is pre-ductile shearing but have had occurred during the post-collision early Tertiary time (e.g. Pecher 1989; Staubli 1989; England *et al.* 1992). Others (e.g. Pognate & Lombardo 1989) consider the earliest metamorphic imprint is pre-Himalayan, possibly Palaeozoic or even older. However, the rocks of the HHCZ are generally considered to be part of the northern margin of the Indian Peninsula of Precambrian age. It is therefore possible that the early deformations and consequently the metamorphism seen in the Chur area may be Precambrian in age. In that event, of course, neither the early deformations nor the progressive metamorphism could be related to the Himalayan orogeny.

Many models have been proposed to explain the inverted metamorphism in the Himalaya. These models are broadly of two types. One group of models postulate inverted metamorphism to be due to thermal perturbation during the Himalayan deformation. These include hot-over-cold model (Oxburgh & Turcotte 1974; Le Fort 1975 and others), heat focus ing in the upper part of the HHCZ by the low-conductive sedimentary rocks of the HHSZ (Jaupart & Provost 1985), shear heating along the MCT (Scholz 1980; Arita 1983; England & Molnar 1993 and others) and thermal buffering by crustal anatexis (Hodges *et al.* 1988). However, in all these models metamorphism needs be syn- to post-tectonic with reference to the movement along the MCT contrary to the observations in the present area. The second group of models implies that the inverted metamorphic isograds is a consequence of some structural geometry. These models include post- (Ray 1947) or syn-metamorphic (Searle & Rex

1989; Treloar *et al.* 1989) recumbent folding and syn- (Jain & Manickavasagam 1993) or post-metamorphic (Brunel & Kienast 1986; Hubbard 1994) ductile shearing/thrusting.

The relationship between deformation episodes and growth of metamorphic mineral suggests that the inverted metamorphic zones in this area is due to post-metamorphic imbrication of thin thrust slices. The thrust slices were derived from a terrain normal (i.e. upward decreasing) Barrovian metamorphic zones. The early thrust slices should comprise lower grade rocks as they would have come from relatively shallow depth. Later thrust slices would bring in higher grade rocks from deeper levels to rest at the top of the lower grade rocks. Although in each thrust sheet metamorphism would be normal, there will be an overall apparent increase in metamorphic grade at higher topographic and structural levels. There is a serious objection to this model of inversion of metamorphic zones by thrust imbrication. It would seem too much of a coincidence for each thrust sheet to bring up a particular metamorphic zone. However, thrust planes and isograds need not be parallel or coincidental. For example, as mentioned earlier, in this area biotite zone in the Chail Formation is truncated by the Jutogh thrust around Haripurdhar. Further, occurrence of staurolite is rather erratic and a more detailed study on the metamorphism than described in this chapter may reveal whether or not the Rajgarh thrust and the garnet-staurolite isograd are parallel or coincidental. The detailed maps showing relationships between isograds and thrusts are rare, primarily because identification of thrust planes in the Himalaya is not always easy and accessibility in this rugged terrain is a formidable problem.

FIGURES AND TABLES

CHAPTER - 6

FIGURE 6.1 PROPHYROBLAST-MATRIX FOLIATION REALTIONS
(a-h schematic, modified after Zwart 1962; Vernon 1978, 1989).

(a) S_e deflected around porphyroblast. The porphyroblast is pretectonic with respect to S_e. Inclusion-rich core and inclusion-free rim suggest two-stage growth. The core is pretectonic to S_e. Inclusion-free rim suggest static overgrowth.

(b) Straight S_i oblique to and abut against S_e. The porphyroblast is pretectonic with S_e but posttectonic with S_i. S_i represent an earlier fabric obliterated during development of a mew fabric in the matrix (S_e).

(c) Spiral S_i continuous with S_e suggesting syntectonic growth with S_e.

(d) Straight S_i continuous with S_e suggesting post-tectonic growth with S_e.

(e) Spiral S_i in the core and inclusion-free rim suggesting two stage growth. the core is syntectonic with a fabric now obliterated in the matrix during the formation of S_e. Swerving S_e and the porphyroblast suggest the porphyroblast is pretectonic with S_e.

(f) During the development of matrix (S_e) a pre-existing rigid porphyroblast is broken into pieces which are strewn along the foliation. This is not a paracrystalline boudinage (cf. Misch 1971).

(g) Crenulation on S_e sharply abut against porphyroblast which is pretectonic with respect to folding as well as Se.

(h) S_e is continuous with S_i and crenulation on Se is tighter than crenulation on S_i. the porphyroblast is post-tectonic with S_e but syntectonic with respect to crenulation folding.

(i) Mylonitic foliation traced by quartz ribbons in granite mylonite deflected around the lensoid shaped K-feldspar megacryst. Undulose extinction in the megacryst and dynamic recrystallisation around the megacryst noticeable. The megacryst is completetly pretectonic with respect to the formation of the mylonitic foliation. Base: 8 mm. Crossed nicols. Location: NE of Chogtali.

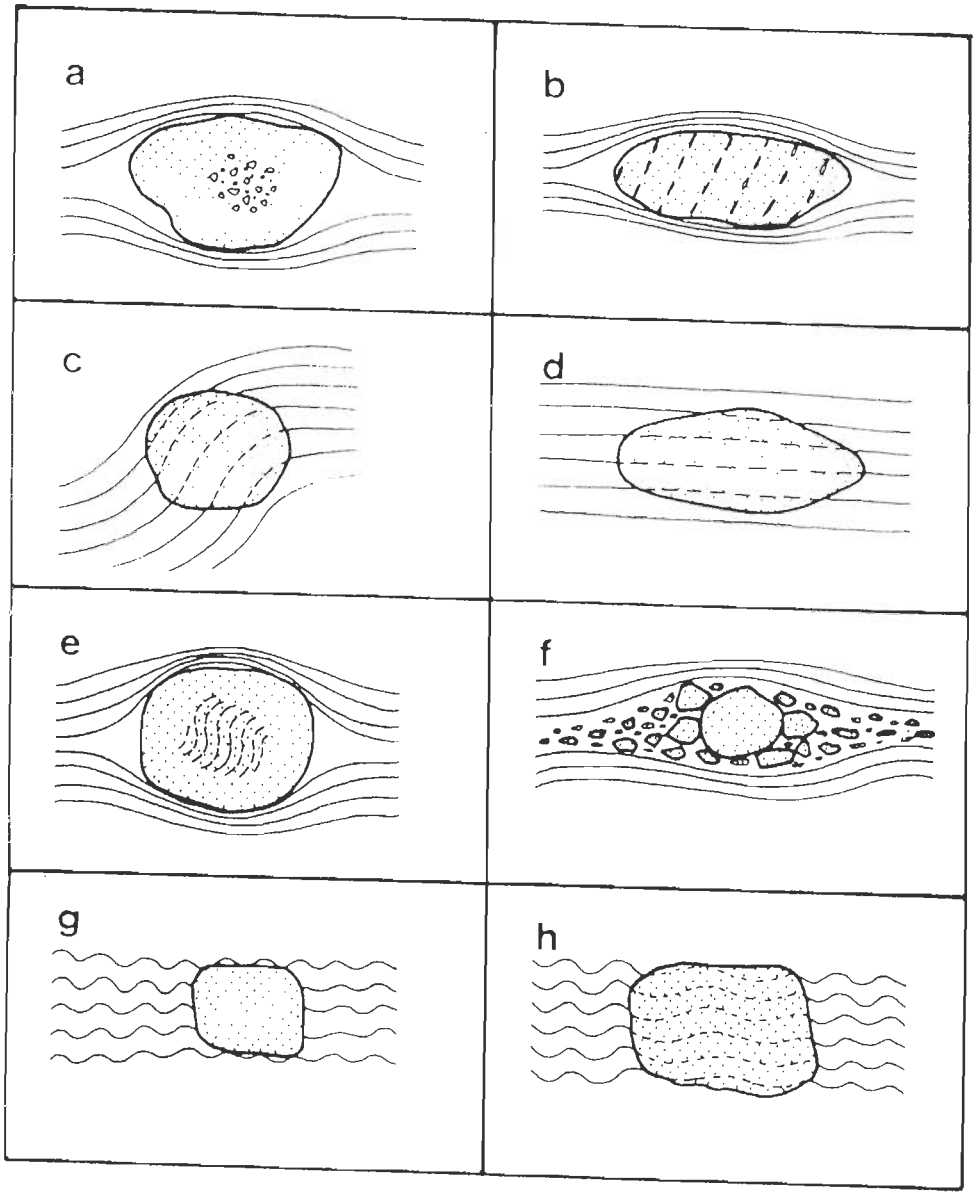

Fig. 6.1

FIGURE 6.2 CHLORITE MICROSTRUCTURES

(a) Straight S_i trail in chlorite porphyroblasts continuous with S_e ($=S_1$) in mica schist. The S_i in the matrix is involved in open F_2 crenulation (not seen in the photograph). The chlorite grains show slight undulose extinction. The chlorite porphyroblasts are post-F_1 but pre-F_2. Base: 2 mm. Plane-polarized light. Location: Bharari.

(b) Crenulated S_i trails in chlorite porphyroblast continuous with crenulated (F_2) S_e ($=S_1$) in the matrix in mica schist. The crenulations traced by S_i is more open than the crenulation in the matrix. The chlorite shows kinked cleavages and strong undulose extinction. The chlorite porphyroblast is syntectonic with F_2. Base: 2 mm. Oblique nicols. Location: Habban.

(c) Retrograde chlorite overgrowing garnet porphyroblast in mica schist. S_i ($=S_1$) in the chlorite porphyroblast noticeable. The retrogression of garnet to chlorite is post-F1. Base: 2 mm. Plane-polarized light. Location: Bharari.

(d) Inclusion-poor chlorite aligned parallel to the mylonitic foliation ($=S_e$) in quartzite. the chlorite is syntectonic with mylonitic foliation. Base: 1.8 mm. Plane-polarized light. Location: 4 Km NE of Kot.

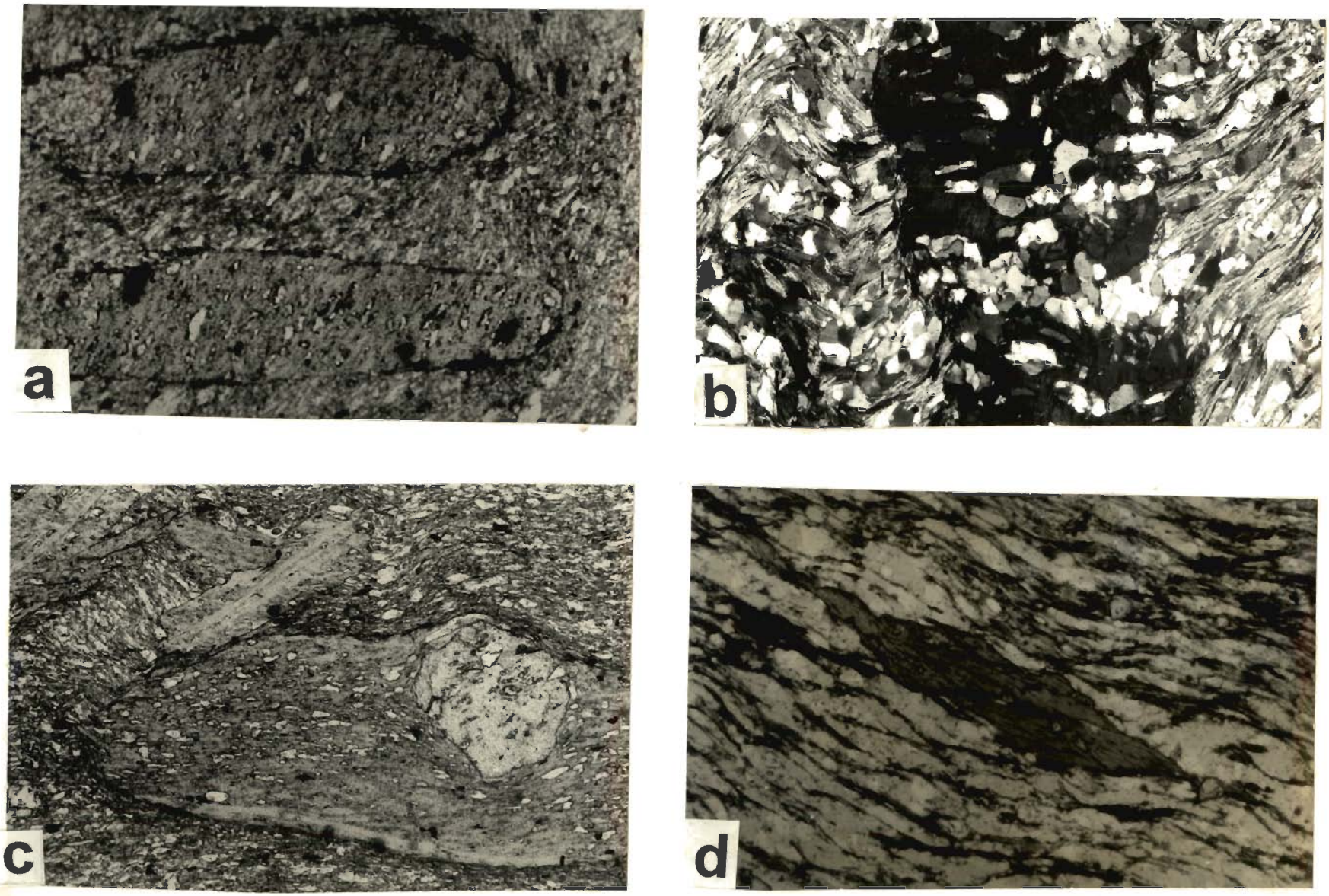

Fig. 6.2

FIGURE 6.3 CHLORITE MICROSTRUCTURES

(a) Slightly curved S_i trails, traced by carbonaceous matter and opaques, in chlorite continuous with mylonitic foliation in the matrix ($S_e = S_m$) in carbonaceous schist. The chlorite is syn- to late-tectonic with respect to ductile shearing. Base: 1 mm. Plane-polarized light. Location: Bogdhar.

(b) Chlorite porphyroblast in lower carbonaceous schist showing "fish"-type structure. The matrix cleavage is mylonitic foliation. Base: 2 mm. Plane-polarized light. Location: Bagi.

(c) Straight S_i ($=S_m$) in chlorite porphyroblast oblique and truncated by a later mylonitic foliaiton (S_e) in lower carbonaceous schist. the chlorite is post-tectonic with reference to the later mylonitic foliation seen in the matrix ($=S_e$). Base: 2 mm. Oblique nicols. Loocation: Bagi.

(d) Straight S_i in chlorite (upper right) nearly perpendicular to the S_e in lower carbonaceous schist. The S_i is an early mylonitic foliation completely obliterated by the later developed mylonitic foliation in the matrix (S_e). The relationship is same as in (c). In the pressure-shadow zone between the garnet (lower left) and the chlorite porphyroblast small needles of chlorite aligned parallel to the matrix mylonitic foliation are present. These chlorite needles are syntectonic to S_e. Base: 2 mm. Oblique nicols. Location: Bagi .

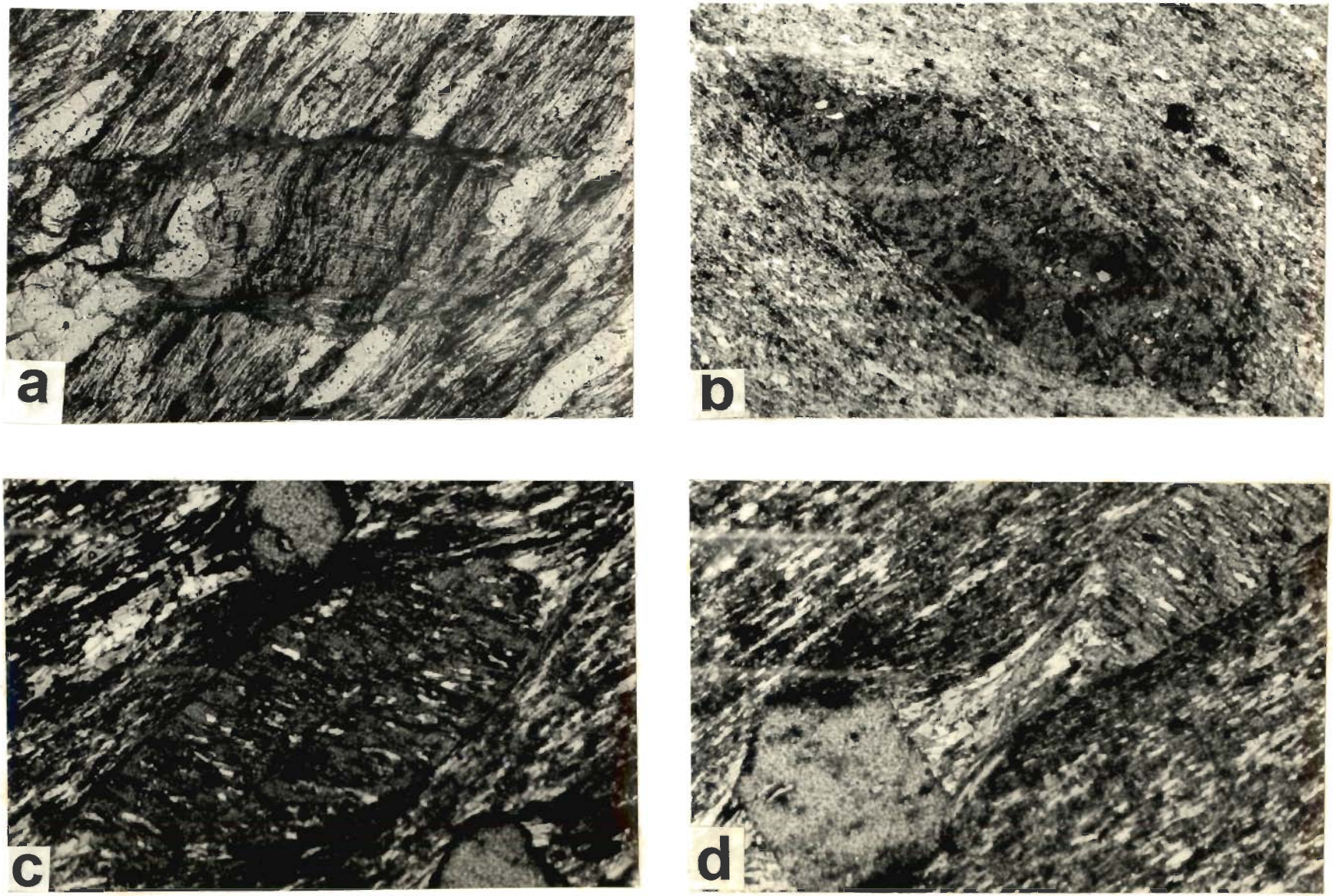

Fig. 6.3

FIGURE 6.4 GARNET MICROSTRUCTURES

(a) Spiral inclusion trails (S_i) in nearly rounded garnet porphroblast continuous with S_e ($=S_1$). The garnet is syntectonic with S_e ($=S_1$) that is with F_1. Base: 5.2 mm. Oblique nicols. Location: 4 Km south of Habban.

(b) Small polygonal garnet porphyroblast against which the S_1 cleavage in the matrix abuts sharply. Note that the core of the garnet contains quartz inclusions but the rim is inclusion free. The garnet is early tectonic with respect to F_1. Base: 0.4 mm. Plane-polarized light. Location: 5 Km east of Rajgarh.

(c) The axial planes of F_2-kinks swerving around a fractured garnet porphyroblast. The garnet is pretectonic with F_2. Base: 5.2 mm. Oblique nicols. Location: Phagu.

(d) Inclusion-free garnet in strongly mylonitized carbonaceous schist. The well developed mylonitic foliation swerves around the porphyroblast. Note that elongated quartz grains and fine muscovite needles in the strain shadows define a cleavage which is oblique to the main mylonitic foliation. The garnet is pretectonic with ductile shearing. Base: 5.2 mm. Crossed nicols. Location: Bharari.

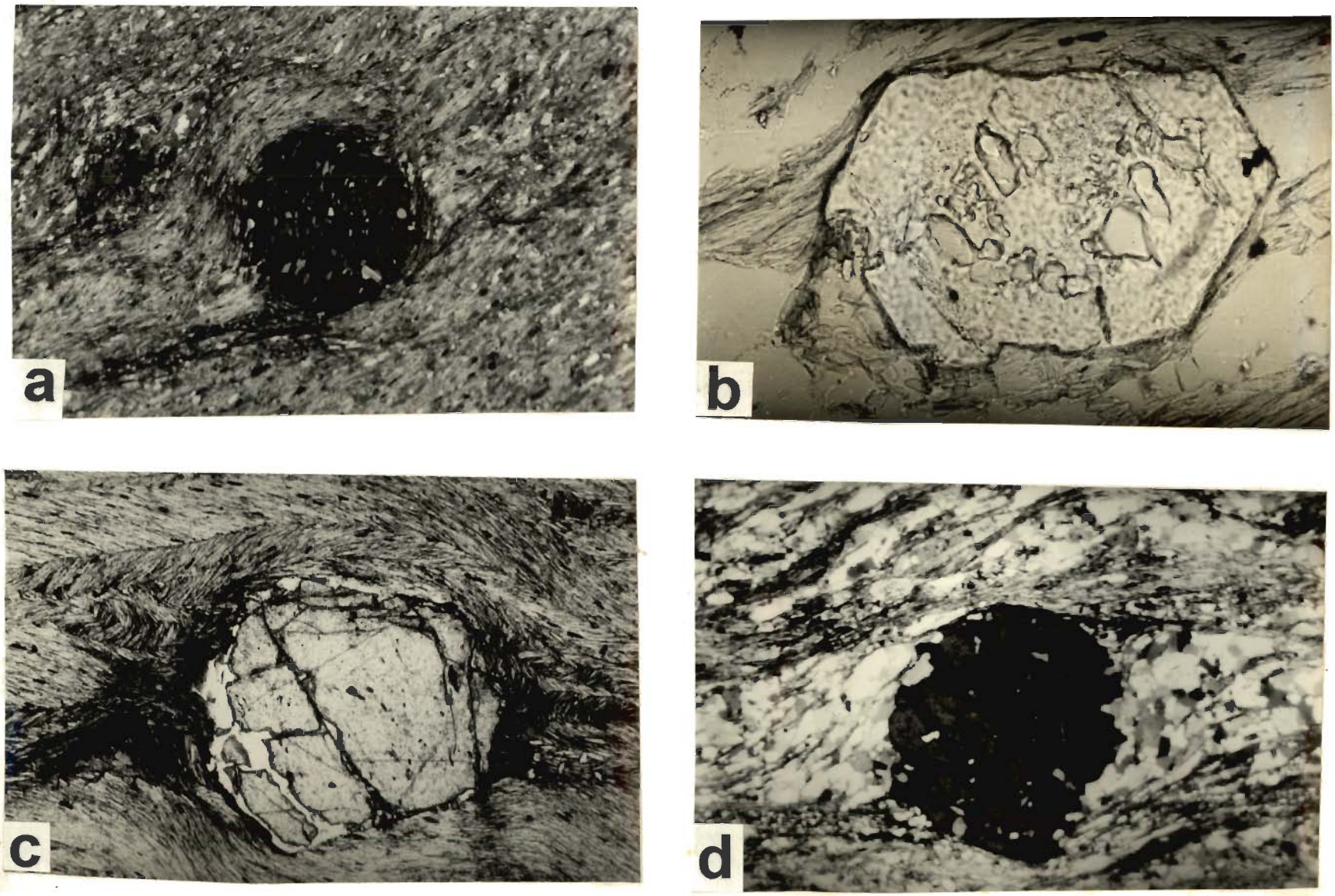

Fig. 6.4

FIGURE 6.5 GARNET MICROSTRUCTURES

(a) Mylonitic foliation in the matrix ($S_e = S_m$) swerving around an elongated garnet porphyroblast. The spiral inclusion trail, ($S_i = S_1$) defined by elongated quartz and opaque grains are not continuous with S_e ($= S_m$). The garnet is pretectonic with ductile shearing. Base: 5.2 mm. Oblique nicols. Location: 2 Km E of Churwadhar.

(b) Crenulations on mylonitic foliaiton ($S_e = S_m$) sharply abut against a rectangular inclusion-free garnet porphyroblast in carbonaceous schist. The wavelengths of the crenulations gradually decrease away from the porphyroblast. The garnet is pretectonic with ductile shearing. Base: 5.2 mm. Plane-polarized light. Location: 4 Km N of Phagu.

(c) The axial planes of isoclinal folds swerving around a garnet porphyroblast in carbonaceous schist. The isoclinal folds are traced by quartz ribbons. The garnet porphyroblast is rich in quartz and opaque inclusions at the core but almost inclusion free near the rim. The garnet is pretectonic with ductile shearing. The inclusion-rich core is early tectonic with F_1 but the inclusion-free rim is post-tectonic with F_1. Base: 5.2 mm. Plane-polarized light. Location: 2 Km N of Bogdhar.

(d) Garnet porphyroblast in mica schist is broken into small fragmentsand strewn along mylonitic foliation during ductile shearing. Base: 2 mm. Oblique nicols. Location: 2 Km N of Bogdhar.

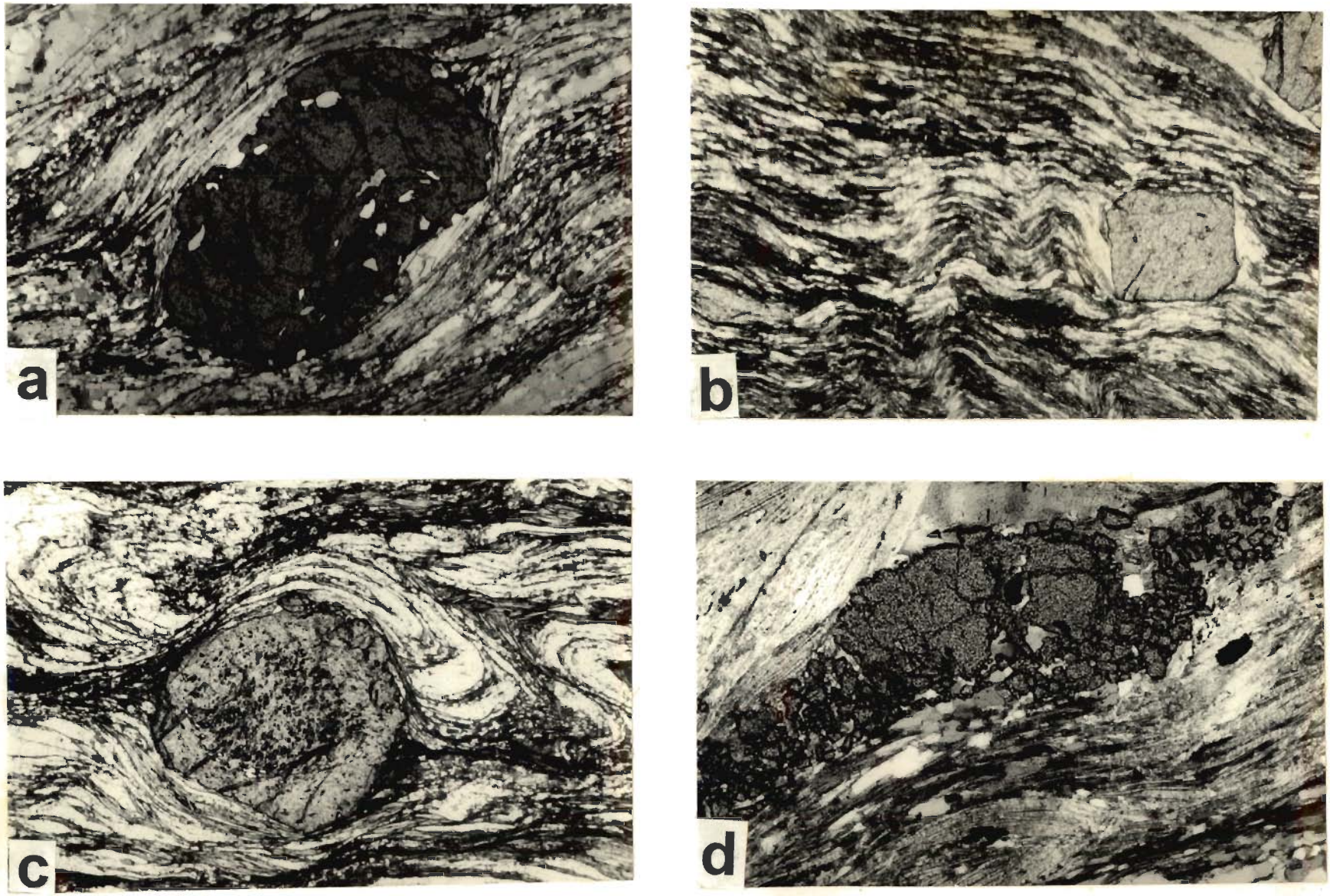

Fig. 6.5

FIGURE 6.6 STAUROLITE, KYANITE AND TOURMALINE MICROSTRUCTURES

(a) Highly fractured staurolite porphyroblast wrapped by mylonitic foliation in mica schist. Note that in the lower right staurolite is broken into small fragments and strewen along the mylonitic foliation ($=S_e$). Staurolite is pretectonic to ductile shearing. Base: 5.2 mm. Oblique nicols. Location: 2 Km E of Didag.

(b) Staurolite porphyroblast boudinaged parallel to the mylonitic foliation in the matrix. At the necking point recrystallised chlorite flakes are oriented at an angle to the fracture plane. Base: 1.6 mm. Plane-polarised light. Location: 4 Km NE of Phagu.

(c) Mylonitic foliation ($=S_e$) swerving around the kyanite porphyroblast. Straight Si in kyanite traced by very fine biotite flakes and elongated quartz is poblique to and abut against Se ($=Sm$). Kynite is pretectonic with ductile shearing. Base: 2 mm. Plane-polarised light. Location: Munalog.

(d) Tourmaline crystal is swerved by mylonitic foliation ($S_e=S_m$) in mica schist. Tourmaline is prekinematic with ductile shearing. Base: 2 mm. Plane-polarised light. Location: 2 Km E of Didag.

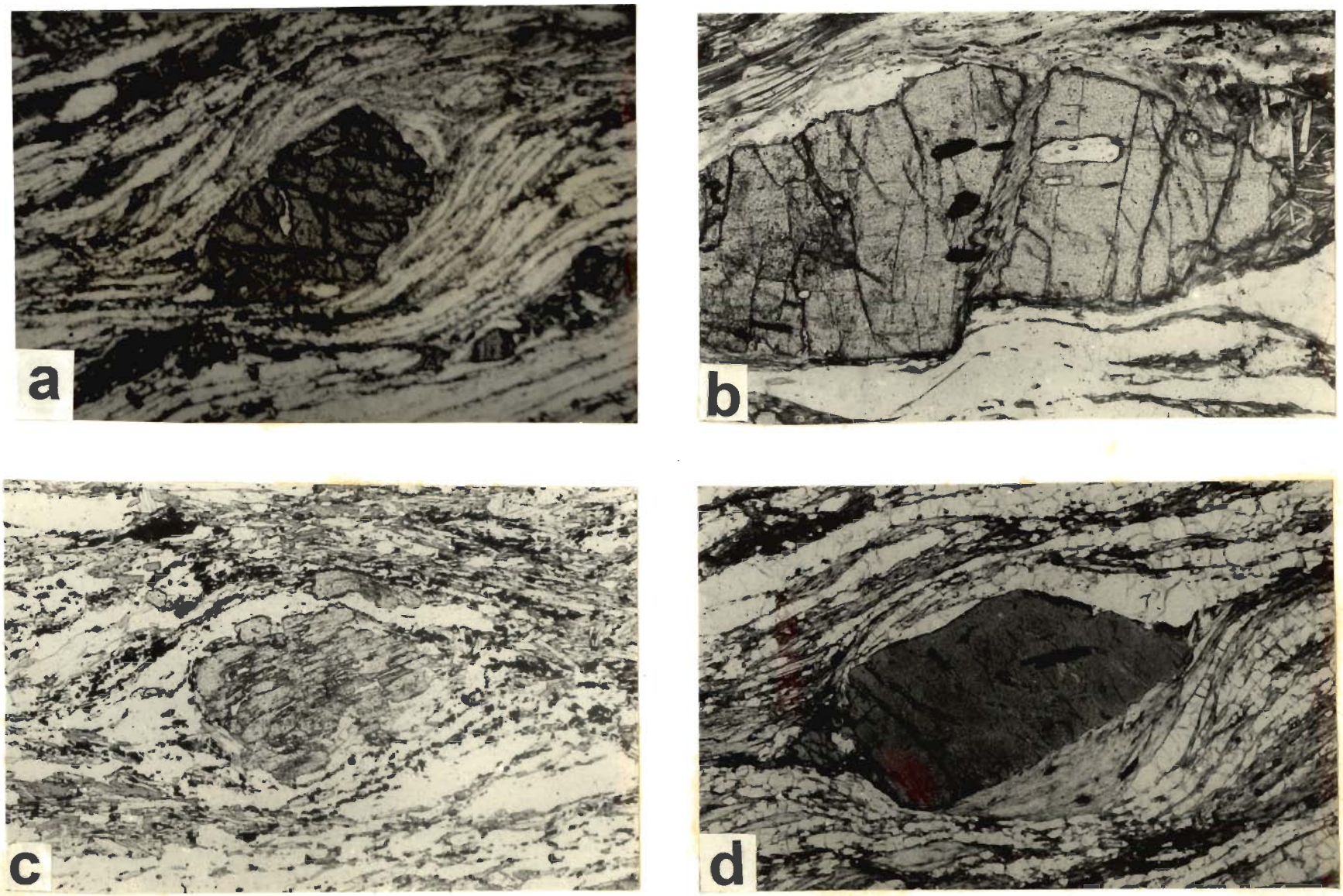

Fig. 6.6

TABLE 6.1

RELATIONSHIP BETWEEN THE CRYSTALLIZATION OF METAMORPHIC MINERALS IN THE BARROVIAN SEQUENCE AND THE DEFORMATION EPISODES

Deformation/ Minerals	F_1	F_2	Ductile shearing
Chlorite	———	———	———
Biotite	———	———	———
Garnet	———		
Staurolite	———		
Kyanite	———		
Sillimanite	———		

CHAPTER - 7
SUMMARY AND CONCLUSIONS

(1) In the Chur half-klippe the Jutogh Group representing the frontal part of the High Himalaya Crystalline thrust sheet, consists of four mappable lithological units, viz., lower carbonaceous schist, quartzite, upper carbonaceous schist and mica schist. These lithological units occur at successively higher topographic levels and the Chur granite overlies the mica schist unit at the highest topographic levels. The Jutogh Group is underlain by the low-grade phyllite and quartzite belonging to the Chail Formation which in turn is underlain by the sedimentary rocks of the Lesser Himalaya Zone.

(2) The topography of the area is like an inverted bowl with highest elevation around the Chur peak. The different lithological units of the Jutogh Group and the Chail Formation are restricted to different but the definite topographic levels. This simple map pattern along with the subhorizontal to gently dipping foliations in a majority of the exposures apparently suggests a sequence of sub-horizontal rock formations with normal stratigraphic succession. In small-scale, however, folds with diverse orientation, style and geometry, and unambiguous evidence of superposed deformations are ubiquitous. Further, contractional and extensional structures typical of ductile shearing are legion from thin sections to outcrop scales. Therefore, the apparently simple map pattern of the area conceals a very complex structural history.

(3) The structures directly observable from thin sections to the outcrop scales can be grouped into (a) the early structures, (b) the structures related to progressive ductile shearing, and (c) the late structures.

(4) The earliest diastrophic structures are a set of very tight to isoclinal, recumbent to gently-plunging reclined/inclined folds (F_1) on stratification planes (S_0) only. A penetrative cleavage (S_1) parallel to the axial planes of the F_1 folds is one of the most dominant planar structures in this area. The axial planes of F_1 folds, the S_1 surfaces as well as the S_0 surfaces have been affected by the folds of the second generation (F_2). Both the F_1 and F_2 folds have more or less similar orientation, style

and geometry. The main difference is that the F_2 folds are described by the cleavage of the first generation whereas the F_1 folds affect only the S_0 surfaces. An axial planar crenulation cleavage (S_2) has developed during the F_2 deformation but it has nowhere completely obliterated the S_1 cleavage surfaces. The geometry of the both the F_1 and F_2 folds suggest their development by a mechanism of buckling (layer parallel compression). However, the F_1 folds show considerable amount of post-buckle flattening perpendicular to the axial planes as compared to the F_2 folds. The F_1 and F_2 folds are coaxial in most of the places resulting in type-3 interference patterns of Ramsay (1967). Occasionally, the F_1 and F_2 folds are not coaxial and the F_1 folds become non-plane as well as non-cylindrical.

(5) The early folds (F_1-F_2) and related structures have been variably affected and obliterated by ductile simple shearing. Shearing is most intense in the two carbonaceous bands and at the contact of the granite body with the mica schist. However, the entire sequence of metasedimentary rocks has also been affected by the ductile shearing to varying extent.

(6) Mylonites are the most common product in the shear zones and vary from protomylonite, through orthomylonite to ultramylonite. Often this variation can be seen in a single outcrop or even within a single thin section. A penetrative mylonitic foliation (S_m), usually defined by quartz and mica ribbons, is very common and obliterates the early cleavage surfaces to varying extent within the ductile shear zones. In the carbonaceous bands and near the granite contact S_m is the most dominant foliation.

(7) Various types of folds can be recognized in the shear zones. Some of them are early folds (i.e. F_1-F_2) and the others have developed during shearing. In many, but not all, outcrops these two groups of folds cannot be distinguished from each other. The early folds and their interference patterns are sometimes caught up and modified in the shear zones. Folds developed during shearing are traced by the S_0 surfaces, the S_1

cleavage surfaces and the mylonitic foliations which was developed during the same shearing movement. One of the most interesting features in the shear zones is the repeated folding of the mylonitic foliations and the development of successive generations of mylonitic foliations and crenulation cleavages. Sheath folds on mylonitic foliation are common but type-2 and type-3 interference patterns are also present. Problem of refolding and repeated crenulation cleavage formation in ductile shear zones have been discussed.

(8) The extensional structures such as extension crenulation cleavage (ecc), foliation boudinage and rotated boudinage structures have extensively developed. These structures affect both the pre-shearing structures as well as structures developed during ductile shearing. The extensional structures do not necessarily envisage any large-scale late-stage extension. They could have formed where pre-existing cleavage surfaces are in the extension field of both the finite and instantaneous strain ellipsoid in a simple shear deformation.

(9) Small-scale thrusts, giving rise to imbricate or schuppen structures, are particularly common in the two carbonaceous bands and adjacent rocks. These thrusts cut up the mylonitic foliations and other shear zone structures.

(10) The late-stage structures are of two types. The first of these is a set of very open folds (F_3) developed on the pre-existing foliation surfaces of both the early generations (S_1-S_2) and the mylonitic foliations. The gentle undulation of foliation surfaces is the only effect of these folds. A set of subvertical fractures cutting through all the earlier structures is the last structures developed in this area. Some of them are faults with normal sense of displacements. These brittle structures have not been studied in detail.

(11) In many outcrops and hand specimen structures of early deformation (i.e. F_1 and F_2) are indistinguishable from structures developed during ductile shearing. This difficulty should make us wary at the time of structural analyses. It is not

uncommon in the literature on the Himalaya to find a sweeping classification of structures into D_1, D_2, D_3 etc. This type of classification is meaningless without detailed description of each of these structures, their interrelations and, most importantly how they are to be distinguished from each other in the field.

(12) The structural analyses suggest isoclinal recumbent to gently-plunging reclined/inclined folding in large scale. However, nowhere in the area hinge zone of any large-scale F_1 fold could be traced. The marble band in the Jutogh mica schist in the southcentral part of the area possibly traces an F_2 fold in the scale of the map. The two subhorizontal carbonaceous bands occurring at two topographic levels do not trace the two limbs of a huge recumbent fold as was originally suggested by Pilgrim and West (1928) and corroborated by later workers. Around Rajgarh in the western part of the area the upper carbonaceous schist band traces a complex map pattern. This map pattern together with the variation in the orientation of the small-scale structures suggest the upper carbonaceous band has been involved in large-scale refolded isoclinal fold. This large-scale folding is traced by mylonitic foliations and, therefore, is related to ductile shearing. Interestingly, this fold affects only the upper carbonaceous band and only in the Rajgarh area. The lower carbonaceous band maintains its flat-lying attitude suggesting a structural discordance.

(13) In the crystalline rocks of the area four thrusts can be recognized, viz., the Chail thrust, the Jutogh thrust, the Rajgarh thrust and the Chur thrust. Of these, the Rajgarh thrust and the Chur thrust have been recognized for the first time. These four thrusts describe an imbricate structure in the frontal part of the HHCZ thrust sheet. However, this pack of four thrust slices also shows evidence of extensive ductile shearing. It can be envisaged that during Himalayan deformation an early ductile shearing was followed by large-scale brittle thrusting.

(14) It is not possible to postulate how extensive is the Rajgarh thrust. But the Chur thrust may potentially be regionally extensive. From this area alone we cannot

predict which of these four thrusts is equivalent to the MCT. However, the significant point is that the MCT represents a zone (the MCT Zone) in which ductile shearing and imbricated thrust slices can be recognized. This, together with the possibility that the Chur thrust may be regionally significant, suggests that the crustal shortening along the MCT may be significantly greater than hitherto estimated. However, estimation of crustal shortening is beyond the scope of the present thesis.

(15) The porphyroblast-matrix foliation relations show that the main phase of progressive regional metamorphism is completely pretectonic with respect to the ductile shearing. Consequently, the progressive Barrovian metamorphism in this area cannot be related to the movement along the MCT. This metamorphism is synchronous with the pre-shearing early phase of deformation episodes whose age is unknown. If this deformation is related to the collision then the metamorphism is Himalayan (i.e. Tertiary) in age. If not, then the early deformations and the metamorphism could be much older (may even be Precambrian) than the Himalayan orogeny. The inverted metamorphic zones is a result of multiple thrusting which brought up higher grade rocks successively from deeper levels.

REFERENCES

Achache, J., Courtillot, V. & Zhou, Y. X. 1984. Paleogeographic and tectonic evolution of southern Tibet since middle Cretaceous time: New paleomagnetic data and synthesis. *J. Geophys. Res.* **89,** 10311-10339.

Arita, K. 1983. Origin of the inverted metamorphism of the Lower Himalayas, Central Nepal. *Tectonophysics* **95**, 42-60.

Auden, J. B. 1937. Structure of Himalaya in Garhwal. *Geol. Surv. India Rec.* **71**, 407-433.

Barnicoat, A. C. & Treloar, P. J. 1989. Himalayan metamorphism - an introduction. *J. Met. Geol.* **7**, 3-8.

Bell, T. H. 1978. Progressive deformation and reorientation of fold axes in a ductile mylonite zone: the Woodroffe thrust. *Tectonophysics* **44**, 285-321.

Bell, T. H. 1985. Deformation partitioning and porphyroblast rotation in metamorphic rocks: a radical reinterpretation. *J. Met. Geol.* **3**, 109-118.

Bell, T. H. & Etheridge, M. A. 1973. Microstructure of mylonites and their descriptive terminology. *Lithos* **6**, 337-348.

Bell, T. H., Forde, A. & Hayward, N. 1992. Do smoothly curving, spiral-shaped inclusion trails signify porphyroblast rotation? *Geology*, **20**, 59-62.

Bell, T. H. & Johnson, S. E. 1989. Porphyroblast inclusion trails: the Key to orogenesis. *J. Met. Geol.* **7**, 279-310.

Bell, T. H. & Rubenach, M. J. 1983. Sequential porphyroblast growth and crenulation cleavage development during progressive deformation. *Tectonophysics* **92**, 171-194.

Berthe, D., Choukroune, P. & Jegouzo, P. 1979. Orthogneiss, mylonite and non coaxial deformation of granites: the example of the South Armorican Shear Zone. *J. Struct. Geol.* **1**, 31-42.

Besse, J. & Courtillot, V. 1988. Paleogeographic maps of the continents bordering the Indian ocean since the early Jurassic. *J. Geophys. Res.* **93**, 11791-11808.

Besse, J., Courtillot, V., Pozzi, J. P., Westphal M. & Zhou, Y. X. 1984. Paleomagnetic estimates of crustal shortening in the Himalayan thrusts and Zangbo suture. *Nature*, **311**, 621-626.

Bhadra, B. K., Ghosh, T. K., Srivastava, D. C. & Mukhopadhyay, D. K., 1993, Thrust imbrication in the Jutogh Series and status of the Chur granite, southeast of Simla Hills, Himachal Pradesh. Seminar on "Himalayan Geology and Geophysics (New Data and New Approaches)", Wadia Instititute of Himalayan Geology, Dehra Dun, India (Abstract)

Bhargava, O. N. 1980. Outline of the stratigraphy of eastern Himachal Pradesh, with special reference to the Jutogh Group. In: Stratigraphy and correlation of Lesser Himalayan Formation (edited by Valdiya, K. S. & Bhatia, S. B.), Hindustan Publishing Corporation (India), New Delhi.

Bhattacharyya, D. S. & Das, K. K. 1982. Inversion of metamorphic zones in the Lower Himalayas at Gangtok, Sikkim, India. *J. Geol.* ***91***, 98-102.

Bird, P. 1978. Initiation of intracontinental subduction in the Himalaya. *J. Geophys. Res.* **83**, 4975-4987.

Bouchez, J. L. & Pêcher, A. 1981. The Himalayan Main Central Thrust pile and its quartz-rich tectonites in central Nepal. *Tectonophysics* **78**, 23-50.

Brown, R. L. & Nazarchuk, J. H. 1993. Annapurna detachment fault in the Greater Himalaya of central Nepal. In: P. J. Treloar & M. P. Searle (eds.), *Himalayan Tectonics, Geol. Soc. Spl. Publ.* **74**, 461-473.

Burchfiel, B. C. & Royden, L. H. 1985. North-south extension within the convergent Himalayan region. *Geology*, **13**, 679-682.

Burchfiel, B. C., Zhiliang, C., Hodges, K. V., Yuping, L., Royden, L. H., Changrong, D. & Jiene, X. 1992. The South Tibet Detachment System, Himalaya Orogeny: Extension contemporaneous with and parallel to shortening in a collision mountain belt. *Geol. Soc. Am. Spl. papers,* 260.

Brunel, M. & Kienast, J. R. 1986. Etude petro-structurale des chevauchements ductiles himalayens sur la transversale de l'Everest-Makalu (Nepal oriental). *Can. J. Earth Sci.* **23**, 1117-1137.

Burg, J. P. & Chen, G. M. 1984. Tectonics and structural zonation of southern Tibet. *Nature* **311**, 219-223.

Burg, J. P., Brunel, M. Gapais, D., Chen, G. M. & Liu, G. H. 1984. Deformation of leucogranites of the crystalline Main Central Sheet in southern Tibet (China). *J. Struct. Geol.* **6**, 535-542.

Carreras, J., Estrada, A. & White, S. H. 1977. The effects of folding on the c-axis fabrics of a quartz. *Tectonophysics* **39**, 3-24

Chatterji, G. C. & Swami Nath, J. 1977. The stratigraphy and structure of parts of the Simla Himalaya - a synthesis. *Mem. Geol. Surv. Ind.* **106**, 408-498.

Cobbold, P. R. & Quinquis, H. 1980. Developments of sheath folds in shear regimes. *J. Struct. Geol.* **2**, 119-126.

Copeland, P., Harrison, T. M., Hodges, K. V., Maruejol, P., Le Fort, P. & Pecher, A. 1991. An early Pliocene thermal disturbance of the Main Central Thrust, Central Nepal: Implications for Himalayan tectonics. *J. Geophys. Res.* **96**, 8475-8500.

Das, B. K. 1991. Petrogenesis of the Chur granites Lesser Himalaya, (H.P.). *J. Scientific Res.* **41B**, 245-261.

Das, B. K. & Rastogi, R. 1988. Petrology of the Jutogh metapelites near Chur, Himachal Himalaya, India. *J. Geol. Soc. Ind.* **31**, 251-266.

Davis, G. H. 1984. Structural geology of rocks and regions. John Wiley & Sons.

Deniel, C., Vidal, P., Fernandez, A., Le Fort, P. & Peucat. J-J. 1987. Isotopic study of the Manslu granite (Himalaya, Nepal): Inferences on the age and source of Himalayan leucogranites. *Contrib. Mineral. Petrol.*, **96**, 78-92.

Dennis, J. G. 1972. Structural Geology. Ronald Press, New York.

Dennis, A. J. & Secor, D. T. 1987. A model for the development of crenulations in shear zones with applications from the Southern Appalachian Piedmont. *J. Struct. Geol.* **9**(7), 809-817.

Dennis, A. J. & Secor, D. T. 1990. On resolving shear direction in foliated rocks deformed by simple shear. *Geol. Soc. Am. Bull.*, **102**, 1257-1267.

Dewey, J. F. & Bird, P. 1970. Mountain belts and the new global tectonics. *J. Geophys. Res.* **75**, 2625-2647

Dietrich, V. & Gansser, A. 1981. The leucogranites of the Bhutan Himalaya (Crustal anatexis versus mantle melting). *Schweiz. Mineral. Petrogr. Mitt.* **61**, 177-202.

Dubey, A. K. & Bhat, M. I. 1991. Structural evolution of the Simla area, NW Himalayas : Implications for crustal thickening. *J. Southeast Asian Earth Sci.* **6**, 41-53.

England, P. & Molnar, P. 1993. The interrelation of inverted metamorphic isograds using simple physical calculations. *Tectonics* **12**, 145-157.

England, P. C. & Thompson, A. B. 1984. Pressure-temperature-time paths of regional metamorphism I. Heat transfer during the evolution of regions of thickened continental crust. *J. Petrol.* **25**, 894-928.

England, P., Le Fort, P., Molnar, P. & Pecher, A. 1992. Heat sources for Tertiary metamorphism and anatexis in the Annapurna-Manaslu region Central Nepal. *J. Geophys. Res.* **97**, 2107-2128

Fuchs, G. 1975. Contributions to the geology of the North-Western Himalayas. *Abh. Geol.* **B. - A32**, 1-59.

Fuchs, G. 1981. Outline of the geology of the Himalaya. *Mitt. Osterr. Geol. Ges.* **74/75**, 101-127.
Gahalaut, V. K. & Chander, R. 1992. On the active tectonics of Dehradun region from observations of ground elevation changes. *J. Geol. Soc. India* **39**, 61-68.
Gansser, A. 1964. Geology of the Himalaya. Interscience, New York.
Gansser, A. 1974. Himalaya. In: Mesozoic-Cenozoic Orogenic Belts (edited by Spencer, A. M.), *Geol. Soc. Lond. Spl. Publ.* **4**, 267-278.
Ghosh, S. K. 1975. Distortion of planar structures around rigid spherical bodies. *Tectonophysics* **28**, 185-208.
Ghosh, S. K. 1977. Drag patterns of planar structures around rigid inclusions. In: Energetics of Geological Processes (edited by Saxena, S. K. & Bhattacharji, S.), 98-120. Springer-Verlag.
Ghosh, S. K. 1993. Structural geology. Fundamentals and Modern Developments. Pergamon Press, Oxford.
Ghosh, S. K. & Ramberg, H. 1976. Reorientation of inclusions by combination of pure shear and simple shear. *Tectonophysics* **34**, 1-70.
Ghosh, S. K. & Sengupta, S. 1984. Successive development of plane noncylindrical folds in progressive deformation. *J. Struct. Geol.* **6**, 703-709.
Ghosh, S. K. & Sengupta, S. 1987. Progressive development of structures in a ductile shear zone. *J. Struct. Geol.* **9**, 277-288.
Gray, D. R. 1977a. Morphological classification of crenulation cleavage. *J. Geol.* **85**, 229-235.
Gray, D. R. 1977b. Differentiation associated with discrete crenulation cleavages. *Lithos* **10**, 89-101.
Gray, D. R. 1979. Microstructure of crenulation cleavages: An indicator of cleavage origin. *Am. J. Sci.* **279**, 97-128.
Gray, D. R. & Durney, D. W. 1979. Crenulation cleavage differentiation: implications of solution-deposition processes. *J. Struct. Geol.* **1**, 73-80.
Gupta, L. N. 1973. A contribution to the geology of Lansdowne area, Garhwal Himalayas, India. *J. Geol. Soc. India* **17**, 449-460.
Gururajan, N. S. 1990. Deformation microstructures and geochemistry of the mylonitic augen gneisses in the Chail thrust zone in Sutlej valley of Himachal Pradesh. *J. Geol. Soc. India* **36**, 290-306.
Gururajan, N. S. 1994. Porphyroblasts-matrix microstructural relationships from the Crystalline Thrust Sheets of Sutlej valley, Himachal Pradesh. *J. Geol. Soc. India* **44**, 367-369.
Gururajan, N. S. & Islam, R. 1991. Petrogenesis of the Khab leucogranite in the Higher Himalayan region of Himachal Pradesh (Sutlej valley) India. *J. Him. Geol.* **2**, 31-37.
Harris, N., Inger, S. & Massey, J. 1993. The role of fluids in the formation of High Himalayan leucogranites. In: Himalayan Tectonics (edited by Treloar, P. J. & Searle, M. P.). *Geol. Soc. Spl. Publ.* **74**, 391-400.
Heim, A. & Gansser, A. 1939. Central Himalaya. Geological observations of the Swiss expedition 1939. *Soc. Helv. Sci. Nat. Mem.* **73**, 1-245. (Reprinted by Hindustan Pub. Corp., New Delhi, 1975).
Herren, E. 1987. The Zanskar Shear Zone: Northeast-Southwest extension within the Higher Himalayas (Ladakh, India). *Geology* **15**, 409-413.
Hirn, A., Lepine, J. C., Jobert, G., Sapin, M., Wittlinger, G., Xin, X. Z., Yuan, G. E., Jing, W. X., Wen, T. J., Bai, X. S., Pandey, M. R. & Tater, J. M. 1984. Crustal structure and variability of the Himalayan border of Tibet. *Nature* **307**, 23-25.
Hobbs, B. E., Means, W. D. & Williams, P. F. 1976. Outline structural geology. Wiley & Sons.

Hodges, K. V., Le Fort. P., & Pecher, A. 1988. Possible thermal buffering by crustal anatexis in collision orogens: Thermobarometric evidence from the Nepalese Himalaya. *Geology* **16**, 707-710.

Hubbard, M. S. 1994. Role of ductile shear on the formation of inverted metamorphism. 9th Himalaya-Karakorum-Tibet workshop, Kathmandu, *J. Nepal Geol. Soc.* **10**, (abstract volume), 68.

Hubbard, M. S. & Harrison, T. M. 1989. 40Ar/39Ar age constraints on deformation and metamorphism in the Main Central Thrust Zone and Tibetan Slab, Eastern Nepal Himalaya. *Tectonics* **8**, 865-880.

Hudleston, P. J. 1986. Extracting information from folds in rocks. *J. Geol. Education* **34**, 237-245.

Ildefonse, B. & Mancktelow, N. S. 1993. Deformation around rigid particles: the influence of slip at the particle/matrix interface. *Tectonophysics* **221**, 345-359.

Jain, A. K. & Manickavasagam, R. M. 1993. Inverted metamorphism in the intracontinental ductile shear zone during Himalayan collision tectonics. *Geology* **21**, 407-410.

Jaupart, C. & Provost, A. 1985. Heat focussing, granite genesis and inverted metamorphic gradients in continental collision zones. *Earth and Planetary Science Letters* **73**, 385-397.

Johnson, S. E. 1993. Testing models for the development of spiral-shaped inclusion trails in garnet porphyroblasts: to rotate or not to rotate, that is the question. *J. Met. Geol.* **11**, 635-659.

Kakkar, R. K. 1988. Geology and tectonic setting of Central Crystalline rocks of southern part of higher Himachal Himalaya. *J. Geol. Soc. India* **31**, 243-250.

Kanwar, R. C. & Singh, I. 1979. Structural history of the Jutogh metasediments, SW of Chur mountain, Sirmur district, Himachal Pradesh. In: Structural Geology of the Himalaya (edited by Saklani, P. S.), Today and Tomorrow's Publishers, New Delhi, 183-200.

Kishore, N. & Kanwar, R. C. 1984a. Petrography, petrochemistry, origin and emplacement of Chor granites. *Bull. Indian. Geol. Asson.* **17**, 1-27.

Kishore, N. & Kanwar, R. C. 1984b. Structural history of the granitic rocks of the Naura-Haripurdhar area of Chor Pluton. *Bull. Indian. Geol. Asson.* **17**, 195-205.

Klootwijk, C. T. 1984. A review of Indian Phanerozoic palaeomagnetism: Implications for the India-Asia collision. *Tectonophysics* **105**, 331-353.

Klootwijk, C. T., Conaghan, P. J. & Powell, C. McA. 1985. The Himalayan arc: Large-scale continental subduction, oroclinal bending and back-arc spreading. *Earth Planet. Sci. Lett.*, **75**, 167-183.

Klootwijk, C. T., Gee, J. S., Peirce, J. W., Smith, G. M. & McFadden, P. L. 1992. An early India-Asia contact: Paleomagnetic constraints from Ninetyeast Ridge, ODP Leg 121. *Geology*, **20**, 395-398.

Knoff, E. B. 1935. Recognition of overthrusts in metamorphic terranes. *Am. J. Sci.* **30**, 198-209.

Lal, R. K., Mukerji, S. & Ackermand, D. 1981. Deformation and Barrovian metamorphism at Tadakh, Darjeeling (Eastern Himalaya). In: Metamorphic Tectonites of the Himalaya (edited by Saklani, P. S.). Today and Tomorrow's Publisher, New Delhi, 231-278.

Lapworth, C. 1885. The Highland controversy in British Geology: its causes, course and consequences. *Nature* **32**, 558-559.

Le Fort, P. 1975. Himalayas: the collided range. Present knowledge of the continental arc. *Am. J. Sci.* **275A**, 1-44.

Le Fort, P. 1981. Manaslu leucogranite: A collision signature of the Himalaya. A model for its genesis and emplacement. *J. Geophys. Res.* **86**, 10545-10568.
Le Fort, P. 1988. Granites in the tectonic evolution of the Himalaya, Karakoram and Southern Tibet. *Phil. Trans. R. Soc. Lond.* **A326**, 281-299.
Le Fort, P. 1989. The Himalayan orogenic segment. In: Tectonic Evolution of the Tethyan Region (edited by Sengor, A. M. C.). Kulwer Academic Publishers, 289-386.
Le Fort, P., Debon, F., & Sonet, J. 1980. The "Lesser Himalayan" cordierite granite belt: Typology and age of the pluton of Manserah (Pakistan). *Peshwar Univ. Geol. Bull. (Spl. Issue)* **13**, 51-61.
Le Fort, P., Cuney, M., Deniel, C., France-Lanord, C., Sheppard, S. M. F., Upreti, B. N. & Vidal, P. 1987. Crustal generation of the Himalayan leucogranites. *Tectonophysics* **134**, 39-57.
Lister, G. S. & Snoke, A. W. 1984. S-C mylonites. *J. Struct. Geol.* **6**, 617-638.
Mattauer, M. 1986. Intracontinental subduction, crust-mantle decollement and crustal stacking wedge in the Himalayas and other collision belts. In: Collision Tectonics (edited by Coward, M. P. & Ries, A. C.). *Geol. Soc. Spl. Publ.* **19**, 37-50.
Metcalfe, R. P. 1993. Pressure, temperature and time constraints on metamorphism across the Main Central Thrust zone and High Himalayan Slab in the Garhwal Himalaya. In: Himayan Tectonics (edited by Treloar, P. J. & Searle, M. P.). *Geol. Soc. Spl. Publ.* **74**, 485-509.
Misch, P. 1970. Paracrystalline microboudinage in a metamorphic reaction sequence. *Geol. Soc. Am. Bull.* **81**, 2483-2486.
Misch, P. 1972. Porphyroblasts and "crystallization force": some textural criteria: a reply. *Geol. Soc. Am. Bull.* **83**, 921-922.
Mohan, A., Windley, B. F. & Searle, M. P. 1989. Geothermobarometry and development of inverted metamorphism in the Darjeeling and Sikkim region of the eastern Himalaya. *J. Met. Geol. 7*, 95-110.
Molnar, P. & England, P. 1990. Temperatures, heat flux and frictional stress near major thrust faults. *J. Geophys. Res.* **95**, 4833-4856.
Molnar, P. & Tapponnier, P. 1975. Cenozoic tectonics of Asia: Effects of a continental collision. *Science* **189**, 419-426.
Molnar, P. & Tapponnier, P. 1978. Active tectonics of Tibet. *J. Geophys. Res.* **83**, 5361-5375
Mueller, R. F. & Saxena, S. K. 1977. Chemical Petrology. Springer-verlag, New York.
Mukhopadhyay, D. K. 1989. Significance of small-scale structures in the Kolar Schist Belt, south India. *J. Geol. Soc. India* **33,** 291-308.
Mukhopadhyay, D. K., Bhadra, B. K., Ghosh, T. K. & Srivastava, D. C. 1994. Thrust imbrication, inverted metamorphism and emplacement of Lesser Himalaya granite around Chur peak, Himachal Himalaya, 9th Himalaya-Karakoram-Tibet Workshop, Kathmandu. *J. Nepal Geol. Soc.* **10**, (Abstract Volume), 89-90.
Naha, K. & Ray, S. K. 1970. Metamorphic history of the Jutogh Series in the Simla Klippe, Lower Himalayas. *Contrib. Mineral. Petrol. 28*, 147-164.
Naha, K. & Ray, S. K. 1971. Evidence of overthrusting in the metamorphic terrane of the Simla Himalayas. *Am. J. Sci.* **270**, 30-42.
Naha, K. & Ray, S. K. 1972. Structural evolution of the Simla Klippe in the Lower Himalayas. *Geol. Rund.* **61**, 1050-1086.
Nakata, T., Otsuki, K., & Khan, S. H. 1990. Active faults, stress field, and plate motion along the Indo-Eurasian Plate Boundary. *Tectonophysics* **181**, 83-95.

Ni, J. & Barazangi, M. 1984. Seismotectonics of the Himalayan Collision Zone: Geometry of the Underthrusting Indian Plate Beneath the Himalaya. *J. Geophys. Res.* **89**, 1147-1163

Oxburgh, E. R. & Turcotte, D. 1974. Thermal gradients and regional metamorphism in overthrust terrains with special reference to the eastern Alps. *Schweiz. Mineral. Petrogr. Mitt.* **54**, 641-662.

Patel, R. C., Singh, S., Asokan, A., Manickavasagam, R. M. & Jain A. K. 1993. Extensional tectonics in the Himalayan orogen, Zanskar, NW India. In: Himalayan Tectonics (edited by Treloar, P. J. & Searle, M. P.). *Geol. Soc. Spl. Publ.* **74**, 445-459.

Paul, S. K. & Roy, A. K. 1991. Significance of satellite imagery in the elucidation of tectonic set-up of Himachal and U.P. Himalaya. In: Mountain Resource Management and Remote sensing (edited by P. N. Gupta and A. K. Roy). Surya Publication, Dehradun.

Pêcher, A. 1975. The Main Central Thrust in the Nepal Himalaya and the related metamorphism in the Modi-Khola cross section (Annapurna Range). *Him. Geol.* **5**, 115-131.

Pêcher, A. 1977. Geology of the Nepal Himalaya: deformation and petrography in the MCT zone. In: Himalaya, Sciences de la Terre, CNRS, Paris, 301-318.

Pêcher, A. 1989. The metamorphism in the Central Himalaya. *J. Met. Geol.* **7**, 31-41.

Pêcher, A. & Le Fort, P. 1977. Origin and significance of the Lesser Himalaya augen gneisses. In: Ecologie et Geologie de l'Himalaya, CNRS, Paris **268**, 319-329.

Pilgrim, G. E. & West, W. D. 1928. The structure and correlation of the Simla rocks. *Geol. Surv. India Mem.* **53**, 1-150.

Platt, J. P. 1979. Extension crenulation cleavage. *J. Struct. Geol.* **1**, 95-96.

Platt, J. P. 1983. Progressive refolding in ductile shear zones. *J. Struct. Geol.* **5**, 619-622.

Platt, J. P. 1984. Secondary cleavages in ductile shear zones. *J. Struct. Geol.* **6**, 432-439.

Platt, J. P. & Vissers, R. L. M. 1980. Extensional structures in anisotropic rocks. *J. Struct. Geol.* **2**, 397-410

Pognante, U. & Lombardo, B. 1989. Metamorphic evolution of the High Himalayan Crystallines in SE Zanskar, India. *J. Met. Geol.* **7**, 9-17

Powell, C. McA. 1979. A morphological classification of rock cleavage. *Tectonophysics*, **58**, 21-34.

Powell, C. McA. & Conaghan, P. J. 1973. Plate tectonics and the Himalayas. *Earth Planet. Sci. Lett.* **20**, 1-12.

Quinquis, H., Andren, C., Brun, J. P. & Cobbold, P. R. 1978. Intense progressive shear in Ile de Groix blueschists and compatibility with subduction or obduction. *Nature*, **273**, 43-45.

Ramsay, J. G. 1967. Folding and fracturing of rocks. McGraw Hill.

Ramsay, J. G. 1980. Shear zone geometry: a review. *J. Struct. Geol.* **2**, 83-99.

Ramsay, J. G. & Allison, I. 1979. Structural analysis of shear zones in an alpinised Hercynian granite. *Schweiz. Mineral. Petrogr. Mitt.* ***59***, 251-279.

Ramsay, J. G. & Graham, R. H. 1970. Strain variation in shear belts. *Can. J. Earth Sci.* **7**, 786-813.

Ramsay, J. G. & Huber, M. 1. 1983. The techniques of modern structural geology. 1 Strain Analysis. Academic Press.

Ramsay, J. G. & Huber, M. 2. 1987. The techniques of modern structural geology. 2 Folds and fractures. Academic Press.

Ray, S. 1947. Zonal metamorphism in the eastern Himalaya and some aspects of local geology. *Quart. J. Geol. Met. Soc. India*, **19**, 117-138.
Rickard, M. J. 1961. A note on cleavage in crenulated rocks. *Geol. Mag.* **98**, 324-332.
Roy, M. K. & Mukherjee, A. B. 1976. The relationship between the metamorphic and movement episodes in the Jutogh Series, west of the Chor granite near Rajgarh, Himachal Pradesh. *Him. Geol.* **6**, 240-246.
Royden, L. H. & Burchfiel, B. C. 1987. Thin-skinned N-S extension within the convergent Himalayan region: gravitational collapse of a Miocene topographic front. In: Continental Extensional Tectonics (edited by Coward, M. P., Dewey J. F. & Hancock, P. J.). *Geol. Soc. Lond. Spl. Publ.* **28**, 611-619.
Scharer, U. & Allegre C. J. 1983. The Palung granite (Himalaya); high-resolution U-Pb systematics in zircon and monazite. *Earth Planet. Sci. Lett.* **63**, 423-432.
Schelling, D. 1992. The tectonostratigraphy and structure of the Eastern Nepal, Himalaya. *Tectonics* **11**, 925-943.
Schelling, D. & Arita, K. 1991. Thrust tectonics, crustal shortening, and the structure of the far-eastern Nepal Himalaya. *Tectonics* **10**, 851-862.
Schneider, C. & Masch, L. 1993. The metamorphism of the Tibetan Series from the Manang area, Marsyandi valley, Central Nepal. In: Himalayan Tectonics (edited by Treloar, P. J. & Searle M. P.). *Geol. Soc. Spl. Publ.* **74**, 357-374.
Scholz, C. H. 1980. Shear heating and the state of stress on faults. *J. Geophys. Res.* **85**, 6174-6184.
Searle, M. P. 1983. Stratigraphy, structure and evolution of the Tibetan-Tethys zone in Zanskar and the Indus Suture Zone in the Ladakh Himalaya. *Trans. R. Soc. Edin. (Earth Sci.)* **73**, 205-219.
Searle, M. P. 1986. Structural evolution and sequence of thrusting in the High Himalayan, Tibetan Tethys and Indus Suture Zones of Zanskar and Ladakh, Western Himalaya. *J. Struct. Geol.* **8**, 923-936.
Searle, M. P., Cooper, D. J. W. & Rex, A. J. 1988. Collision tectonics of the Ladakh-Zanskar Himalaya. *Phil. Trans. R. Soc. Lond.* **A326**, 117-150.
Searle, M. P., Metcalfe, R. P., Rex, A. J. & Norry, M. J. 1993. Field relations, petrogenesis and emplacement of the Bhagirathi leucogranite, Garhwal Himalaya. In: Himalayan Tectonics (edited by Treloar, P. J. & Searle, M. P.). *Geol. Soc. Spl. Publ.* **74**, 429-444.
Searle, M. P. & Rex, A. J. 1989. Thermal model for the Zanskar Himalaya. *J. Met. Geol.* **7**, 127-134.
Searle, M. P., Windley, B. F., Coward, M. P., Cooper, D. J. W., Rex, A. J., Rex, D., Tingdong, L., Xuchang, X., Jan, M. Q., Thakur, V. C. & Kumar, S. 1987. The closing of Tethys and the tectonics of the Himalaya. *Geol. Soc. Am. Bull.* **98**, 678-701.
Seeber, L., Armbruster, J. G. & Quittmeyer, R. C. 1981. Seismicity and continental subduction in the Himalayan arc. In: Zagros, Hindukush, Himalaya Geodynamic evolution (edited by Gupta, H. K. & Delany, F. M.). *Am. Geophys. Union Geodyn. Ser.* **3**, 215-242.
Shankar, R. & Ganesan, T. M. 1973. A note on the Garhwal nappe. *Him. Geol.* **3**, 72-82.
Sharma, K. K. 1976. A contribution to the geology of the Sutlej valley, Kinnaur, Himachal Pradesh, India. *Coll. Inter. CNRS: Himalaya Sci. de la Terra C.N.R.S.* **268**, 369-378.
Shi, Y. & Wang, C-Y. 1987. Two-dimensional modelling of the P-T-t paths of regional metamorphism in simple overthrust terrains. *Geology* **15**, 1048-1051.

Sibson, R. H. 1977. Fault rocks and fault mechanisms. *J. Geol. Soc. Lond.* **133**, 191-233.
Sinha, A. K. 1981. Geology and tectonics of the Himalayan region of Ladakh, Himachal, Garhwal-Kumaun and Arunachal Pradesh: A review. In: Zagros, Hindukush, Himalaya Geodynamic evolution (edited by Gupta, H. K. & Delany, F. M.). *Am. Geophys. Union Geodyn. Ser.* **3**, 122-148.
Sinha-Roy, S. 1982. Himalayan Main Central Thrust and its implications for Himalayan Inverted Metamorphism. *Tectonophysics* **84**, 197-224.
Sinha-Roy, S. & Sengupta, S. 1986. Precambrian deformed granites of possible basement in the Himalayas. *Precamb. Res.* **31**, 209-235.
Srikantia, S. V. & Bhargava, O. N. 1974. The Salkhalas and the Jutogh relationship in the Kashmir and Himachal Himalaya - a reappraisal. *Him. Geol.* **4**, 396-413.
Srikantia, S. V. & Bhargava, O. N. 1985. 'Chail Series' of the Himachal Himalaya. *J. Geol. Soc. Ind.* **26**, 350-355.
Srikantia, S. V. & Bhargava, O.N. 1988. The Jutogh Group of metasediments of the Himachal Himalaya: its lithostratigraphy. *J. Geol. Soc. Ind.* **32**, 279-274.
Srikantia, S. V., Jangi, B. L. & Reddy, K. P. 1978. The Kainchwa granitic complex of the Jutogh belt of the Chaur mountain area, Simla Himalaya. *J. Geol. Soc. Ind.* **19**, 169-170.
Spry, A. H. 1969. Metamorphic textures. Pergamon Press.
Staubli, A. 1989. Polyphase metamorphism and the development of the Main Central Thrust. *J. Met. Geol.* **7**, 73-93.
Stocklin, J. 1980. Geology of Nepal and its regional frame. *J. Geol. Soc. Lond.* **137**, 1-34.
Tapponnier, P., Peltzer, G., Le Dain, Y., Armijo, R. & Cobbold, P.R.1982. Propagating extrusions tectonics in Asia: New insights from simple experiments with plasticine. *Geology*, **10**, 611-616.
Thakur, V. C. 1980. Tectonics of the Central Crystallines of Western Himalaya. *Tectonophysics* **62**, 141-154.
Thakur, V. C. 1981. An overview of the thrusts and nappes of western Himalaya. In: Thrust and Nappe Tectonics (edited by McClay, K. R. & Price, N. J.), *Geol. Soc. Lond. Spl. Publ.* **9**, 381-392.
Thakur, V. C. 1983. Granites of western Himalayas and Karakorum - structural framework, geochronology and tectonics. In: Granites of Himalayas, Karakorum and Hindu Kush (edited by Shams, F.A.). Institute of Geology, Punjab University, Lahore, Pakistan, 327-339.
Treloar, P. J., Broughton, R. D., Williams, M. P., Coward, M. P. & Windley, B. F. 1989. Deformation, metamorphism and imbrication of the Indian plate, south of the Main Central Thrust, north Pakistan. *J. Met. Geol.* **7**, 111-125.
Trivedi, J. R., Gopalan, K., & Valdiya, K. S. 1984. Rb-Sr ages of granitic rocks within the Lesser Himalayan Nappes, Kumaun, India. *J. Geol. Soc. Ind.* **25**, 641-654.
Tullis, J., Snoke, A. W. & Todd, V. R. 1982. Significance and petrogenesis of mylonitic rocks. *Geology* **10**, 227-230.
Valdiya, K. S. 1980a. The two intracrustal boundary thrusts of the Himalaya. *Tectonophysics* **66**, 323-348.
Valdiya, K. S. 1980b. Geology of Kumaun Lesser Himalaya. Wadia Institute of Himalayan Geology, Dehra Dun, India.
Valdiya, K. S. 1988. Tectonics and evolution of the central sector of the Himalaya. *Phil. Trans. R. Soc. Lond.* **A326**, 151-175.

Valdiya, K. S., Rana, R. S., Sharma, P. K., & Dey, P. 1992. Active Himalayan Frontal Fault, Main Boundary Thrust and Ramgarh Thrust in southern Kumaon. *J. Geol. Soc. India* **40**, 509-528.

Vernon, R. H. 1978. Porphyroblast-matrix microstructural relationships in deformed metamorphic rocks. *Geol. Rund.* **67**, 288-305.

Vernon R. H. 1989. Porphyroblast-matrix microstructural relationships: recent approaches and problems. In: Evolution of Metamorphic Belts (edited by Daly, J. S., Cliff, R. A. & Yardley, B. W. D.), *Geol. Soc. Spl. Publ.* **43**, 83-102.

Vidal, P., Cocherie, A. & Le Fort, P. 1982. Geochemical investigations of the origin of the Manaslu leucogranite (Himalaya, Nepal). *Geochim. Cosmocim. Acta* **46**, 2279-2292.

Virdi, N. S. 1979. Status of the Chail Formation vis-a-vis Jutogh-Chail relationship in the Himachal Lesser Himalaya. *Him. Geol.* **9**, 111-125.

Virdi, N. S. 1981. Chail metamorphics of the Himachal Lesser Himalaya. In: Metamorphic Tectonites of the Himalaya (edited by Saklani, P. S.), Today and Tomorrow's Publication, New Delhi, 89-100.

White, S. H. 1976. The effects of strain on the microstructures, fabrics, and deformation mechanisms in quartzites. *Phil. Trans. R. Soc. Lond.* **A283**, 69-86.

White, S. H., Burrows, S. E., Carreras, J., Shaw, N. D. & Humphreys, F. J. 1980. On mylonites in ductile shear zones. *J. Struct. Geol.* **2**, 175-187.

Williams, P. F. 1970. A criticism of the use of style in the study of deformed rocks. *Geol. Soc. Am. Bull.* **81**, 3283-3296.

Williams, P. F. & Price, G. P. 1990. Origin of kinkbands and shear-band cleavage in shear zones: an experimental study. *J. Struct. Geol.* **12**, 145-164.

Windley, B. F. 1988. Tectonic framework of the Himalaya, Karakoram and Tibet, and problems of their evolution. *Phil. Trans. R. Soc. Lond.* **A326**, 3-16.

Wise, D. U., Dunn, D. E., Engelder, T. J., Geiser, P. A., Hatcher, R. D.(Junior) Kish, S. A., Odom, A. L. & Schamel, S. 1984. Fault-related rocks: Suggestions for terminology. *Geology* **12**, 391-394.

Yardley, B. W. D. 1989. An introduction of Metamorphic Petrology. Longman.

Yeats, R. S. & Lillie, R. J. 1991. Contemporary tectonics of the Himalayan frontal fault system: folds, blind thrusts and the 1905 Kangra earthquake. *J. Struct. Geol.* **13**, 215-225.

Zeck, H. P. 1974. Cataclastites, hemiclastites, holoclastites, blastoditto and myloblastites. ~~= cataclastic rocks~~. *Am. J. Sci.* **274**, 1064-1073.

Zwart, H. J. 1962. On the determination of polymetamorphic mineral associations, and its application to the Bosot area (Coastal Pyrenees). *Geol. Rund.* **52**, 38-65.

* Additional References

Patriarch, P. E. & Achache, J. 1984. India-Eurasia collision chronology has implications for crustal shortening and driving mechanism of plates. *Nature* **311**, 615-621.

Turner, F. J. & Weiss, L. E. 1963. Structural analysis of metamorphic tectonites. McGraw-Hill Book Co.

Windley, B. F. 1983. Metamorphism and tectonics of the Himalaya. *J. Geol. Soc. Lond.* **140**, 849-865.